Universidad Nacional Autónoma de México

POSGRADO EN CIENCIAS FÍSICAS

RANDOM SEARCHES IN INTERMITTENT ENVIRONMENTS

TÉSIS

QUE PARA OPTAR POR EL GRADO DE:

DOCTOR EN CIENCIAS (FÍSICA)

PRESENTA:

JOSÉ GABRIEL MERCADO VÁSQUEZ

TUTOR PRINCIPAL:

DR. DENIS PIERRE BOYER

INSTITUTO DE FÍSICA, UNAM

MIEMBROS DEL COMITÉ TUTORIAL:

DR. FRANCISCO JAVIER SEVILLA PÉREZ

INSTITUTO DE FÍSICA, UNAM

DR. PEDRO EDUARDO MIRAMONTES VIDAL

FACULTAD DE CIENCIAS, UNAM

CIUDAD UNIVERSITARIA, CD. MX., AGOSTO 2022

Contents

Chapter 1

Introduction

First passage problems find ubiquitous applications in several areas of science, as numerous phenomena are controlled by the time taken by a process to reach for the first time a specified site in space, or threshold, or configuration [108, 122, 61]. In biological systems, first passage processes allow us to predict the sizes of neuronal avalanches in neocortical circuits [12] or the search strategies adopted by foraging animals to find food [140, 75]. In chemistry, processes are often limited by reaction rates which can be understood in terms of a mean first passage time (MFPT), such as the mean encounter time between two diffusing molecules, or the two diffusive ends of a polymer chain in solution [134, 43], or between remote DNA segments [147, 38].

Many search problems are modelled as a random walk or a Brownian particle and a fixed target site to be found, such that the process ends instantaneously upon first encounter [100]. However, in many applications, due to errors or imperfections in the binding or detection phase, a search may be completed only after several passages on the target region. On discrete lattices, partial absorption can be modelled by introducing an absorption probability lower than unity each time the searcher occupies the target site [87, 33, 27]. In the continuous limit, this rule becomes equivalent to a radiation boundary condition, where the absorption probability flux is proportional to the probability density at the target [108, 124, 105].

However, some systems cannot be described by partial absorption only: this is the case when the environment of the searcher fluctuates in time, for instance, when the target sites are subject to an internal dynamics, such as a switching process between an active and an inactive state, or detectable and undetectable, where the target can be hidden or inactive for long periods, and thus not available for reaction or encounter of the searcher [16, 18, 113].

In cell biology, ion channels are targets for ions in the cell and can be modelled as gates that stochastically open and close to control the flux of ions that cross the membrane, affecting transport of material, cell signaling, or drug delivery [29, 110]. Studies on single ion-channels have shown that opening or closing events of the pore occur over characteristic dwell times ranging from 0.5 to hundreds of ms [76, 115]. These times are comparable or much larger than the diffusion times of K^+ or Ca^{2+} ions at the scale of a cell ($\tau_D \sim 0.1$ ms) [47]. Hence, first hitting times are likely to be limited by the channel state [84, 91].

Random switching processes between different states are also common in gene expres-

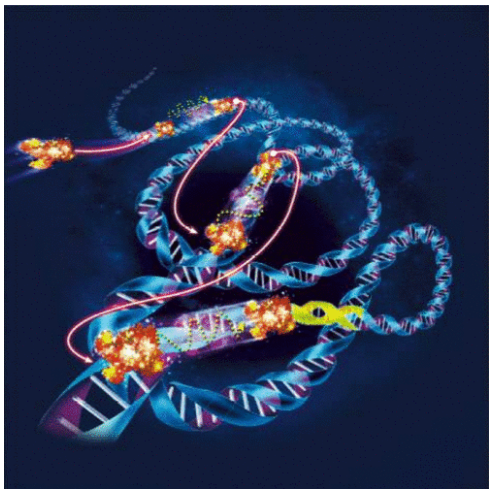

Figure 1.1: Protein performing $1d$ sliding along the DNA strands with 3d diffusion in the volume cell. Reprinted figure with permission from [17].

sion. A transcription factor may diffuse to reach its target promoter in order to activate the gene expression [42, 70, 73, 120], and this can be achieved by a combination of sliding along the DNA contour, and diffusive hops within the volume of the cell (see Fig. 1.1). In any case, gene expression is possible only if the binding target site along the DNA chain is accessible to the transcription factors [94, 136]. When the chromatin is in the unfolded state, the binding site is accessible and gene expression may start, however, when the chromatin is folded, transcription is not allowed [102, 146, 48]. It has been proposed that the accessibility of the binding sites is governed by a Poisson distributed switching process, with fixed transition rates between the reactive and non-reactive states [102].

Switching processes are of relevance in foraging ecology as well. To prevent attacks from predators, several organisms adopt crypsis as their primary defense [114]. Many species may conceal by camouflaging themselves for some periods of time in their environment to make their detection more difficult [131, 137, 49]. In some cases, cryptic prey prefer to rest for a long time in a particular area, where its background matching is better [64, 67], in other cases, prey are able to be cryptic and undetectable for long periods of time by hiding behind an object or adopting a subterranean lifestyle, thus forcing predators to develop different mechanisms to recognize them, either by forming a search image or by varying their searching rate [49, 114, 62, 104].

The search of intermittent targets is also of interest in rescue operations, which are often carried out in scenarios where a target must be located within the shortest amount of time possible. In the case of a person lost in nature, for instance, minimizing the searching time can be crucial for survival. However, such target may not remain always detectable due to varying climatic conditions, or because the person is unable to call continuously for help, or may have an emitter with limited battery. Some experiments have simulated random search problems by using robots equipped with a receptor in search of intermittent electromagnetic signals emitted by a fixed source [128, 127].

Despite the wide range of phenomena that we can find in nature that involve reaction with intermittent targets, there are surprisingly few theoretical studies that have focused on the consequences of target intermittency on first encounter statistics. The problem

in which diffusive ligands bind to a protein that stochastically switches between two conformational states, and it is only reactive in one state was first studied in [135]. In this paper, target encounters are described in terms of the effective flux of ligands that bind to the protein. A more recent extension of this work has been done in [31]. The inclusion of the intermittent target with its own dynamics independent of the dynamics of the searcher has been also modeled in [113], where the intermittence is taken into account in the target state and the absorption or capture is only possible when the target is in the active state. However, this work focuses on the mean time in which the target is found by a set of searchers.

The time-scale associated with the own dynamics of the target introduces a new parameter, additional to the absorption probability, that markedly affects the first passage time properties, as we will see in this work. Further, when we consider the intermittence as an intrinsic property of the target (and not as a consequence of the walk strategy of the searcher), this allows us to face the question of the time needed to find a target, among a set of targets having independent internal dynamics.

Whereas the first passage properties of diffusive processes with fluctuating targets have not been well studied, in recent years a significant interest has been dedicated to understanding the search mechanisms that can improve target encounter. An example is the case of intermittent search [15, 28, 17], where slow diffusive phases of search are interspersed with fast phases of ballistic motion, during which target detection by the searcher is not possible. It can be proven [15] that, with this strategy, the mean encounter time can be minimized with respect to the rate at which the searcher switches between the diffusing and the relocation or ballistic phase. Intermittent search is favorable as it allows the searcher to explore different regions of space with little overlap between them, which would be covered much more slowly by a simple Brownian motion.

The growing interest in non-Brownian search strategies lies in the fact that many organisms, ranging from motile cells to animals, perform non-Brownian motions in order to efficiently explore their environment [71, 45, 123]. Special interest has been dedicated to search processes such as Lévy flights [139, 138, 140, 83], ballistic movements [139, 10] and run-and-tumble motion [7, 89]. Of special interest in this work is the run-and-tumble (RT) motion, which consists of straight-line motion at constant speed (run) interspersed with random re-orientations occurring with a constant rate (tumble). Despite of its simplicity, the RT motion has served to model a wide range of non-equilibrium systems such as self-propelled particles [51, 89], electron collisions in a Lorentz gas [90] or the motion of bacteria such as *E. coli*, *Salmonella* or the marine bacteria *P. haloplanktis* [20, 132]. The motility of microswimers in diverse environments has been better understood thanks to analytical results on the RT model. In confined environments, run-and-tumble particles (RTP) tend to accumulate near the boundaries [89, 51]. In the presence of steady potentials, transitions between active and passive-like behaviour have been observed [46]. RTPs subject to periodic and asymmetric potentials exhibit a so-called active ratchet effect [6]. In [4] a run-and-tumble particle in the presence of imperfect boundaries has been considered. These studies have brought evidence that run-and-tumble particles exhibit properties that contrast with those of their Brownian counterparts.

Particularly important for the optimization of search processes is also the case of diffusion with stochastic resetting, in which the motion of a searcher is randomly interrupted and restarted from the initial position [54, 55]. Resetting allows the searcher to explore

new paths and to cut-off those unfruitful trajectories that explore regions that are far from the target region [59]. In search problems, restarting (or resetting) to the initial configuration causes drastic effects on the behaviour of the first passage times. Under this scheme, the mean first passage time (MFPT), which is infinite for free diffusion in infinite domains, becomes finite; furthermore, it is found that this quantity can be minimized with respect to the resetting rate. In Brownian diffusion under resetting, the optimal resetting rate depends on the diffusion coefficient and the distance between the target and the starting point. In unbounded domains and in the absence of absorbing targets, stochastic resetting also generates non-equilibrium steady states. For a diffusive particle, for instance, the probability density tends to an asymptotic distribution, in marked contrast with the non-stationary Gaussian profiles that characterize free diffusion [54, 58].

Despite the fact that the features of diffusion with resetting are interesting, implementing this process in a lab experiment with a physical particle is challenging since, at least in its original form, it considers that the restart process occurs infinitely fast and with perfect precision to the initial configuration, *i.e.*, the searcher must immediately restart from exactly the same position. Both aspects make experiments difficult (if not impossible) to carry out. Therefore, the original model must be modified in order to take into account physical constraints. In addition, it is worth noting that the resetting process can be viewed as a diffusive process in fluctuating environments, in which intermittent forces (more specifically time-dependent potentials) constrain the motion of the particle. This last approach is the one we use in the present document. Although the two problems are different, the methods and theoretical techniques developed for the intermittent target problem will be useful to model a realistic resetting process.

In the present work we address several problems of search processes in intermittent media: i) a diffusive particle searching for an intermittent target and ii) a model of diffusion with stochastic resetting that can be implemented in lab experiments. For the first case, the target will stochastically transit between two phases of detection, whereas the movement of the particle will be Brownian diffusion. Extensions to other types of diffusion such as diffusion with stochastic resetting or run-and-tumble motion will be considered. We will focus on the full distribution of the first hitting times in this problem. In the second problem, we will study a diffusive particle driven by the action of a confining potential that is applied during random time intervals. We will explore all the relevant features of this system when there is no target and when a steady target is placed at a certain distance of the potential minimum. The present document is organized as follows:

We begin in chapter 2 with a brief background of the work and what has been done up to now in relation with first passage processes. We start by mentioning the most well-known works on the subject and their main results. Next, we review first passage time problems with fluctuating boundaries. Following this, we present the model of diffusion with stochastic resetting. In this part, we analyze the first hitting properties of this problem and discuss the difficulties that arise when implementing in real experiments.

In Chapter 3 we expose the main objectives we are pursuing, as well as the problems we want to cover and the results we hope to achieve in this work.

In chapter 4 we provide an introduction to the main mathematical methods that will be needed later to carry out our research project. This chapter presents useful tools in the area of first passage problems and defines the main relevant quantities, such as the survival probability, the first hitting time distribution, and the mean first hitting

time. We dedicate section 4.2 to the deduction of the backward Fokker-Planck equation that will be essential for calculating the temporal behavior of the survival probability. Equally important is section 4.4 where we establish the boundary conditions associated to the Fokker-Planck equation for the most simple cases with absorbing and reflecting boundaries. We also include the partial absorption case.

In the following two chapters we introduce the problems we are studying and present their analysis. In chapter 5 we investigate random searches of fluctuating targets. Here we focus on the statistical properties of the first hitting time of a diffusive particle to an intermittent target located at a fixed position. The target dynamics are governed by a Markov process which consists of randomly switching between two states, where target detection is allowed only in one of the two.

We start in section 5.1 with the study of a Brownian particle in the presence of an intermittent target. The exact first passage time distribution on the infinite line is derived. We find that in the limit of high transition rates target intermittency has little effects on first passage times, independently of the crypticity. In the general case, the typical first hitting time is substantially increased due to the target dynamics. In section 5.1.5 we analyze the shape of the first hitting time density for long times, finding a scaling regime in $t^{-1/2}$, followed by the well known asymptotic behavior in $t^{-3/2}$ dependence. At the end of this chapter, we carefully analyze the conditions that lead to the presence of this intermediate regime as a function of the intermittency parameters.

In Section 5.2 we extend the above study to Brownian motion with stochastic resetting. We investigate how the implementation of resetting affects the statistical properties of the first hitting time to the intermittent target. We observe that the search time is minimum at an optimal resetting rate that depends on the target transition rates. When the target relaxation rate is much larger than both the resetting rate and the inverse diffusion time, the system becomes equivalent to a partially absorbing boundary problem. In other cases, however, the optimal resetting rate can be a non-monotonic function of the target rates, a feature not observed in partial absorption. We compute the relative fluctuations of the first hitting time around its mean and compare our results with the ungated case. The usual universal behavior of these fluctuations for resetting processes at their optimum breaks down due to the target internal dynamics.

Section 5.3 is dedicated to the run and tumble searcher. In this case, we analyze two scenarios: the finite domain size where the particle is confined between two reflective walls and the infinite domain. For the bounded case, the problem allows us to compute a mean first hitting time, that we find becomes minimal when the particle performs ballistic motion. To better comprise the behaviour of the first hitting time density, we calculate the relative variance that it has a non-trivial dependence with the target dynamic parameters. As in the Brownian case, in the infinite domain we found again the scaling decay $t^{-1/2}$ for intermediate times before to the standard $t^{-3/2}$ decaying. We interestingly found that a persistent searcher slightly lengthens the duration of the intermediate regime and thus, Brownian motion appears as the best option to diminish the effect of the target dynamics.

Chapter 6 is devoted to the study of random searches in fluctuating media. In Section 6.1 we explore the nonequilibrium diffusive process of a Brownian particle driven by a piece-wise linear potential that intermittently turns on and off. We find a non monotonic behaviour of the mean first hitting time as a function of the switched-on and switched-off rates, and this mean time can be optimized. When the potential strength is varied, it

is possible to observe first and second order transitions in the optimal rates. Our model extends previous works in the literature related to stochastic resetting processes such that several limiting cases can be recovered from it. In the absence of the absorbing barrier, the system reaches a non-equilibrium steady state, irrespective of the switched-on and switched-off rates and the potential strength.

In Section 6.2 we extend our study for more general potentials of the form $v(x) = k|x - x_0|^n/n$. In particular, we focus on the harmonic potential case with $n = 2$. We also recover previous results for the linear potential ($n = 1$). Similarly to the piece-wise potential case, the MFPT to a fixed target can get optimized by intermittently applying a confining potential. Again, we observe that the system undergoes a second order transition in the optimal rates.

Finally, in chapter 7 we summarize the results of this research project and discuss our findings.

Chapter 2

Background

In this chapter we make a brief review of the theory of first passage times from a historical perspective, starting from the earliest works on this field up to the most recent advances related with first passage problems in fluctuating media.

We start in Section 2.1 by presenting one of the first addressed problems that relate with first passage times, namely, the *gambler's ruin* problem. Following this, we present the main works and achievements that have been made in order to mathematically formalize this type of problems.

In Section 2.2 we discuss the problem of diffusion in fluctuating media, where the reactivity of the system boundaries varies in time and the diffusive particles are not always absorbed upon boundary encounter. We named a few interesting cases that have been observed in nature where this situation happens and we introduce the partial absorption process that arises as the main way in which this phenomenon can be modeled.

Finally, Section 2.3 is devoted to presenting an interesting kind of stochastic processes that is observed in real systems, and that finds many applications, namely, intermittent search processes. The attention that these processes have gained in recent years surges from the fact that they show rich features with respect to first passage properties. We focus on instantaneous resetting processes which are a class of intermittent search. Introducing instantaneous resetting processes is fundamental to understand our work in Chapter 6.

2.1 First passage problems

The interest in first passage time distributions has a long history. Perhaps the oldest study that we can find related to first passage times in a random process is the well known *gambler's ruin* problem, that Pascal first proposed to Fermat in 1656 [50]. In this problem, two gamblers play a game of chance. The gambler A starts with k units of money, whereas the opponent B starts with $N - k$. In each trial of the game, the player A wins a unit of money from B with probability p, or loses one unit to B with probability $q = 1 - p$. Conversely, the player B wins from A or loses to A with probability q and p, respectively. The game ends when one player loses all his money. Pascal was interested in the probability that the gambler A (or B) wins the game, and he could find a solution using his knowledge of probability theory that was surging in these years.

In 1657, just a year later, Huygens announced the problem (without giving Pascal

credit) in his *De ratiociniis in ludo aleae*, which is the first published book on probability theory [129]. In this work, he proposed another solution that agreed with Pascal's. The *gambler's ruin* problem rapidly gained the attention of the mathematics community and it arose the question of determining the duration of play, *i.e.*, the number of trials before the gambler wins or loses. The first solutions for this question were given by Montmort, Nicholas Bernoulli, and de Moivre, which, without rigorous proofs, were able to compute an expression for the expected duration of play [129]. What they found was in fact the mean first passage time for a discrete random process and it represented one of the first important results in the theory of first passage problems.

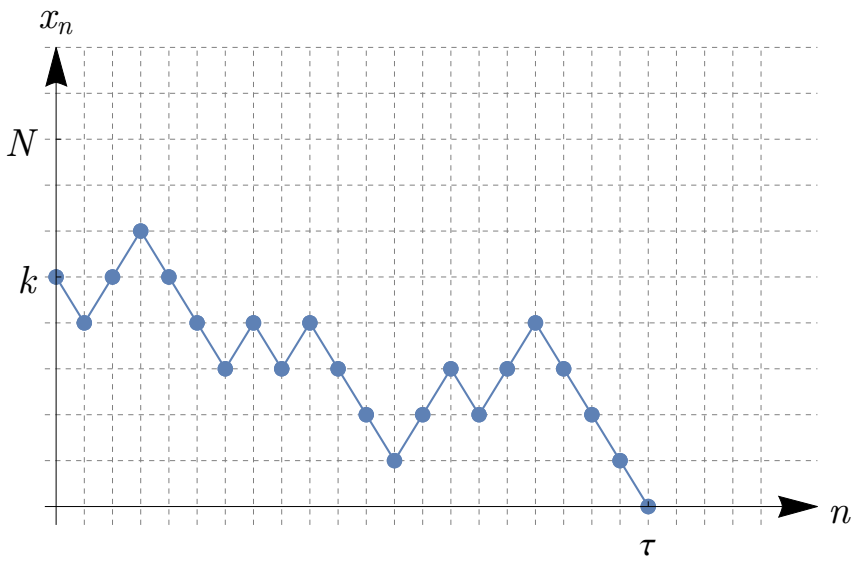

Figure 2.1: Simulation of a gambler's ruin problem with $k = 5$, $N = 8$ and $p = q = 1/2$. In this case, the duration of play is $\tau = 21$ steps.

Nowadays, the *gambler's ruin* problem is described in terms of a random walk in $1d$, where the money of the gambler represents a walker with position x_n at the trial n, starting at $x_0 = k \in (0, N)$. Each trial the walker jumps to the right with probability p, or to the left with probability $1 - p$ (see figure 2.1). When the walker reaches N for the first time the gambler wins, and when it first reaches the origin the gambler loses. The ruin and the win conditions represent two absorbing states of the system; once the walker reaches one of them, it will be impossible to exit that state, and the process ends. The time τ at which the ruin or the win occurs is the duration of the play and this number is a random variable.

Expressing the mean duration of play $\langle\tau\rangle$ in terms of a inhomogeneous differential equation [74], one can find

$$\langle\tau\rangle = \begin{cases} k(N-k) & \text{if} \quad p = q, \\ \frac{1}{q-p}\left(k - N\frac{1-(q/p)^k}{1-(q/p)^N}\right) & \text{if} \quad p \neq q, \end{cases} \tag{2.1}$$

which has an interesting behaviour in the limit $N \to \infty$: if $q > p$, the mean duration reaches the finite value $\langle\tau\rangle = k/(q-p)$, otherwise, the mean duration tends to infinity.

Problems like the gambler ruin caused a great expectation among mathematicians, who sought for a formal theory that proved these first results, which most of the time came from their intuition or from combinatorial analysis, as was the case of the Fermat's solution of the gambler's ruin problem (see [50]). It was not until the development of probability theory and statistical physics, in the first decades of the 20th century, that first passage problems began to be formally treated.

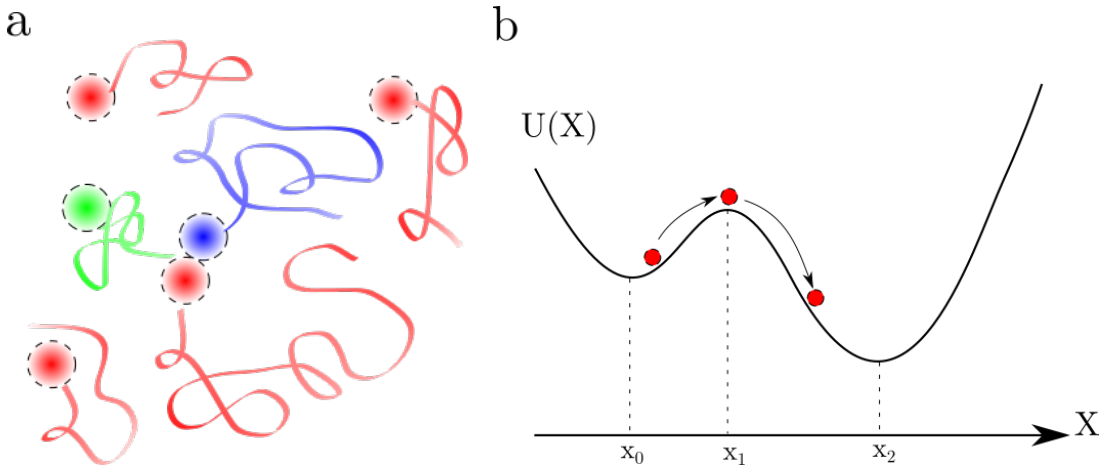

Figure 2.2: a) A molecule A (blue point) diffuses in the presence of a concentration of molecules B (red point). When they interact for the first time a reaction occurs and a new molecule AB (green point) is created. Lines represent the path that the diffusive particles travel. b) Potential $U(X)$ for the Kramer's problem.

Particularly important are the pioneering works of E. Schrödinger [117] and Smoluchovsky [141] (see [122] for a brief discussion of these works), where the first passage time problem for a continuous random process was posed and first attempts for solving it were carried out. These works have had a great impact not only in physics and mathematics but in other areas of science such as chemistry and biology. The Smoluchovsky rate theory allowed us to understand reactions rates between molecules using the diffusion-controlled approach. The simplest case where two molecules A and B interact and react to form a new complex molecule AB (see Fig. 2.2a) can be described in terms of a first passage time problem, since reaction occurs at first encounter [39, 134, 108, 29]. As we have mentioned in the introduction, this problem is of great interest since the principle of diffusion-reaction underlies many other phenomena, such as animal foraging [140, 75], in which a predator "reacts" with a prey when hunting, or proteins binding to DNA for expressing a gene [147, 38, 135]. In the next section, we will return to this problem for the case of fluctuating media and gated reactions, as it relates with the problem of intermittent targets.

In a more realistic description of a chemical reaction, two nearby interacting molecules are separated by a potential barrier, in such a way that the reaction occurs only if they have enough energy to overcome it [61, 112]. This is the well known Kramer's problem after the work of Kramer in 1940 [77]. In this problem, a Brownian particle is subject to the action of a bimodal potential $U(x)$ that has two local minima and a local maximum, where x is the particle position, as depicted in Fig. 2.2b. When the particle is on the left side around x_0, due to thermal fluctuations, there exists a probability that, after some

time τ, the particle crosses the maxima at x_1 for the first time, passing to the right side. The time τ is in fact a first passage time and controls the reaction time. Certainly, once the particle is around the minima x_2 it can return to the left side in the same way by crossing the barrier at x_1. This is a problem of bistability where the process randomly transits between two stable points around x_0 and x_2. Let suppose that a molecule A is initially at x_0 and other molecule B is at x_2. If one assumes that the barrier height $U(x_1) - U(x_0)$ is very large, one can obtain the Arrhenius formula [61, 112]:

$$\frac{1}{\langle\tau\rangle} = \frac{D}{2\pi kT}\sqrt{|U''(x_1)|\,U''(x_0)}\exp\left(-\frac{U(x_1)-U(x_0)}{kT}\right), \tag{2.2}$$

where T is absolute temperature, D is the diffusion constant and k is the Boltzmann constant. Eq. (2.2) gives the mean rate $1/\langle\tau\rangle$ at which a reaction occurs.

With this advances, new mathematical concepts surged, such as the first passage time distribution (the probability density of the random variable τ) and the survival probability defined as the probability that the particle has not reached the target yet at time t, a quantity related to the first one. Shortly after Kramer's work, Siegert [122, 44] extended some of the results of Schrödinger, Smoluchovsky, and others, giving a new perspective to the diffusion processes. He also showed that the survival probability is solution of the backward Fokker-Planck equation. We would like to mention that all these concepts will be rigorously introduced in the following chapter, however, we emphasize the fact that these are the most relevant quantities involved in first passage problems and contains all the information that typically one would like to know in order to describe the first passage properties of a system under study.

Since the gambler's ruin problem, discrete random processes have been also extensively studied (see references in [60, 61, 108, 109]) and the random walk model gained much relevance for physicist, since it allowed to make an amalgamation of discrete-time processes with continuous one. Specially important for our study is the work of Sparre Andersen [2, 3], which gave the proof of a general result, pointing to a surprizing universality of discrete time processes. Consider a walker such as the one in Fig. 2.1, performing at each step random increments ℓ drawn from a distribution $p(\ell)$. What Sparre Andersen showed is that, no matters what kind of distribution $p(\ell)$ is followed by the walker steps, as long as it is symmetrical, $p(\ell) = p(-\ell)$, and ℓ is continuous, the probability that the position of the walker has remained always non-negative up to step n is

$$Q(0,n) = \binom{2n}{n} 2^{-2n}, \tag{2.3}$$

which in the limit of large n decays, to leading order, as

$$Q(0,n) \sim \frac{1}{\sqrt{\pi n}}. \tag{2.4}$$

$Q(0,n)$ is also called the survival probability at n when the walker starts at $x = 0$. As the interpretation of this result requires some care, we will discuss it in section 4.9.

Another work that ought to be mentioned is the Montroll's paper of 1965 [101], which represented a significant advance in the formalization of the first passage properties of random walks. In this work, he was able to calculate important quantities such as the

moments of the first passage time distribution, the mean number of points visited r times, or the probability for the walker to return to the origin for the first time after n steps. This paper is also the cornerstone of subsequent works that initiated the field of anomalous diffusive transport (see [121] for a brief historical review of Montroll's work).

Currently, the theory of first passage time is a rich and constantly growing field that comprises the analysis of many different problems in diverse areas of science such as physics, mathematics, biology, and more recently in computer science or economy, among others. We refer the reader to [108, 29, 61], where he or she will find a complete exposition of the state of the art on the theory of first passage processes and applications. The richness of this field is largely due to the fact that many phenomena rely on the time it takes a random process to first reach a configuration. This is the case of fluctuating media, in which sometimes a certain configuration cannot be reached immediately by the random process. As this is a wide and interesting topic to be discussed, it deserves a section apart.

2.2 Fluctuating media

As we have seen, the first passage theory deals with processes that randomly reach some configuration for the first time. In the works mentioned above, it has been considered that these configurations are always available for the random process. In the chemical reaction theory of Smoluchovsky, for instance, a reaction occurs immediately after a first interaction between the molecules A and B and they form a new compound AB. In the Kramer's problem, the particle crosses the barrier as soon as it reaches the local maximum. In the gambler's ruin problem, the player is ruined as soon as he loses all his money and therefore cannot play again. All these situations are examples in which the configurations or boundaries of the system are perfectly absorbent; the random process ends once it reaches the boundary.

Mathematically, this condition on the system imposes a survival probability that vanishes at the boundaries. This means that there will be no more chances for the process to continue when it first reaches the boundaries. However, there are many situations in which the random process may not end upon the first encounter and needs to reach the boundaries many times before to be absorbed. Suppose, for example, that in the gambler's problem, when the player is ruined, with some probability p' the opponent lends him a unit of money for playing once again. In the random walk solution, this would mean that when the walker crosses the origin, with a probability p' it is reflected, and the walk continues. Strictly speaking, in this case, we do not talk of first passage time, but first hitting time since we are measuring the time in which a first hit or reaction with the boundaries occurs.

These scenarios are observed in natural phenomena, as is the case of oxygen molecules diffusing in blood cells to bind hemoglobin and myoglobin. It is found that, in some cases, the oxygen cannot bind due to the presence of other proteins that block the entrance of the heme pockets [135]. The proteins behave as gates that stochastically open and close, controlling the binding of oxygen. This system has been modeled as a controlled-diffusive reaction (as in Smoluchovky theory) in which the reactive molecules A randomly switches to an unreactive state A' where they cannot interact with the molecules B [95, 135].

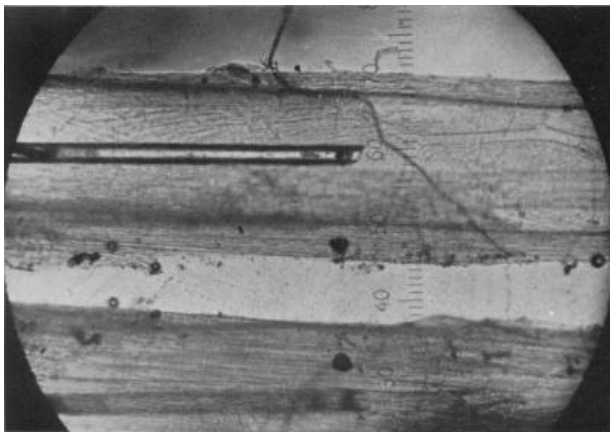

Figure 2.3: Photomicrograph of an electrode inside a squid giant axon. This is how Hodgkin and Huxley saw the axon in the microscope. Image taken from [72].

In a similar fashion, ion channels in the cell membrane can control the flux of K^+ and Na^+ ions into and out of cell [29]. The latter was investigated by Hudgkin and Huxley in a series of papers that eventually led them to share the Nobel prize in Physiology or Medicine in 1963 (see [119]). In these works, they studied the squid giant axon (see Fig. 2.3) and were able to describe the mechanism that underlies ions transport. They observed that a difference in the Sodium and Potassium ions concentration within and outside the cell generated a voltage difference on the lipid bilayer membrane, which produced a change in its permeability. They found out that some protein channels, that remained closed at the rest voltage, began to open and close stochastically at a voltage-dependent rate; these channels act as intermittent random gates [53].

One of the most important mechanisms that controls gene expression is transcriptional regulation. This mechanism is mediated by proteins known as transcription factors, which serve as switches that turn gene expression on and off [29]. The transcription factors that are responsible for turning the expression off are called repressors. These proteins bind to the promoter region along the DNA, preventing the mRNA molecule from transcribing the gene code. Some transcription factors, such as the *lac* repressor of the bacterium *Escherichia coli*, enhance repression by simultaneously binding to two DNA sites [133], which causes the DNA to run into itself and form a loop. Despite the energetic cost of deforming the DNA, the looped conformation can be sustained for long periods of time [37], after which the DNA unwinds. In this case, a patter of intermittency can be observed (see figure 2.4).

In a quite different context, patterns of intermittency been observed in animal foraging. Arctic ground squirrels can alternate in phases above and below ground during a day [145]. In the phases above ground, these semi-fossorial animals spend time foraging for food and going on excursions to mate, despite the high risk of predation. Certainly, they can reduce this risk by remaining below ground, albeit the energy cost this may represent as they are not foraging. They have to compensate for both dynamics, performing intermittent patterns in their activity as depicted in Fig. 2.4. It is interesting to notice that, due to the lactation and maternal care, females have to return more often to their burrows. The natural predators of arctic squirrels such as the red fox (*Vulpes vulpes*), the grey wolf (*Canis lupus*), or golden eagles (*Aquila chrysaetos*), have to deal with this intermittent

behaviour when hunting.

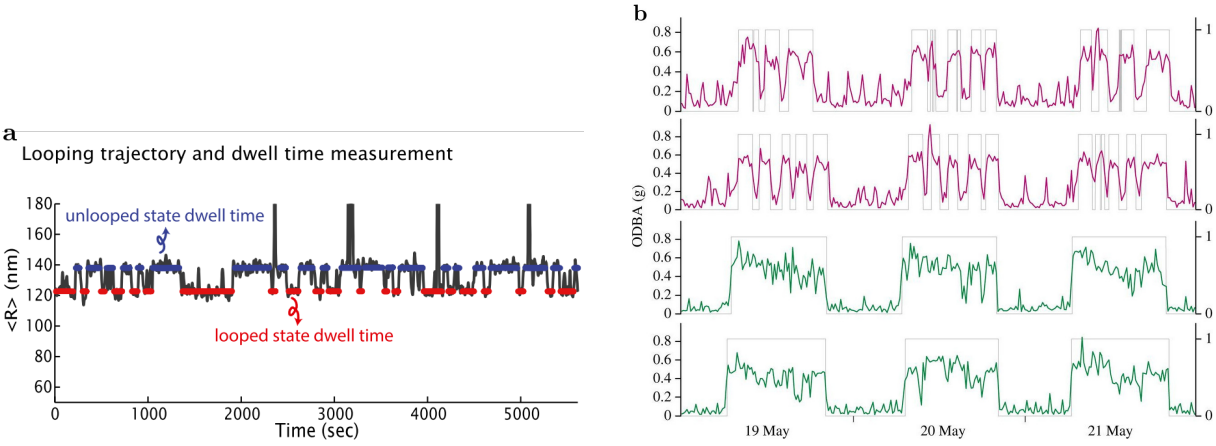

Figure 2.4: a) Time that the DNA of the bacterium *Escherichia coli* spends in the looped/unlooped state measured by tethered particle motion. Image taken from [37]. b) Time spend above/below ground deduced from the overall dynamic body acceleration (ODBA) on 19-21 May 2015, from two females (top panels) and two males arctic ground squirrels (bottom panels). Image taken from [145].

Systems where absorption does not occur instantaneously have been modelled by partial absorption boundaries, which have the property that, with some probability, they absorb or reflect the random process [14, 108], as in the modified gambler's problem that we mentioned above. For the continuum case of controlled-diffusion, the partial absorption condition is described in terms of the average difference of the flux of particles that react and those that do not. The mathematical treatment for these boundary conditions will be seen more in detail in chapter 4.

The partial absorption model has allowed treating many real systems and has had a favorable acceptance in the field of first passage problems. However, as it reduces the absorbing condition to a simple probability, it does not capture the rich features that the dynamics of the boundaries can have [68]. One of our main aims in this work is to face the problem of imperfect absorption from a perspective in which the dynamics of the boundaries (or targets) are independent of those of the searching entities.

2.3 Stochastic search strategies

The first passage properties of real systems strongly depend on the strategy that the searcher adopts in order to expedite the target encounter. This can be observed in the search process of transcription factors in the cellular environment. As we have mentioned in the introduction, it has been shown experimentally that these proteins perform a 3D diffusion in the volume cell combined with a $1d$ sliding on the DNA strands where they search for their specific binding site [18, 70, 73, 120, 52]. When the transcription factors alternate between these two diffusing phases they can reduce the search duration or the first passage time to the binding side. Nevertheless, experiments also show that changes in the DNA conformation or a partial folding of the protein can accelerate or decelerate target detection [126]; faster excursions (that are possible when the binding energies are

low) cannot allow target recognition, whereas slower scanning with high binding energies retards target encounter.

From the above example, we can see that fluctuations in real systems are not only present at the boundaries, but also in the bulk, and this affects the dynamics of the search and hence, the first passage properties of the search dynamics. The particular dynamics in which target detection is allowed only in one phase of the search process is called intermittent search [15]. Typically, in this process, target recognition is allowed during a slow motion phase, whereas faster motion is used to relocate the searcher [17]. With this model, the behaviour of real systems (such as transcription factors) can be emulated and very interesting properties result from these dynamics. It is worth noting that this model bears a certain analogy with intermittent dynamic targets. But the two problems are not equivalent, except in specific particular cases. In one case, the target is intermittently invisible, whereas, in the other, the searcher is intermittently "blind". When there are many targets, the two problems are thus very different.

Let us exemplify a one-dimensional model of intermittent search [15]. Suppose that with rate λ_1 the searcher switches from the recognition phase, where it diffuses slowly with constant diffusion D, to a ballistic phase with velocities v or $-v$, where v is a constant. Conversely, with rate λ_2 the searcher switches from the ballistic to the diffusive motion. It can be found that, in a finite domain of size L with periodic boundary conditions and with a target located at $x = 0$, intermittency becomes favorable for the search, at least for L large enough, since the mean first passage time $\langle \tau \rangle \propto L$, whereas for pure diffusion $\langle \tau \rangle \propto L^2$. Furthermore, fixing λ_1, the MFPT can be minimized at the non-trivial optimal rate λ_2 given by (see [15] for more details):

$$\lambda_2^{\text{opt}} = \begin{cases} \left(\frac{4v^2}{3D}\right)^{1/3} \lambda_1^{2/3} & \text{if} \quad \lambda_1 \ll v^2/D, \\ \left(\frac{2\sqrt{2}v^2}{D}\right)^{1/3} \lambda_1^{3/5} & \text{if} \quad \lambda_1 \gg v^2/D. \end{cases} \tag{2.5}$$

From Eq. 2.3 we can see that when $\lambda_1 \ll v^2/D$, the optimal rate λ_2 is greater than λ_1, and then the searcher spends more time scanning than moving. On the other hand, if $\lambda_1 \gg v^2/D$, the optimal rate λ_2 is less than λ_1, and then the searcher spends more time moving than scanning.

Intermittent searches can combine different types of motion (for instance, diffusive and ballistic) can be generalized to a wide variety of models that exhibit interesting first passage properties (see reference [17] for a review). One of the most studied intermittent dynamics in the last years are diffusive processes with stochastic resetting. This search protocol was first introduced in [54, 55] as an idealized intermittent search in which relocation is infinitely fast. Processes under resetting may be viewed as the simplest intermittent search models.

Let us consider a one-dimensional Brownian particle with position $X(t)$, which is reset at rate r to an initial position x_0, from where it starts again (see Fig. 2.5). The probability density $p(x, t|x_0)$ that the particle is at x at time t, given that at time $t = 0$ was at x_0, will evolve as [55]

$$\frac{\partial p(x,t|x_0)}{\partial t} = D\frac{\partial^2 p(x,t|x_0)}{\partial x^2} - rp(x,t|x_0) + r\delta(x - x_0), \tag{2.6}$$

where the second and third term of the right hand accounts for the loss of probability

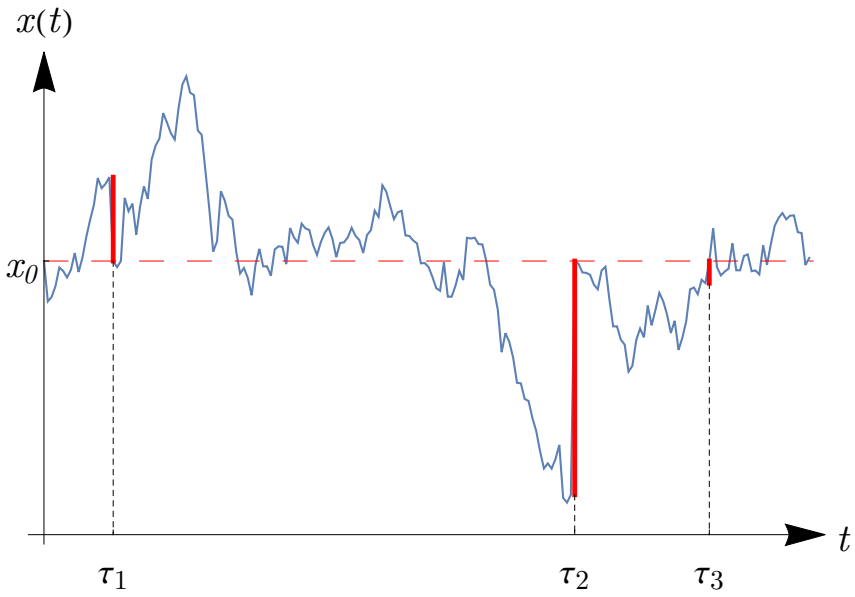

Figure 2.5: Representation of a diffusive search with stochastic resetting. At the times τ_i, randomly generated from an exponential distribution with rate r, the Brownian particle is relocated to the initial position x_0.

flux at x due to the interruptions, and a gain of probability flux at the initial position x_0 due to the reset.

This simple resetting mechanism has two strong consequences on the diffusion process:

i) in the unbounded domain, at large times, $p(x,t|x_0)$ tends to a non-zero stationary distribution that represents a non-equilibrium steady state (NESS), given by

$$p(x|x_0) = \frac{\sqrt{r/D}}{2} e^{-\sqrt{r/D}|x-x_0|}, \tag{2.7}$$

which is the solution of Eq.(2.6) when the time derivative is set to zero. By NESS it is meant that there is a flow of probability even at long times, in contrast to an equilibrium state where detail balance holds and probability currents vanish [55, 59].

ii) in the semi-infinite domain, the mean first passage time T to an absorbing target that is placed at the origin is finite. This is in marked contrast with the case of simple diffusion where it is infinite (recall the gambler's ruin problem where we showed that the mean duration of the play for any $k > 0$ is infinite for the symmetric walk). The MFPT is given by

$$T(x_0) = \frac{e^{x_0\sqrt{r/D}} - 1}{r}, \tag{2.8}$$

which has a non-monotonous dependence with the resetting rate r, since it diverges in the limits $r \to 0$ and $r \to \infty$. This implies that the MFPT can be minimized at the particular rate $r^* = (z^*)^2 D/x_0^2$, where $z^* = 1.59362...$ (see [55] for more details). Therefore, resetting can expedite target encounter and the search process can be optimized with respect to r.

The latter is an important feature of many resetting processes (see [59] for a review). The qualitative explanation for the existence of an optimal mean first passage time resides in the fact that excursions in which the particle travels far away from the target region are

interrupted at some time and restarted from the initial position, giving a new opportunity for more favorable trajectories.

Perhaps the main weakness of this model is its inherent nonphysical meaning since it implies an instantaneous renewal process and an exact relocation, which in practice is not feasible. However, modifications of the original model can be made to handle these difficulties. In reference [56] it was considered instantaneous resetting with refractory periods in which the particle remains immobile at the origin for some time after each instantaneous resetting. The idea is to mimic the time it takes for the particle to return to the origin. Recent studies [25, 24, 92] have been proposed non-instantaneous resetting, in which the diffusive particle performs different types of motion during the return phase, *e.g.* return at a constant speed, at a constant acceleration and under the action of a harmonic force.

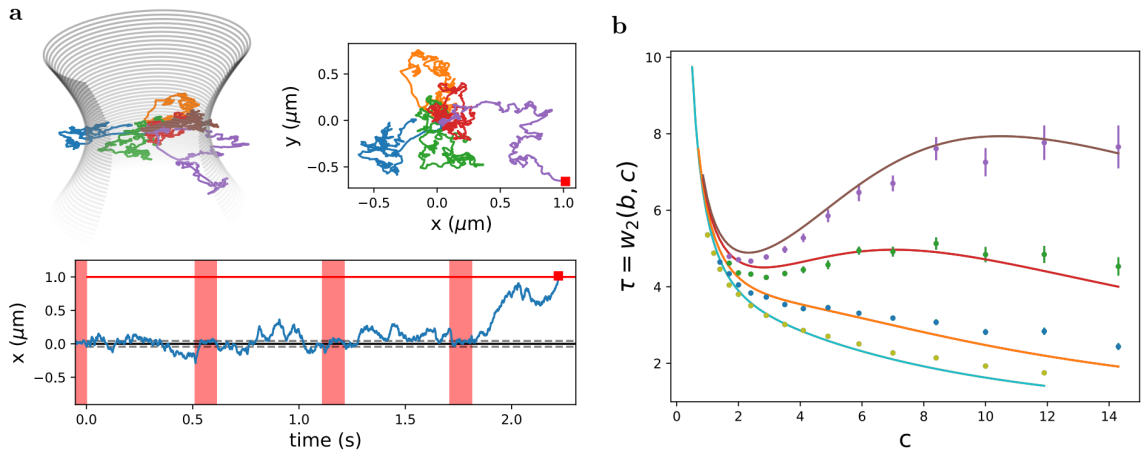

Figure 2.6: a) The upper figures depict an schematic representation of the Brownian particle optically trapped in 2d, whereas the bottom figure represents the $1d$ trajectory with periodic resetting at each constant time $T = 0.5$s. The red bars represent the time interval in which the particle is relax toward the potential minimum. Red horizontal line represents the target position at a distance $X = 1\mu m$ from the origin. b) MFPT τ in units of D/L^2 as a function of the parameter $c = \sqrt{r/D}L$ for $b = 3$ (orange curve), $b = 2.3$ (red curve) and $b = 2$ (brown curve), where $b = L/\sigma$. Symbols represent experimental data. Images taken from [21].

Recently, an experiment with optical tweezers was carried out in order to physically study some features of resetting processes [21]. In this experiment, a Brownian particle with constant diffusion D is tracked in 2d and at a time T (that can be exponentially distributed with rate r or fixed to a constant) the particle is optically trapped and relaxed toward a potential minimum. Before releasing the particle for its following Brownian excursion, the search process is suspended and one waits for a sufficiently long time to let the particle equilibrate in the harmonic profile generated by the laser trap (see Fig. 2.6a). Although the position of the particle is tracked in the (X, Y)-plane, this study focuses on the X-component.

The first passage τ time to a target that is placed at $x = L$ can be obtained from the particle tracking. In order to compare experimental results with the theoretical ones, the time spent by the particle equilibrating in the harmonic profile is not counted, in other words, τ is the net diffusion time spent by the particle before reaching the target [21]. Despite the difficulties the experiment can present, rich behaviors were observed for the

MFPT as a function of the resetting rate r (or period T) and the width σ of the Gibbs-Boltzmann distribution generated by the potential when it is on. Particularly relevant is the metastability that the MFPT exhibits as a function of the parameter $c = \sqrt{r/D}L$ for different values of the constant $b = L/\sigma$, as depicted in Fig. 2.6b. For values of b below a critical value $b_c \approx 2.53$, the MFPT reaches a minimum at $c = \infty$, whereas above b_c, in addition to the minimum at $c = \infty$, a metastable minimum for finite c appears. In the limit $b = \infty$, the system reaches a single minimum at $c^* = 1.59362....$

In the present work, we will propose a new model that allows us to physically reproduce a resetting process, viewed as a diffusion in a fluctuating potential. The model will have the advantage that it does not require to track the position X of the diffusive particle nor waiting for its relaxation to equilibrium.

Chapter 3

Objectives

In the previous chapter, we have presented some aspects of the theory of first passage times and discussed how fluctuations in the environment can affect the first passage properties of the search dynamics. We focused on those phenomena that involve the presence of imperfect boundaries that may not absorb upon a first encounter with the searcher. We saw that, in real systems, temporal fluctuations are also present in the bulk, which modifies the searcher dynamics. We emphasized the fact that, in order to expedite target encounters, searchers can combine slow reactive movements with fast unreactive relocations. This behaviour belongs to the category of search strategies known as intermittent search. A particular case of intermittent strategies are resetting processes, which in general are more efficient than simple diffusion.

Now we would like to point out the objectives of the present work.

Main objective:

Our work points to the understanding of the first passage properties of stochastic processes that evolve in environments that fluctuate in time. Since fluctuations can be present at the system boundaries as well as in the bulk, we are interested in the search dynamics with fluctuating targets or under the action of time-dependent potentials.

Specific objectives:

- We study the problem of a random searcher in the presence of non-instantaneous absorbing targets, from the perspective that the targets have their own dynamics independent of the dynamics of the searcher. To model non-instantaneous absorption, each target will have an internal state that fluctuates in time such that the absorption or capture is only possible when the target is in the active state.

- We address the question of the time it takes the searcher to be absorbed by these fluctuating targets, therefore, we will be mainly interested in calculating the first passage time distribution, as well as other relevant quantities such as the survival probability or the mean first passage time.

- As a first approach, we start by studying the case of a diffusive searcher on the infinite line with a Markovian target placed at the origin. The internal state of the

target will be characterized by a time dependent variable $\sigma(t)$ which takes values 0 and 1. Capture is allowed only in the state $\sigma = 1$.

- Further we will consider other kinds of search processes with dynamical targets, such as run-and-tumble motion and normally diffusive particles with stochastic resetting to the origin. We will also study problems with non-Markovian targets, as well as consider several fluctuating targets.

- We also wish to study problems in which fluctuations in the environment constrain the motion of the searcher. These fluctuations will be modelled through time-dependent potentials. We are interested in the mean first passage time to a steady, absorbing target, as well as the probability distribution of the position of the random searcher when there is no target.

- The first problem that we addressed is the case of a Brownian searcher with position X subject to an external confining potential of the form $V(X) = \mu|X|$, and that is switched on and off stochastically. We wish to compute the mean first passage time when a perfect absorbing target is placed at a distance L from the origin. We also wish to calculate the distribution of the position of the searcher in the absence of the target.

- Finally we extend this study to more general potentials. Particularly, for potentials of the form $V(X) = K^n/n|X - X_0|^n$. In this study we recover our previous results of the linear potential ($n = 1$), and explore the first passage properties for potentials with more general shapes, such as the harmonic potential.

Chapter 4

Methods and Mathematical Techniques

From the introduction and the objectives of this work, it can be seen that all the systems we are studying involve a diffusion process that reaches some threshold or target for the first time. Whether the threshold intermittently changes of state to avoid detection or the particle diffuses in the presence of an external potential, in all the problems we will require to know the probability density that the particle reaches the target for the first time at time t. A related quantity is the survival probability, or the probability that the particle has not reached the target yet at time t. To achieve this goal, it will be necessary to calculate the equation of motion for the survival probability and then, from this quantity, to obtain the distribution of the first hitting time.

In this chapter we develop all the mathematical techniques that we will need later on to solve the different problems we are interested in. We start by formally defining the survival probability and we deduce the backward Fokker-Planck equation that governs it for a simple diffusion process. We will show how to solve this differential equation and how its solution relates with the first hitting time distribution. We briefly introduce the run-and-tumble motion, a dynamics that is of interest to us for the subsequent chapters. At the end of the chapter, we will briefly talk about the Sparre Andersen theorem, which shows a universal scaling behaviour in the diffusion process with discrete jumps. Throughout this chapter, the analysis we do is for the one-dimensional case.

4.1 Survival probability

Let some diffusing particle be initially at the position $x \in (a, b)$, where a and b are some thresholds of the system. The survival probability (SP) is defined as the probability that, at time t, the particle remains in the interval (a, b) [61]:

$$Q(x,t) \equiv \int_a^b P(x',t|x,0)dx', \tag{4.1}$$

where $P(x',t|x,0)dx'$ is the conditional probability that the particle is in the interval $[x', x'+dx']$ at time t given that, at time $t = 0$, it was at x. We notice that this conditional probability is in fact the distribution $p(x',t)$ that the particle is near to x' at

time t, with the initial condition $p(x', 0) = \delta(x' - x)$. On the other hand, this last equality implies that at $t = 0$, $Q(x, 0) = 1$.

The term *survival* comes from the fact that, in many problems, it is usual for one or both thresholds to be an absorbing barrier, and the process ends when the particle reaches a threshold, namely, its does not "survive" or it stops diffusing. In the context of foraging search, for instance, when a predator (diffusive particle) hunts an immobile prey (system threshold) the search ends, and then the term survive, which in this case refers to the prey survival, fits well.

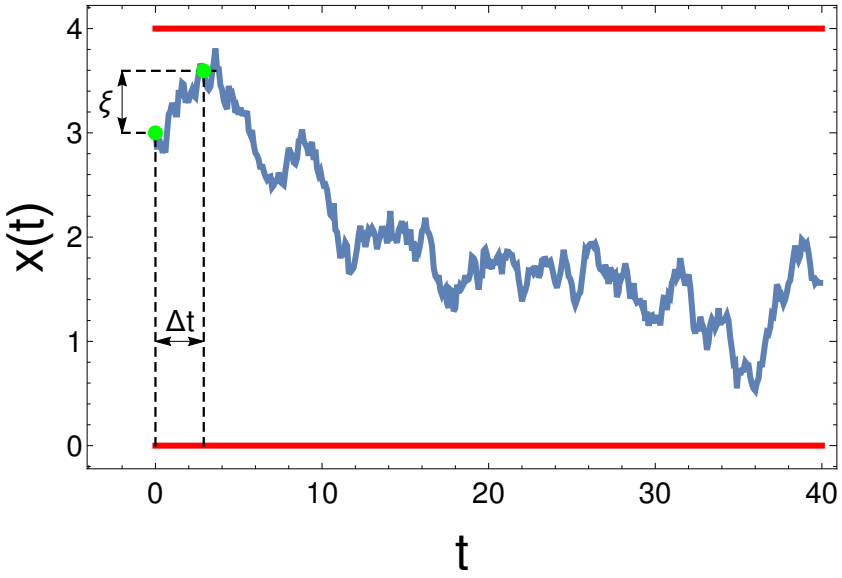

Figure 4.1: Particle position as a function of time. The particle starts diffusing from $x = 3$. After Δt the particles moves to a new random position $x' = x + \xi'$. Red lines represents the thresholds at $a = 0$ and $b = 4$.

From equation (4.1) we see that the probability $Q(x, t)$ only depends on the initial position x and on the time. The time evolution of this probability will be given in terms of the variation of its initial conditions. Figure 4.1 depicts a realization of a diffusion process in which the particle starts at $x = 3$ and during the time Δt diffuses to a new position which is closer, in this example, to the barrier located at x=4. Our intuition could tell us that, in this case, the probability that the particle does not reach the barrier from this new position is less than when it was at $x = 3$, due to the proximity of the barrier. In the next section we will see how the SP evolves with time.

4.2 Backward Fokker-Planck equation

The Fokker-Planck equation (FPE) was first introduced in the study of Brownian motion and was further generalized to a large class of very interesting stochastic processes [61]. Although it was first used to describe the time evolution of the probability distribution density $p(x', t)$ for a particle diffusing in the presence of deterministic and stochastic forces [112], the FPE can also be used to describe the evolution of the survival probability.

When the FPE involves x', the position reached by the particle at a time t larger than the initial time (t'), then it is called forward FPE. When the variable is x, *i.e.*, a position reached at a previous time t' smaller than the present time t it is called backward FPE. In this section we derive the backward FPE equation for the survival probability using the formalism of the Kramers-Moyal expansion [112].

Let $\Delta t > 0$ an small time increment, then the SP at $t + \Delta t$ can be calculated with the Chapman-Kolmogorov equation

$$P(x', t + \Delta t|x, 0) = \int d\xi P(x', t + \Delta t|x + \xi, \Delta t)P(x + \xi, \Delta t|x, 0). \tag{4.2}$$

The above equation indicates that the transition probability density $P(x', t + \Delta t|x, 0)$ is the sum over all the possible trajectories going from x to $x + \xi$ (where ξ is a random displacement) during the time interval $[0, \Delta t]$ and then going from $x + \xi$ to x' during $[\Delta t, \Delta t + t]$ (see Figure 4.1).

Integrating equation 4.2 for x' in the interval (a, b) and setting $P(x + \xi, \Delta t|x, 0) \equiv P_{\Delta t}(x, \xi)$, one obtains

$$Q(x, t + \Delta t) = \int d\xi Q(x + \xi, t)P_{\Delta t}(x, \xi). \tag{4.3}$$

Note that Δt has disappeared in Q, owing to the translational invariance of the diffusion process.

Now, if one makes a Taylor expansion of $Q(x + \xi, t)$ in powers of ξ

$$Q(x + \xi, t) = \sum_{n=0}^{\infty} \frac{\xi^n}{n!} \frac{\partial^n Q(x, t)}{\partial x^n}, \tag{4.4}$$

and inserts it in Eq. (4.3), one obtains

$$Q(x, t + \Delta t) = Q(x, t) + \sum_{n=1}^{\infty} \frac{M_n(x, \Delta t)}{n!} \frac{\partial^n Q(x, t)}{\partial x^n}. \tag{4.5}$$

where $M_n(x, \Delta t) = \int d\xi \xi^n P_{\Delta t}(x, \xi)$ is the $n-$th moment of the distribution $P_{\Delta t}(x, \xi)$[1], assuming that this moments exist. This expression is general and the values of the moments depend on the particular diffusive process under consideration.

Now, we can assume that the moments $M_n(x, \Delta t)$ can be expanded in a Taylor series with respect to Δt, thus

$$\frac{M_n(x, \Delta t)}{n!} = D_n(x)\Delta t + \text{h.o.terms}. \tag{4.6}$$

Setting $\Delta t = 0$, one sees that $M_n(x, \Delta t) = 0$, as $P(x + \xi, 0|x, 0) = \delta(x + \xi - x) = \delta(\xi)$.

If one divides by $\Delta t \neq 0$ and takes the limit $\Delta t \to 0$, one gets the Kramer-Moyal backward expansion for the survival probability

$$\frac{\partial Q(x, t)}{\partial t} = \sum_{n=1}^{\infty} D_n(x) \frac{\partial^n Q(x, t)}{\partial x^n}. \tag{4.7}$$

[1]To be precise, in general $M_n(x, \Delta t)$, and the subsequent coefficient $D_n(x)$ defined in Eq. (4.6), could also depend on the initial time, that we have set to $t = 0$. For simplicity we have omitted this in the notation.

In order to solve the Kramer-Moyal expansion we need to compute the coefficients $D_n(x)$, something which at first glance appears to be an arduous task. In the following we make use of the Pawula's theorem, which states that for Q to be a positive definite function, the expansion may stop either after the first term or after the second term, otherwise it can contain an infinite number of terms [112]. We thus carry out a truncation of the Kramel-Moyal expansion to second order, obtaining from Eq. (4.7) the expression:

$$\frac{\partial Q(x,t)}{\partial t} = D_1(x)\frac{\partial Q(x,t)}{\partial x} + D_2(x)\frac{\partial^2 Q(x,t)}{\partial x^2}. \tag{4.8}$$

This is the well known backward FPE and it will describe the time evolution of the SP in terms of the initial position, where D_1 is called the drift coefficient and D_2 the diffusion coefficient [112]. Then, in order to solve this equation we need to know D_1 and D_2 that, from Eq. (4.6), can be calculated as

$$D_n(x) = \frac{1}{n!}\frac{\partial M_n(x,t)}{\partial t}\Big|_{t=0}. \tag{4.9}$$

Evidently, the transition probability $P(x',t|x,0)$ (and then the probability density $p(x',t)$) also satisfies the FPE (4.8): one can follow all the above steps without integrating the transition probability in (a,b), to get

$$\frac{\partial P(x',t|x,0)}{\partial t} = D_1(x)\frac{\partial P(x',t|x,0)}{\partial x} + D_2(x)\frac{\partial^2 P(x',t|x,0)}{\partial x^2}. \tag{4.10}$$

For completeness, we contrast this expression with the forward FPE, that gives the time evolution of $P(x',t|x,0)$ as a variation of the final position x' [112]:

$$\frac{\partial P(x',t|x,0)}{\partial t} = -\frac{\partial}{\partial x'}D_1(x')P(x',t|x,0) + \frac{\partial^2}{\partial x'^2}D_2(x')P(x',t|x,0). \tag{4.11}$$

This expression can be also deduced from a Chapman-Kolmogorov equation, now summing over all the possible trajectories going from x to $x'-\xi$ during the time interval $[0,t]$ and then going from $x'-\xi$ to x' during $[t,t+\Delta t]$. As both contributions of this equation depend on the final position x', its expansion in series of ξ will lead to Eq.(4.11), where the probability distribution $P(x',t)$ and the Kramer-Moyal coefficients $D_n(x)$ must be derived (see Reference [112] for more details).

We see that this equation can be written as the continuity equation

$$\frac{\partial P(x',t|x,0)}{\partial t} + \frac{\partial J(x',t|x,0)}{\partial x'} = 0, \tag{4.12}$$

where $J(x',t|x,0) = D_1(x')P(x',t|x,0) - \frac{\partial}{\partial x'}D_2(x')P(x',t|x,0)$ is the probability flux. This concept will be helpful when we defined the boundary conditions of $Q(x,t)$.

4.3 Langevin equation

In general, the coefficients $D_n(x)$ depend on the system dynamics and are defined by the transition probability $P(x',t|x,0)$, thus, as we have said, we will need to take into account

the presence of deterministic and random forces acting on the particle. Then, in order to obtain the coefficients D_1 and D_2, we have to make assumptions on the microscopic dynamics of the diffusing particle. For instance, one can propose a stochastic Langevin equation for the particle motion.

The stochastic Langevin equation describes, at the microscopical level, the random motion of a particle subject to forces. In the general case, a particle embedded in some media will experiment friction forces, systematic forces due to external potentials and random forces due to thermal fluctuations. If one takes into account all this forces, the equation of moment conservation is

$$m\frac{d^2x}{dt^2} = -\alpha\frac{dx}{dt} + F_e(x,t) + \Gamma(t). \tag{4.13}$$

where m, α, F_e and Γ are the mass of the particle, the friction coefficient, the external force and the fluctuating force which comes from the thermal noise, respectively.

If we assume that the friction is large we can neglect the second derivative with respect to time, and thus we obtain the equation of motion in the over-damped limit

$$\frac{dx}{dt} = \frac{F_e(x,t)}{\alpha} + \Gamma(t), \tag{4.14}$$

where the term $\Gamma(t)/\alpha$ has been re-defined as $\Gamma(t)$.

Now, some reasonable assumptions can be made for the stochastic force Γ. First, we consider that, on average, it does not produce a net force on the particle, *i.e.*, the atoms of the media hit the diffusing particle in all directions with the same probability. Second, we suppose that the random force is delta-correlated in time, which means that the time between collisions is much shorter than the characteristic time of motion of the particle, and do not determine future collisions, thus, $\Gamma(t)$ will represent a Gaussian noise with zero mean and delta-correlations. These two assumptions will be represented as a

$$\langle\Gamma(t)\rangle = 0, \tag{4.15}$$

$$\langle\Gamma(t)\Gamma(t')\rangle = 2D\delta(t-t'), \tag{4.16}$$

where D is the diffusion constant.

Reminding that $P(x',t|x,0)$ is the distribution $p(x',t)$ with the initial condition $p(x',0) = \delta(x'-x)$, the moments $\langle(x'-x)^n\rangle = \langle\xi^n\rangle = \int \xi^n P_{\Delta t}(x,\xi)d\xi$ can be calculated from solving Eq. (4.14) to obtain the Kramer-Moyal coefficients $D_n(x)$.

In general, the Langevin equation for a stochastic variable or position ξ could be written more generally as

$$\frac{d\xi}{dt} = h(\xi,t) + g(\xi,t)\Gamma(t), \tag{4.17}$$

where $h(\xi,t)$ and $g(\xi,t)$ are functions determined by the system.

It is important to note that Eq. (4.17) cannot be solved by the usual calculus techniques, since ξ is a stochastic variable. Instead of this, it is necessary to use the formalism of stochastic calculus. Because the introduction of these mathematics tools is far beyond the scope of this chapter, we only show two results that can be obtained from the definition of the Stratonovich integral, and connect the Kramer-Moyal coefficients with the

functions $h(\xi,t)$ and $g(\xi,t)$ [112]:

$$D_1(x,t) = h(x,t) + g(x,t)\frac{\partial g(x,t)}{\partial x}D, \tag{4.18}$$

$$D_2(x,t) = [g(x,t)]^2 D. \tag{4.19}$$

Now that we have obtained the drift and the diffusion coefficient, we only need to define boundary conditions in order to completely solve Eq. (4.8). The following section is devoted to presenting the most common boundary conditions that are found in many physical systems, and that we will help us to solve a variety of interesting problems.

4.4 Boundary conditions

At the beginning of this chapter, we mentioned that the term survival refers to the fact that, in some cases, the particle could be absorbed upon the first encounter with a threshold, and as we saw in the introduction, this problem is relevant to many systems in nature. Nevertheless, the thresholds do not need to be always absorbing. In this section we introduce two kind of boundaries that will be important in our work: the reflecting and the absorbing boundary. In the following, we suppose that there is only one threshold in the system, represented by a wall or barrier placed at $x = b$; the particle diffuses in the interval $(-\infty, b)$ (in the definition of the SP we let $a \to -\infty$).

We say that a barrier is perfectly absorbing (or absorbing for short), if any particle that hits it is immediately absorbed, *i.e.*, particles cannot continue to diffuse after the first encounter, which means that any particle that starts at $x = b$ will have a probability $p(x,t) = 0$ to be at $x \in (-\infty, b)$ at any posterior time $t > 0$ [61, 108], then

$$Q(x = b, t) = 0. \tag{4.20}$$

Formally, we may say that the SP satisfies the Dirichlet boundary condition when the boundary is absorbing, since this function takes a specified value at the boundary [9].

On the other hand, a boundary is called reflective if, as the name suggests, the particle reflects when it hits the barrier but continues diffusing, then the probability flux is zero at the boundary, *i.e.*, $J(x', t|x, 0)|_{x=b} = 0$ (see Eq. 4.12).

For a general coefficient $D_1(x)$ and supposing that $D_2(x) \neq 0$, we can use the backward and the forward FPE to prove that the reflective boundary condition reduces to [61]

$$\left.\frac{\partial Q(x,t)}{\partial x}\right|_{x=b} = 0. \tag{4.21}$$

Unlike an absorbing barrier, a reflecting boundary is of the Neumann boundary condition type, in these cases the normal derivative of the SP takes a specified value at the boundary [9].

We would like to remark that these are not the only boundary conditions one could find in physical systems. In some cases, it is possible to have a boundary that partially absorbs and partially reflects, in this case we talk of mixed, or Robin, boundary condition (RBC), which will be given by [124]:

$$-J(x' = b, t|x, 0) = \kappa p(x' = b, t|x, 0), \tag{4.22}$$

where κ is a positive constant. Eq. (4.22) is widely used in effective medium descriptions of spatially heterogeneous interfaces containing both reflecting and reactive zones [148, 11, 19]. When we analyze the problem of intermittent target we will return to this boundary condition, as it will be relevant to that problem.

4.5 Solution of the backward Fokker-Planck equation

The backward FPE belongs to the more general class of parabolic second-order differential equations and, as we have seen, its solution will depend on the coefficients $D_1(x)$, $D_2(x)$ and on the boundary conditions; the latter will determine a unique solution (given an initial condition) and will characterize its behaviour, for instance, if the solution is stable or not [112, 9].

There is no one way by which the FPE can be solved, nevertheless, one mathematical technique that will be helpful to solve the backward FPE for the SP, and that we will use in this work, is the Laplace transform. This mathematical tool transforms time derivatives into a linear algebraic equation that involves the Laplace variable. The FPE reduces, in the 1D case, to a second-order differential equation of the space variable.

The Laplace transform $\widetilde{F}(s)$ of a function $F(t)$ is defined by [8]

$$\widetilde{F}(s) = \mathcal{L}\left\{F(t)\right\} = \int_0^\infty dt\ e^{-st} F(t), \tag{4.23}$$

where we notice that, the transformed $\widetilde{F}(s)$ function depends on the conjugate variable s. Assuming that the function $F(t)$ satisfies certain properties so that Eq. (4.23) is well-defined (see the more specialized texts [8, 130, 1]), we want to directly use the Laplace transform and see how a time derivative changes under such transformation. Then, taking the Laplace transform of the first derivative of a function $F(t)$ one obtains

$$\mathcal{L}\left\{\frac{dF(t)}{dt}\right\} = \int_0^\infty dt\ e^{-st}\frac{dF(t)}{dt} = s\mathcal{L}\{F(t)\} - F(t=0) \tag{4.24}$$

Now, we are able to convert the backward FPE (4.8) into an ordinary differential equation (ODE), just by applying the Laplace transform on each side of the equation, to get

$$s\widetilde{Q}(x,s) - 1 = D_1(x)\frac{\partial \widetilde{Q}(x,s)}{\partial x} + D_2(x)\frac{\partial^2 \widetilde{Q}(x,s)}{\partial x^2}. \tag{4.25}$$

where we have used the initial condition $Q(x, t = 0) = 1$, and $\widetilde{Q}(x,s)$ is the Laplace transform of $Q(x,t)$. This equation holds if $x \neq b$.

If the diffusion coefficient $D_2(x) \neq 0$, Eq. (4.25) can be recast as

$$\frac{\partial^2 \widetilde{Q}(x,s)}{\partial x^2} + \frac{D_1(x)}{D_2(x)}\frac{\partial \widetilde{Q}(x,s)}{\partial x} - \frac{s}{D_2(x)}\widetilde{Q}(x,s) = -\frac{1}{D_2(x)}. \tag{4.26}$$

Although we have reduced a partial differential equation into an inhomogeneous linear ODE, whose solution can be given as a sum of the solution to the homogeneous part of Eq. (4.26) and a particular one [26], the main problem will arise when we want to retrieve

the solution $Q(x,t)$ from the reciprocal $\widetilde{Q}(x,s)$. This means that we have to find the inverse Laplace transform of $\widetilde{Q}(x,s)$.

The task of calculating an inverse transform of a function $\widetilde{F}(s)$ is not always easy, and sometimes it is not possible to find an analytical solution of the inverse transform. In this case, one may resort to numerical methods [8]. However, in some cases the Laplace transform can be easily found by using tables of Laplace transforms [1]. Very often, the Laplace transform represents a useful mathematical tool to analyze the asymptotic behaviour of $Q(x,t)$ in the limits $t \to 0$ and $t \to \infty$. This point will be analysed in more detail when we consider the problem of intermittent target.

4.6 First Hitting Time

Now that we have defined the survival probability and the equation that gives its evolution, together with the boundary conditions, we can introduce the first hitting time distribution. This distribution is of great application in many context of science, since it gives a probability that an event occurs at a given time [108, 122, 61].

Formally, the first hitting time distribution (FHTD), that we denote as $P(x,t)$, is defined as the probability density of the first hitting time t, which is a random variable. The first hitting time is the time it takes for a diffusing particle, or any other stochastic of process, to first reach a specified site (or set of sites), from the initial position x [108]. With this definition it is easy to see that the probability that the particle has not reached any of the target sites or thresholds at time t, namely the survival probability $Q(x,t)$, is equal to the probability that the particle first reaches any threshold at later time $t' > t$:

$$Q(x,t) = \int_t^\infty P(x,t')dt', \tag{4.27}$$

hence, the first hitting time distribution will be given by

$$P(x,t) = -\frac{\partial Q(x,t)}{\partial t}. \tag{4.28}$$

Once we know the survival probability for a given problem, we immediately can calculate the FHTD, using (4.28).

One can prove that, defined in this way, $P(x,t)$ is a probability distribution. First, we see that $P(x,t) \geq 0$ given that $Q(x,t)$ cannot increase with time due to causality. On the other hand, $P(x,t)$ satisfies the normalization condition $\int_0^\infty P(x,t)dt = Q(x,0) = 1$. In recurrent systems, such that $Q(x,t) \to 0$ as $t \to \infty$, the hitting time density also tends smoothly to 0 at large times. In non-recurrent systems, such that $Q(x,t) \to \text{cst} > 0$ as $t \to \infty$, $P(x,t)$ contains a singular part at $t = \infty$, corresponding to trajectories that never find the target.

In the previous section we saw that the Laplace transform is useful in reducing a time derivation into an algebraic equation, then if we transform $P(x,t)$ and use the relation (4.28), we obtain

$$P(x,s) = 1 - sQ(x,s). \tag{4.29}$$

Depending on the phenomena under study, sometimes one may be interested in calculating the mean hitting time. This quantity corresponds to the the first moment of the

FHTD, defined as the mean first hitting time (MFHT)

$$T(x) = \int_0^\infty tP(x,t)dt. \tag{4.30}$$

In some cases this quantity is infinite. The FHTD plays an important role, as its asymptotic behaviour at large t determines whether the first moment of the distribution exists or not.

Integrating by parts, Eq. (4.30) can be written in the form

$$T(x) = \int_0^\infty Q(x,t)dt \tag{4.31}$$

where we have used the relation given by Eq. (4.28).

If we integrate over $t \in (0,\infty)$ the backward FPE for the survival probability given by Eq. (4.8), we immediately see that the MFHT satisfies

$$-1 = D_1(x)\frac{\partial T(x)}{\partial x} + D_2(x)\frac{\partial^2 T(x)}{\partial x^2}, \tag{4.32}$$

that is a inhomogeneous linear ODE. From Eq. (4.31) it is easy to see that $T(x) = \widetilde{Q}(x, s=0)$, therefore, the MFHT can be calculated directly from the Laplace transform of the SP just by setting the Laplace variable $s = 0$.

4.7 Standard case (Brownian motion)

To exemplify the formalism exposed in the above sections we analyze the problem of a Brownian particle with an absorbing barrier placed at $x = 0$ (see Fig. 4.2). The diffusive particle has a initial position $x > 0$. We will call the solution of this problem as the standard solution, in contrast with other cases with more complex configurations.

In this system, the particle movement is only caused by thermal fluctuations, *i.e.*, without drift forces. Then, the Langevin equation will be given by

$$\frac{dx}{dt} = \Gamma(t). \tag{4.33}$$

Solving for x, from (4.33), we will have

$$\xi(t) = x' - x = \int_0^t \Gamma(\tau)d\tau, \tag{4.34}$$

and

$$\langle \xi(t) \rangle = \int_0^t \langle \Gamma(\tau) \rangle d\tau = 0, \tag{4.35}$$

$$\langle \xi^2(t) \rangle = \int_0^t \int_0^t \langle \Gamma(\tau)\Gamma(\tau') \rangle d\tau d\tau' = 2Dt. \tag{4.36}$$

If one does not neglect the second derivative in (4.13), it can be found that

$$D = \frac{kT}{\alpha}, \tag{4.37}$$

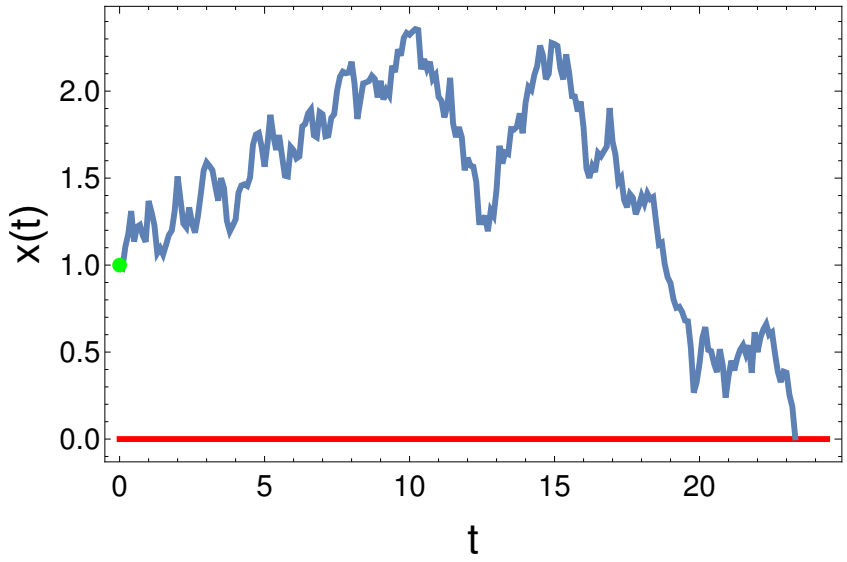

Figure 4.2: Particle position as a function of time. The particle starts diffusing from $x = 1$. Red line represents the thresholds at $x = 0$.

where D is the diffusion coefficient, k is the Boltzmann constant, T is the absolute temperature and α is the friction coefficient. This is the well known fluctuation-dissipation relation that was first deduced by Einstein [112, 61].

With these results we show that $D_1 = 0$ and the diffusion coefficient $D_2 = D$, in complete agreement with Eqs. (4.18)-(4.19). Then, we have that the FPE obeyed by the SP in this problem is

$$\frac{\partial Q(x,t)}{\partial t} = D\frac{\partial^2 Q(x,t)}{\partial x^2}. \tag{4.38}$$

Now, if we use the Laplace transform, Eq. (4.38) is recast as

$$\frac{\partial^2 \widetilde{Q}(x,t)}{\partial x^2} - \frac{s}{D}\widetilde{Q}(x,s) = -\frac{1}{D}. \tag{4.39}$$

This equation admits homogeneous solutions of the form $Q_h(x,s) = A_1 e^{-x\sqrt{s/D}} + A_2 e^{x\sqrt{s/D}}$, with the particular solution $Q_p = 1/s$.

Next in order is to apply the boundary conditions. First, we expect that the probability does not exponentially increase with the distance x, since it has to be bounded by 1. This implies that $A_2 = 0$. On the other hand, the absorbing barrier placed at $x = 0$ imposes $Q(x = 0, s) = 0$, which is the Dirichlet boundary condition given by Eq. (4.20). Therefore, the solution of Eq. (4.39) subject to the absorbing boundary at $x = 0$ is

$$\widetilde{Q}^{st}(x,s) = \frac{1 - e^{-x\sqrt{s/D}}}{s}, \tag{4.40}$$

where the label "st" stands for the "standard case". From Eq. (4.29) we have that the Laplace transform of the standard FHTD is

$$\widetilde{P}^{st}(x,s) = e^{-x\sqrt{s/D}}. \tag{4.41}$$

The inverse Laplace transforms of this two expressions can be found in [1] and read

$$Q^{st}(x,t) = \text{erf}\left(\frac{x}{\sqrt{4Dt}}\right), \tag{4.42}$$

$$P^{st}(x,t) = \frac{x}{\sqrt{4\pi D t^3}} e^{-\frac{x^2}{4Dt}}. \tag{4.43}$$

Equation (4.43) is the well known Lévy-Smirnov distribution [60, 36].

Finally, we want to analyze the asymptotic behaviour of both Q^{st} and P^{st} in the long time regime, which is typical of diffusion processes in one spatial dimension. Whereas these behaviours can be determined easily from Eqs. (4.42)-(4.43), we may choose to derive them directly from the corresponding Laplace transforms, given by Eqs. (4.40)-(4.41). This method will be useful in the following chapter, where the expressions in the time domain will be less easy to handle.

The long time analysis can be carried out by noting that this regime corresponds to the small s regime in the Laplace transform. Roughly speaking, this can be seen by noticing that the product of the conjugate variables s and t that appears in the definition of the Laplace transform allows to change the limit $t \to \infty$ by $s \to 0$. Reciprocally, the short time regime corresponds a large s. This result is analogous to the reciprocity between frequency and time in the Fourier transform. For more details one can consult [130, 61].

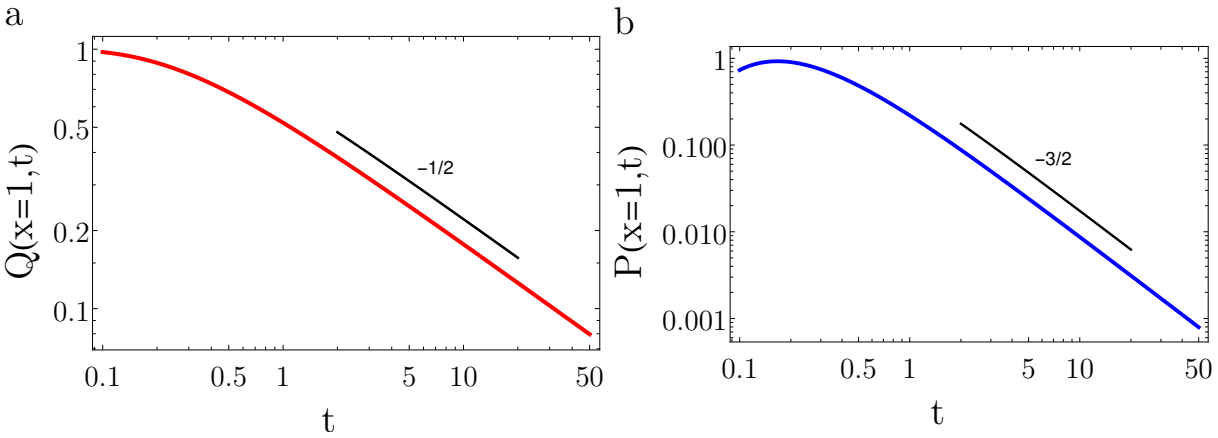

Figure 4.3: a) Survival probability and b) first hitting time distribution as a function of time for a initial position $x = 1$ and a diffusion coefficient $D = 1$. One can see the asymptotic behaviour of each function for long times. Black lines indicate the exponent of the power-law decay, $-1/2$ for the SP and $-3/2$ for the FHTD.

Let us expand $\tilde{Q}(x,s)$ in series of s. To do this we will need to suppose that $\sqrt{s} \ll x/\sqrt{D}$, which, in the time domain means $x^2/D \ll t$, where x^2/D is a characteristic time of the diffusion process. We obtain

$$Q(x,s) \approx \frac{x/\sqrt{D}}{\sqrt{s}}, \tag{4.44}$$

which can be exactly inverted as [1]

$$Q(x,t) \approx \frac{x}{\sqrt{\pi D t}}. \tag{4.45}$$

Further, with Eq. (4.28) we will obtain

$$P(x,t) \approx \frac{x}{\sqrt{4\pi D t^3}}. \tag{4.46}$$

Hence, we have shown that in the long time regime, the SP and the FHTD scales with time as $\sim t^{-1/2}$ and $\sim t^{-3/2}$, respectively (see figure 4.3). This scaling behaviour is characteristic of the one-dimensional diffusion processes and has important consequences on the mean absorption time: the MFHT is actually infinite, as the distribution decays more slowly than t^{-2}.

4.8 Run-and-tumble motion

In the description of the microscopic dynamics of diffusive particles we made in Section 4.3, we have considered that the stochastic force that produces the erratic movement of the particles is delta-correlated in time. As we mentioned, this consideration assumes that the time between collisions is much shorter than the characteristic time of motion of the particle, and do not determine future collisions. However, some systems in nature that are out of equilibrium do not fulfill this assumption. One of the most common examples is the case of the bacteria *E. coli*. In the searching for food, bacteria uses chemotaxis; they direct their movement towards different sites in which the concentration of chemicals increases [20, 132]. In a typical excursion, bacteria travel towards a specific site where they search for food. After a short period of time in which the bacteria randomly explores the site, they resume its excursion and move toward other possible sources of food [20]. The preference in direction introduces correlations in their movement that cannot be described by a delta-correlated noise. Instead, their actual movement depends on the history of the trajectory.

The run-and-tumble (RT) motion, also called as persisting Brownian motion, is a relatively simple model that mimics the dynamics of self-propelled particles such as the bacteria *E. coli*. The motion consists in ballistic "run" phases at constant speed v, followed by "tumble" periods, occurring with a fixed rate, say γ, and leading to a full randomization of the direction of motion [20, 90].

In one-dimension, the RT dynamics is governed by the overdamped stochastic Langevin equation

$$\frac{dx}{dt} = \theta(t), \tag{4.47}$$

where $\theta(t)$ is a dichotomous stochastic noise that switches between the values $\sigma = v$ and $\sigma = -v$ with rate γ. The run and tumble process is sometimes referred to as "telegraphic noise" to describe the evolution of $\theta(t)$ [90, 142]. The autocorrelation function of the telegraphic noise $\theta(t)$ is given by [90]

$$\langle \theta(t_1)\theta(t_2)\rangle = v^2 e^{-2\gamma|t_1-t_2|}. \tag{4.48}$$

In the limit $\gamma \to \infty$, $v \to \infty$, and keeping the ratio $v^2/(2\gamma) = D$ fixed, the noise $\theta(t)$ becomes a white noise with correlator $\langle \theta(t_1)\theta(t_2)\rangle = 2D\delta(t_1 - t_2)$, that coincides with the noise $\Gamma(t)$ in Eq. (4.16) for the Brownian particle case. Therefore, under such limit run-and-tumble leads to Brownian motion.

The run-and-tumble motion has been extensively studied and many interesting properties of its dynamics have been observed. In confined environments, for instance, run-and-tumble particles (RTP) tend to accumulate near the boundaries [89, 51]. When a steady potential is applied, phases of active and passive-like behaviour appear [46]. The first passage properties of RT particles in confinement and in the semi-infinite domain have been studied before [89, 5]. For completeness, in the following we deduce the the survival probability of a RT particle in the presence of a absorbing boundary at the origin in the semi-infinite line.

We start by denoting as $Q^+(x,t)$ [and $Q^-(x,t)$] the probability that the particle has not reacted up to time t, given the initial particle position $x > 0$ and the initial velocity $+v$ [$-v$, respectively]. Now, let us suppose that, at time $t = 0$, the particle starts with velocity $+v$. During the small time interval $[0, \Delta t]$, with probability $\gamma \Delta t$ the particle will change its velocity to $-v$, or will remain with $+v$ with probability $1 - \gamma \Delta t$. If we sum these contributions, the survival probability can be written as

$$Q^+(x, t + \Delta t) = (1 - \gamma \Delta t) Q^+(x + v\Delta t, t) + \gamma \Delta t Q^-(x + v\Delta t, t). \tag{4.49}$$

Expanding the r.h.s. of (4.49) in Taylor series and retaining only the terms of order Δt, we obtain

$$\frac{\partial Q^+(x,t)}{\partial t} = v \frac{\partial Q^+(x,t)}{\partial x} - \gamma Q^+(x,t) + \gamma Q^-(x,t), \tag{4.50}$$

Similarly, one can deduce the evolution of the survival probability $Q^-(x,t)$, given the initial velocity $-v$:

$$\frac{\partial Q^-(x,t)}{\partial t} = -v \frac{\partial Q^-(x,t)}{\partial x} - \gamma Q^-(x,t) + \gamma Q^+(x,t). \tag{4.51}$$

In order to solve the system of Eqns. (4.50)-(4.51), it is convenient to first take the Laplace transform, to obtain

$$v \frac{\partial \widetilde{Q}^+(x,t)}{\partial x} - (s + \gamma) \widetilde{Q}^+(x,t) + \gamma \widetilde{Q}^-(x,t) = -1 \tag{4.52}$$

$$-v \frac{\partial \widetilde{Q}^-(x,t)}{\partial x} - (s + \gamma) \widetilde{Q}^-(x,t) + \gamma \widetilde{Q}^+(x,t) = -1, \tag{4.53}$$

whose solutions, that satisfies the absorbing boundary condition $Q^-(0,t) = 0$, and that do not have an exponential growing with x, are given by [57]

$$\widetilde{Q}^+(x,t) = \frac{1}{s} + \frac{1}{\gamma s} \left[v_0 \lambda - (s + \gamma) \right] e^{-\lambda x}, \tag{4.54}$$

$$\widetilde{Q}^-(x,t) = \frac{1}{s} \left[1 - e^{-\lambda x} \right], \tag{4.55}$$

where $\lambda = \sqrt{s(s + 2\gamma)}/v$.

Assuming a symmetric velocity initial condition, that is, an equal probabilities for the initial positive and negative particle velocities, we have

$$\widetilde{Q}(x,s) \equiv \frac{1}{2} \left[\widetilde{Q}^+(x,s) + \widetilde{Q}^-(x,s) \right] = \frac{1}{s} + \frac{1}{2\gamma s} \left[v_0 \lambda - (s + 2\gamma) \right] e^{-\lambda x}. \tag{4.56}$$

From this solution we can analyze the long-time behaviour of the survival probability, and thus, of the first passage time distribution, by considering the $s \to 0$ limit. Making the approximation $\sqrt{s(s+2\gamma)} \approx \sqrt{2\gamma s}$, in the limit $s \to 0$ Eq. (4.56) can be recast as

$$\widetilde{Q}(x,s) \approx \frac{1 - e^{-\sqrt{2\gamma s}x/v}}{s}, \tag{4.57}$$

which coincides with the expression in Eq. 4.41, with $D = v^2/(2\gamma)$. Thus, in the long-time limit, the survival probability, and thus the first passage time distribution, of a run-and-tumble particle behaves the same as for a Brownian particle.

4.9 Sparre Andersen theorem

Up to now, we have only discussed continuous random processes and we have introduced the principal quantities involved in first passage problems, with special emphasis on the survival probability. When we derived the backward FPE for $Q(x,t)$ we started from the Champan-Kolmogorov equation that is a recursive manner in which the survival probability could be calculated. We saw the remarkable role that the transition probability plays in the derivation of the FPE, since its moments will completely define the time evolution of the SP through the Kramer-Moyal expansion. However, what happens if the moments of this distribution diverge? In this case, it is clear that we will not be able to make an expansion of the Kramer-Moyal type.

In an attempt to answer the above question, we would like to conclude the present chapter by mentioning a relevant result that falls into an universality behaviour of the first passage time for discrete-time random processes, namely, the Sparre Andersen theorem [88, 86]. We will see how the survival probability for the discrete-time process is essentially different from that of the continuous process, although under some limit both solutions can match.

Let us start with a discrete-time random walker that jumps on a line. Each time step the walker performs a jump, such that its position x_n after n steps, with $n \geq 1$ and starting at x_0, evolves following the rule

$$x_n = x_{n-1} + \xi_n, \tag{4.58}$$

where ξ_n is an i.i.d. random variable drawn from the distribution $\phi(\xi)$, which is normalized, symmetric and with zero mean.

Due to the central limit theorem, we know that if the distribution $\phi(\xi)$ has a finite variance σ^2, for large n the discrete-time process $x(n)$ converges to the continuous Brownian motion $x(t)$ that is ruled by the Langevin equation (4.33). We also know that the probability that a Brownian particle does not cross the origin up to time t, starting at $x_0 \geq 0$ at $t = 0$, behaves as $Q(x_0,t) \sim x_0/\sqrt{\pi D t}$, which is zero for the initial position $x_0 = 0$.

The fact that the survival probability vanishes when the particle starts at the origin can be understood from the recurrence property of Brownian trajectories in 1D, which cross and re-cross the origin many times within a short period. However, in a discrete process this behaviour is different, and a random walk that starts at $x_0 = 0$ can perform

several jumps before first crossing the origin [88]. The fraction of trajectories that do not immediately cross the origin will account for the probability $q(x_0, n)$ that the particle remains at the positive side before n steps.

What the Sparre Andersen theorem tells us is that, for a discrete-time random walk with a symmetric and continuous jump distribution $\phi(\xi)$, given the initial position $x_0 = 0$, the survival probability is given by [88, 86]

$$Q(0, n) = \binom{2n}{n} 2^{-2n}. \tag{4.59}$$

Surprisingly, the survival probability is independent of the jump distribution. This result is universal and holds for several types of discrete-random walks, including Lévy flights characterized by their infinite variance. We remark that the universality in the Sparre Andersen theorem is only observed if the walker starts at the origin. For an initial position $x_0 \geq 0$, there exists an explicit solution which is known as the Pollaczek-Spitzer formula (see reference [86]) that in general depends on the jump distribution and reduces to Eq. (4.59) when $x_0 = 0$.

In the limit of large n, the survival probability in Eq. (4.59) has the scaling decay

$$Q(0, n) \sim \frac{1}{\sqrt{\pi n}}. \tag{4.60}$$

Despite the similarities between the $1/\sqrt{n}$ algebraic decay of the Sparre Andersen theorem and the $1/\sqrt{t}$ decay of the survival probability in the Brownian motion, both results are essentially different and have distinct origins. Only in the limit case in which $x_0 \sim n^{1/2}$ for large n, the discrete-time solution matches with the Brownian one and, in both cases, the survival probability goes to zero with the starting point [86]. In general, for Lévy flights with index $\mu \in (0, 2]$, a more rigorous analysis of the Pollaczek-Spitezer solution shows that, when the initial position scales as $n^{1/\mu}$ for large n, the discrete and the continuous process coincide (see reference [88] for more details).

Chapter 5

Random searches of fluctuating targets

In this chapter we address the problem of random searches of fluctuating targets. We are mainly interested in the statistical properties of the first hitting time of diffusive searchers to an intermittent target. For the target dynamics we consider the two-state model; the target switches between a reactive state and a non-reactive one. For the motion of the searcher we consider three different strategies: Brownian motion, diffusion with stochastic resetting and run-and-tumble motion. The chapter is organized as follows:

We start in Section 5.1 by considering a Brownian searcher. We deduce the governing equation for the survival probability and obtain the first hitting time. We analyze the behavior of this distribution for short and long times. At high crypticity, that is, when the target spends most of the time in the inactive state, an unexpected rate limited power-law regime emerges for the first hitting time density, which markedly differs from the classic $t^{-3/2}$ scaling for steady targets. Our problem admits an asymptotic mapping onto a mixed, or Robin, boundary condition.

In Section 5.2, we extend our analysis by examining a Brownian particle under the action of stochastic resetting. As is usual in resetting processes, the mean first hitting time (MFHT) can be optimized by a suitable choice of the resetting rate. We study the behaviour of the optimal resetting rate as a function of the target dynamical parameters. From our analysis emerges a strong connection between our model and the problem of diffusion with stochastic resetting in the presence of a partially absorbing target. We show how the two problems actually become equivalent in the limit of high transition rates, or when the target is in the non-reactive state most of the time. We also analyse the relative variance of the first hitting time around the mean and study its dependence with respect to the target rates and the resetting rate. The relative fluctuations are no longer unity at the optimal resetting rate, and can take much larger values instead. This is due to the fact that the dynamics of the target state is independent of the resetting process itself. The problem therefore differs from the one considered in [30], where the search of a gated target by diffusion under resetting was studied through a renewal approach, that assumed that the resetting process also acted on the target state.

Finally, in Section 5.3 we investigate the one-dimensional run-and-tumble dynamics. Here we analyze the RT motion in several geometries: (*i*) the finite domain, with the particle bounded by two reflective walls symmetrically placed around the target, (*ii*) the

infinite line, as a special case in which the walls are infinitely far away. In the first case, quantities of primary interest are the mean first hitting time (MFHT) and the standard deviation of the hitting time around this mean. We find that the global MFHT averaged over the particle initial positions is always minimal for a ballistic particle, whereas less persistent searchers are suboptimal. However, the relative variance of the first hitting time can take very large values and exhibits a non-monotonic behaviour with respect to the parameters that control the intermittent dynamics of the target. In the unbounded case, the MFHT diverges and we study the asymptotic behaviour of the full first hitting time distribution (FHTD). The decay of the distribution at large hitting times t is decomposed into two scaling regimes: a $t^{-3/2}$ asymptotic regime that is characteristic of unbiased motion, and an intermediate regime varying as $t^{-1/2}$, which represents a much slower decay and whose range can be varied depending on the target and particle rates.

5.1 Simple diffusion

In this section we study the dynamics of a one-dimensional Brownian particle hitting an intermittent target located at the origin of the system. The target internal state is characterized by a time dependent variable $\sigma(t)$ which can take two values: $\sigma = 1$ when the target is visible, which means that the Brownian particle can detect it upon encounter, and $\sigma = 0$ when the target is invisible, meaning that it cannot be detected even if the Brownian searcher crosses the origin. The target visibility randomly switches between these two states, which last for time intervals that are exponentially distributed. Then, the target in state $\sigma = 0$ changes to state $\sigma = 1$ at rate α, whereas the transition from state $\sigma = 1$ to state $\sigma = 0$ occurs at rate β. Therefore, the mean duration of the visible (invisible) phase is $1/\beta$ ($1/\alpha$, respectively) and the overall probability to find the target in the visible state is $\alpha/(\alpha + \beta)$.

5.1.1 Governing equations

The searcher starts at time $t = 0$ from a positive position x. As shown in Fig. 5.1, during a trajectory the walker may cross the origin and perform several excursions on the positive and negative sides before hitting the target for the first time.

To calculate some first passage quantities in this problem, one needs to specify, in addition to the initial position of the particle, the initial target state. Let us define $Q_\sigma(x,t)$ as the probability that the particle has survived up to time t given that it started at $t = 0$ from x and with the target in state σ (0 or 1). Averaging over the initial target states yields the average survival probability, denoted as $Q_{av}(t)$:

$$Q_{av}(x,t) = \frac{\beta}{\alpha+\beta} Q_0(x,t) + \frac{\alpha}{\alpha+\beta} Q_1(x,t). \tag{5.1}$$

The first passage time distribution $P_i(x,t)$ is obtained from the usual identity $Q_i(x,t) = \int_t^\infty d\tau P_i(x,\tau)$ or

$$P_i(x,t) = -\frac{\partial Q_i(x,t)}{\partial t}, \tag{5.2}$$

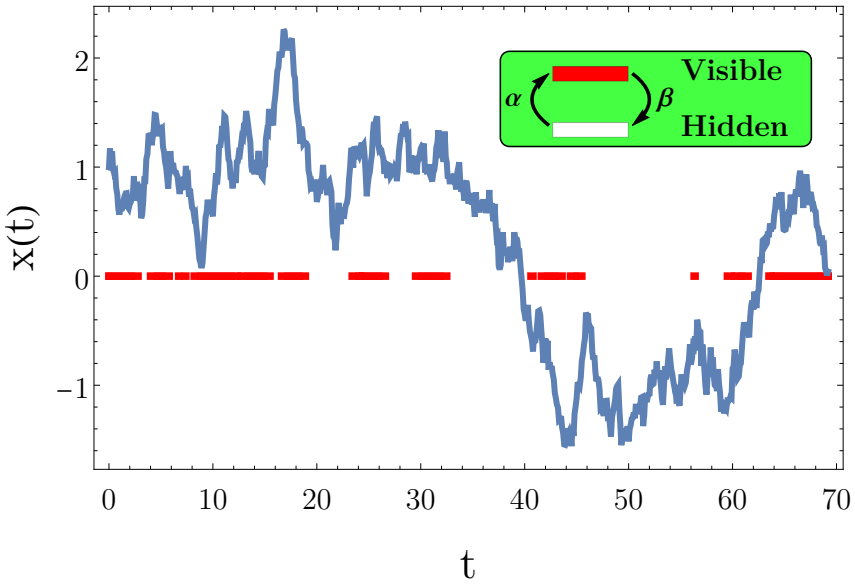

Figure 5.1: Brownian trajectory in the presence of an intermittent target located at the origin. The red segments represent the target in the visible state, separated by time intervals in the hidden state. The Brownian particle is absorbed when it reaches the target in the visible state for the first time.

where $i \in \{0, 1, av\}$. The survival probabilities $Q_{\sigma=0,1}(x,t)$ satisfy two coupled backward Fokker-Planck equations, which read:

$$\frac{\partial Q_0(x,t)}{\partial t} = D\frac{\partial^2 Q_0(x,t)}{\partial x^2} + \alpha[Q_1(x,t) - Q_0(x,t)] \tag{5.3}$$

$$\frac{\partial Q_1(x,t)}{\partial t} = D\frac{\partial^2 Q_1(x,t)}{\partial x^2} + \beta[Q_0(x,t) - Q_1(x,t)] \tag{5.4}$$

To derive Eq. (5.3) for Q_0, one follows the method used in chapter 4. We notice that during a small time interval $[0, \Delta t]$, the target can switch to the state $\sigma = 1$ with probability $\alpha\Delta t$ or remain in $\sigma = 0$ with probability $1 - \alpha\Delta t$. Summing these two contributions, one obtains a relation for the quantity $Q_0(x_0, t + \Delta t)$:

$$Q_0(x,t+\Delta t) = \alpha\Delta t \int_{-\infty}^{\infty} d\xi P_{\Delta t}(\xi) Q_1(x+\xi,t) + (1-\alpha\Delta t)\int_{-\infty}^{\infty} d\xi P_{\Delta t}(\xi) Q_0(x+\xi,t). \tag{5.5}$$

At time Δt, the particle position is $x + \xi$ (where ξ is a small random increment), which serves as a new initial condition for the rest of the trajectory comprised in the time interval $[\Delta t, t + \Delta t]$, of duration t. In (5.5) we have used the fact that the process is time translational invariant. The random displacement ξ of the Brownian particle is drawn from the Gaussian distribution $P_{\Delta t}(\xi)$ with zero mean and variance $\langle \xi^2 \rangle = 2D\Delta t$ (see section 4.7). As we have done in 4.2, a Taylor expansion of the probabilities $Q_\sigma(x + \xi, t)$ in powers of ξ up to second order (the first non-zero average contribution) leads to Eq. (5.3), after grouping the terms of order Δt and taking the limit $\Delta t \to 0$. We obtain Eq. (5.4) from a similar reasoning.

This coupled system of PDEs must satisfy the boundary conditions

$$Q_1(x = 0, t) = 0, \tag{5.6}$$

$$\left.\frac{\partial Q_0(x,t)}{\partial x}\right|_{x=0} = 0, \tag{5.7}$$

and the initial conditions $Q_0(t=0) = Q_1(t=0) = 1$.

Whereas Eq. (5.6) simply asserts that the target is absorbing in the visible state, relation (5.7) is a bit more subtle. It can be understood, for instance, by considering the case $\beta = 0$, which corresponds to a target in state 0 at $t = 0$ and that irreversibly transits to the visible state at rate α. The calculation of Q_0 is performed in the following section by using simple probabilistic arguments and one checks that the solution actually fulfills condition (5.7). For $\beta \neq 0$ the particle is less visible, or more often reflecting, therefore Eq. (5.7) must be valid as well.

5.1.2 Boundary condition for $Q_0(x,t)$

In this section, we solve the problem for the particular case $\beta = 0$ and examine from there the boundary conditions.

We suppose that at $t = 0$, the target site at $x = 0$ is in the dormant state $\sigma(t=0) = 0$. The probability that the target switches to the active state $\sigma(t') = 1$ for the first time at time t' is given by the exponential distribution with rate α. If we choose $\beta = 0$, once the target has switched to the active state, it will remain active for ever. Since the Brownian particle starts at $x > 0$ at $t = 0$ and diffuses in the unbounded free space, it will be located at a Gaussianly distributed position x' at time t'. This position x' represents a new initial position for the standard first passage problem with a permanent target. Therefore, when $\beta = 0$, the survival probability at time t is given by

$$Q_0(x,t) = \int_0^\infty dt' \alpha e^{-\alpha t'} \int_{-\infty}^\infty dx' \frac{e^{-\frac{(x'-x)^2}{4Dt'}}}{\sqrt{4\pi D t'}} \begin{cases} 1, & \text{if } t' > t, \\ Q^{st}(x', t-t'), & \text{if } t' < t, \end{cases} \tag{5.8}$$

where $Q^{st}(x,t)$ stands for the standard survival probability with a steady target. In Eq. (5.8), we have used the fact that the particle cannot be absorbed while the target is inactive ($t < t'$), and the averages over x' and t' are taken. Let us further take the Laplace transform of Eq. (5.8), denoted as $\widetilde{Q}_0(x,s) = \int_0^\infty dt\ e^{-st} Q_0(x,t)$. After changing the order of the integrals, we obtain

$$\widetilde{Q}_0(x,s) = \alpha \int_0^\infty dt' e^{-\alpha t'} \int_{-\infty}^\infty dx' \frac{e^{-\frac{(x'-x)^2}{4Dt'}}}{\sqrt{4\pi D t'}} \left(\int_0^{t'} dt\ e^{-st} + \int_{t'}^\infty dt\ e^{-st} Q^{st}(x', t-t') \right) \tag{5.9}$$

The first integral of the term between parenthesis in Eq. (5.9) is simply $\frac{1-e^{-st'}}{s}$ and does not depend on x', thus, the integral over x' gives unity. For the second integral, we make a change of variable $u = t - t'$ and obtain the Laplace transform of $Q^{st}(x,u)$ multiplied by a factor $e^{-st'}$. Therefore:

$$\begin{aligned} \widetilde{Q}_0(x,s) =& \alpha \int_0^\infty dt' e^{-\alpha t'} \left(\frac{1-e^{-st'}}{s} + e^{-st'} \int_{-\infty}^\infty dx' \frac{e^{-\frac{(x'-x)^2}{4Dt'}}}{\sqrt{4\pi D t'}} \widetilde{Q}^{st}(x', s) \right) \\ =& \frac{1}{s+\alpha} + \alpha \int_{-\infty}^\infty dx' \frac{e^{-|x'-x|\sqrt{(s+\alpha)/D}}}{\sqrt{4D(s+\alpha)}} \widetilde{Q}^{st}(x', s). \end{aligned} \tag{5.10}$$

Given that $\widetilde{Q}^{st}(x',s) = \frac{1-e^{-|x'|\sqrt{s/D}}}{s}$ (see Eq. 4.40) we substitute this expression into Eq. (5.10) and obtain

$$\widetilde{Q}_0(x,s) = \frac{1}{s+\alpha} + \frac{\alpha}{2s\sqrt{D(s+\alpha)}} \int_{-\infty}^{\infty} dx' e^{-|x'-x|\sqrt{(s+\alpha)/D}} \left(1 - e^{-|x'|\sqrt{s/D}}\right) \tag{5.11}$$

After integrating in Eq. (5.11), we obtain

$$\widetilde{Q}_0(x,s) = \frac{1}{s} + \frac{\sqrt{s}e^{-x\sqrt{(s+\alpha)/D}} - \sqrt{s+\alpha}e^{-x\sqrt{s/D}}}{s\sqrt{s+\alpha}}. \tag{5.12}$$

Further we will see that this result coincides with the full solution given by Eq. (5.27) and with $\beta = 0$. It is also easy to see that Eq. (5.12) satisfies the boundary condition

$$\left.\frac{\partial \widetilde{Q}_0(x,s)}{\partial x}\right|_{x=0} = 0, \tag{5.13}$$

for any s, which implies that

$$\left.\frac{\partial Q_0(x,t)}{\partial x}\right|_{x=0} = 0, \tag{5.14}$$

for any t. Hence, it is "as if " the boundary in $x = 0$ was always reflective, given its initial reflecting state $\sigma = 0$. This may look surprizing, since the target is actually reactive (absorbing) any time after the switch-on time t'.

In the general case, one can derive a relation between Q_0 and Q_1 to show that the boundary condition (5.14) for Q_0 still holds. As before, we suppose that the initial target state is $\sigma_0 = 0$. The particle starts from the position $x > 0$ and freely diffuses until the first transition to the state $\sigma = 1$ occurs, at a time t'. During the interval $[0, t']$ the particle has reached the Gaussianly distributed position x'. At this point, the deduction departs from the case of $\beta = 0$; now, the survival probability function for times $t > t'$ is no longer the standard survival probability but $Q_1(x', t - t')$, since a renewed diffusion process starts from x' with $\sigma_0 = 1$ at time t'. Thus, the survival probability at time t will be

$$Q_0(x,t) = \int_0^{\infty} dt' \alpha e^{-\alpha t'} \int_{-\infty}^{\infty} dx' \frac{e^{-\frac{(x'-x)^2}{4Dt'}}}{\sqrt{4\pi D t'}} \begin{cases} 1, & \text{if } t' > t, \\ Q_1(x', t-t'), & \text{if } t' < t. \end{cases} \tag{5.15}$$

In Eq. (5.15), Q_1 does not depend on the initial position x, thus, if one takes the derivative with respect to x, it will only apply to the exponential term in the integral. Evaluating $\partial Q_0(x,t)/\partial x$ in $x = 0$ gives

$$\left.\frac{\partial Q_0(x,t)}{\partial x}\right|_{x=0} = \int_0^{\infty} dt' \alpha e^{-\alpha t'} \int_{-\infty}^{\infty} dx' \frac{x' e^{-\frac{x'^2}{4Dt'}}}{2Dt'\sqrt{4\pi D t'}} \begin{cases} 1, & \text{if } t' > t, \\ Q_1(x', t-t'), & \text{if } t' < t. \end{cases} \tag{5.16}$$

From the parity of the Gaussian function and of Q_1 with respect to x', namely, $Q_1(-x', t - t') = Q_1(x', t - t')$, we see that the integral over x' in Eq. (5.16) vanishes. Hence, we have shown that the boundary condition in Eq. (6) in the main text is valid for any β.

5.1.3 Solution in Laplace space

We use the Laplace transform defined by $\tilde{Q}_\sigma(x,s) = \int_0^\infty Q_\sigma(x,t)e^{-st}dt$ and obtain from Eqs. (5.3)-(5.4) the following system:

$$D\frac{\partial^2 \tilde{Q}_0(x,s)}{\partial x^2} + \alpha \tilde{Q}_1(x,s) - (\alpha+s)\tilde{Q}_0(x,s) = -1 \tag{5.17}$$

$$D\frac{\partial^2 \tilde{Q}_1(x,s)}{\partial x^2} + \beta \tilde{Q}_0 x,s) - (\beta+s)\tilde{Q}_1(x,s) = -1, \tag{5.18}$$

where the initial condition $Q_\sigma(x, t=0) = 1$ has been used. The homogeneous part of Eqs. (5.17)-(5.18) admits solutions of the form $e^{\lambda x}$ that satisfy

$$\begin{pmatrix} D\lambda^2 - (\alpha+s) & \alpha \\ \beta & D\lambda^2 - (\beta+s) \end{pmatrix} \begin{pmatrix} \tilde{Q}_0 \\ \tilde{Q}_1 \end{pmatrix} = 0. \tag{5.19}$$

The eigenvalues are

$$\lambda_1 = \pm\sqrt{\frac{s}{D}}, \quad \lambda_2 = \pm\sqrt{\frac{s+\alpha+\beta}{D}}, \tag{5.20}$$

with their corresponding eigenstates:

$$v_1 = \begin{pmatrix} 1 \\ 1 \end{pmatrix}, \quad v_2 = \begin{pmatrix} -\frac{\alpha}{\beta} \\ 1 \end{pmatrix}. \tag{5.21}$$

The inhomogeneous part of both Q_0 and Q_1 is independent of the starting position x and simply given by $1/s$. Setting $x > 0$, one notices that $\tilde{Q}_\sigma(x,s)$ must tend to $1/s$ as $x \to \infty$, since $Q_\sigma(x,t)$ remains equal to unity when the particle is very far from the target. Hence, only the negative eigenvalues are acceptable. One deduces

$$\tilde{Q}_0(x,s) = Ae^{-\sqrt{\frac{s}{D}}x} - \frac{\alpha}{\beta}Be^{-\sqrt{\frac{s+\alpha+\beta}{D}}x} + \frac{1}{s}, \tag{5.22}$$

$$\tilde{Q}_1(x,s) = Ae^{-\sqrt{\frac{s}{D}}x} + Be^{-\sqrt{\frac{s+\alpha+\beta}{D}}x} + \frac{1}{s}, \tag{5.23}$$

with A and B two constants. In the following, employ the notation

$$a = x/\sqrt{D}. \tag{5.24}$$

Thus, $\tau_D \equiv a^2$ is the typical diffusion time to reach the target region.

Enforcing the boundary conditions (5.6)-(5.7) yields

$$A = -\frac{\alpha\sqrt{s+\alpha+\beta}}{s\left(\alpha\sqrt{s+\alpha+\beta} + \beta\sqrt{s}\right)}, \tag{5.25}$$

$$B = -\frac{\beta}{\sqrt{s}\left(\alpha\sqrt{s+\alpha+\beta} + \beta\sqrt{s}\right)}. \tag{5.26}$$

The solutions are thus given by

$$\tilde{Q}_0(x,s) = -\frac{\alpha\sqrt{s+\alpha+\beta}}{\sqrt{s}\left(\alpha\sqrt{s+\alpha+\beta} + \beta\sqrt{s}\right)}\left(\frac{e^{-a\sqrt{s}}}{\sqrt{s}} - \frac{e^{-a\sqrt{s+\alpha+\beta}}}{\sqrt{s+\alpha+\beta}}\right) + \frac{1}{s}, \tag{5.27}$$

$$\tilde{Q}_1(x,s) = -\frac{\alpha\sqrt{s+\alpha+\beta}}{\sqrt{s}\left(\alpha\sqrt{s+\alpha+\beta} + \beta\sqrt{s}\right)}\left(\frac{e^{-a\sqrt{s}}}{\sqrt{s}} + \frac{\beta}{\alpha}\frac{e^{-a\sqrt{s+\alpha+\beta}}}{\sqrt{s+\alpha+\beta}}\right) + \frac{1}{s}. \tag{5.28}$$

The average survival probability is obtained from Eq. (5.1):

$$\tilde{Q}_{av}(x,s) = -\frac{\alpha\sqrt{s+\alpha+\beta}}{\alpha\sqrt{s+\alpha+\beta}+\beta\sqrt{s}}\left(\frac{e^{-a\sqrt{s}}}{s}\right)+\frac{1}{s}. \tag{5.29}$$

Alternately, equations (5.27)-(5.29) can be recast under the form

$$\tilde{Q}_i(x,s) = -\frac{\alpha\sqrt{s+\alpha+\beta}}{\sqrt{s}\left(\alpha\sqrt{s+\alpha+\beta}+\beta\sqrt{s}\right)}\left(\frac{e^{-a\sqrt{s}}}{\sqrt{s}} - C_i\frac{e^{-a\sqrt{s+\alpha+\beta}}}{\sqrt{s+\alpha+\beta}}\right)+\frac{1}{s}, \tag{5.30}$$

where $i = \{0, 1, av\}$ and the constants C_i take the values: $C_0 = 1$, $C_1 = -\frac{\beta}{\alpha}$ and $C_{av} = 0$. The Laplace transform of the first passage time distribution is deduced from the general relation $\tilde{P}_i(x,s) = 1 - s\tilde{Q}_i(x,s)$, which stems from taking the Laplace transform of Eq. (5.2). Hence,

$$\tilde{P}_i(x,s) = \frac{\alpha\sqrt{s+\alpha+\beta}\sqrt{s}}{\alpha\sqrt{s+\alpha+\beta}+\beta\sqrt{s}}\left(\frac{e^{-a\sqrt{s}}}{\sqrt{s}} - C_i\frac{e^{-a\sqrt{s+\alpha+\beta}}}{\sqrt{s+\alpha+\beta}}\right), \tag{5.31}$$

which in the case of P_{av} is simply

$$\tilde{P}_{av}(x,s) = \frac{\alpha\sqrt{s+\alpha+\beta}}{\alpha\sqrt{s+\alpha+\beta}+\beta\sqrt{s}}\, e^{-a\sqrt{s}}. \tag{5.32}$$

With the above expressions at hand, several comments are in order.

Limit $\beta = 0$.

For Q_{av} or P_{av}, this case corresponds to a target always in the visible state. As expected, one recovers from Eqs. (5.29) and (5.32) the well known results of the standard case shown in 4.7, see Eq.(4.40)-(4.41):

$$\tilde{Q}_{av}(x,s) = \tilde{Q}^{st}(x,s) \equiv \frac{1-e^{-a\sqrt{s}}}{s}, \tag{5.33}$$

$$\tilde{P}_{av}(x,s) = \tilde{P}^{st}(x,s) \equiv e^{-a\sqrt{s}}, \tag{5.34}$$

where the label "st" stands for the standard case of a target without intermittent dynamics. The inversion of Eq. (5.34) yields

$$P^{st}(a,t) = \frac{a}{\sqrt{4\pi t^3}}e^{-\frac{a^2}{4t}} \simeq \frac{a}{\sqrt{4\pi}}\, t^{-\frac{3}{2}} \quad \text{for } t \gg \tau_D. \tag{5.35}$$

Limit $\alpha, \beta \gg 1/a^2$.

For very large values of the two transition rates compared to the inverse diffusion time, but keeping β/α constant, it is easy to see from Eq. (5.30) or (5.31) that the three first passage quantities tend to those of the standard problem, too:

$$\tilde{Q}_i(x,s) \to \tilde{Q}^{st}(x,s). \tag{5.36}$$

This result seems intriguing, as it implies that at very high transition rates, the target is always detectable by the Brownian particle, *even if it is actually invisible most of the time, i.e., with* $\beta/\alpha \gg 1$. This property is in marked contrast with the radiation boundary condition problem, where the standard case is recovered only when the boundary is mostly absorbing. The fast absorption can be understood here by the recurrence of Brownian trajectories in $1d$: a particle crossing the origin will cross it many times within a short amount of time. If, in the meantime, the target transits very rapidly from one state to the other, as soon as it becomes visible it will be hit by the nearby particle. Hence, the duration of the visible state with respect to the invisible one is not a key factor. As a corollary, if the particle starts very far away from the target ($a^2 \gg \alpha, \beta$), the target dynamics and initial state will play minor roles on the first passage statistics as well (see further Section 5.1.5).

Diffusion limited and intermittency limited survivals

The analytical expression of the survival probability allows us to discuss an important property of the first passage statistics which is not met by the standard case nor radiation boundary problems. Let us consider the limit of infinitely fast diffusion $D \to \infty$, which corresponds to taking $a \to 0$ from the definition (5.24). In the standard case, the target is found immediately if diffusion is infinitely fast, or $Q^{st}(a = 0, t) = 0$ for $t > 0$, see Eq. (5.33). However, when the target is intermittent, Q_{av} and Q_0 admit non-trivial limits. If one defines $Q^I(t) \equiv Q_{av}(a = 0, t)$, the survival probability for any value of a can be decomposed into two parts:

$$Q_{av}(a, t) = Q^I(t) + Q^D(a, t). \tag{5.37}$$

By construction, the contribution $Q^D(a, t)$ vanishes as $a \to 0$ and it therefore represents the diffusion limited part of the overall survival probability. Conversely, $Q^I(t)$ is independent of the diffusion coefficient or starting position, but depends only on α and β. Therefore, it represents the part of Q_{av} limited by the on/off dynamics of the target. Owing to Eq. (5.2), $P_{av}(a, t)$ obviously admits the same type of decomposition $P^I(t) + P^D(a, t)$. From Eq. (5.29), one obtains in the Laplace domain

$$\tilde{Q}^I(s) = \frac{\beta}{\sqrt{s}(\alpha\sqrt{s+\alpha+\beta} + \beta\sqrt{s})}, \tag{5.38}$$

$$\tilde{Q}^D(a, s) = \frac{\alpha\sqrt{s+\alpha+\beta}}{\alpha\sqrt{s+\alpha+\beta} + \beta\sqrt{s}} \left(\frac{1 - e^{-a\sqrt{s}}}{s}\right). \tag{5.39}$$

The intermittent part arises from the fact that the target can be initially invisible and therefore undetectable while it remains in such state, no matter how fast diffusion occurs. A decomposition like in Eq. (5.37) can be performed for Q_0 as well. From Eq. (5.30),

$$\tilde{Q}_0^I(s) = \frac{\alpha + \beta}{\sqrt{s}(\alpha\sqrt{s+\alpha+\beta} + \beta\sqrt{s})}, \tag{5.40}$$

$$\tilde{Q}_0^D(a, s) = \frac{\alpha\sqrt{s+\alpha+\beta}}{\alpha\sqrt{s+\alpha+\beta} + \beta\sqrt{s}} \left(\frac{1 - e^{-a\sqrt{s}}}{s} - \frac{1 - e^{-a\sqrt{s+\alpha+\beta}}}{\sqrt{s}\sqrt{s+\alpha+\beta}}\right). \tag{5.41}$$

One notice that $Q_0^I(t) = \frac{\alpha+\beta}{\beta} Q^I(t)$. This quantity represents the probability that the particle starting right at the target position, with the target initially invisible, has still not hit the target at time t. One can also notice that the average survival probability can be expressed from $\tilde{Q}^I$ and $\tilde{Q}^{st}$:

$$\tilde{Q}_{av}(a,s) = \tilde{Q}^{st}(a,s) + e^{-a\sqrt{s}}\tilde{Q}^I(s). \tag{5.42}$$

5.1.4 Exact Laplace inversion

The general expression (5.30) does not seem to admit an exact Laplace inverse transform in terms of elementary functions. Instead, we obtain $Q_i(a,t)$ by using the convolution theorem. To this end, we write Eq. (5.30) in terms of two functions of s (Eqs. 5.43-5.44) and then, we calculate its convolution. We define the following functions:

$$f(s) = \frac{\sqrt{s} - \frac{\beta}{\alpha}\sqrt{s+\alpha+\beta} + \frac{\alpha+\beta}{\sqrt{s}}}{(\alpha-\beta)s + \alpha^2} \tag{5.43}$$

$$g_\sigma(a,s) = \frac{e^{-a\sqrt{s}}}{\sqrt{s}} - C_\sigma \frac{e^{-a\sqrt{s+\alpha+\beta}}}{\sqrt{s+\alpha+\beta}} \tag{5.44}$$

Once defining these functions, we are able to write $Q_\sigma(a,s) = 1/s - \frac{\alpha^2}{\alpha+\beta} f(s) g_\sigma(a,s)$. If we denote the inverse Laplace transform of $f(s)$ and $g_\sigma(a,s)$ as $F(t)$ and $G_\sigma(a,t)$, respectively, we will have:

$$Q_\sigma(a,t) = 1 - \frac{\alpha^2}{\alpha+\beta}\int_0^t F(u) G_\sigma(a,t-u)du. \tag{5.45}$$

$G_\sigma(a,t)$ and $F(t)$ are calculated below.

To obtain the FPTD of the state σ as a function of time ($P = -dQ/dt$), we need to calculate the time derivative of Eq. (5.45):

$$P_\sigma(a,t) = \frac{\alpha^2}{\alpha+\beta}\int_0^t F(u)\frac{\partial G_\sigma(a,t-u)}{\partial t}du, \tag{5.46}$$

where we have use the fact that $F(t)G(0^+) = 0$, which can be shown from the definitions of G and F in Eqs. (5.47)-(5.48).

The first function $G_\sigma(a,t)$ can be found by direct inversion:

$$G_\sigma(a,t) = \frac{1}{\sqrt{\pi t}} e^{-\frac{a^2}{4t}}\left(1 - C_\sigma e^{-(\alpha+\beta)t}\right). \tag{5.47}$$

For $F(t)$ it is necessary to divide the problem into two cases, $\alpha = \beta$ and $\alpha \neq \beta$. One finds:

$$F(t) = \begin{cases} \dfrac{e^{-2\alpha t}-1}{2\alpha^2\sqrt{\pi t^3}} + \dfrac{2}{\alpha\sqrt{\pi t}}, & \text{for} \quad \alpha = \beta, \\ \dfrac{\beta^2}{\alpha\sqrt{(\alpha-\beta)^3}} e^{-\frac{\alpha^2}{\alpha-\beta}t}\left[\operatorname{erfi}\left(\sqrt{\dfrac{\beta^2}{\alpha-\beta}t}\right) - \operatorname{erfi}\left(\sqrt{\dfrac{\alpha^2}{\alpha-\beta}t}\right)\right] + \dfrac{\alpha - \beta e^{-(\alpha+\beta)t}}{\alpha(\alpha-\beta)\sqrt{\pi t}}, & \text{for} \quad \alpha \neq \beta, \end{cases} \tag{5.48}$$

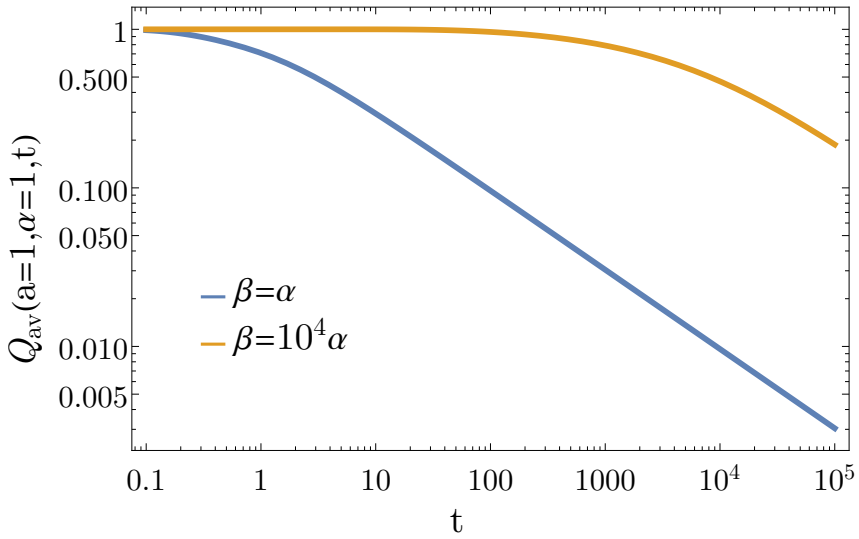

Figure 5.2: Average survival probability for the values $\alpha = 1$, $\beta = 1, 10^4$ with $x = 1$ and $D = 1$. One can appreciate how fast the probability decays with $\beta = \alpha$ compared to $\beta = 10^4\alpha$.

where $\mathrm{erfi}(z) = -i\,\mathrm{erf}(iz)$, with the error function defined by

$$\mathrm{erf}(x) = \frac{2}{\pi}\int_0^x d\tau e^{-\tau^2}. \tag{5.49}$$

Figure (5.2) depicts the survival probability for two different values of β and constant α. One can see how this probability decays slower and remains close to unity for a long time when β increases. On the other hand, the exact solution for P_{av} obtained above is checked successfully with Monte Carlo simulations in Figure 5.4, for several values of β. At large times ($> 10^5$), we can observe the scaling decay $\sim t^{-3/2}$ as in the standard case (see Eq. (4.46)), however, when the target is *cryptic* with $\beta/\alpha \gg 1$, in which case the target is invisible most of the time, a new scaling regime $\sim t^{-1/2}$ emerges. This will be explain more in detail in Section 5.1.5.

Mean first passage time and search efficiency.

The mean search time (also averaged over initial target states) is given by the general relation $\langle T\rangle_{av} = \int_0^\infty dt\ tP_{av}(x,t) = \tilde{Q}_{av}(x, s=0)$. It is easy to see from Eq. (5.30) that $\langle T\rangle_{av} = \langle T\rangle_0 = \langle T\rangle_1 = \infty$. One can nevertheless define a search efficiency based on the mean inverse time $\langle 1/T\rangle = \int_0^\infty dt\ P_{av}(x,t)/t = \int_0^\infty ds\ \tilde{P}(x,s)$, which is a finite quantity. One has:

$$\left\langle \frac{1}{T}\right\rangle_{av} = \int_0^\infty ds \frac{\alpha\sqrt{s+\alpha+\beta}}{\alpha\sqrt{s+\alpha+\beta}+\beta\sqrt{s}}\ e^{-a\sqrt{s}}. \tag{5.50}$$

The search efficiency is obviously less than in the non-intermittent case $\beta = 0$. Opposite to this standard case is that of targets with long periods of visibility and invisibility compared to the diffusion time (β and α both $\ll 1/a^2$). In this case $\sqrt{s+\alpha+\beta} \simeq \sqrt{s}$ when the decaying exponential contribute most in (5.50), therefore

$$\left\langle \frac{1}{T}\right\rangle_{av} \simeq \frac{\alpha}{\alpha+\beta}\int_0^\infty ds\ e^{-a\sqrt{s}} = \frac{\alpha}{\alpha+\beta}\left(\frac{2}{a^2}\right). \tag{5.51}$$

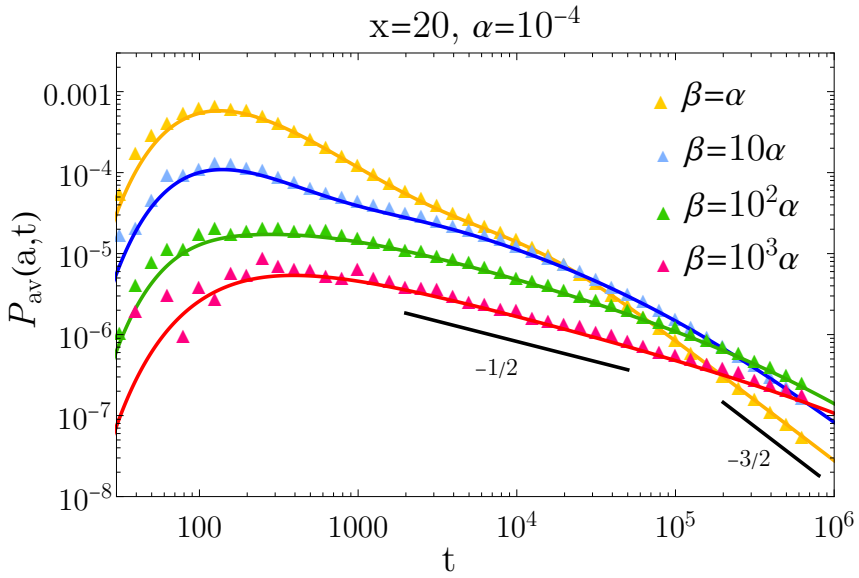

Figure 5.3: Average FHTD for $\alpha = 10^{-4}$ and varying β with a diffusion constant $D = 1/2$. Symbols represent simulation results and lines the exact solution.

Hence, compared to the standard case, the efficiency is degraded by a factor $\alpha/(\alpha+\beta)$, which is also the probability that the target is found in the visible state.

5.1.5 Asymptotic behavior of $Q_{av}(a,t)$

Though we have already found the exact solution of the survival probability, it is given in an integral form that makes it cumbersome to analyze its dependence with the diffusion coefficient and the intermittency parameters. To overcome this difficulty, we can study the behaviour of $Q_{av}(x,t)$ for long and short times, using the properties of the Laplace transform that we have seen in Section 4.5. With this we can obtain an approximation of the behaviour of a function $F(t)$ for long (short) times if we evaluate its corresponding Laplace transform $f(s)$ at the limit $s \to 0$ ($s \to \infty$).

Before of making the asymptotic analysis, we notice that there are two basic time scales involved in the system. The first time scale that we have already mentioned is given by $\tau_D = a^2$, this is the typical diffusion time to reach the target region from the starting position. On the other hand, the target intermittency sets another time scale defined as $\tau_{ta} = 1/(\alpha+\beta)$; this is the mean time in which a target state transition occurs. In addition to these two time scales, in the following we will see that a third one emerge, that will divide the asymptotic behaviour of the survival probability into two regimes.

Long times.

From the above discussion, the long time regime is reached when $\max(\tau_D, \tau_{ta}) \ll t$. In Laplace space this is satisfied if $s \ll \alpha+\beta$ and $s \ll a^{-2}$. The first assumption allow us to write $\sqrt{s+\alpha+\beta} \approx \sqrt{\alpha+\beta}$, and then Eq. (5.29) becomes

$$\tilde{Q}_{av}(a,s) = \frac{1}{s}\left(1 - \frac{e^{-a\sqrt{s}}}{1+K\sqrt{s}}\right), \tag{5.52}$$

where we have defined

$$K = \frac{\beta}{\alpha\sqrt{\alpha+\beta}}. \tag{5.53}$$

Eq. (5.52) can be directly inverted [1] to obtain the survival probability

$$Q_{av}(a,t) = \operatorname{erfc}\left(\frac{\sqrt{t}}{K} + \frac{a}{2\sqrt{t}}\right)\exp\left(\frac{a}{K} + \frac{t}{K^2}\right) + \operatorname{erf}\left(\frac{a}{2\sqrt{t}}\right), \tag{5.54}$$

and the FPTD

$$P_{av}(a,t) = \frac{1}{K\sqrt{\pi t}}\exp\left(-\frac{a^2}{4t}\right) - \frac{1}{K^2}\operatorname{erfc}\left(\frac{\sqrt{t}}{K} + \frac{a}{2\sqrt{t}}\right)\exp\left(\frac{a}{K} + \frac{t}{K^2}\right), \tag{5.55}$$

where $\operatorname{erfc}(\cdot) = 1 - \operatorname{erf}(\cdot)$ is the complement of the error function, defined in Eq. (5.49).

Although these expressions are still complex, we now can directly analyze their behaviour at large times as a function of the intermittent parameters. Nevertheless, another calculation allows us to carry out this analysis in a simpler way. Let us take the assumption $s \ll a^{-2}$ and write $e^{-a\sqrt{s}} \approx 1 - a\sqrt{s}$. Hence, from Eq. (5.52) we find two possible scenarios:

(i) If $K\sqrt{s} \ll 1$, we can make a series expansion of the term $1/(1+K\sqrt{s})$ to obtain $\tilde{Q}_{av} \simeq (a+K)/\sqrt{s}$. By inversion, this yields $Q_{av}(a,t) \simeq (a+K)/\sqrt{\pi t}$ and the first passage probability will approximate to

$$P_{av}(a,t) \simeq \frac{a+K}{2\sqrt{\pi t^3}}. \tag{5.56}$$

Hence, at large times, when the first term of (5.55) dominates, the long time behaviour is the same as in the standard case, except that the prefactor of the power-law $t^{-3/2}$ depends on the target visibility dynamic through the constant K.

Following orders in Eq. (5.56) can be obtained if we expand Eq. (5.52) for small s. In this case, we will have that

$$Q_{av}(s) \simeq \frac{a+K}{\sqrt{s}} - \left(a + aK + K^2\right) + \frac{a^3 + 3a^2K + 6aK^2 + 6K^3}{6}\sqrt{s} + \text{h.o.terms}, \tag{5.57}$$

Whereas the leading order in Eq. (5.57) leads to (5.56), the Laplace transform of the constant term does not contribute for long times. The third term of the right side in Eq. (5.57) must be treated apart. As this term does not diverges when $s \to 0$, we cannot invert it directly. Instead, we can use the following result that holds for the Laplace transform $\widetilde{F}(s)$ of a function $f(t)$ [78]:

$$-\frac{d\widetilde{F}(s)}{ds} = -\frac{d}{ds}\int_0^\infty f(t)e^{-st}dt = \int_0^\infty t f(t)e^{-st}dt. \tag{5.58}$$

If $F(s) = \sqrt{s}$, it follows that $\int_0^\infty t f(t)e^{-st}dt = -1/(2\sqrt{s})$, *i.e.*, the Laplace transform of $tf(t)$ is $1/(2\sqrt{s})$. Therefore, by simple inversion we have that $tf(t) = -1/(2\sqrt{\pi t})$, that leads to $f(t) = -1/(2\sqrt{\pi t^3})$. Now we can invert Eq. (5.57) and use the relation $P = -dQ/dt$ to obtain the FHTD

$$P_{av}(a,t) \simeq \frac{a+K}{2\sqrt{\pi t^3}} - \frac{a^3 + 3a^2K + 6aK^2 + 6K^3}{8\sqrt{\pi t^5}} + \mathcal{O}\left(t^{-7/2}\right). \tag{5.59}$$

(ii) There exists a second case, where we have at the same time $s \ll a^{-2}$, $s \ll \alpha+\beta$ and $K\sqrt{s} \gg 1$ for a wide range of values of s. This is possible if $a = 0$ or very small, and if K is sufficiently large compared to $1/\sqrt{\alpha+\beta}$. In this case, $\tilde{Q}_{av} \simeq \frac{1}{s}\left(1 - 1/K\sqrt{s}\right)$ and immediately we will have $\tilde{P}_{av} = 1 - s\tilde{Q}_{av} = 1/K\sqrt{s}$. This form allows us to derive an important result: in an intermediate time interval, we thus have

$$P_{av}(t) \simeq \frac{1}{K\sqrt{\pi t}}. \tag{5.60}$$

From the above analysis we see that the asymptotic behaviour of the FHTD drastically changes at the time scale

$$\tau_c \equiv K^2 = \frac{\beta^2}{\alpha^2(\alpha+\beta)}, \tag{5.61}$$

which sets a crossover time that separates the standard scaling $t^{-3/2}$ modified by the prefactor $(a + K)$, from a new regime $t^{-1/2}$ that holds in the range $\max(\tau_D, \tau_{ta}) \ll t \ll \tau_c$. It is worth noting that the crossover time only depends on the target intermittent dynamics and will be observed only if

$$\frac{\tau_c}{\tau_{ta}} = \left(\frac{\beta}{\alpha}\right)^2 \gg 1, \tag{5.62}$$

which is satisfied for high cryptic targets with $\beta \gg \alpha$. Interestingly, this regime can be sustained for several decades. Summarizing, we have found that

$$P_{av}(a,t) \simeq \begin{cases} 1/(K\sqrt{\pi t}), & \text{if} \quad \max(\tau_D, \tau_{ta}) \ll t \ll \tau_c, \\ (a+K)/(2\sqrt{\pi t^3}), & \text{if} \quad \tau_c \ll t. \end{cases} \tag{5.63}$$

In figure (5.4) we plot $P_{av}(a,t)$ for an extreme case in which $\beta \gg \alpha$. We include the curve given by the complete solution given in section 5.1.4. It can be appreciated that at time $\tau_c = K^2$ the slope of the curve changes from $t^{-1/2}$ to $t^{-3/2}$.

Short times

As we have done before, to analyze the behaviour of the FPTD for short times we calculate the Laplace transform of the function $\tilde{Q}_{av}(a,s)$ in the corresponding limit $s \to \infty$. To do this, we rewrite Eq. (5.29) as

$$\tilde{Q}_{av} = \frac{1 - e^{-a\sqrt{s}}}{s} + \frac{1}{1 + \frac{\alpha}{\beta}\sqrt{(s+\alpha+\beta)/s}}\left(\frac{e^{-a\sqrt{s}}}{s}\right) \tag{5.64}$$

and we make the series expansion $\sqrt{(s+\alpha+\beta)/s} \approx 1 + \frac{\alpha+\beta}{2s} - \mathcal{O}(s^{-2})$ to obtain

$$\tilde{Q}(a,s) = \frac{1}{s} - \frac{\alpha}{\alpha+\beta}\frac{e^{-a\sqrt{s}}}{s} - \frac{\alpha\beta}{2(\alpha+\beta)}\frac{e^{-a\sqrt{s}}}{s^2} + \frac{\beta(3\alpha^2+\alpha\beta)}{8(\alpha+\beta)}\frac{e^{-a\sqrt{s}}}{s^3} + \mathcal{O}(s^{-4}) \tag{5.65}$$

and the FPTD in the Laplace space will be

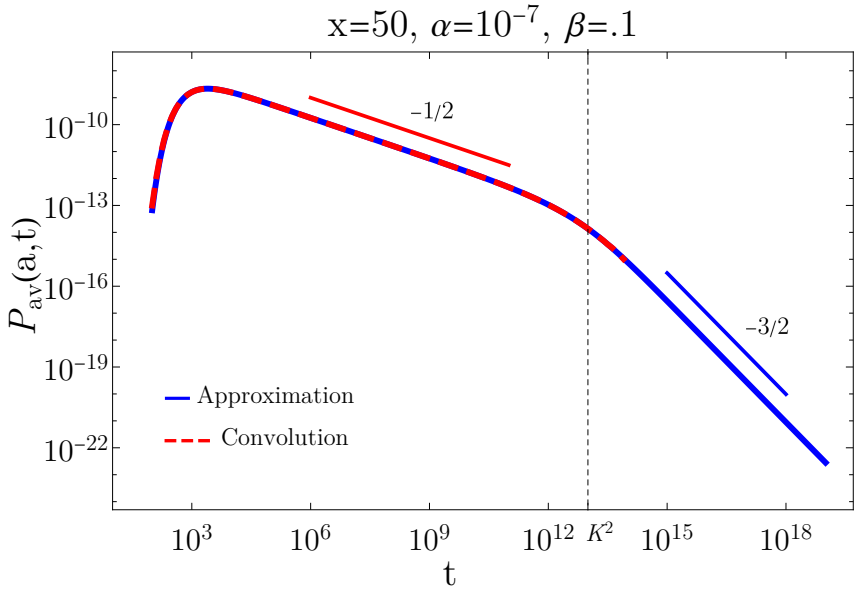

Figure 5.4: Average first passage time density for the values $\alpha = 10^{-7}$, $\beta = 0.1$ and the starting position of the searcher $x = 50$ and $D = 1/2$. With this values $K^2 \approx 10^{13}$. Dashed red line correspond to the exact solution. This is given in section 5.1.4.

$$\tilde{P}(a,s) = \frac{\alpha}{\alpha+\beta} e^{-a\sqrt{s}} \left[1 + \frac{\beta}{2s} - \frac{\beta(3\alpha+\beta)}{8s^2} + \mathcal{O}(s^{-3}) \right] \tag{5.66}$$

From this equation we immediately see one important result that departs from the standard case: when $a \to 0$ there will be a non vanishing contribution to the FPTD given by the intermittency behaviour of the target as we discussed in section 5.1.3. Then, if we invert Eq. (5.66) in this limit ($a = 0$) we will have

$$P_{av}(t) = \frac{\alpha}{\alpha+\beta} \left[\delta(t) + \frac{\beta}{2} - \frac{\beta(3\alpha+\beta)}{8} t + \mathcal{O}(t^2) \right] \tag{5.67}$$

The total FPTD will be given by

$$P_{av}(a,t) = \frac{\alpha}{\alpha+\beta} \left[\frac{a}{\sqrt{4\pi t^3}} e^{-\frac{a^2}{4t}} + \frac{\beta}{2} \operatorname{erfc}\left(\frac{a}{2\sqrt{t}} \right) - \mathcal{O}(t) \right] \tag{5.68}$$

We observe that at short times, the first passage time behaves as the standard case weighted by the probability $\alpha/(\alpha+\beta)$.

5.1.6 Relation with mixed boundary condition problems

Since the target switches between absorbing and reflecting phases (the latter being equivalent to hidden in the present geometry), one may wonder about a possible connection with diffusion in the presence of a mixed, or Robin, boundary condition (RBC) introduced at section 4.4. For a Brownian particle, the general mixed boundary condition Eq. 4.22 reduces to [124]:

$$D \frac{\partial p}{\partial z}\bigg|_{z=0} = \kappa p(z=0,t), \tag{5.69}$$

where κ is a positive constant and $p(z,t)$ is the probability density of the position $z \in [0,\infty)$. The exact survival probability in $1d$ of a particle starting at $z = x$ and obeying a RBC [116, 105] actually coincides with our Eq. (5.52) or (5.55) for all t, where K must be replaced by $\sqrt{D}/\kappa$. Since these Eqs. (5.52) or (5.55) are valid for $t \gg 1/(\alpha+\beta)$, both problems become equivalent for times larger than the target time. We deduce the formula

$$\kappa = \frac{\alpha}{\beta}\sqrt{\alpha+\beta}\sqrt{D}. \tag{5.70}$$

As one may expect, the boundary is absorbing ($\kappa \to \infty$) when $\beta \to 0$ and reflecting ($\kappa \to 0$) when $\alpha \to 0$. Non trivially, it is also absorbing as $\alpha, \beta \to \infty$, β/α being fixed, as mentioned earlier. The two-state process thus provides a new, rigorous example of application of the RBC (5.69), extending the relevance of the latter to the study of fluctuating biophysical systems. Both problems differ for t smaller than the target time-scale, though, as the RBC does not involve such a time-scale. A similar asymptotic analogy with the RBC was shown some time ago for diffusion into a partially absorbing medium [14].

5.2 Diffusion with resetting

In this section, we study the first hitting time statistics between a particle, which stochastically resets to its initial position on the semi-infinite line, and a gated target that intermittently switches between two states: a reactive state that absorbs the diffusive particle upon encounter, and a non-reactive one which reflects the particle. We calculate the survival probabilities of the particle at time t, and further deduce quantities of interest such as the first two moments of the hitting time distribution. This section is organized as follows: we begin in Section 5.2.1 by introducing the model and deduce the equations of motion that govern the survival probabilities, which are solved in the Laplace space. With these solutions, in Section 5.2.2 we find an exact expression for the MFHT and analyze its behaviour as a function of the target transition rates and of the resetting rate. In Section 5.2.3 we discuss the connection between our model and the partial absorption problem. Section 5.2.4 is devoted to the analysis of the relative variance of the first hitting times. A comparison between our findings and those of [30] is discussed in more details in 5.2.5.

5.2.1 The problem and its solution

Let us consider on the semi-infinite line a Brownian particle with diffusion coefficient D, starting at $t = 0$ from a position $x_0 > 0$, and which is subject to a stochastic Poissonian resetting process of rate r. The resetting position is denoted as $x_r > 0$. At the origin, a stochastically gated target is placed. The dynamics of the target will be characterized by the time-dependent binary variable $\sigma(t)$, which takes the value $\sigma = 0$ when the target is non-reactive, and $\sigma = 1$ when it is reactive. The target stochastically switches from the state 0 to 1 with rate α, whereas it switches from the state 1 to 0 with rate β (see Fig. 5.5). The diffusing particle is absorbed upon its first encounter with the target in the reactive state.

We define $Q_0(x_0,t)$ as the probability that the particle has not hit the target up to time t, given the initial position x_0 and initial target state $\sigma(t=0) = 0$ [the variable

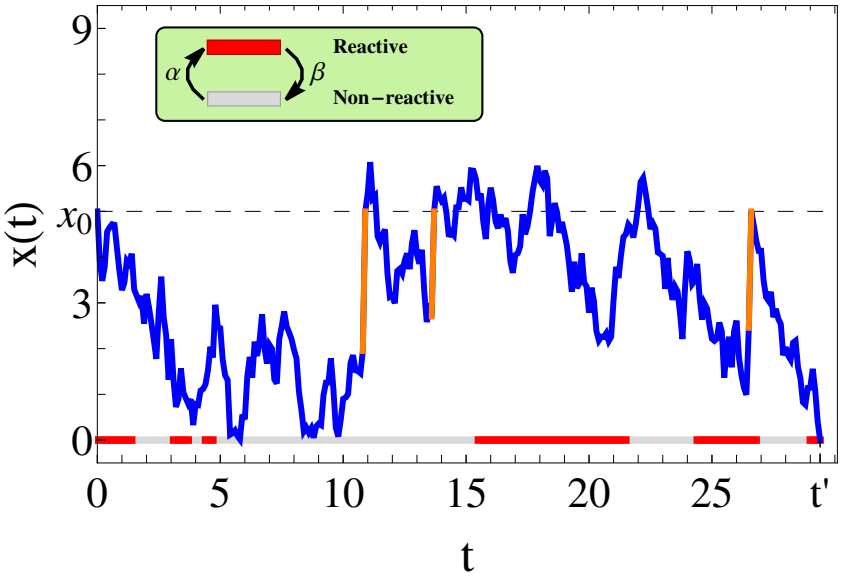

Figure 5.5: Trajectory of a diffusive particle (blue line) in 1D, in the presence of an intermittent target placed at the origin. The periods of time during which the target is reactive (or absorbing) are represented by red segments, whereas the gray intervals represent the target in the non-reactive (or reflective) state. At exponentially distributed time intervals with mean $1/r$, the particle is reset to the position x_r (orange line), which coincides in this example with the initial position x_0.

x_r is implicit]. Similarly, we define $Q_1(x_0,t)$ for the initial target state $\sigma(t=0)=1$. In Appendix A.2 we show that these probabilities satisfy the coupled backward Fokker-Planck equations

$$\frac{\partial Q_0(x_0,t)}{\partial t} = D\frac{\partial^2 Q_0(x_0,t)}{\partial x_0^2} + \alpha(Q_1(x_0,t)-Q_0(x_0,t)) + r(Q_0(x_r,t)-Q_0(x_0,t)), \quad (5.71)$$

$$\frac{\partial Q_1(x_0,t)}{\partial t} = D\frac{\partial^2 Q_1(x_0,t)}{\partial x_0^2} + \beta(Q_0(x_0,t)-Q_1(x_0,t)) + r(Q_1(x_r,t)-Q_1(x_0,t)). \quad (5.72)$$

The system of equations (5.71) and (5.72) will satisfy the following boundary conditions:

$$Q_1(x_0=0,t)=0, \quad (5.73)$$

$$\left.\frac{\partial Q_0(x_0,t)}{\partial x_0}\right|_{x_0=0} = 0. \quad (5.74)$$

Eq. (5.73) enforces the absorbing condition of the target in the reactive state, whereas Eq. (5.74) asserts that the target in the non-reactive state will reflect the diffusive particle upon encounter (see Section 5.1 for a detailed derivation of the latter condition).

We also define the average survival probability $Q_{av}(x_0,t)$ for the particle starting at x_0 that results from averaging over the initial target states generated by the steady-state distribution of the two-state Markov chain:

$$Q_{av}(x_0,t) = \frac{\beta}{\alpha+\beta}Q_0(x_0,t) + \frac{\alpha}{\alpha+\beta}Q_1(x_0,t). \quad (5.75)$$

The probability distributions of the first hitting time t are denoted as $P_0(x_0,t)$ and $P_1(x_0,t)$, with the same notations as before for the initial conditions. These first hitting

time densities (FHTDs) are deduced from the survival probabilities through the usual relation [108]:

$$P_{0,1}(x_0,t) = -\frac{\partial Q_{0,1}(x_0,t)}{\partial t}. \tag{5.76}$$

Introducing the Laplace transforms $\widetilde{Q}_{0,1}(x_0,s) = \int_0^\infty e^{-st} Q_{0,1}(x_0,t)dt$ and using the initial condition $Q_{0,1}(x_0,t=0) = 1$ for $x_0 > 0$, Eqs. (5.71) and (5.72) become

$$D\frac{\partial^2 \widetilde{Q}_0(x_0,s)}{\partial x_0^2} + \alpha \widetilde{Q}_1(x_0,s) - (s+\alpha+r)\widetilde{Q}_0(x_0,s) = -1 - r\widetilde{Q}_0(x_r,s), \tag{5.77}$$

$$D\frac{\partial^2 \widetilde{Q}_1(x_0,s)}{\partial x_0^2} + \beta \widetilde{Q}_0(x_0,s) - (s+\beta+r)\widetilde{Q}_1(x_0,s) = -1 - r\widetilde{Q}_1(x_r,s), \tag{5.78}$$

and the boundary conditions (5.73) and (5.74) read

$$\widetilde{Q}_1(x_0=0,s) = 0, \tag{5.79}$$

$$\left.\frac{\partial \widetilde{Q}_0(x_0,s)}{\partial x_0}\right|_{x_0=0} = 0. \tag{5.80}$$

By using Eq. (5.76) and integrating by parts, the Laplace transform of the FHTD will be simply given by

$$\widetilde{P}_0(x_0,s) = 1 - s\widetilde{Q}_0(x_0,s) \text{ and } \widetilde{P}_1(x_0,s) = 1 - s\widetilde{Q}_1(x_0,s). \tag{5.81}$$

We consider $Q_0(x_r,s)$ and $Q_1(x_r,s)$ as unknown inhomogeneous terms in the differential equations (5.77) and (5.78). The homogeneous part of this system is solved with the ansatz $\boldsymbol{\xi} e^{\lambda x_0}$, where the vector $\boldsymbol{\xi}$ and λ are determined from solving

$$\begin{pmatrix} D\lambda^2 - (\alpha+r+s) & \alpha \\ \beta & D\lambda^2 - (\beta+r+s) \end{pmatrix} \boldsymbol{\xi} = 0. \tag{5.82}$$

After straightforward algebra, the general solution $\widetilde{\mathbf{Q}} = \begin{pmatrix} \widetilde{Q}_0 & \widetilde{Q}_1 \end{pmatrix}^T$ is given by the following linear combination

$$\widetilde{\mathbf{Q}} = A_1\boldsymbol{\xi}_1 e^{-\lambda_1 x_0} + A_2\boldsymbol{\xi}_1 e^{\lambda_1 x_0} + A_3\boldsymbol{\xi}_2 e^{-\lambda_2 x_0} + A_4\boldsymbol{\xi}_2 e^{\lambda_2 x_0} + \widetilde{\mathbf{Q}}^{inh}, \tag{5.83}$$

where $\widetilde{\mathbf{Q}}^{inh} = \begin{pmatrix} \widetilde{Q}_0^{inh} & \widetilde{Q}_1^{inh} \end{pmatrix}^T$ is the constant solution given by

$$\widetilde{Q}_0^{inh} = \frac{1 + r\widetilde{Q}_0(x_r,s)}{D\lambda_1^2} + \frac{r\alpha\left[\widetilde{Q}_1(x_r,s) - \widetilde{Q}_0(x_r,s)\right]}{D\lambda_1^2\lambda_2^2}, \tag{5.84}$$

$$\widetilde{Q}_1^{inh} = \frac{1 + r\widetilde{Q}_1(x_r,s)}{D\lambda_1^2} + \frac{r\beta\left[\widetilde{Q}_0(x_r,s) - \widetilde{Q}_1(x_r,s)\right]}{D^2\lambda_1^2\lambda_2^2}. \tag{5.85}$$

The factors A_k are determined from the boundary conditions and the no-divergence of the probabilities $Q_{0,1}$ as $x_0 \to \infty$. The roots λ_1 and λ_2 in Eqs. (5.83)–(5.85) are given from (5.82) by

$$\lambda_1 = \sqrt{\frac{s+r}{D}}, \quad \lambda_2 = \sqrt{\frac{s+\alpha+\beta+r}{D}}, \tag{5.86}$$

whereas the vectors $\boldsymbol{\xi}_1$ and $\boldsymbol{\xi}_2$ are

$$\boldsymbol{\xi}_1 = \begin{pmatrix} 1 \\ 1 \end{pmatrix}, \quad \boldsymbol{\xi}_2 = \begin{pmatrix} -\frac{\alpha}{\beta} \\ 1 \end{pmatrix}.$$

To avoid infinite solutions at $x_0 \to \infty$, we must set $A_2 = A_4 = 0$ in Eq. (5.83). From the boundary conditions (5.79)-(5.80) we obtain the remaining constants,

$$A_1 = -\frac{\alpha\lambda_2 \widetilde{Q}_1^{inh}}{\alpha\lambda_2 + \beta\lambda_1}, \tag{5.87}$$

and $A_3 = \frac{\beta\lambda_1}{\alpha\lambda_2} A_1$. Substituting these factors into Eq. (5.83),

$$\widetilde{Q}_0(x_0, s) = -\tfrac{\alpha\lambda_2}{\alpha\lambda_2+\beta\lambda_1}\left(e^{-\lambda_1 x_0} - \tfrac{\lambda_1}{\lambda_2} e^{-\lambda_2 x_0}\right) \widetilde{Q}_1^{inh} + \widetilde{Q}_0^{inh}, \tag{5.88}$$

$$\widetilde{Q}_1(x_0, s) = -\tfrac{\alpha\lambda_2}{\alpha\lambda_2+\beta\lambda_1}\left(e^{-\lambda_1 x_0} + \tfrac{\beta\lambda_1}{\alpha\lambda_2} e^{-\lambda_2 x_0}\right) \widetilde{Q}_1^{inh} + \widetilde{Q}_1^{inh}. \tag{5.89}$$

The average survival probability takes a slightly simpler form:

$$\widetilde{Q}_{av}(x_0, s) = -\frac{\alpha\lambda_2 \widetilde{Q}_1^{inh}}{\alpha\lambda_2 + \beta\lambda_1} e^{-\lambda_1 x} + \frac{1 + r\widetilde{Q}_{av}(x_r, s)}{D\lambda_1^2}. \tag{5.90}$$

Substituting Eqs. (5.84)-(5.85) into Eqs. (5.88)-(5.89), and then setting $x_r = x_0$, one obtains in a self-consistent way the survival probabilities $\tilde{Q}_0(x_0, s)$ and $\tilde{Q}_1(x_0, s)$, *i.e.*, when the initial position is the resetting position:

$$\widetilde{Q}_0(x_0, s) = \frac{\alpha\lambda_2\left(e^{\lambda_1 x_0} - 1\right) + \lambda_1\left(\beta + (\alpha + r)e^{-\lambda_2 x_0}\right)e^{\lambda_1 x_0} - \frac{s\lambda_1 r}{\alpha+\beta+s} e^{(\lambda_1 - \lambda_2)x_0}}{\alpha\lambda_2 r + s e^{\lambda_1 x_0}\left[(\beta\lambda_1 + \alpha\lambda_2) + \frac{\beta\lambda_1 r}{\alpha+\beta+s} e^{-\lambda_2 x_0}\right]}, \tag{5.91}$$

$$\widetilde{Q}_1(x_0, s) = \frac{\alpha\lambda_2\left(e^{\lambda_1 x_0} - 1\right) + \beta\lambda_1\left(1 - e^{-\lambda_2 x_0}\right)e^{\lambda_1 x_0}}{\alpha\lambda_2 r + s e^{\lambda_1 x_0}\left[(\beta\lambda_1 + \alpha\lambda_2) + \frac{\beta\lambda_1 r}{\alpha+\beta+s} e^{-\lambda_2 x_0}\right]}. \tag{5.92}$$

whereas the average survival probability is

$$\widetilde{Q}_{av}(x_0, s) = \frac{\alpha\lambda_2\left(1 - e^{-\lambda_1 x_0}\right)(s + \alpha + \beta) + \beta\lambda_1\left(r e^{-\lambda_2 x_0} + s + \alpha + \beta\right)}{\alpha\lambda_2\left(r e^{-\lambda_1 x_0} + s\right)(s + \alpha + \beta) + s\beta\lambda_1\left(r e^{-\lambda_2 x_0} + s + \alpha + \beta\right)}. \tag{5.93}$$

5.2.2 Mean first hitting time

In the following we keep considering $x_r = x_0$ (resetting to the starting position) and define the mean first hitting time given the initial target condition $\sigma = 0$ ($\sigma = 1$, respectively) as $T_0(x_0)$ ($T_1(x_0)$, respectively). These quantities are obtained from the usual relation $T_{0,1}(x_0) = \int_0^\infty Q_{0,1}(x_0, t)dt = \widetilde{Q}_{0,1}(x_0, s = 0)$. Setting $s = 0$ in Eqs. (5.91) and (5.92), one deduces

$$T_0(x_0) = \frac{e^{\sqrt{\frac{r}{D}}x_0} - 1}{r} + \frac{\beta + (r + \alpha)e^{-\sqrt{\frac{r+\alpha+\beta}{D}}x_0}}{\alpha\sqrt{r(r + \alpha + \beta)}} e^{\sqrt{\frac{r}{D}}x_0}, \tag{5.94}$$

$$T_1(x_0) = \frac{e^{\sqrt{\frac{r}{D}}x_0} - 1}{r} + \frac{\beta}{\alpha}\left(\frac{1 - e^{-\sqrt{\frac{r+\alpha+\beta}{D}}x_0}}{\sqrt{r(r + \alpha + \beta)}}\right) e^{\sqrt{\frac{r}{D}}x_0}. \tag{5.95}$$

From Eq. (5.93), the average mean first hitting time reads

$$T_{av}(x_0) = \frac{e^{\sqrt{\frac{r}{D}}x_0} - 1}{r} + \frac{\beta e^{\sqrt{\frac{r}{D}}x_0}(\alpha + \beta + re^{-\sqrt{\frac{r+\alpha+\beta}{D}}x_0})}{\alpha(\alpha+\beta)\sqrt{r(r+\alpha+\beta)}}. \tag{5.96}$$

As well-known for the case of perfectly absorbing targets [55, 54], one of the main consequence of introducing resetting in the dynamics of the diffusive particle is to make the mean of the FHTD finite, unlike in free diffusion, where it diverges. Furthermore, the different MFHTs here can be minimized by a suitable choice of the resetting rate.

The solution of the mean first hitting time of the gated problem calls for several comments. As expected, if we set $\beta = 0$ in Eq. (5.94) or (5.95), we recover the expression of the MFHT for the ungated case, denoted as $T_r(x_0)$ here:

$$T_{av}(x_0, \beta = 0) = T_r(x_0) = \frac{e^{\sqrt{\frac{r}{D}}x_0} - 1}{r}. \tag{5.97}$$

T_r is a non-monotonic function of r that is minimum at the optimal resetting rate $r^*(\beta = 0) = 2.53963...D/x_0^2$, a result first deduced in [55].

The solution for the average MFHT in Eq. (5.96) also exhibits a non-monotonic behaviour with a single minimum (Fig. 5.6a), for all parameter values $\alpha, \beta > 0$ of the intermittent target. The optimal resetting rate r^* that minimizes the MFHT varies with the switching parameters α and β. Increasing the parameter β makes the target less reactive, which causes an increase of the MFHT. As shown by Fig. 5.6b, at a fixed resetting rate, the MFHT increases monotonically with β. Even when the switching parameter β is high, an optimal resetting rate $r = r^*(\beta)$ can always be found. Therefore, fixing α, it is possible to draw a minimal curve for the MFHT as a function of β. As depicted in Fig. 5.6b, any MFHT with another value of r will lie above the curve corresponding to $r^*(\beta)$. One can also notice the non-monotonic variations of the MFTH with r: the MFHT first decreases with r until it reaches its minimal value at $r^*(\beta)$, which is of order one. For $r > r^*(\beta)$, the MFPT increases with r. A very good agreement with numerical simulations is obtained.

In Eq. (5.96), the dependence of the MFHT with respect to the target rates is not as simple as one would wish and obtaining an analytical expression for r^* seems beyond reach. Below, we derive a simplified expression in the limiting case when the target rapidly switches between the reactive and non-reactive states, and compare the results with the numerical minimization of the exact solution (5.96).

In the limit of large α and β compared to r, we approximate $\sqrt{r+\alpha+\beta} \approx \sqrt{\alpha+\beta}$ in Eq. (5.96) and can always neglect the term proportional to $e^{-x_0\sqrt{\frac{r+\alpha+\beta}{D}}}$ to obtain

$$T_{av}(x_0) \approx \frac{e^{\sqrt{\frac{r}{D}}x_0} - 1}{r} + \frac{\beta e^{\sqrt{\frac{r}{D}}x_0}}{\alpha\sqrt{r(\alpha+\beta)}}. \tag{5.98}$$

Defining the dimensionless parameters

$$z = x_0\sqrt{\frac{r}{D}}, \tag{5.99}$$

$$w = \frac{\beta\sqrt{r}}{2\alpha\sqrt{\alpha+\beta}}, \tag{5.100}$$

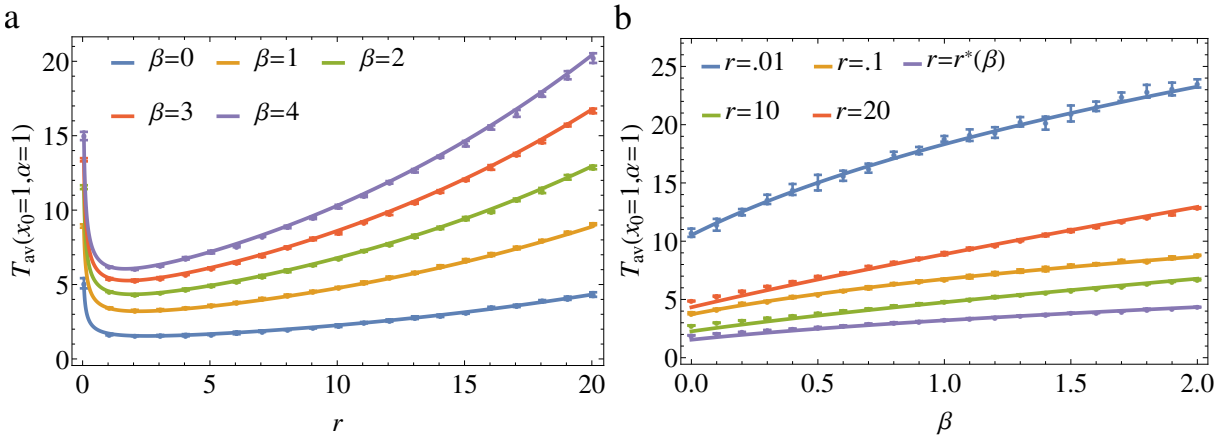

Figure 5.6: (a) Mean first hitting time T_{av} as a function of r for several values of β ($x_0 = 1$, $D = 1$ and $\alpha = 1$). (b) Same quantity as a function of β for several values of r. Symbols represent simulation results obtained with the Gillespie algorithm [63].

the approximate optimal resetting rate obeys the transcendental equation

$$\frac{z}{2} - 1 + e^{-z} + w(z-1) = 0. \tag{5.101}$$

The solution of Eq. (5.101) as a function of β is shown in Fig. 5.7a (dashed lines), together with the exact optimal parameter obtained from numerical minimization of Eq. (5.96). Clearly, the two solutions show a good agreement for all β only if $\alpha \gg r^*$. Otherwise, the differences are significant in the intermediate regime of β.

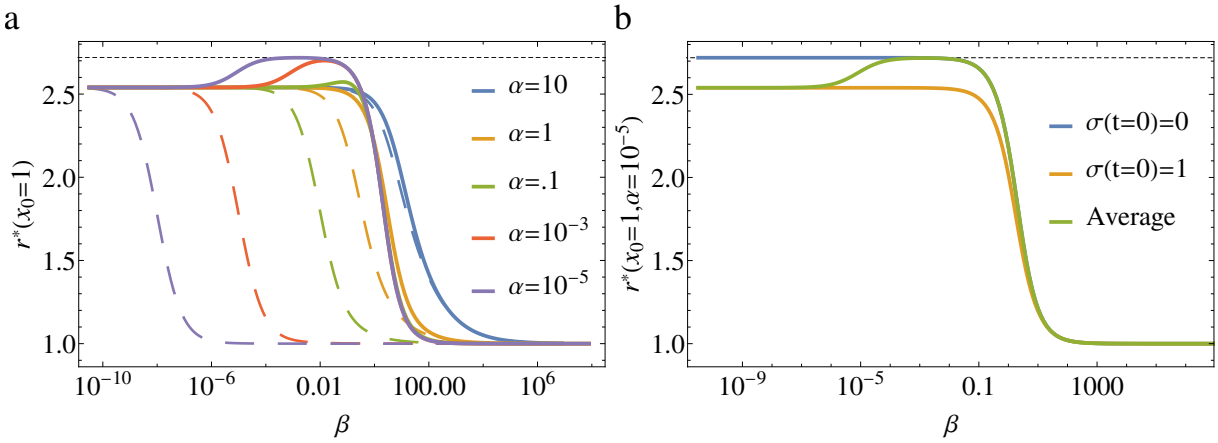

Figure 5.7: a) Optimal resetting rate r^* as a function of β and several values of α (fixing $x_0 = 1$ and $D = 1$). The continuous lines are obtained from numerical minimization of the exact result (5.96), whereas the dashed lines represent the solution of the approximate Eq. (5.101). b) Optimal resetting rates obtained from the minimizations of the functions T_0, T_1 and T_{av}, respectively, see Eqs. (5.94), (5.95) and (5.96), for a small value of α (10^{-5}). In both figures, the upper horizontal dotted line represents the maximum value 2.72033...D/x_0^2 that r^* can reach, which is given by minimizing Eq. (5.103).

In the high transition rates regime, if the target is mostly non-reactive ($r \ll \alpha \ll \beta$, such that $w \gg 1$), the first three terms of the left hand side of Eq. (5.101) can be neglected and we arrive at the simple solution $z = 1$. From Eq. (5.99), the optimal resetting rate

in the limit $\beta = \infty$ is therefore given by

$$r^*(\beta = \infty) = D/x_0^2, \tag{5.102}$$

which is substantially lower than the optimal rate $r^*(\beta = 0) = 2.53963...D/x_0^2$ for the ungated target (see Fig. 5.7a). Therefore, to optimize the search process of a poorly reactive target, one must opt for less frequent resetting compared with the perfectly reactive case, at a rate exactly given by the inverse diffusion time D/x_0^2. It is also worth noting that, even though the expression (5.101) is obtained in the high transition rates limit, we can recover the solution for the ungated case: setting $\beta = 0$, it reduces to the transcendental equation $\frac{z^*}{2} - 1 + e^{-z^*} = 0$, whose solution is $z^* = 1.59362...$ or $r^*(\beta = 0) = 2.53963...D/x_0^2$.

As shown by Fig. 5.7a, r^* always remains of the order of the inverse diffusion time D/x_0^2. Nevertheless, the (exact) optimal resetting rate does not always decrease as the target becomes less reactive. At odds with the solution given by Eq. (5.101), r^* can exhibit a clear non-monotonic shape with respect to β, with a maximum at a value above $2.53963...D/x_0^2$. This occurs when the parameter α is fixed to a small value (compared to the inverse diffusion time), a regime where the approximation (5.98) is no longer valid. In this case, r^* is maximum for a value of β which is larger than α, namely, in a situation where the target is most of the time inactive.

This non-monotonic shape of the optimal resetting rate stems from properties exhibited by the two MFHTs T_0 and T_1. As depicted in Fig. 5.7b, the resetting rates that minimize T_0 and T_1 taken separately are different. If the target is initially reactive, it remains so during a random time of mean $1/\beta$ until it switches to the non-reactive state. For a small transition rate β, the initial reactive phase can thus be very long and the target is considered as practically ungated: r^* coincides with the optimal rate $r^*(\beta = 0) = 2.53963...D/x_0^2$. On the contrary, if the target is initially non-reactive, the searcher will diffuse and reset without being absorbed during a random time of mean $1/\alpha$ until the target becomes reactive. If this first transition happens after a long time (α small), the searcher will have a random position approximately distributed along the non-equilibrium steady state in the presence of the reflecting boundary. If in addition the transition rate β is small, once the target activates, it can be considered as practically ungated and the problem becomes analogous to the standard one, but with a distribution of starting positions. As a consequence, the value of the optimal resetting rate is larger, as shown in Fig. 5.7b (see also Eq. (5.103) below).

Since T_{av} represents the average over the initial target states in Eq. (5.75), for values of β much smaller than α, the target is likely to be initially reactive, and the main contribution to T_{av} comes from T_1. Conversely, when β becomes greater than α (but still $\ll r^*$), the contribution of T_0 is dominant. Therefore the resetting rate that minimizes T_{av} increases and reaches the value that minimizes T_0. Eventually, in the regime $\beta \gg r^*$ the resetting rate drops to the value D/x_0^2 discussed previously. These considerations explain the non-monotonic behaviour of r^* at small α seen in Figs. 5.7a-b.

The upper bound reached by the optimal resetting rate r^* in our problem can be calculated as follows. With $\beta = 0$, the value of r that minimize T_0 becomes independent of α at small α. This can be noticed by setting $\beta = 0$ and expanding Eq. (5.94) around

$\alpha = 0$:

$$T_0(x_0, \alpha, \beta = 0) \approx \frac{e^{\sqrt{\frac{r}{D}}x_0} - 1}{r} + \frac{1 - \sqrt{\frac{r}{D}}x_0}{2r} + \frac{1}{\alpha} + \mathcal{O}(\alpha). \tag{5.103}$$

In the limit $\alpha \to 0$, all the terms of order α or higher can be neglected. Therefore, the minimization of Eq. (5.103) with respect to r will only involve the first two terms of the right hand side, leading to an optimal resetting rate of $2.72033...D/x_0^2$, independent of α. This is the maximum value that the optimal resetting rate r^* can reach here, over all the possible values of the parameters α and β, as illustrated in Figs. 5.7a-b.

5.2.3 The regime $\alpha, \beta \gg r$ and the partial absorption problem

We comment that the same expression (5.101) was deduced in reference [143] for diffusion under resetting with partial absorption: in that case, the dimensionless parameter w was given by $w = \sqrt{rD}/2\kappa$, where κ is the absorption velocity of the target.

The physical meaning of the approximation (5.98) can therefore be traced back to the problem of diffusion under resetting in the presence of a partially absorbing target [143]. In that problem, a searcher performs diffusion with stochastic resetting to the initial position whereas a partially absorbing target is located at the origin (see Section 4.4). Upon target encounters, the searcher will not be necessarily absorbed at the target boundary but instead reflected at some rate, such that the probability density $p(x,t)$ of the position x will satisfy the so-called radiation boundary condition

$$D\frac{\partial p(x,t)}{\partial y}\Big|_{x=0} = \kappa p(x=0,t), \tag{5.104}$$

where the absorption velocity κ is the rate at which the searcher is absorbed at the target boundary. A different interpretation of κ can be found in Ref. [118] , where the searcher can diffuse inside the target, which is considered to have a certain thickness. In this configuration, κ is proportional to the rate at which the searcher is absorbed while it is in the target region. Both interpretations lead to the same results when the target size tends to zero, which is the case of interest here.

It is found that the mean time at which the searcher reacts with the target is given by [143]

$$T_p(x_0) = \frac{e^{\sqrt{\frac{r}{D}}x_0} - 1}{r} + \frac{e^{\sqrt{\frac{r}{D}}x_0}}{\kappa\sqrt{r/D}}, \tag{5.105}$$

where the other parameters r, x_0 and D are the same as in our model.

By simple inspection, one can notice that Eq. (5.105) has the same form as the approximation (5.98) of T_{av} in the limit of high transition rates (α, β). Although the radiation boundary condition does not assume any internal target dynamics, we can make a mapping between the parameters α and β and an absorption velocity κ through the equation

$$\kappa = \frac{\alpha}{\beta}\sqrt{\alpha + \beta}\sqrt{D}. \tag{5.106}$$

In other words, the optimal resetting rate in the problem of partial absorption is given by solving Eq. (5.101) with $w = \sqrt{rD}/2\kappa$ [143]. Therefore, the solution $r^*(\beta = \infty) =$

D/x_0^2 of Eq. (5.102) coincides with the optimal rate in the case of weak absorption, $\kappa \ll \sqrt{Dr}$ [143, 118]. However, this mapping between the two models is not valid for intermediate values of the transition rates. With the radiation boundary condition (5.104), the behaviour of the optimal resetting rate r^* is monotonic with respect to the absorption velocity κ, whereas the gating dynamics on time-scales comparable or longer than the diffusion time give rise to a new non-monotonic behaviour with respect to the target reactivity (Fig. 5.7).

These findings point out a close connection between partially absorbing and intermittent boundaries, a connection that has been revealed before in the context of simple diffusion (see Sec. 5.1.6). Eq. (5.106) is independent of the resetting rate and actually coincides with the expression found in Eq. (5.70) for a free Brownian particle. Furthermore, in [80], it was proved that the mean solution of the diffusion equation with a boundary condition switching infinitely fast between Dirichlet and Neumann conditions and with the boundary being in the Neumann condition most of the time, satisfies the Robin condition in a form equivalent to Eq. (5.106) above. Similar homogenization methods have been applied for the solutions of parabolic partial differential equations with intermittent boundaries [81].

5.2.4 Coefficient of variation

In this section we analyze the coefficient of variation defined as $C_{av} = \langle (t - T_{av})^2 \rangle / T_{av}^2$. This quantity represents the relative fluctuations of the first hitting time t, distributed according to the density $P_{av}(x,t)$, around its mean T_{av}. With the help of the relation (5.76), the coefficient of variation can be easily calculated:

$$C_{av} = -\frac{2}{T_{av}^2} \frac{\partial \widetilde{Q}_{av}(x_0,s)}{\partial s}\bigg|_{s=0} - 1. \tag{5.107}$$

Given the expression of the survival probability $\widetilde{Q}_{av}(x_0,s)$ in Eq. (5.93), we can obtain the coefficient of variation in a straightforward manner after some algebraic manipulations. However, it is convenient here to rewrite Eq. (5.93) in terms of the survival probability $\widetilde{Q}_r(x_0,s)$ for the ungated case, given by [55]

$$\widetilde{Q}_r(x_0,s) = \frac{1 - e^{-x_0\sqrt{\frac{s+r}{D}}}}{re^{-x_0\sqrt{\frac{s+r}{D}}} + s}. \tag{5.108}$$

Let us introduce the function

$$\widetilde{F}_r(x_0,s) = \frac{re^{-\sqrt{\frac{s+r}{D}}x_0} + s}{\sqrt{s+r}}. \tag{5.109}$$

With these definitions, the average survival probability is

$$\widetilde{Q}_{av}(x_0,s) = \frac{\alpha \widetilde{F}_r(x_0,s)\widetilde{Q}_r(x_0,s) + \beta \widetilde{F}_r(x_0,s+\alpha+\beta)/(s+\alpha+\beta)}{\alpha \widetilde{F}_r(x_0,s) + s\beta \widetilde{F}_r(x_0,s+\alpha+\beta)/(s+\alpha+\beta)}. \tag{5.110}$$

After taking the derivative with respect to s, we obtain

$$\left.\frac{\partial \widetilde{Q}_{av}(x_0,s)}{\partial s}\right|_{s=0} = \left.\frac{\partial \widetilde{Q}_r(x_0,s)}{\partial s}\right|_{s=0} - \left[T_{av}(x_0) - T_r(x_0)\right]\left[T_{av}(x_0) + \tfrac{1}{\alpha+\beta}\right] + \tfrac{\beta}{\alpha(\alpha+\beta)}\tfrac{\partial}{\partial s}\left(\frac{\widetilde{F}_r(x_0,s+\alpha+\beta)}{\widetilde{F}_r(x_0,s)}\right)\Bigg|_{s=0}, \tag{5.111}$$

where $T_r(x_0)$ is the MFPT for the ungated case given by Eq. (5.97). From the above expression, C_{av} is obtained in terms of the coefficient of variation C_r in the ungated case, which is calculated from an equation equivalent to Eq. (5.107), namely

$$C_r = -\frac{2}{T_r^2}\left.\frac{\partial \widetilde{Q}_r(x_0,s)}{\partial s}\right|_{s=0} - 1. \tag{5.112}$$

Substituting the partial derivative of $\widetilde{Q}_r(x_0,s)$ with respect to s into Eq. (5.112), one gets

$$C_{av} = \left(\tfrac{T_r(x_0)}{T_{av}(x_0)}\right)^2 (C_r+1) + 2\left[1 - \tfrac{T_r(x_0)}{T_{av}(x_0)}\right]\left[1 + \tfrac{1}{(\alpha+\beta)T_{av}(x_0)}\right] - \tfrac{2\beta}{\alpha(\alpha+\beta)[T_{av}(x_0)]^2}\tfrac{\partial}{\partial s}\left(\frac{\widetilde{F}_r(x_0,s+\alpha+\beta)}{\widetilde{F}_r(x_0,s)}\right)\Bigg|_{s=0} - 1. \tag{5.113}$$

The advantage of expressing the coefficient of variation C_{av} in terms of C_r is to elucidate how different the fluctuations of the FHT for a dynamical target are from those of a simple target. Specially important to us is to see whether a generic feature of processes under resetting at the optimal rate also holds in our model. It is known that search processes under stochastic resetting which are optimal at a non-zero resetting rate, which is the case here, have a coefficient of variation equal to unity at optimality [111, 107, 13]. This property holds true if the process is brought to the same initial state after each reset. In our case, this condition is not fulfilled, as resetting only acts on the particle and not on the target: after resetting the particle position, the target may not be in the state it occupied at $t = 0$ (we compare in 5.2.5 our results with the case where both the particle and the target are subject to resetting, as studied in [30]). In the following, we see that the aforementioned generic property holds in the limits $\beta \to 0$ and $\beta \to \infty$, but is violated in the more general intermediate regime.

It is straightforward to notice that when $\beta = 0$, we recover from Eq. (5.113) the coefficient of variation for the ungated case, or $C_{av}(\beta = 0) = C_r$ [recall that $T_{av}(\beta = 0) = T_r$]. In the limit $\beta \to \infty$, the first hitting times diverges as $T_{av} \propto \sqrt{\beta}$ (see Eq. 5.98), and it is not difficult to see from the definition of $\widetilde{F}_r(x_0,s)$ that, in the limit of large β and at the optimal resetting rate $r^*(\beta = \infty) = D/x_0^2$,

$$\frac{\partial}{\partial s}\left(\frac{\widetilde{F}_r(x_0,s+\alpha+\beta)}{\widetilde{F}_r(x_0,s)}\right)\Bigg|_{s=0} \propto \sqrt{\beta}. \tag{5.114}$$

One deduces from Eq. (5.113) that $C_{av}(r^*, \beta \to \infty) \to 1$. These limiting behaviours are checked in Fig. 5.8b with the exact solution.

Whereas the relative fluctuations of the first hitting times are unity at optimality in the cases $\beta = 0$ and $\beta = \infty$, this property is not general. The intricate way in which Eq. (5.113) depends on the target intermittency parameters does not allow an explicit analysis

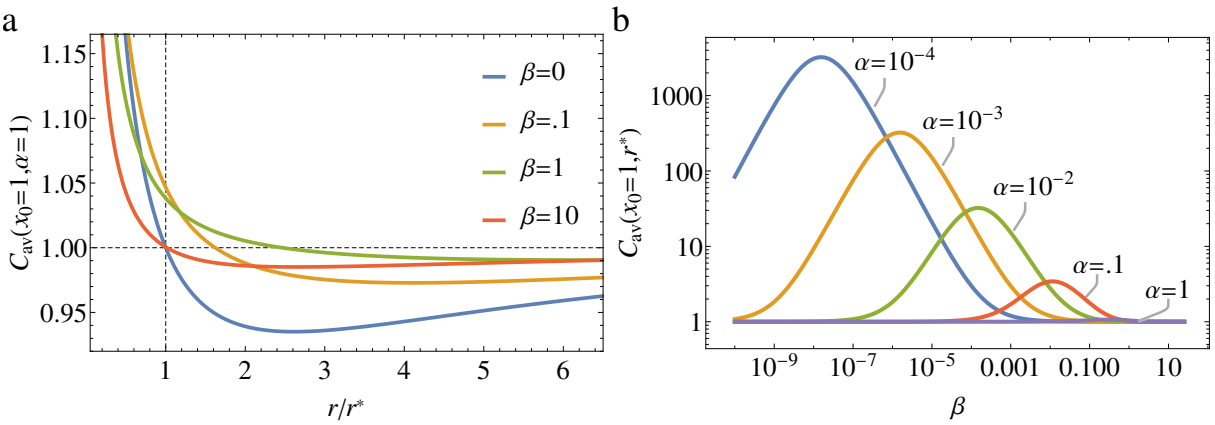

Figure 5.8: a) Coefficient of variation C_{av} as a function of r/r^* for fixed $x_0 = 1$, $D = 1$, $\alpha = 1$ and several values of β. b) Same quantity as a function of β at the optimal rate r^* (for $x_0 = 1$, $D = 1$).

at finite α and β. Nevertheless, we performed a numerical evaluation of Eq. (5.113) in a wide range of values of β and α at the corresponding optimal resetting rate r^*. The results are shown in Figs. 5.8a-b, where the coefficient of variation takes values different from unity. As displayed in Fig. 5.8b, when the target spends long periods of time in the two states, *i.e.*, when $\alpha, \beta \ll D/x_0^2$, the quantity C_{av} can take values much larger than 1 at optimality, even when the target is reactive most of the time ($\beta \ll \alpha$).

5.2.5 Comparison with the Bressloff's model

In this section we compare our expression for the MFHT, Eq. (5.96), with the analogous quantity deduced by Bressloff in [30]. In this work, a one dimensional Brownian particle diffuses in the interval $[0, L]$ and is subject to stochastic resetting to the initial position x_0, with $0 < x_0 < L$. A dynamic target placed at the origin switches between an active absorbing state and a reflecting state which prevents absorption. The MFHT for this model is given by equation (4.19) in [30], from which we can obtain the MFHT in the semi-infinite domain by taking the limit $L \to \infty$:

$$T_B(x_0) = \frac{e^{\sqrt{\frac{r}{D}}x_0} - 1}{r} + \frac{\beta e^{\sqrt{\frac{r}{D}}x_0}}{\alpha\sqrt{r(r+\alpha+\beta)}}, \tag{5.115}$$

with the same notation for the switching rates α and β than ours. Although the model studied in [30] is very similar, it bears an important difference. In [30], when the particle is reset to x_0, the state of the target is also re-initialised to the state $\sigma = 0$ [with probability $\beta/(\alpha+\beta)$] or $\sigma = 1$ [with probability $\alpha/(\alpha+\beta)$]. Conversely, in our model, the dynamics of the intermittent target is completely independent of the particle dynamics and not subject to resetting. This leads to quite different results for the behaviour of the mean time to absorption.

Eq. (5.115) can be rewritten in terms of $T_{av}(x_0)$ here as

$$T_B(x_0) = T_{av}(x_0) - \frac{\beta\sqrt{r}e^{\left(\sqrt{\frac{r}{D}} - \sqrt{\frac{r+\alpha+\beta}{D}}\right)x_0}}{\alpha(\alpha+\beta)\sqrt{r+\alpha+\beta}}, \tag{5.116}$$

which implies that T_B is lower than T_{av} for all non-zero values of the parameters α, β and r. It is easy to notice that the difference between both quantities can become very large for cases in which α and β are $\ll r$ (see Figs. 5.9a-c).

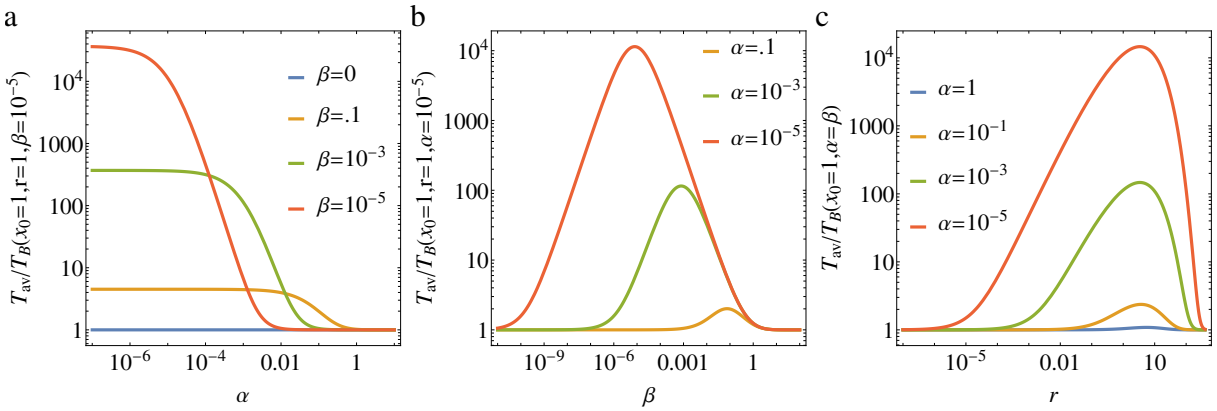

Figure 5.9: (a) Mean first hitting times T_{av}/T_B as a function of α and several values of β at $r = 1$. (b) Same quantity as a function of β for several values of α. (c) T_{av}/T_B as a function of r for several values of α (and $\beta = \alpha$). In all cases, $x_0 = 1$ and $D = 1$.

To further contrast between these results, let us analyse the limiting case in which the particle resets to the origin ($x_0 = 0$) at infinite rate ($r = \infty$). In this scenario, once the search process has started the particle immediately returns to the origin, with the target still being in its initial state. If the target is initially in the reactive state ($\sigma = 1$), the particle will be immediately absorbed, yielding to $T_1 = 0$. If the target is initially in the non-reactive state ($\sigma = 0$), the particle will remain at the origin (due to the infinitely frequent resetting) until the target switches to the reactive state with rate α, in this case $T_0 = 1/\alpha$. Therefore, from the definition of T_{av}, one obtains

$$T_{av}(x_0 = 0, r = \infty) = \frac{\beta}{\alpha(\alpha + \beta)}, \tag{5.117}$$

which in fact coincides with Eq. (5.96). Conversely, from Eq. (5.115) one can easily see that

$$T_B(x_0 = 0, r = \infty) = 0, \tag{5.118}$$

i.e., in [30] the particle is immediately absorbed irrespective the initial target state. This is a consequence of the resetting process which, being infinitely frequent, makes the target rapidly active, even if $\frac{\alpha}{\alpha+\beta} \ll 1$. In this model, stochastic resetting enhances target detection not only by means of the particle motion but also by promoting target activation.

We notice in Fig. 5.9 that T_{av} approaches T_B in the limit of high switching rates, *i.e.*, when $\alpha, \beta \gg r$. This can be seen directly from Eq. (5.116), where the second term of the right-hand-side approaches zero in this limit. Furthermore, when $\beta \to 0$, the two solutions $T_{av}(x_0)$ and $T_B(x_0)$ tend to that of the ungated case, given by $T_r(x_0)$ in Eq. (5.97).

5.3 Run-and-tumble

In this section we study the first hitting time statistics between a one-dimensional run-and-tumble particle and a target site that switches intermittently between visible and invisible phases. The two-state dynamics of the target is independent of the motion of the particle, which can be absorbed by the target only in its visible phase. This section is organized as follows: we begin in Section 5.3.1 by introducing the model and deduce the governing equations for the survival probabilities, which are solved in the Laplace domain in the general case. With the help of these results, in Section 5.3.2 we compute the MFHT and analyze this quantity for several limiting cases of the intermittent dynamic parameters and of the particle motion. Subsequently, in Section 5.3.3 we calculate the relative variance of the first hitting times. Section 5.3.4 is devoted to analyzing the FHTD in the unbounded case.

5.3.1 General setup and solution

We start by defining a time-dependent binary variable $\sigma(t)$ that describes the state of a target placed at the origin of a one-dimensional space, and that takes the value $\sigma = 1$ when it is visible (or active) and $\sigma = 0$ when it is hidden (or inactive). The target state switches at exponentially distributed times, with rate a for the transition $0 \to 1$ and with rate b for the transition $1 \to 0$. Therefore, the mean duration of the active (inactive) phase is $1/b$ ($1/a$, respectively) and the overall probability to find the target in the active state is $a/(a+b)$. We then consider a run-and-tumble particle that moves at constant speed v and changes its direction at a rate γ. Thus, the motion is governed by the equation

$$\frac{dx}{dt} = \Gamma(t) \tag{5.119}$$

where $\Gamma(t)$ is a dichotomous noise which takes constant values, $+v$ or $-v$, during exponentially distributed time intervals of mean duration $1/\gamma$. Two reflective barriers are placed at the positions $\pm L$, constraining the movement of the particle to the interval $(-L, L)$.

Fig. 5.10 depicts an example of first encounter in which the RTP (blue line) starts from $x(t=0) = L/2$ and with the initial velocity $+v$, whereas the target is initially in the visible state (in red). During the search process, the particle reverses its direction of motion randomly through tumble events or by reflections against the walls. If the particle crosses the origin while the target is hidden (white line), there is no encounter and the RTP simply follows its way; however, if the target is visible, it is detected and the process ends at the first hitting/encounter time t'.

In order to analyze the statistics of t' in this system, let us denote as $Q_0^+(x,t)$ [and $Q_0^-(x,t)$] the probability that the particle has not reacted up to time t, given the initial target state $\sigma(t=0) = 0$, the initial particle position $x \in (-L, L)$ and the initial velocity $+v$ [$-v$, respectively]. Similarly, we denote as $Q_1^+(x,t)$ and $Q_1^-(x,t)$ the survival probabilities when the target initial state is $\sigma(t=0) = 1$. We show in Appendix A.3 that these

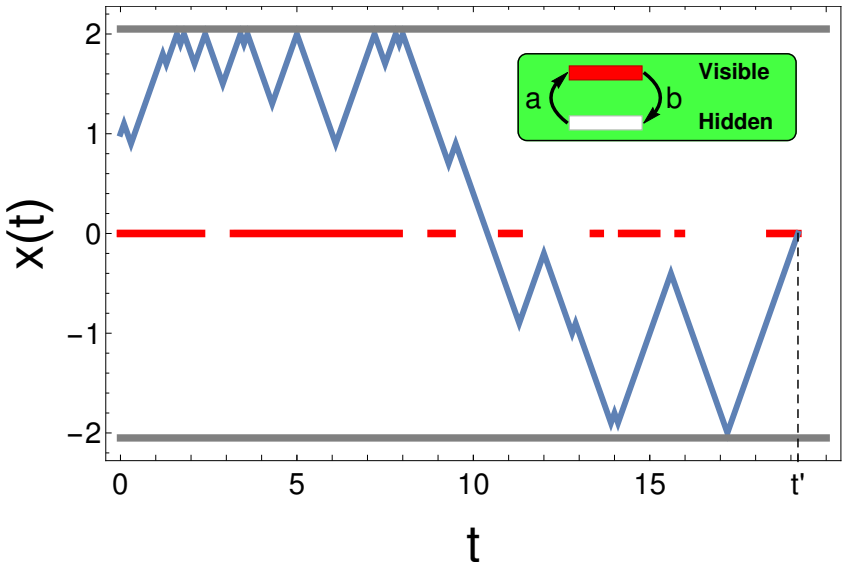

Figure 5.10: Run-and-tumble motion (blue line) in 1D in the presence of an intermittent target placed at the origin. The periods of the target in the visible state are represented by red segments, whereas the white intervals represent the target in its hidden state. The gray lines represent the reflective boundaries located at L and $-L$, with $L = 2$.

four probabilities satisfy the backward Fokker-Planck equations

$$\begin{aligned}
\frac{\partial Q_0^+}{\partial t} &= v\frac{\partial Q_0^+}{\partial x} - \gamma(Q_0^+ - Q_0^-) - a(Q_0^+ - Q_1^+),\\
\frac{\partial Q_0^-}{\partial t} &= -v\frac{\partial Q_0^-}{\partial x} - \gamma(Q_0^- - Q_0^+) - a(Q_0^- - Q_1^-),\\
\frac{\partial Q_1^+}{\partial t} &= v\frac{\partial Q_1^+}{\partial x} - \gamma(Q_1^+ - Q_1^-) - b(Q_1^+ - Q_0^+),\\
\frac{\partial Q_1^-}{\partial t} &= -v\frac{\partial Q_1^-}{\partial x} - \gamma(Q_1^- - Q_1^+) - b(Q_1^- - Q_0^-).
\end{aligned} \tag{5.120}$$

For the initial particle position $x > 0$, the system (5.120) will satisfy the following boundary conditions:

$$Q_1^-(x = 0^+, t) = 0, \tag{5.121}$$
$$Q_0^+(x = 0, t) = Q_0^-(x = 0, t), \tag{5.122}$$
$$Q_0^+(x = L, t) = Q_0^-(x = L, t), \tag{5.123}$$
$$Q_1^+(x = L, t) = Q_1^-(x = L, t). \tag{5.124}$$

The first condition asserts that the particle detects the target in state $\sigma = 1$ when it goes leftward from its immediate vicinity on the right. Eq. (5.122) stems from symmetry, as the target is placed in the middle of the domain. Eqs. (5.123)-(5.124) set the reflective condition on the wall placed at $x = L$.

We can also average over the initial target states and assume equal probabilities for the initial positive and negative particle velocities. The resulting average survival probability

is thus:

$$Q_{av}(x,t) = \frac{b}{a+b}\left(\frac{Q_0^+(x,t)+Q_0^-(x,t)}{2}\right) + \frac{a}{a+b}\left(\frac{Q_1^+(x,t)+Q_1^-(x,t)}{2}\right). \tag{5.125}$$

The probability distributions of the first hitting time (t) are denoted as $P_0^+(x,t)$, $P_0^-(x,t)$, $P_1^+(x,t)$ and $P_0^-(x,t)$ with the same notations as before for the initial conditions. These first hitting time densities (FHTD) are deduced from the survival probabilities through the usual relation [108]:

$$P_{0,1}^{\pm}(x,t) = -\frac{\partial Q_{0,1}^{\pm}(x,t)}{\partial t}. \tag{5.126}$$

In the following, it is convenient to set γ^{-1} as the unit of time and $v\gamma^{-1}$ as the unit of length, so that the system (5.120) can be recast, in the dimensionless variables $\tau = t\gamma$ and $z = x\gamma/v$, as

$$\begin{aligned}
\frac{\partial Q_0^+}{\partial \tau} &= \frac{\partial Q_0^+}{\partial z} - (Q_0^+ - Q_0^-) - \alpha(Q_0^+ - Q_1^+),\\
\frac{\partial Q_0^-}{\partial \tau} &= -\frac{\partial Q_0^-}{\partial z} - (Q_0^- - Q_0^+) - \alpha(Q_0^- - Q_1^-),\\
\frac{\partial Q_1^+}{\partial \tau} &= \frac{\partial Q_1^+}{\partial z} - (Q_1^+ - Q_1^-) - \beta(Q_1^+ - Q_0^+),\\
\frac{\partial Q_1^-}{\partial \tau} &= -\frac{\partial Q_1^-}{\partial z} - (Q_1^- - Q_1^+) - \beta(Q_1^- - Q_0^-).
\end{aligned} \tag{5.127}$$

which only depends on two parameters, the dimensionless rates:

$$\alpha = a\gamma^{-1}, \tag{5.128}$$

$$\beta = b\gamma^{-1}. \tag{5.129}$$

In these dimensionless units, the particle is thus restricted to $z \in (-\ell, \ell)$, where ℓ is the re-scaled domain size

$$\ell = L\gamma/v. \tag{5.130}$$

Introducing the Laplace transform $\widetilde{Q}(z,s) = \int_0^\infty e^{-s\tau} Q(z,\tau)d\tau$ and using the initial condition $Q(z,\tau=0) = 1$ for $0 < z < \ell$, the Laplace transform of Eqs. (5.127) gives

$$\frac{\partial}{\partial z}\begin{pmatrix}\widetilde{Q}_0^+\\ \widetilde{Q}_0^-\\ \widetilde{Q}_1^+\\ \widetilde{Q}_1^-\end{pmatrix} = \mathbb{A}\begin{pmatrix}\widetilde{Q}_0^+\\ \widetilde{Q}_0^-\\ \widetilde{Q}_1^+\\ \widetilde{Q}_1^-\end{pmatrix} - \begin{pmatrix}1\\ -1\\ 1\\ -1\end{pmatrix} \tag{5.131}$$

where

$$\mathbb{A} = \begin{pmatrix}1+s+\alpha & -1 & -\alpha & 0\\ 1 & -1-s-\alpha & 0 & \alpha\\ -\beta & 0 & 1+s+\beta & -1\\ 0 & \beta & 1 & -1-s-\beta\end{pmatrix} \tag{5.132}$$

The homogeneous part of Eq. (5.131) can be solved with the ansatz $\boldsymbol{\xi}e^{\lambda z}$, where λ and the vector $\boldsymbol{\xi}$ must be determined by diagonalizing (5.132), whereas the inhomogeneous solution is simply $\widetilde{Q}^{\pm}_{0,1} = 1/s$. After straightforward algebra, the general solution $\widetilde{\mathbf{Q}} = \begin{pmatrix}\widetilde{Q}_0^+ & \widetilde{Q}_0^- & \widetilde{Q}_1^+ & \widetilde{Q}_1^-\end{pmatrix}^T$ is given by the following linear combination of terms

$$\widetilde{\mathbf{Q}} = A_1\boldsymbol{\xi}_1 e^{-\lambda_1 z} + A_2\boldsymbol{\xi}_2 e^{\lambda_1 z} + A_3\boldsymbol{\xi}_3 e^{-\lambda_2 z} + A_4\boldsymbol{\xi}_4 e^{\lambda_2 z} + \widetilde{\mathbf{Q}}_{inh}, \tag{5.133}$$

where the factors A_k are determined by the boundary conditions and $\widetilde{\mathbf{Q}}_{inh}$ is the inhomogeneous solution with each entry equal to $1/s$. In Eq. (5.133), the eigenvalues λ_1 and λ_2 are positive and given by

$$\lambda_1 = \sqrt{s}\sqrt{2+s}, \quad \lambda_2 = \sqrt{\alpha+\beta+s}\sqrt{2+\alpha+\beta+s}, \tag{5.134}$$

whereas the eingenvectors are

$$\boldsymbol{\xi}_1 = \begin{pmatrix} 1+s-\lambda_1 \\ 1 \\ 1+s-\lambda_1 \\ 1 \end{pmatrix}, \boldsymbol{\xi}_2 = \begin{pmatrix} 1+s+\lambda_1 \\ 1 \\ 1+s+\lambda_1 \\ 1 \end{pmatrix},$$

$$\boldsymbol{\xi}_3 = \begin{pmatrix} -\frac{\alpha(1+s+\alpha+\beta-\lambda_2)}{\beta} \\ -\frac{\alpha}{\beta} \\ 1+s+\alpha+\beta-\lambda_2 \\ 1 \end{pmatrix}, \boldsymbol{\xi}_4 = \begin{pmatrix} -\frac{\alpha(1+s+\alpha+\beta+\lambda_2)}{\beta} \\ -\frac{\alpha}{\beta} \\ 1+s+\alpha+\beta+\lambda_2 \\ 1 \end{pmatrix}.$$

From Eq. (5.125), the average survival probability takes a simpler form:

$$\widetilde{Q}_{av}(z,s) = \frac{s+2-\lambda_1}{2}A_1 e^{-\lambda_1 z} + \frac{s+2+\lambda_1}{2}A_2 e^{\lambda_1 z} + \frac{1}{s}. \tag{5.135}$$

The boundary conditions in the Laplace domain are recast as

$$\widetilde{Q}_1^-(z=0^+,s) = 0, \tag{5.136}$$

$$\widetilde{Q}_0^+(z=0,s) = \widetilde{Q}_0^-(z=0,s), \tag{5.137}$$

$$\widetilde{Q}_0^+(z=\ell,s) = \widetilde{Q}_0^-(z=\ell,s), \tag{5.138}$$

$$\widetilde{Q}_1^+(z=\ell,s) = \widetilde{Q}_1^-(z=\ell,s). \tag{5.139}$$

With these conditions, the general solution in Eq. (5.133) admits a unique solution with the factors A_k given by

$$A_1 = -\frac{e^{\lambda_1\ell}(s+\lambda_1)\,\mathrm{csch}(\lambda_1\ell)}{2s\left(\lambda_1\coth(\lambda_1 l) + \frac{s}{\alpha}\left(\alpha+\beta+\frac{\beta\lambda_2\coth(\lambda_2\ell)}{\alpha+\beta+s}\right)\right)}, \tag{5.140}$$

$$A_2 = \frac{e^{-\lambda_1\ell}(s-\lambda_1)\,\mathrm{csch}(\lambda_1\ell)}{2s\left(\lambda_1\coth(\lambda_1 l) + \frac{s}{\alpha}\left(\alpha+\beta+\frac{\beta\lambda_2\coth(\lambda_2\ell)}{\alpha+\beta+s}\right)\right)}, \tag{5.141}$$

$$A_3 = -\frac{\beta e^{\lambda_2\ell}(s+\alpha+\beta+\lambda_2)(s+\alpha+\beta)^{-1}\mathrm{csch}(\lambda_2\ell)}{2\alpha\sqrt{s}\left(\lambda_1\coth(\lambda_1 l) + \frac{s}{\alpha}\left(\alpha+\beta+\frac{\beta\lambda_2\coth(\lambda_2\ell)}{\alpha+\beta+s}\right)\right)}, \tag{5.142}$$

$$A_4 = \frac{\beta e^{-\lambda_2\ell}(s+\alpha+\beta-\lambda_2)(s+\alpha+\beta)^{-1}\mathrm{csch}(\lambda_2\ell)}{2\alpha\sqrt{s}\left(\lambda_1\coth(\lambda_1 l) + \frac{s}{\alpha}\left(\alpha+\beta+\frac{\beta\lambda_2\coth(\lambda_2\ell)}{\alpha+\beta+s}\right)\right)}. \tag{5.143}$$

Inserting these expressions into the average survival probability (5.135) yields

$$\widetilde{Q}_{av}(z,s) = \frac{1}{s} - \frac{\lambda_1 \mathrm{csch}\left(\lambda_1 \ell\right) \cosh\left(\lambda_1 (z-\ell)\right)}{s\lambda_1 \coth \lambda_1 \ell + \frac{s^2}{\alpha}\left(\alpha+\beta+\frac{\beta\lambda_2 \coth(\lambda_2 \ell)}{\alpha+\beta+s}\right)}. \tag{5.144}$$

The FHTD can be obtained from relation (5.126) and the fact that, in the Laplace domain, $\partial Q(z,\tau)/\partial\tau$ transforms into $-1 + s\widetilde{Q}(z,s)$. Therefore, we have

$$\widetilde{P}_{av}(z,s) = \frac{\lambda_1 \mathrm{csch}\left(\lambda_1 \ell\right) \cosh\left(\lambda_1 (z-\ell)\right)}{\lambda_1 \coth \lambda_1 \ell + \frac{s}{\alpha}\left(\alpha+\beta+\frac{\beta\lambda_2 \coth(\lambda_2 \ell)}{\alpha+\beta+s}\right)} \quad . \tag{5.145}$$

Seeking for an inversion of Eqs. (5.144) or (5.145) does not look as simple as we would wish. However, one can exactly obtain from the above solution the mean first hitting time (MFHT), the second moment of the first hitting time distribution, as well as the behaviors of the tails of the full distribution. In the following sections we calculate the MFHT and the variance. We leave for section 5.3.4 the analysis of the FHTD in the limit $\ell \to \infty$.

5.3.2 Mean first hitting time

The mean first hitting time is given by $t_1(x) = \int_0^\infty t P_{av}(x,t)dt$, which, in units of γ^{-1}, can be written as $\tau_1(z) = \int_0^\infty \tau P_{av}(z,\tau)d\tau$. It is obtained from the Laplace transform of the survival probability if we use the relation (5.126) and integrate by parts to get $\tau_1(z) = \widetilde{Q}_{av}(z, s=0)$. Evaluating Eq. (5.144) in the limit $s \to 0$, we thus obtain the dimensionless MFHT

$$\begin{aligned}\tau_1(z) =& (2\ell - z)z + \ell + \frac{\beta\ell}{\alpha} \\ &+ \frac{\beta\ell}{\alpha}\sqrt{\frac{\alpha+\beta+2}{\alpha+\beta}} \coth \ell\sqrt{\alpha+\beta}\sqrt{\alpha+\beta+2}.\end{aligned} \tag{5.146}$$

It is convenient to define the global MFHT (in units of γ^{-1}), τ_G, which is obtained by averaging $\tau_1(z)$ over z, which corresponds to having a uniform distribution of starting positions:

$$\tau_G = \frac{1}{\ell}\int_0^\ell \tau_1(z)dz, \tag{5.147}$$

or, from Eq. (5.147),

$$\begin{aligned}\tau_G =& \ell + \frac{2}{3}\ell^2 + \frac{\beta\ell}{\alpha} \\ &+ \frac{\beta\ell}{\alpha}\sqrt{\frac{\alpha+\beta+2}{\alpha+\beta}} \coth \ell\sqrt{\alpha+\beta}\sqrt{\alpha+\beta+2}.\end{aligned} \tag{5.148}$$

The global MFPT is split into two contributions: one part corresponding to the case of a perfectly absorbing target (setting $\beta = 0$), and another which depends on both the parameters of the RTP (through $\ell = L\gamma/v$) and on the re-scaled target switching rates. In fact, one can see that $\tau_1(z)$ and τ_G are strictly increasing with β: the longer the target

is found in the hidden state, the longer it takes for the RTP to be absorbed. Figures 5.11a-b depict the mean global time given by Eq. (5.148) as a function of β for several values of α. It is interesting to notice that due to the hyperbolic function, the global MFPT abruptly increase at small β, as depicted in figure 5.11b. We successfully compare the analytic results with simulations that use the Gillespie algorithm [63].

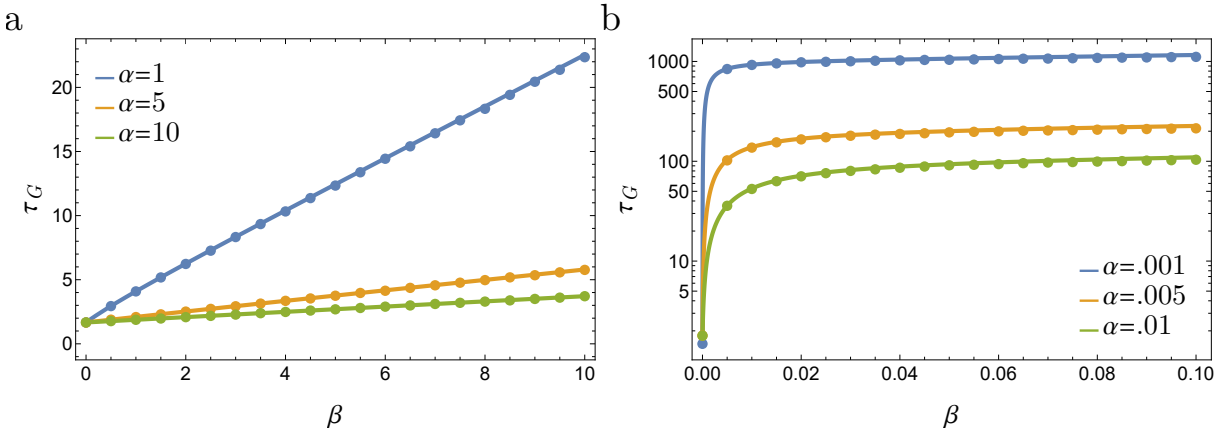

Figure 5.11: Global mean first hitting time as a function of β for $\ell = 1$. a) $\alpha = \{1, 5, 10\}$ and b) $\alpha = \{.001, .005, .01\}$. Symbols represent the results from an average of $50,000$ Gillespie simulations.

Defining

$$\epsilon = \frac{\alpha}{\alpha + \beta + \beta\sqrt{\frac{\alpha+\beta+2}{\alpha+\beta}}\coth \ell\sqrt{\alpha+\beta}\sqrt{\alpha+\beta+2}}, \tag{5.149}$$

equation (5.146) can be recast as

$$\tau_G = \frac{\ell}{\epsilon} + \frac{2}{3}\ell^2. \tag{5.150}$$

With this notation, we notice that τ_G takes the same expression as for a RTP confined on one side by a partially reflecting boundary at the origin, with absorption coefficient ϵ, and on the other side by a totally reflecting boundary placed at ℓ [4]. In such model there is no target dynamics: at each passage at the origin, the RTP is absorbed with probability $\eta \equiv 2\epsilon/(1+\epsilon)$ and reflected with probability $1-\eta$ [4, 93]. In our problem, yet, due to the temporal variations of the target state, η is not simply given by $\alpha/(\alpha+\beta)$, the probability that the target is found in the visible state, but depends in a more intricate way on the target rates and the effective turning rate ℓ. The effective absorption probability in our problem is thus affected by the relative time scales associated with target switching (with respect to the turning time of the RTP) and by the relative time needed by a ballistic particle to cross the whole domain (ℓ).

In physical units, the global MFHT is given by

$$t_G = \gamma^{-1}\tau_G, \tag{5.151}$$

and can be expressed from Eqs. (5.149)-(5.150) using the dimensional parameters as

$$t_G = \frac{L}{\kappa} + \frac{2L^2\gamma}{3v^2}. \tag{5.152}$$

where $\kappa = v\epsilon$ is given by

$$\kappa = \frac{va}{a+b+b\sqrt{\frac{a+b+2\gamma}{a+b}}\coth\frac{L\sqrt{a+b}\sqrt{a+b+2\gamma}}{v}}. \tag{5.153}$$

Several limiting cases ought to be mentioned:

(i) Perfect absorption, $\beta = 0$: From Eq. (5.149), one obtains $\epsilon = 1$, *i.e.*, the perfect absorption boundary condition. Hence, we recover the global mean first passage time

$$\tau_G(\beta = 0) = \ell + \frac{2}{3}\ell^2, \tag{5.154}$$

which was previously derived in [7].

(ii) High transition rates $\alpha \gg 1$ and $\beta \gg 1$: In this scenario, the target transitions are so fast that the RTP only "sees" a partial absorbing boundary with an absorption coefficient $\epsilon \approx \frac{\alpha}{\alpha+2\beta}$. This leads to $\eta \approx \alpha/(\alpha+\beta)$, *i.e.*, the probability that the particle is absorbed is equal to the probability that the target is found in the visible state. The global mean first passage time reads

$$\tau_G \approx \frac{\alpha+2\beta}{\alpha}\ell + \frac{2}{3}\ell^2. \tag{5.155}$$

(iii) Low transition rates $\alpha \ll 1$ and $\beta \ll 1$: In this case the absorption coefficient approaches

$$\epsilon \approx \frac{\alpha}{\alpha+\beta+\beta\sqrt{\frac{2}{\alpha+\beta}}\coth\ell\sqrt{2}\sqrt{\alpha+\beta}}. \tag{5.156}$$

(iv) Ballistic particle $\gamma = 0$: The other parameters being fixed, from Eq. (5.152) one can notice that t_G reaches a minimum at $\gamma = 0$ and

$$t_G(\gamma = 0) = \left(\frac{a+b}{av} + \frac{b}{av}\coth\frac{L(a+b)}{v}\right)L. \tag{5.157}$$

As in the stationary target case, the optimal strategy to react quickly with the dynamical target is ballistic motion. In this scenario, the particle performs straight line movements and only flips its direction when reflecting at the walls, crossing the origin periodically until it coincides with the target in the active state. On average, less persistent searchers waste time in fruitless excursions, not returning to the origin often enough to detect the target. In Appendix B we deduce Eq. (5.157) by another method, from purely probabilistic arguments.

(v) Brownian limit, $v \to \infty$, $\gamma \to \infty$ and v^2/γ fixed: Taking the limit of large v and γ with $v^2/(2\gamma) \equiv D$, the stochastic noise $\Gamma(t)$ in Eq. (5.119) becomes a white noise, leading to a Brownian motion with diffusion constant D [89, 125, 46]. In this limit, Eq. (5.152) becomes [134]

$$t_G = \frac{L}{\kappa} + \frac{L^2}{3D}, \tag{5.158}$$

with the effective reactivity coefficient given by

$$\kappa = \frac{a}{b}\sqrt{D(a+b)}\tanh L\sqrt{\frac{a+b}{D}}. \tag{5.159}$$

Eq. (5.158) coincides with the expression for a bounded Brownian particle with a partially absorbing boundary on one side, obeying the Robin boundary condition:

$$D\frac{d\rho}{dx}\Big|_{x=0} = \kappa\rho(x=0) \tag{5.160}$$

where ρ is the particle probability density. We remark that, when $L \longrightarrow \infty$, one recovers the reactivity coefficient $\kappa = \frac{a}{b}\sqrt{D(a+b)}$ that was first deduced in Section 5.1 for an unbounded Brownian particle. Therefore, Eq. (5.159) generalizes the connection that exists between partially absorbing and intermittent boundaries for Brownian particles.

5.3.3 Coefficient of variation

The Laplace transform of the FHTD given by Eq. (5.145) seem rather difficult to invert, however we can obtain from this expression the second moment of the distribution. Let us define the coefficient of variation of the first hitting time as

$$C_v = \frac{\langle\overline{[\tau' - \tau_G]^2}\rangle_z}{\tau_G^2}, \tag{5.161}$$

where the average $\langle\dot{\cdot}\rangle_z$ runs over both the realizations of the process and the starting position z. We use this quantity to assess the global fluctuations of τ' around its global mean, re-scaled by τ_G^2. Therefore,

$$C_v = \frac{\frac{1}{\ell}\int_0^\ell dz \int_0^\infty d\tau' P_{av}(z,\tau')(\tau' - \tau_G)^2}{\tau_G^2} \tag{5.162}$$

Integrating by parts and using the relation (5.126), the coefficient of variation can be written as

$$C_v = -\frac{2}{\ell\tau_G^2}\int_0^\ell dz \frac{\partial\widetilde{Q}_{av}(z,s)}{\partial s}\Big|_{s=0} - 1. \tag{5.163}$$

Using Eq. (5.144), one obtains

$$\begin{aligned} C_v =& 1 + \frac{2\ell^2}{\tau_G^2}\left[\frac{4\ell^2}{45} - \frac{1}{3}\right. \\ &\left. + \frac{\beta(1+\alpha+\beta)}{\alpha(\alpha+\beta)}\left(\operatorname{csch}^2 X + \frac{\coth X}{(1+\alpha+\beta)X}\right)\right], \end{aligned} \tag{5.164}$$

where X is defined as

$$X = \ell\sqrt{\alpha+\beta}\sqrt{\alpha+\beta+2}. \tag{5.165}$$

In the limit $\beta \to \infty$, τ_G diverges (the target is always invisible) and $C_v \to 1$, whereas for $\beta = 0$ (the target is always visible) the coefficient of variation only depends on ℓ. From Eq. (5.154) one gets

$$C_v(\beta = 0) = \frac{15 + 4\ell(15 + 7\ell)}{5(3+2\ell)^2}. \tag{5.166}$$

To the best of our knowledge, this expression has not been derived in the literature on RTPs.

Eq. (5.166) tells us that $C_v(\beta = 0)$ increases monotonically with the dimensionless length ℓ, which can be varied by moving the reflective walls further apart, or by changing the particle velocity v, or the turning rate γ. The coefficient of variation for a non-gated target is restricted to the interval $1/3 \leq C_v(\beta = 0, \ell) < 7/5$ (see Fig. 5.12). However, for the more general case with $\beta > 0$ and $\alpha > 0$, the full expression of the coefficient of variation suggests a more intricate dependence with ℓ. From numerical evaluations of Eq. (5.164) we observe that C_v can take values $\gg 1$ and also reaches a minimum at a non-trivial length $\ell^*(\alpha, \beta)$, as depicted in Fig. 5.12. Given α and β, the searcher can thus minimise the uncertainty on the first hitting time by adjusting its velocity to reach $\ell^*(\alpha, \beta)$.

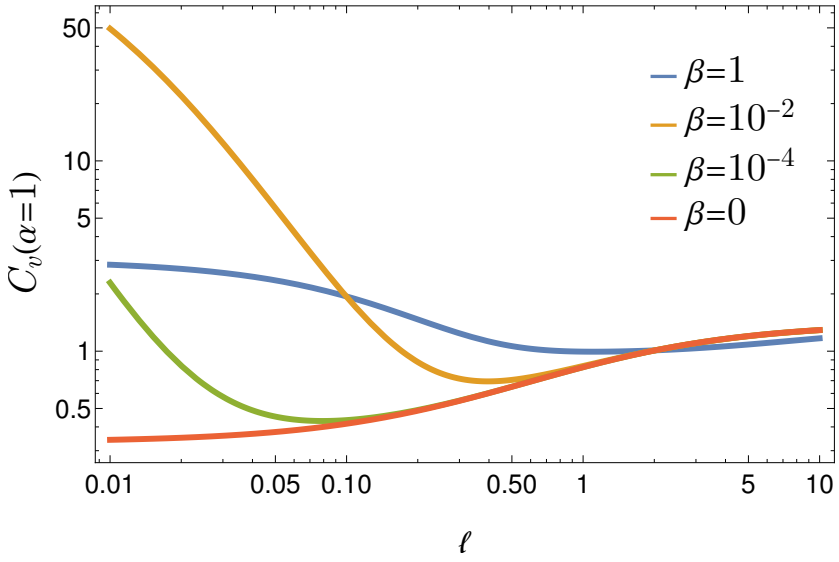

Figure 5.12: Relative variance as a function of ℓ for several values of β at fixed $\alpha = 1$. Symbols represent simulation results obtained with the Gillespie algorithm.

The curves of Fig. 5.12 also show a rather unexpected behaviour of the coefficient of variation: at fixed ℓ and α, C_v varies non-monotonically with β. As shown in Figures 5.13a-b and numerical evaluations of Eq. (5.164), C_v reaches a maximum as the switching rates β or α are varied at fixed ℓ. This maximum indicates that the distribution suddenly widens around its mean for a particular value of the target rate. In those situations, the first hitting times become less predictable and the MFHT less meaningful. Notably, the coefficient of variation can reach values much larger than unity when the re-scaled rates become small ($\alpha, \beta \ll 1$). Fixing $\alpha \ll 1$ and $\ell = 1$, we observe in Fig. 5.13a that C_v peaks at a value β^* which is much smaller than α, *i.e.*, when the inactive phases of the target are relatively brief compared to the active phases. This finding is paradoxical: the reaction time becomes widely unpredictable due to the target dynamics, but the target is most of the time reactive! On the other hand, when one fixes $\beta \ll 1$ and $\ell = 1$, one finds that C_v peaks at a value α^* which is of the same order as β (see Fig.5.13b), that is, when the target spends on average the same time in the active phase as in the inactive phase.

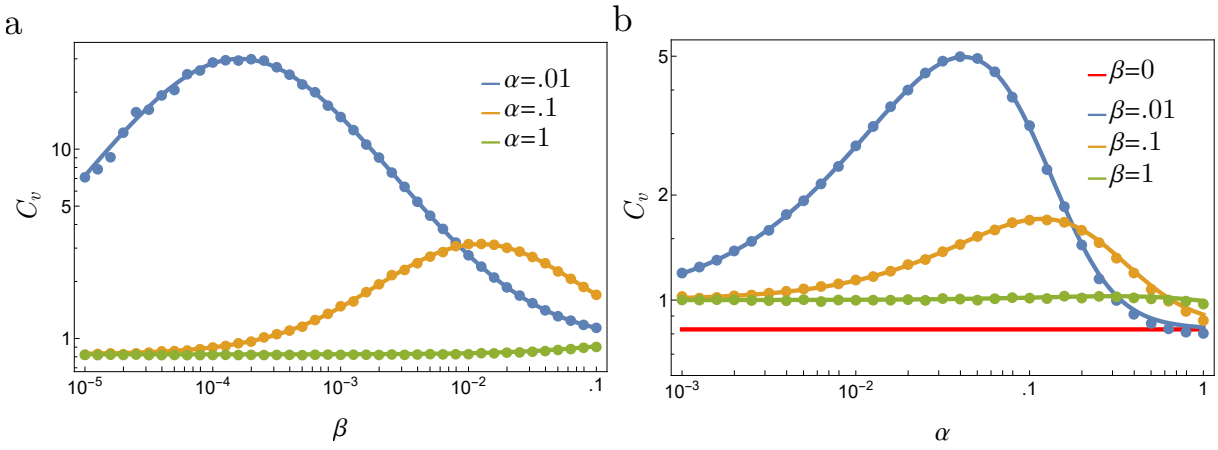

Figure 5.13: a) Coefficient of variation as a function of β for several values of α at fixed $\ell = 1$, b) Same quantity as a function of α for several values of β. In both cases, $\ell = 1$. Symbols represent simulation results obtained with the Gillespie algorithm.

5.3.4 Infinite domain

In this section, we study the RTP and the intermittent target in the limit of infinite domain size. In this case, the asymptotic forms of the survival probability can be obtained explicitly. For convenience, in the following analysis we will work with the dimensional variables $\{x, t, \gamma, a, b\}$ and use the Laplace transform $\widetilde{Q}(x,u) = \int_0^\infty e^{-ut} Q(x,t)dt$, which is equivalent to take $\widetilde{Q}(x,u) = \gamma^{-1}\widetilde{Q}(z,s)$ in Eq. (5.144), with $u = s\gamma$. By taking the limit $\ell \to \infty$ in Eq. (5.144), we get

$$\widetilde{Q}_{av}(x,u) = \frac{1}{u} - \frac{e^{-\frac{x}{v}\sqrt{u(u+2\gamma)}}}{u + \frac{u}{a}\sqrt{\frac{u}{u+2\gamma}}\left(a+b+b\sqrt{\frac{u+a+b+2\gamma}{u+a+b}}\right)}. \tag{5.167}$$

Despite the fact that this expression has not a simple form allowing an exact inversion from the Laplace domain, it is possible to analyze the long time behaviour of the survival probability and the associated first hitting time distribution. The long time regime can be extracted from the small u expansion of the image function $\widetilde{Q}_{av}(x,u)$. Making the approximations $\sqrt{u(u+2\gamma)} \approx \sqrt{2\gamma u}$, $\sqrt{u/(u+2\gamma)} \approx \sqrt{u/(2\gamma)}$ and $\sqrt{a+b+u} \approx \sqrt{a+b}$, Eq. (5.167) becomes

$$\widetilde{Q}_{av}(x,u) \simeq \frac{1}{u}\left(1 - \frac{e^{-\frac{x}{v}\sqrt{2\gamma u}}}{1+R\sqrt{u}}\right) \tag{5.168}$$

where we have defined $R = \frac{1}{\sqrt{2\gamma a}}\left(a+b+b\sqrt{\frac{a+b+2\gamma}{a+b}}\right)$. The above expression can be exactly inverted [1] to yield

$$Q_{av}(x,t) \simeq \operatorname{erfc}\left(\frac{\sqrt{t}}{R} + \frac{x}{v}\sqrt{\frac{\gamma}{2t}}\right)\exp\left(\frac{x\sqrt{2\gamma}}{vR} + \frac{t}{R^2}\right) + \operatorname{erf}\left(\frac{x}{v}\sqrt{\frac{\gamma}{2t}}\right), \tag{5.169}$$

and, from Eq. (5.126),

$$P_{av}(x,t) \simeq \frac{1}{R\sqrt{\pi t}} \exp\left(-\frac{\gamma x^2}{2tv^2}\right) - \frac{1}{R^2}\,\mathrm{erfc}\left(\frac{\sqrt{t}}{R} + \frac{x}{v}\sqrt{\frac{\gamma}{2t}}\right) \exp\left(\frac{x\sqrt{2\gamma}}{vR} + \frac{t}{R^2}\right), \tag{5.170}$$

where $\mathrm{erf}(z) = \frac{2}{\sqrt{\pi}} \int_0^z e^{-\xi^2} d\xi$ is the error function and $\mathrm{erfc}(z) = 1 - \mathrm{erf}(z)$ the complementary error function. Due to the approximations made, Eqs. (5.169)-(5.170) hold for t larger than both the target relaxation time $t_{ta} \equiv (a+b)^{-1}$ and the tumble time $t_{tb} \equiv (2\gamma)^{-1}$.

From the above equations one can see that the first hitting time distribution (and also the survival probability) is determined by two characteristic timescales: a diffusive time $t_D = x^2\gamma/(2v^2)$, which is the typical time needed for the particle to reach the origin, and the time

$$t_c = R^2 = \frac{1}{2\gamma a^2}\left(a + b + b\sqrt{\frac{a+b+2\gamma}{a+b}}\right)^2, \tag{5.171}$$

that sets a crossover time that separates two different scaling regimes in the asymptotic behaviour of the FHTD. These regimes are deduced from Eq. (5.170) as follows (the analysis can also be done directly from the image function $\widetilde{Q}_{av}(x,u)$ in Eq. (5.168), see Section 5.1):

- *The true asymptotic limit $t \gg t_c$:* in this limit we can use the approximation $\mathrm{erfc}(x) \approx \frac{e^{-x^2}}{\sqrt{\pi}x}\left(1 - \frac{1}{2x^2} + \dots\right)$ to get

$$P_{av}(x,t) \simeq \frac{x\sqrt{2\gamma}/v + R}{2\sqrt{\pi t^3}}, \quad t \gg t_c, \tag{5.172}$$

  which is the tail of the Lévy-Smirnov distribution typical of Brownian motion and random walks [60], but with a different prefactor. The modification of this prefactor is a phenomenon that has also been observed in random search problems with fluctuating targets on networks, including the case of non-Markovian switching dynamics [34, 32].

- *The intermediate regime:* if t_c is much larger than all the other characteristic times, or $t_c \gg \max(t_D, t_{ta}, t_{tb})$, the arguments in the exponential and the complementary error functions are small and we notice that, before the true asymptotic regime, an intermediate time regime appears:

$$P_{av}(x,t) \simeq \frac{1}{R\sqrt{\pi t}}, \quad \max(t_D, t_{ta}, t_{tb}) \ll t \ll t_c. \tag{5.173}$$

Eq.(5.173) represents a much slower decay than the standard $t^{-3/2}$ scaling. For simplicity, in the following we will assume $t_D \ll t_{ta}, t_{tb}$, a condition which is easily enforced by choosing $x = 0$, *i.e.*, by initially placing the particle right on the target. As we have done in Section 5.3.2, we analyze below different limiting cases.

(i) Perfect absorption, $b = 0$: From Eq. (5.171) one obtains $t_c = t_{tb}$, therefore the conditions for the existence of the intermediate regime are not fulfilled and we find the asymptotic decay [89]

$$P_{av}(x,t) \simeq \left(x\sqrt{2\gamma}/v + 1/\sqrt{2\gamma}\right)/\sqrt{4\pi t^3}. \tag{5.174}$$

(ii) High transition rates $a, b \gg \gamma$: In this case $\max(t_{ta}, t_{tb}) = t_{tb}$ and $t_c \simeq \left(\frac{a+2b}{\sqrt{2\gamma}a}\right)^2$, therefore

$$\frac{t_c}{t_{tb}} \simeq \left(\frac{a+2b}{a}\right)^2. \tag{5.175}$$

(iii) Low transition rates $a, b \ll \gamma$: Here, $\max(t_{ta}, t_{tb}) = t_{ta}$ and $t_c \simeq \frac{b^2}{a^2(a+b)}$, then

$$\frac{t_c}{t_{ta}} \simeq \frac{b^2}{a^2}. \tag{5.176}$$

(iv) Ballistic particle $\gamma = 0$: From the inversion of Eq. (5.167), one obtains that, for the ballistic searcher, $P_{av}(x,t) = \frac{a\delta(t-x/v)}{2(a+b)}$ for $t > 0$, which is the condition for the particle to start at $x > 0$ and move, with probability $1/2$, in a straight line towards the origin and then, with probability $a/(a+b)$, hit the target.

(v) Brownian limit, $v \to \infty$, $\gamma \to \infty$ and v^2/γ fixed: In this case we recover the result

$$\frac{t_c}{t_{ta}} = \frac{b^2}{a^2} \tag{5.177}$$

deduced in Section 5.1 for a Brownian particle, and which actually coincides with Eq. (5.176).

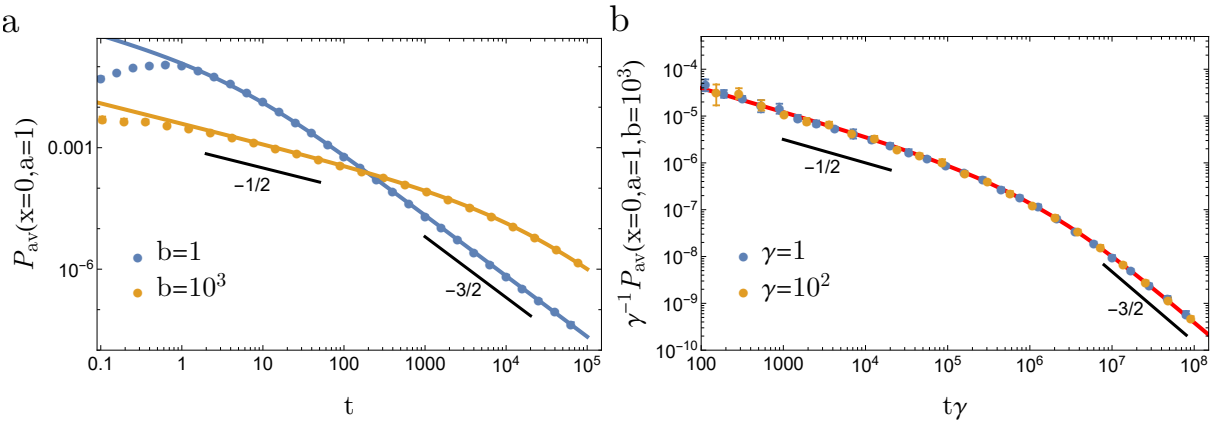

Figure 5.14: a) FHTD for a run-and-tumble particle that start at $x = 0$, with $a = 1$, $\gamma = 1$ and $b = \{1, 10^3\}$. b) Same quantity for $b = 10^3$ and $\gamma = \{1, 10^2\}$. Lines are the analytical solution given by Eq. (5.170) and symbols represents simulation results.

From Eqs. (5.175)-(5.177), we conclude that the intermediate scaling regime $\sim t^{-1/2}$ of the FHTD emerges when the target is cryptic, *i.e.*, when $b \gg a$ (see Fig. 5.14a). We also see that the crossover time becomes longer as β increases. In addition to this, the result in Eq. (5.177) is interesting since it implies that the Brownian motion becomes

the best strategy that the searcher can opt in order to reduce (as much as possible) the slow decay range ($\sim t^{-1/2}$) in the FHTD. This is owing to the recurrence property of the Brownian motion, that ensures that the particle recrosses the origin many times within a short period of time.

Chapter 6

Random searches in the presence of fluctuating media

In this chapter we address the problem of random searches in the presence of fluctuating media. Here a Brownian particle will be embedded in a media that fluctuates in time. These fluctuations will be modeled through the application of external intermittent potentials. The chapter is organized as follows:

We start in Section 6.1 by studying the non-equilibrium steady states and first passage properties of a Brownian particle with position X subject to an external confining potential of the form $V(X) = \mu|X|$, and that is switched on and off stochastically. Applying the potential intermittently generates a physically realistic diffusion process with stochastic resetting toward the origin, a topic which has recently attracted a considerable interest in a variety of theoretical contexts but has remained challenging to implement in lab experiments. The present system exhibits rich features, not observed in previous resetting models. The mean time needed by a particle starting from the potential minimum to reach an absorbing target located at a certain distance can be minimized with respect to the switch-on and switch-off rates. The optimal rates undergo continuous or discontinuous transitions as the potential strength μ is varied across non-trivial values. A discontinuous transition with metastable behavior is also observed for the optimal strength at fixed rates.

In section 6.2 we extend our study to more general intermittent potentials. In particular, we analyze the case of a potential of the form $V(X) = K|X - X_0|^n/n$. We focus on the mean first passage time to a fixed absorbing target, and analyze its behaviour as a function of the potential stiffness K and the rates that governs the switch-on and switch-off rates. Similarly to the piece-wise potential case, the MFPT to a fixed target can get optimized by intermittently applying a confining potential. Again, we observe that the system undergoes order transitions in the optimal rates. We particularly focus on the harmonic potential case with $n = 2$, and recover previous results for the linear potential ($n = 1$).

6.1 Intermittent piecewise linear potential

In this section, we study another first passage problem for a particle in a fluctuating environment. We consider a Brownian particle in one dimension with diffusion constant D and friction coefficient α, driven by the action of an intermittent external potential. The state of the potential is described by a time dependent binary variable $\sigma(t)$, where $\sigma(t) = 0$ means that the potential is switched off and $\sigma(t) = 1$ that it is applied. In the "on" state, the potential has a V-shape, given by $V(X) = f|X|$ with X the position and $f > 0$, whereas $V(X) = 0$ in the "off" state. The two-state process σ is Markovian and characterized by constant transition rates, R_0 (for the transition $0 \to 1$) and R_1 (for $1 \to 0$).

Due to the action of the external potential that confines the particle diffusion, we expect a non-equilibrium stationary density for the particle position (irrespective of the potential state), on the unbounded line. Further, when an absorbing target is placed at a fixed position, we whish to calculate the mean first passage time (MFPT), if it is finite.

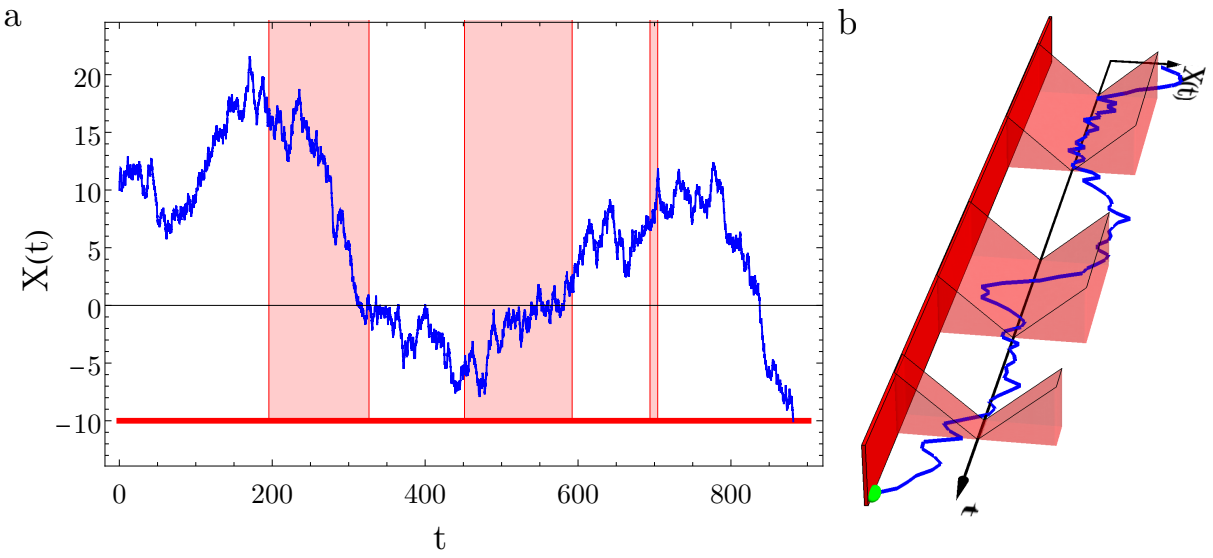

Figure 6.1: a) Trajectory of a diffusive particle with diffusion constant $D = 1$, in an intermittent resetting potential ($\mu = 0.1$). The shaded zones represent the time intervals when the potential is turned on ($R_0 = R_1 = 0.005$). An absorbing boundary is placed at $X = -10$. b) $3D$ representation of a particle trajectory in the time-dependent potential ($\mu = 1$).

Figure 6.1 depicts trajectories in the presence of an absorbing boundary (target) at the position $-L = -10$. Free diffusion is interspersed with random periods of potential reset, during which the particle it is attracted toward the origin. This dynamics is somehow similar to diffusion with a non-instantaneous resetting protocol for the particle, with three important differences compared to recent studies on this subject: 1) the return toward the origin is not deterministic but stochastic, owing to diffusion; 2) the particle is not necessarily at the potential minimum $X = 0$ when the potential is switched off, as the dynamics of $\sigma(t)$ is independent of the particle position; 3) the target at $-L$ is always detectable, *i.e.*, it can be found when the potential state is either 0 or 1. Therefore the search process is not suspended during the "on" phase, an often assumed. This assumption will have important consequences, as seen further.

In the following we introduce the Langevin equation for the particle motion. Like in the previous sections, we first develop the backward Fokker-Planck equation for the survival probability, which is a preliminary step to find the MFPT. Recall that in the previous problem of free diffusion with intermittent targets, the MFPT was infinite. After analysing the MFPTs, we will turn to the calculation of the probability density of the particle position in an unbounded $1d$ domain, without absorbing target.

6.1.1 Langevin equation

When we introduced the Langevin equation in Section 4.3, we mentioned that, in order to determine the backward Fokker-Planck equation we would have to calculate the Kramer-Moyal coefficients. For Brownian motion, inertia is neglected and diffusion is due to the friction forces (the Stokes' force) and thermal fluctuations. When an external potential is applied, one has to add the external force to the Langevin equation.

Then, the evolution of the particle position $X(t)$ in the time-varying potential $V(X) = f|X|$ will be given by the Langevin equation

$$m\frac{d^2X}{dt^2} = F_{friction} + F_{ext} + F_{random} \tag{6.1}$$

where $F_{friction} = -\alpha dX/dt$ is the Stokes' force, F_{random} is the random force due to thermal fluctuations, and $F_{ext} = -\left(dV/dx\right)\sigma(t) = -f\,\mathrm{sgn}(X)\sigma(t)$ is the force owing to the external potential that is applied according to the two state stochastic process $\sigma(t)$ defined previously (the term $\mathrm{sgn}(X)$ comes from the derivative of the potential). If we neglect the left hand side (inertia), we obtain

$$\frac{dX}{dt} = -\mu\,\mathrm{sgn}(X)\sigma(t) + \Gamma(t), \tag{6.2}$$

with $\mu = f/\alpha$ and $\Gamma(t)$ a Gaussian white noise with zero mean and correlations $\langle\Gamma(t)\Gamma(t')\rangle = 2D\delta(t-t')$. The V-shaped potential is convenient for analytical calculations, but we expect other confining potentials to yield qualitatively similar results.

For convenience, we introduce the dimensionless space and time variables $x = X/L$ and $t/(L^2/D)$ (which we renote as t). The problem is fully described by three dimensionless parameters:

$$r_0 = R_0L^2/D, \tag{6.3}$$
$$r_1 = R_1L^2/D, \tag{6.4}$$
$$\gamma = \mu L/D, \tag{6.5}$$

namely, the re-scaled "on" and "off" rates, and the re-scaled potential strength, respectively.

Before to proceed to the next section, we would like to briefly mention several limiting cases that we will be important for the understanding of the model. In the limit $r_1 = 0$ and if $\sigma(t=0) = 1$, the potential is stationary and, in the unbounded domain, $x(t)$ follows the Boltzmann-Gibbs equilibrium distribution $\propto \exp\left(-\gamma|x|\right)$ at long times. Another limit is that of infinite strength, more specifically $\gamma \to \infty$, which corresponds to an instantaneous resetting to the origin, followed by a refractory time (exponentially distributed and of

mean $1/r_1$) during which the particle stays immobile (see [56]). If $\gamma = \infty$ and $r_1 \to \infty$, one recovers the standard diffusion problem with stochastic resetting at rate r_0 to the origin, where the particle is released immediately after resetting [55].

6.1.2 Survival probability

Let us consider an absorbing boundary placed at -1 in dimensionless units and define $Q_0(x,t)$ as the probability that the particle has not hit the boundary up to time t, given the initial position x and the potential initially in the off state $\sigma(t=0)=0$. Similarly, $Q_1(x,t)$ when the potential is initially on, or $\sigma(t=0)=1$. These two survival probabilities satisfy the backward Fokker-Planck equations

$$\frac{\partial Q_0}{\partial t} = \frac{\partial^2 Q_0}{\partial x^2} + r_0(Q_1 - Q_0), \tag{6.6}$$

$$\frac{\partial Q_1}{\partial t} = \frac{\partial^2 Q_1}{\partial x^2} - v'(x)\frac{\partial Q_1}{\partial x} + r_1(Q_0 - Q_1), \tag{6.7}$$

where $v(x) = \gamma|x|$ is the dimensionless potential. To derive this system of equations, one first notices that $x(t)$ obeys the adimensionalised version of Eq. (6.2):

$$\frac{dx}{dt} = -\sigma(t)\gamma\,\mathrm{sgn}(x) + \eta(t), \tag{6.8}$$

where $\eta(t)$ is now a dimensionless Gaussian noise with zero mean and correlations $\langle \eta(t)\eta(t')\rangle = 2\delta(t-t')$.

Let us consider that the particle starts from x at time $t=0$, whereas the potential is in the state $\sigma(t=0)=0$. During the interval $[0,\Delta t]$ the particle travels from x to $x+\xi$, where ξ is a random displacement and Δt is an small time increment. When the particle is at $x+\xi$, with probability $r_0\Delta t$ the potential turns on and then, the particle will driven by the external potential and the thermal fluctuations from $x+\xi$ to x' during $[\Delta t, t+\Delta t]$, otherwise, with probability $1-r_0\Delta t$ the particle will diffuse from $x+\xi$ to x' with the potential turned off. This can be expressed by the Chapman-Kolmogorov equation

$$Q_0(x,t+\Delta t) = (1-r_0\Delta t)\int d\xi P_{\Delta t}(\xi) Q_0(x+\xi,t) + r_0\Delta t \int d\xi P_{\Delta t}(\xi) Q_1(x+\xi,t), \tag{6.9}$$

where $P_{\Delta t}(\xi)$ is the transition probability density of the random displacement ξ (see Section 4.2). Similarly, for the initial state $\sigma(t=0)=1$ we obtain

$$Q_1(x,t+\Delta t) = r_1\Delta t \int_{-\infty}^{\infty} d\xi P_{\Delta t}(\xi) Q_0(x+\xi,t) + (1-r_1\Delta t)\int_{-\infty}^{\infty} d\xi P_{\Delta t}(\xi) Q_1(x+\xi,t). \tag{6.10}$$

Performing a Taylor series of $Q_\sigma(x+\xi,t)$ in powers of ξ up to second order, we get

$$\begin{aligned} Q_\sigma(x,t+\Delta t) =& (1-r_\sigma\Delta t)\int d\xi P(\xi)\left\{Q_\sigma(x,t) + \frac{\partial Q_\sigma(x,t)}{\partial x}\xi + \frac{1}{2}\frac{\partial^2 Q_\sigma(x,t)}{\partial x^2}\xi^2\right\} \\ &+ r_\sigma\Delta t \int d\xi P(\xi)\left\{Q_{1-\sigma}(x,t) + \frac{\partial Q_{1-\sigma}(x,t)}{\partial x}\xi + \frac{1}{2}\frac{\partial^2 Q_{1-\sigma}(x,t)}{\partial x^2}\xi^2\right\}, \end{aligned} \tag{6.11}$$

which allows us to carry out of the integral terms that do not depend on ξ, namely, the survival probability $Q_\sigma(x,t)$ and its derivatives. With this, the right hand side of Eq. (6.11) can be expressed in terms of the moments $\langle \xi^n \rangle$.

From Eq. 6.8 we have that, if the potential is switched off ($\sigma = 0$), the particle freely diffuses, hence integration gives $\langle \xi \rangle = 0$ and $\langle \xi^2 \rangle = 2\Delta t$. On the other hand, if the potential is switched on ($\sigma = 1$), $\langle \xi \rangle = -\gamma \,\mathrm{sgn}(x)\Delta t$ whereas the term $\langle \xi^2 \rangle$ produces a contribution of order Δt^2, which is neglectable.

Let us denote $Q_0^+(x) = Q_0(x)$ with $x > 0$ and $Q_0^-(x) = Q_0(x)$ with $x < 0$. Similarly, $Q_1^+(x) = Q_1(x)$ with $x > 0$ and $Q_1^-(x) = Q_1(x)$ with $x < 0$. Keeping terms only up to $\mathcal{O}(\Delta t)$, Eq. (6.11) becomes

$$\begin{aligned} Q_0^+(x,t+\Delta t) =& (1 - r_0\Delta t)\Big\{ Q_0^+(x,t) + \frac{\partial^2 Q_0^+(x,t)}{\partial x^2}\Delta t \Big\} \\ &+ r_0\Delta t\Big\{ Q_1^+(x,t) - \frac{\partial Q_1^+(x,t)}{\partial x}\gamma\Delta t + \frac{\partial^2 Q_1(x,t)}{\partial x^2}\Delta t \Big\}, \end{aligned} \tag{6.12}$$

$$\begin{aligned} Q_0^-(x,t+\Delta t) =& (1 - r_0\Delta t)\Big\{ Q_0^-(x,t) + \frac{\partial^2 Q_0^-(x,t)}{\partial x^2}\Delta t \Big\} \\ &+ r_0\Delta t\Big\{ Q_1^-(x,t) + \frac{\partial Q_1^-(x,t)}{\partial x}\gamma\Delta t + \frac{\partial^2 Q_1^-(x,t)}{\partial x^2}\Delta t \Big\}, \end{aligned} \tag{6.13}$$

$$\begin{aligned} Q_1^+(x,t+\Delta t) =& (1 - r_1\Delta t)\Big\{ Q_1^+(x,t) - \frac{\partial Q_1^+(x,t)}{\partial x}\gamma\Delta t + \frac{\partial^2 Q_1^+(x,t)}{\partial x^2}\Delta t \Big\} \\ &+ r_1\Delta t\Big\{ Q_0^+(x,t) + \frac{\partial^2 Q_0^+(x,t)}{\partial x^2}\Delta t \Big\}. \end{aligned} \tag{6.14}$$

$$\begin{aligned} Q_1^-(x,t+\Delta t) =& (1 - r_1\Delta t)\Big\{ Q_1^-(x,t) + \frac{\partial Q_1^-(x,t)}{\partial x}\gamma\Delta t + \frac{\partial^2 Q_1^-(x,t)}{\partial x^2}\Delta t \Big\} \\ &+ r_1\Delta t\Big\{ Q_0^-(x,t) + \frac{\partial^2 Q_0^-(x,t)}{\partial x^2}\Delta t \Big\}. \end{aligned} \tag{6.15}$$

In the limit $\Delta t \to 0$ we obtain Eqs. (6.6)-(6.7).

Using the Laplace transform, $\tilde{Q}(x,s) = \int_0^\infty dt e^{-st} Q(x,t)$, the system (6.6)-(6.7) can be written in the Laplace domain as

$$\frac{\partial^2 \tilde{Q}_0^+}{\partial x^2} + r_0\tilde{Q}_1^+ - (r_0 + s)\tilde{Q}_0^+ = -1, \tag{6.16}$$

$$\frac{\partial^2 \tilde{Q}_1^+}{\partial x^2} - \gamma\frac{\partial \tilde{Q}_1^+}{\partial x} + r_1\tilde{Q}_0^+ - (r_1 + s)\tilde{Q}_1^+ = -1, \tag{6.17}$$

where we have used the initial condition $Q_{0,1}^+(x, t = 0) = 1$. We notice at this point that a system like (6.16)-(6.17) is difficult to solve exactly *a priori*. Whereas the inhomogeneous solution is given by $\tilde{Q}_0^+ = \tilde{Q}_1^+ = 1/s$, seeking for homogeneous solutions of the form $e^{\lambda x}$ yields the equation

$$\begin{vmatrix} \lambda^2 - (r_0 + s) & r_0 \\ r_1 & \lambda^2 - \gamma\lambda - (r_1 + s) \end{vmatrix} = 0. \tag{6.18}$$

This determinant yields a 4th order polynomial for the eigenvalues λ, which seems arduous to solve. The same system is obtained for $\tilde{Q}^-$, with a change in the sign in front of γ.

In the following we are interested in the mean first passage time $t_0(x)$ (in units of L^2/D) given the initial particle position x and the initial potential state $\sigma = 0$ (with the target at the dimensionless position -1), which is given by

$$t_0(x) = \int_0^\infty tP_0(x,t)dt = \int_0^\infty t\frac{\partial Q_0(x,t)}{\partial t}dt = \int_0^\infty Q_0(x,t)dt = \widetilde{Q}_0(x, s=0). \tag{6.19}$$

Anagolously, for the initial potential state $\sigma = 1$, the MFPT $t_1(x) = \widetilde{Q}_1(x, s = 0)$. With $s = 0$, Eq. (6.18) simplifies, as one eigenvalue is always 0 and the remaining three are the roots of a cubic polynomial.

The system (6.16)-(6.17) with $s = 0$ gives the equations satisfied by the re-scaled MFPTs $t_0(x)$ and $t_1(x)$. By denoting $t_0^+(x)$ and $t_1^+(x)$ as the MFPTs for $x > 0$, we have:

$$\frac{\partial^2 t_0^+(x)}{\partial x^2} + r_0[t_1^+(x) - t_0^+(x)] = -1, \tag{6.20}$$

$$\frac{\partial^2 t_1^+(x)}{\partial x^2} - \gamma\frac{\partial t_1^+(x)}{\partial x} + r_1[t_0^+(x) - t_1^+(x)] = -1. \tag{6.21}$$

whereas on the negative side ($-1 \leq x < 0$) we have

$$\frac{\partial^2 t_0^-(x)}{\partial x^2} + r_0[t_1^-(x) - t_0^-(x)] = -1, \tag{6.22}$$

$$\frac{\partial^2 t_1^-(x)}{\partial x^2} + \gamma\frac{\partial t_1^-(x)}{\partial x} + r_1[t_0^-(x) - t_1^-(x)] = -1. \tag{6.23}$$

These equations need to be solved on each side and matched at $x = 0$, through the continuity of the MFPTs and their derivatives. Hence, there are six boundary conditions (BCs):

$$t_\sigma^+(x=0) = t_\sigma^-(x=0) \tag{6.24}$$

$$\frac{\partial t_\sigma^+(x)}{\partial x}\Big|_{x=0} = \frac{\partial t_\sigma^-(x)}{\partial x}\Big|_{x=0} \tag{6.25}$$

$$t_\sigma^-(x=-1) = 0, \tag{6.26}$$

with $\sigma = \{0, 1\}$ and where the last condition enforces absorption at $x = -1$. We can also obtain a MFPT averaged over the initial conditions of the potential with their respective weights:

$$t_{av}(x) = \frac{r_0}{r_0 + r_1}t_1(x) + \frac{r_1}{r_0 + r_1}t_0(x). \tag{6.27}$$

6.1.3 Exact solution of the MFPT

From Eqs. (6.23)-(6.21), we note that we can write $t_0^+(t_0^-)$ in terms of $t_1^+(t_1^-$, respectively):

$$t_0^+(x) = -\frac{1}{r_1}\frac{\partial^2 t_1^+(x)}{\partial x^2} + \frac{\gamma}{r_1}\frac{\partial t_1^+(x)}{\partial x} + t_1^+(x) - \frac{1}{r_1}, \tag{6.28}$$

$$t_0^-(x) = -\frac{1}{r_1}\frac{\partial^2 t_1^-(x)}{\partial x^2} - \frac{\gamma}{r_1}\frac{\partial t_1^-(x)}{\partial x} + t_1^-(x) - \frac{1}{r_1}, \tag{6.29}$$

and then substitute these expressions into Eqs. (6.20)-(6.22) to obtain a fourth-order differential equation for $t_1^+(x)$ and $t_1^-(x)$:

$$\frac{\partial^4 t_1^+(x)}{\partial x^4} - \gamma\frac{\partial^3 t_1^+(x)}{\partial x^3} - (r_1+r_0)\frac{\partial^2 t_1^+(x)}{\partial x^2} + r_0\gamma\frac{\partial t_1^+(x)}{\partial x} = r_1 + r_0, \tag{6.30}$$

$$\frac{\partial^4 t_1^-(x)}{\partial x^4} + \gamma\frac{\partial^3 t_1^-(x)}{\partial x^3} - (r_1+r_0)\frac{\partial^2 t_1^-(x)}{\partial x^2} - r_0\gamma\frac{\partial t_1^-(x)}{\partial x} = r_1 + r_0. \tag{6.31}$$

Let us focus on t_1^+ first, the solution with $x > 0$. It is clear that t_1^+ admits the inhomogeneous solution $(r_0+r_1)x/r_0\gamma$, whereas the homogeneous part can be solved with the anzats $e^{\lambda x}$, which leads to the characteristic polynomial

$$\lambda\left[\lambda^3 - \lambda^2\gamma - \lambda(r_1+r_0) + r_0\gamma\right] = 0. \tag{6.32}$$

This polynomial also follows from Eq. (6.18) with $s = 0$.

In addition to the simple root $\lambda_0 = 0$, there are three other roots to this polynomial [1]:

$$\lambda_k = \frac{1}{3}\left[\gamma + 2b\cos\frac{\theta + 2(k-1)\pi}{3}\right] \tag{6.33}$$

where $k = \{1, 2, 3\}$ and

$$b = \sqrt{3(r_0+r_1) + \gamma^2} \tag{6.34}$$

$$\theta = \arccos\left[\frac{9\gamma(r_1 - 2r_0) + 2\gamma^3}{2(3(r_0+r_1)+\gamma^2)^{3/2}}\right]. \tag{6.35}$$

It is relatively straightforward to show that the argument in Eq. (6.35) is comprised in the interval $[-1, 1]$ for any non-zero positive γ, r_0 and r_1; therefore the three roots λ_k are real. We next wish to determine their sign and retain only those that are negative to avoid exponential divergences of the MFPT as $x \to +\infty$. The polynomial $P(\lambda) = \lambda^3 - \lambda^2\gamma - \lambda(r_1+r_0) + r_0\gamma$ has $P(0) = r_0\gamma > 0$ and $P'(0) = -r_1 - r_0 < 0$. Combined to the fact that $P(\lambda)$ decreases over a single finite interval (since it is of degree 3), these inequalities imply that one root must be negative and the other two positive. To find which root is negative, we notice that $\frac{2(k-1)\pi}{3} \leq \frac{\theta+2(k-1)\pi}{3} \leq \frac{(2k-1)\pi}{3}$, since $0 \leq \theta \leq \pi$. With $k = 2$ the argument of the cosine in Eq. (6.33) is thus in the interval $[\frac{2\pi}{3}, \pi]$ and consequently the cosine smaller than $-1/2$. Since $b > \gamma$ by definition, we conclude that $\lambda_2 < 0$. In summary,

$$\lambda_1 > 0,\ \lambda_3 > 0,\ \lambda_2 < 0. \tag{6.36}$$

Then, the admissible roots are $\lambda_0 = 0$ and λ_2, as they avoid exponential divergence at $x \to +\infty$, and t_1^+ takes the form::

$$t_1^+(x) = A_0^+ + A_2^+ e^{\lambda_2 x} + \frac{r_1+r_0}{r_0\gamma}x, \tag{6.37}$$

with $A_{0,2}^+$ two constants. Similarly, in the interval $-1 \leq x < 0$, the inhomogeneous solution of Eq. (6.60) for $t_1^-(x)$ is $-x(r_1+r_0)/(r_0\gamma)$, and the homogeneous solutions take

the form $e^{-\lambda x}$, with λ a root of the same polynomial (6.32). In this case all the roots are admissible, since $-1 \leq x < 0$. Therefore

$$t_1^-(x) = A_0^- + \sum_{k=1}^{3} A_k^- e^{-\lambda_k x} - \frac{r_1 + r_0}{r_0 \gamma} x. \tag{6.38}$$

Thus we have a total of 6 constants to determine, from the 6 boundary conditions (6.24)-(6.26). Using Eqs. (6.28)-(6.29), t_0 is deduced from t_1 on each side as:

$$t_0^+(x) = A_0^+ + \frac{1}{r_0} + A_2^+ \left[1 + \frac{\lambda_2(\lambda_1 + \lambda_3)}{r_1}\right] e^{\lambda_2 x} + \frac{r_1 + r_0}{r_0 \gamma} x \tag{6.39}$$

and

$$t_0^-(x) = A_0^- + \frac{1}{r_0} + \sum_{k=1}^{3} A_k^- \left[1 + \frac{\lambda_k(\lambda_i + \lambda_j)}{r_1}\right] e^{-\lambda_k x} - \frac{r_1 + r_0}{r_0 \gamma} x, \tag{6.40}$$

where we have used the identity $\lambda_1 + \lambda_2 + \lambda_3 = \gamma$ and where i, j represent the two indices different from k. The boundary conditions (6.24)-(6.26) lead to the system:

$$\begin{pmatrix} 1 & -1 & -1 & -1 & 1 & -1 \\ \lambda_2(\lambda_1+\lambda_3) & -\lambda_3(\lambda_1+\lambda_2) & -\lambda_2(\lambda_1+\lambda_3) & -\lambda_1(\lambda_2+\lambda_3) & 0 & 0 \\ \lambda_2 & \lambda_3 & \lambda_2 & \lambda_1 & 0 & 0 \\ \lambda_2^2(\lambda_1+\lambda_3) & \lambda_3^2(\lambda_1+\lambda_2) & \lambda_2^2(\lambda_1+\lambda_3) & \lambda_1^2(\lambda_2+\lambda_3) & 0 & 0 \\ 0 & e^{\lambda_3} & e^{\lambda_2} & e^{\lambda_1} & 0 & 1 \\ 0 & \lambda_3(\lambda_1+\lambda_2)e^{\lambda_3} & \lambda_2(\lambda_1+\lambda_3)e^{\lambda_2} & \lambda_1(\lambda_2+\lambda_3)e^{\lambda_1} & 0 & 0 \end{pmatrix} \begin{pmatrix} A_2^+ \\ A_3^- \\ A_2^- \\ A_1^- \\ A_0^+ \\ A_0^- \end{pmatrix} = \begin{pmatrix} 0 \\ 0 \\ -2\frac{r_1+r_0}{r_0\gamma} \\ 0 \\ -\frac{r_1+r_0}{r_0\gamma} \\ -\frac{r_1}{r_0} \end{pmatrix}. \tag{6.41}$$

Although the MFPTs can be determined for all $x > -1$ by this method, in the following we will present the results corresponding to the case $x = 0$, *i.e.*, for a particle starting at the potential minimum. This case is typical of experiments using optical tweezers. The MFPTs we are interested in are:

$$t_1^+(x=0) = A_0^+ + A_2^+, \tag{6.42}$$

$$t_0^+(x=0) = A_0^+ + \frac{1}{r_0} + A_2^+ \left[1 + \frac{\lambda_2(\lambda_1 + \lambda_3)}{r_1}\right]. \tag{6.43}$$

For convenience we use the notation

$$\Lambda_1^- = \lambda_1 - \lambda_2, \qquad \Lambda_1^+ = \lambda_1 + \lambda_2, \tag{6.44}$$

$$\Lambda_2^- = \lambda_2 - \lambda_3, \qquad \Lambda_2^+ = \lambda_2 + \lambda_3, \tag{6.45}$$

$$\Lambda_3^- = \lambda_3 - \lambda_1, \qquad \Lambda_3^+ = \lambda_3 + \lambda_1. \tag{6.46}$$

Solving the system (6.41) with the help of Mathematica, yields

$$A_0^+ = -\left(\frac{r_0+r_1}{\gamma r_0}\right)\left[\frac{2\lambda_2^2 e^{\Lambda_3^+}\Lambda_3^+\Lambda_3^-}{\lambda_1\lambda_3\Lambda_1^+\Lambda_2^+} + \frac{\lambda_3 e^{\Lambda_1^+}\Lambda_1^-}{\lambda_1\lambda_2} + \frac{e^{\lambda_3}\Lambda_1^-\left(\left(\frac{2}{\lambda_1}+1\right)\lambda_3 - \frac{\gamma r_1}{\Lambda_1^+(r_0+r_1)}\right)}{\Lambda_2^+}\right.$$
$$+ \frac{e^{\lambda_1}\Lambda_2^-\left(\lambda_1\left(\frac{2}{\lambda_3}+1\right) - \frac{\gamma r_1}{\Lambda_2^+(r_0+r_1)}\right)}{\Lambda_1^+} + \frac{e^{\lambda_2}\Lambda_3^-\left(-\frac{2((\gamma+1)r_0+r_1)}{\lambda_1\lambda_3} - \frac{\gamma r_1}{\Lambda_3^+(r_0+r_1)} - 4\right)}{2\lambda_2}$$
$$\left. + \frac{\lambda_1 e^{\Lambda_2^+}\Lambda_2^-}{\lambda_3\lambda_2} - \frac{\gamma\Lambda_1^-\Lambda_2^-\Lambda_3^- r_1}{\lambda_2\Lambda_1^+\Lambda_2^+\Lambda_3^+(r_0+r_1)}\right]\left(\frac{e^{\lambda_3}\lambda_3\Lambda_1^-}{\Lambda_2^+} + \frac{e^{\lambda_1}\lambda_1\Lambda_2^-}{\Lambda_1^+} + \frac{1}{2}e^{\lambda_2}\Lambda_3^-\right)^{-1}. \tag{6.47}$$

and

$$A_2^+ = -\frac{\Lambda_1^- e^{\lambda_3} + \Lambda_3^- e^{\lambda_2} + \Lambda_2^- e^{\lambda_1} + \frac{r_1\gamma}{2(r_0+r_1)}\frac{\Lambda_1^-\Lambda_2^-\Lambda_3^-}{\Lambda_1^+\Lambda_2^+\Lambda_3^+}}{\frac{r_0\gamma\lambda_2}{r_0+r_1}\left(\frac{\lambda_3\Lambda_1^-}{\Lambda_2^+}e^{\lambda_3} + \frac{1}{2}\Lambda_3^- e^{\lambda_2} + \frac{\lambda_1\Lambda_2^-}{\Lambda_1^+}e^{\lambda_1}\right)} \tag{6.48}$$

Although the constants A_0^+ and A_2^+ do not take a simple form, making difficult to analytically analyze the MFPT as a function of the dimensionless parameters r_0, r_1 and γ, it is easy to evaluate the expressions of the MFPTs numerically to study their behaviors. In the following section we start by analyzing the MFPT $t_1(x=0)$ in the (r_0, r_1)-plane for a fixed strength potential γ, seeking the rates that minimize this function. We recall that we will be mainly interested in the results that correspond to $x = 0$, *i.e.*, when the particle starts at the minimum of the potential. We will drop the x dependence in when it is clear from the context. Due to the contrasting behaviour that we observe between t_1 and t_0, we present the analysis of each function in separate sections. Regardless of this numerical analysis, we will seek, when it is possible, to re-derive the results in some particular limits in order to better understand the behaviors of the MFPTs.

6.1.4 Optimal MFPT t_1^*

Taking $x = 0$, fixing the strength (γ) and varying the rates, let us define

$$t_1^*(\gamma) = \min_{r_0,r_1} t_1(\gamma, r_0, r_1), \tag{6.49}$$

whereas $r_0^*(\gamma)$ adn $r_1^*(\gamma)$ as the corresponding optimal rates. The optimal mean first passage time $t_1^* = t_1(r_0^*, r_1^*)$ only depends on the scaled strength γ. Its variations are shown in Figure 6.2a, from very weak to very confining potentials. Figures 6.2b and 6.2c reports the pairs of optimal rates $[r_1^*(\gamma), r_0^*(\gamma)]$ as a function of γ.

The optimal MFPT t_1^* exhibits a "second-order", continuous transition at a non-trivial critical potential slope

$$\gamma_c = 1.228780... \tag{6.50}$$

For $\gamma \leq \gamma_c$, the resetting protocol that optimizes t_1 consists in keeping the potential always turned on, or

$$r_1^*(\gamma) = 0, \tag{6.51}$$

while r_0 is irrelevant.

The optimal MFPT is thus given in this regime by the equilibrium Kramers' time (solving Eqs. (6.21) and (6.23) with $r_1 = 0$ [58]):

$$t_1^*(\gamma) = t_{eq}(\gamma) = \frac{2}{\gamma^2}(e^\gamma - 1) - \frac{1}{\gamma}. \tag{6.52}$$

The curve of $t_{eq}(\gamma)$ is represented by the orange line in Fig. 6.2a: it first decreases with γ and reaches a minimum at $\gamma_{eq}^* = 1.244678...$, which is *slightly larger* than γ_c, as clear from the inset.

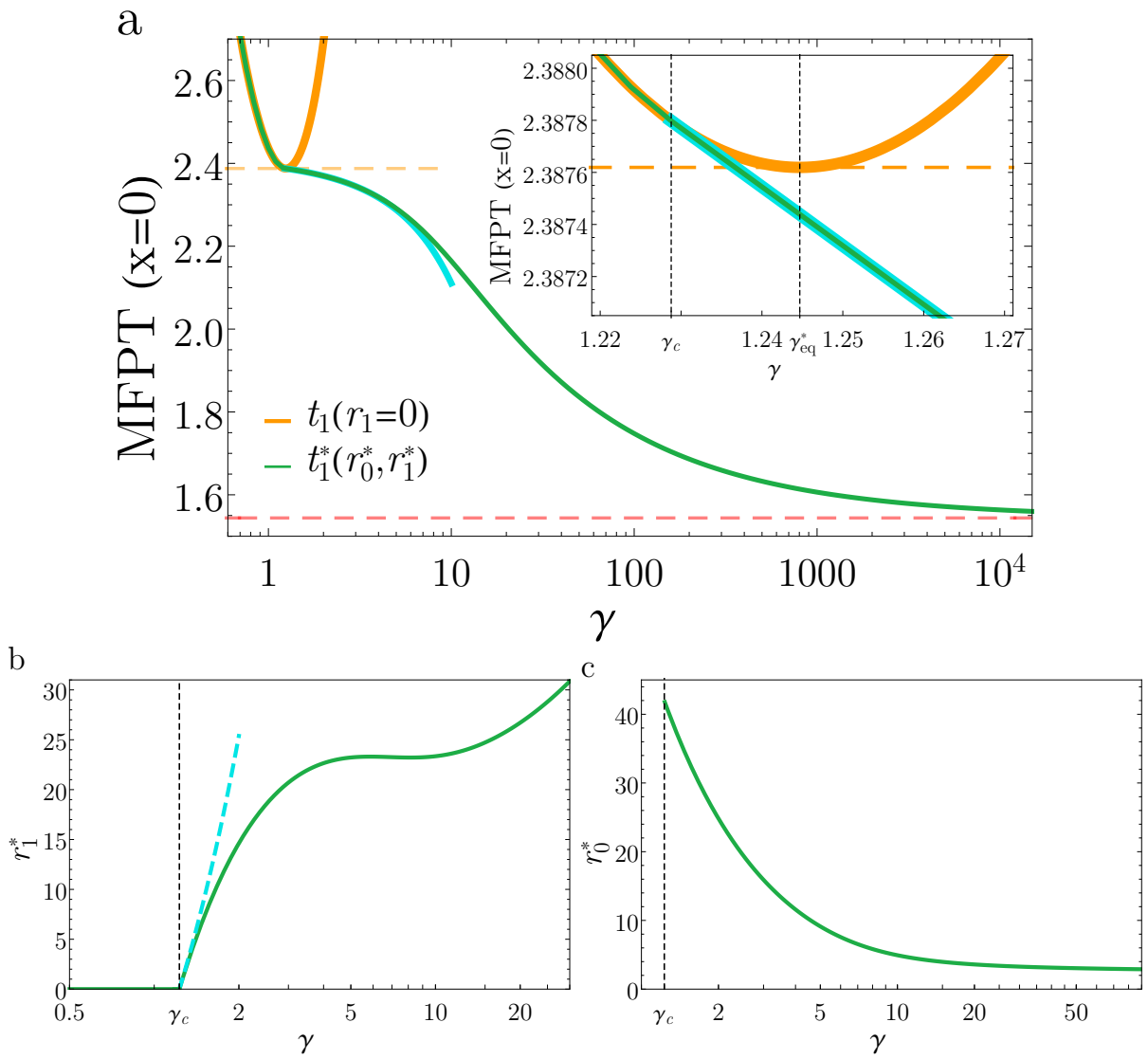

Figure 6.2: (a) Minimal MFPT t_1^* as a function of γ (green line), obtained from numerical minimization of the exact solution. The orange line represents t_1 for a particle in a steady potential ($r_1 = 0$), and the aqua line the analytical expression (6.53) for $\gamma > \gamma_c = 1.2287...$. The lower horizontal dotted line denotes the limit $\gamma \to \infty$. Inset: zoom of the transition region ($\gamma \sim \gamma_c$). The corresponding optimal rates $r_1^*(\gamma)$ and $r_0^*(\gamma)$ are shown in (b) and (c), respectively. For $\gamma \leq \gamma_c$, the optimal choice consists in keeping the potential steady, or $r_1^* = 0$, whereas above γ_c, r_0^* and r_1^* are non-zero.

For $\gamma > \gamma_c$, $t_1(\gamma)$ can be improved compared to $t_{eq}(\gamma)$ by applying a non-trivial resetting protocol. As shown by the inset of Fig. 6.2a, t_1^* start to deviate from the equilibrium

line when it reaches the value $t_{eq}(\gamma_c) = 2.387797...$, strikingly close but definitely above the equilibrium minimum $t^*_{eq} = 2.387619...$ For potentials of slope above but close to γ_c,

$$t^*_1(\gamma) = t_{eq}(\gamma_c) - 0.0225432...\,(\gamma - \gamma_c) - 0.00103404...\,(\gamma - \gamma_c)^2 + \text{h. o. terms}, \quad (6.53)$$

a relation which remains quite accurate up to $\gamma - \gamma_c \sim 10$ (Fig. 6.2a). Above the critical point, r^*_1 increases in a linear fashion from zero:

$$r^*_1(\gamma) = 32.91301557...(\gamma - \gamma_c) + \text{h. o. terms}, \quad (6.54)$$

as shown in Fig. 6.2b (dotted line). In contrast, the optimal switch-on rate $r^*_0(\gamma)$ decreases with γ. Right at the transition, it is finite and surprisingly large:

$$r^*_0(\gamma_c) = 41.969027... \quad (6.55)$$

At large potential strength, the particle rapidly returns to $x = 0$ when the potential is on. The process thus becomes closer to the well-known problem of diffusion with instantaneous resetting to the origin with the dimensionless rate r_0. In the limit $\gamma \to \infty$, as expected, the optimal protocol corresponds to $r_1 \to \infty$ (the potential is applied for very short periods of time) and $r_0 = 2.539638...$, which is the optimal rate of instantaneous resetting [58].

a) Perturbative analysis

Some of the results described above can be obtained exactly from a perturbation theory, considering $r_1 \ll r_0$ and γ in the vicinity of γ_c. Before going into the details, we first present a simple heuristic argument which can explain qualitatively the origin of the equilibrium-non-equilibrium transition for t^*_1, *i.e.*, between a zero and non-zero optimal rate r^*_1. It consists in approximating the problem by a particle diffusing in a steady potential, given by the mean potential felt by the original particle, *i.e.* $v_{eff}(x) = \gamma_{eff}|x|$ with $\gamma_{eff} = r_0\gamma/(r_0 + r_1) \leq \gamma$. The MFPT in this effective description satisfies the equation

$$\frac{\partial^2 t_{eff}}{\partial x^2} - \frac{\partial v_{eff}(x)}{\partial x}\frac{\partial t_{eff}}{\partial x} = -1, \quad (6.56)$$

The solution of Eq. (6.56) evaluated at $x = 0$ is given by Eq. (6.52), where γ has to be replaced by γ_{eff}:

$$t_{eff}(x = 0) = t_{eq}(\gamma_{eff}). \quad (6.57)$$

As mentioned earlier, the equilibrium time t_{eq} is a non-monotonous function of its argument and reaches a minimum at $\gamma^*_{eq} = 1.244678...$. Hence, at fixed γ there are two ways of minimizing $T(x = 0)$ in Eq. (6.56): If $\gamma < \gamma^*_{eq}$, on the decreasing side of the curve, the argument γ_e should be as large as possible, *i.e.*, $\gamma_e = \gamma$, which implies $r^*_1 = 0$. But if $\gamma > \gamma^*_{eq}$, γ_e can be tuned to match the optimal parameter γ^*_{eq} by choosing the rates such that:

$$\gamma^*_{eq} = \frac{r^*_0(\gamma)}{r^*_0(\gamma) + r^*_1(\gamma)}\gamma. \quad (6.58)$$

The above relation implies $r^*_1(\gamma) \neq 0$, since $\gamma^*_{eq} < \gamma$. Hence, a transition would occur when γ crosses γ^*_{eq}, between optimal protocols with zero and non-zero switch-off rate. It

is reasonable to think that when the potential is very confining, one needs to switch it off from time to time to let the particle find the target.

Nevertheless, the above argument is not correct, as the true critical point γ_c is lower that γ^*_{eq}, albeit by less than two percents, a feature suggestive of a more complex transition mechanism. In addition, this argument does not predicts that, after the transition, $t_1^*(\gamma)$ can be lower than (and not equal to) the optimal equilibrium time t^*_{eq}.

b) Calculation of γ_c and $r_0^*(\gamma_c)$

We retake the exact fourth-order differential equations for $t_1^+(x)$ and $t_1^-(x)$, obtained from combining Eqs. (6.20)-(6.23) [1]:

$$\frac{\partial^4 t_1^+(x)}{\partial x^4} - \gamma \frac{\partial^3 t_1^+(x)}{\partial x^3} - (r_1 + r_0)\frac{\partial^2 t_1^+(x)}{\partial x^2} + r_0\gamma \frac{\partial t_1^+(x)}{\partial x} = r_1 + r_0, \tag{6.59}$$

$$\frac{\partial^4 t_1^-(x)}{\partial x^4} + \gamma \frac{\partial^3 t_1^-(x)}{\partial x^3} - (r_1 + r_0)\frac{\partial^2 t_1^-(x)}{\partial x^2} - r_0\gamma \frac{\partial t_1^-(x)}{\partial x} = r_1 + r_0 \tag{6.60}$$

By defining the operator $\mathcal{L}_\gamma \equiv \frac{\partial^2}{\partial x^2} - \operatorname{sgn}\gamma \frac{\partial}{\partial x}$ and dividing by r_0, Eqs. (6.59)-(6.60) read

$$\left[\frac{1}{r_0}\frac{\partial^2}{\partial x^2} - 1\right]\mathcal{L}_\gamma t_1^+ - \frac{r_1}{r_0}\frac{\partial^2 t_1^+}{\partial x^2} = 1 + \frac{r_1}{r_0}, \tag{6.61}$$

$$\left[\frac{1}{r_0}\frac{\partial^2}{\partial x^2} - 1\right]\mathcal{L}_{-\gamma} t_1^- - \frac{r_1}{r_0}\frac{\partial^2 t_1^-}{\partial x^2} = 1 + \frac{r_1}{r_0}. \tag{6.62}$$

We introduce the small parameter $\epsilon = \frac{r_1}{r_0} \ll 1$, hence Eqs. (6.61)-(6.62) are recast as

$$\left[\frac{1}{r_0}\frac{\partial^2}{\partial x^2} - 1\right]\mathcal{L}_\gamma t_1^+ - \epsilon\frac{\partial^2 t_1^+}{\partial x^2} = 1 + \epsilon, \tag{6.63}$$

$$\left[\frac{1}{r_0}\frac{\partial^2}{\partial x^2} - 1\right]\mathcal{L}^-_{-\gamma} t_1^- - \epsilon\frac{\partial^2 t_1^-}{\partial x^2} = 1 + \epsilon. \tag{6.64}$$

To solve this PDEs we write the general solution as a series expansion in ϵ, or $t_1(x) = t_1^{(0)}(x) + \epsilon t_1^{(1)}(x) + \epsilon^2 t_1^{(2)}(x) + \ldots$, where the $t_1^{(i)}$ are functions of order unity to be determined for $x > 0$ and $-1 < x < 0$.

In the following, let us define $t_1^{+(i)}(x) = t_1^{(i)}(x)$ with $x > 0$ and $t_1^{-(i)}(x) = t_1^{(i)}(x)$ with $-1 < x < 0$. Hence, at leading order one has:

$$\left[\frac{1}{r_0}\frac{\partial^2}{\partial x^2} - 1\right]\mathcal{L}_\gamma t_1^{+(0)}(x) = 1, \tag{6.65}$$

$$\left[\frac{1}{r_0}\frac{\partial^2}{\partial x^2} - 1\right]\mathcal{L}_{-\gamma} t_1^{-(0)}(x) = 1, \tag{6.66}$$

a relation which is satisfied if $\mathcal{L}_{\pm\gamma} t_1^{\pm(0)}(x) = -1$. We recover at this order the equilibrium time t_{eq} in a potential $\gamma|x|$. Its expression is obtained by applying the boundary conditions

[1] It is easy to see that the effective description of Eq. (6.56) becomes exact when r_0 and r_1 tend to ∞, the ratio r_1/r_0 being fixed.

(6.24)-(6.26), and was calculated in [58]:

$$t_1^{+(0)}(x) = t_{eq}^{+}(x,\gamma) = \frac{2(e^{\gamma}-1)-(1-x)\gamma}{\gamma^2}, \tag{6.67}$$

$$t_1^{-(0)}(x) = t_{eq}^{-}(x,\gamma) = \frac{2(e^{\gamma}-e^{-\gamma x})-(x+1)\gamma}{\gamma^2}, \tag{6.68}$$

A relation allowing the exact determination of the critical point γ_c can be obtained at the following order ϵ. From Eqs. (6.63)-(6.64), one get

$$\left[\frac{1}{r_0}\frac{\partial^2}{\partial x^2}-1\right]\mathcal{L}_{\gamma}t_1^{+(1)} = 1+\frac{\partial^2 t_1^{+(0)}}{\partial x^2}, \tag{6.69}$$

$$\left[\frac{1}{r_0}\frac{\partial^2}{\partial x^2}-1\right]\mathcal{L}_{-\gamma}t_1^{-(1)} = 1+\frac{\partial^2 t_1^{-(0)}}{\partial x^2}. \tag{6.70}$$

Solving for $t_1^{+(1)}$, the homogeneous part of (6.69) is given by a constant plus a linear combination of $e^{-\sqrt{r_0}x}$, $e^{\sqrt{r_0}x}$ and $e^{\gamma x}$, where the coefficient of the last two terms must be 0 to avoid divergence at $x=\infty$. From Eq. (6.67), the right-hand-side of (6.69) for $t_1^{+(1)}$ is 1, which yields x/γ for the inhomogeneous solution. Similarly, $t_1^{-(1)}$ is a linear combination of a constant, $e^{-\sqrt{r_0}x}$, $e^{\sqrt{r_0}x}$ and $e^{-\gamma x}$, which are all acceptable ($-1<x<0$). The right-hand-side of (6.69) for $t_1^{-(1)}$ is obtained from Eq. (6.68) as $1-2e^{-\gamma x}$, which yields the inhomogeneous solution $-[2r_0xe^{-\gamma x}/(r_0-\gamma^2)+x]/\gamma$. To sum up, $t_1^{(1)}(x)$ takes the form

$$t_1^{+(1)}(x) = C^{+} + A^{+}e^{-\sqrt{r_0}x} + \frac{x}{\gamma} \tag{6.71}$$

$$t_1^{-(1)}(x) = C^{-} + A^{-}e^{-\sqrt{r_0}x} + B^{-}e^{\sqrt{r_0}x} + D^{-}e^{-\gamma x} - \frac{2r_0xe^{-\gamma x}}{\gamma\left(r_0-\gamma^2\right)} - \frac{x}{\gamma}. \tag{6.72}$$

Three relations between the six unknown coefficients above are given by the BCs: $t_1^{+(1)}(0) = t_1^{-(1)}(0)$, $dt_1^{+(1)}(0)/dx = dt_1^{-(1)}(0)/dx$ and $t_1^{-(1)}(-1)=0$. The remaining three relations stem from the same conditions applied to $t_0^{\pm(0)}(x)$ in the ϵ-expansion of $t_0(x) = t_0^{(0)} + \epsilon t_0^{(1)} + \ldots$. From Eqs. (6.21) and (6.23), t_0 is related to t_1 through the exact relation

$$t_0^{\pm} = t_1^{\pm} - \frac{1}{r_1}\left(\mathcal{L}_{\pm\gamma}t_1^{\pm}+1\right). \tag{6.73}$$

At order $1/\epsilon$, one recovers $\mathcal{L}_{\pm\gamma}t_1^{\pm(0)}(x) = -1$, which was already solved. At order ϵ^0,

$$t_0^{\pm(0)} = t_1^{\pm(0)} - \frac{1}{r_0}\mathcal{L}_{\pm\gamma}t_1^{\pm(1)}. \tag{6.74}$$

When applying the BCs to $t_0^{(0)}$ above, we obtain 3 new relations that involve only A^{+}, A^{-} and B^{-}, which are easily solved and substituted into the other 3 relations for the remaining coefficients. At $x=0$ one has $t_1^{(1)} = C^{+} + A^{+}$, which gives after some algebra:

$$t_1^{(1)}(\gamma,r_0) = -\gamma\frac{\partial t_1^{(0)}}{\partial\gamma} + \frac{\sqrt{r_0}e^{-\sqrt{r_0}}\left[2\left(e^{\gamma}-1\right)\left(e^{-\sqrt{r_0}}+\frac{\gamma}{\sqrt{r_0}}\right)+4e^{\gamma}-1+\frac{\gamma^2}{r_0}\right]}{\left(\gamma+\sqrt{r_0}\right)\left(r_0-\gamma^2\right)} \tag{6.75}$$

$$+\frac{2\left(e^{\gamma}-1\right)-2e^{\gamma}\gamma-\frac{\gamma}{\sqrt{r_0}}+e^{-2\sqrt{r_0}}}{r_0-\gamma^2} + \frac{4r_0e^{\gamma}\left(\frac{\gamma}{\sqrt{r_0}}-e^{\gamma-\sqrt{r_0}}\right)}{\left(r_0-\gamma^2\right)^2}.$$

The complete expressions of $t_1^{(1)}$ for $x \geq 0$ and $x \leq 0$ are shown in the Appendix C.

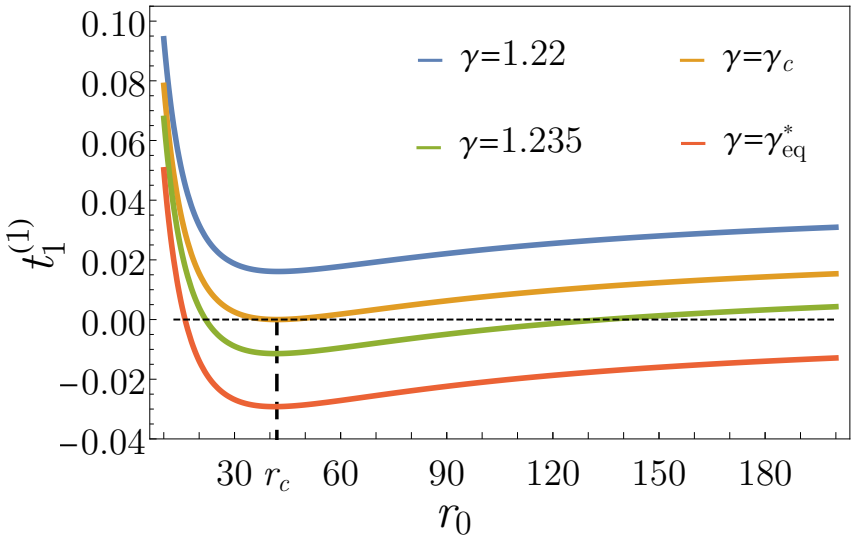

Figure 6.3: "Dispersion relation" $t_1^{(1)}$ given by Eq. (6.75) as a function of r_0. At $\gamma_c = 1.228780...$, the correction is non-negative but vanishes at $r_0 = r_c$.

The critical potential γ_c is determined from Eq. (6.75) as follows. At fixed γ, if $t_1^{(1)}$ is positive for all r_0, then applying a resetting protocol with a small r_1 will always produce an increase in t_1, as the first correction will be positive (recall that $\epsilon \geq 0$). On the other hand, if at fixed γ there exist a range of r_0 such that $t_1^{(1)} < 0$, then the MFPT can be decreased by applying the potential intermittently. In such case, the non-equilibrium search process becomes more efficient than the equilibrium one. The critical γ_c is given by the marginal situation between these two cases. Figure 6.3 shows $t_1^{(1)}$ given by expression (6.75) as a function of r_0 for a few values of γ. This quantity plays the role of a "dispersion relation", in analogy with instabilities in pattern formation problems: it is non monotonic and positive for γ below a threshold, whereas for $\gamma = \gamma_c \equiv 1.228780...$, $t_1^{(1)}$ is non-negative but tangent to the line $t_1^{(1)} = 0$ at some point r_c. This special point is given numerically by $r_c \equiv 41.969027...$, which is the value taken by the optimal rate r_0^* for $\gamma = \gamma_c$, as given by our previous analysis of the full exact solution in Eq. (6.55). Setting a small $\gamma - \gamma_c > 0$, the curve will present negative values over a small interval centered around r_c, and one thus must choose $r_0 \simeq r_c$ to minimize the MFPT at ϵ fixed. A similar reasoning is used to find the fastest growing mode in pattern formation problems.

c) Behaviour of t_1^* and r_1^* near γ_c

To summarize, the exact series expansion of the MFPT in powers of $\epsilon = r_1/r_0$,

$$t_1(\gamma, \epsilon, r_0) = t_{eq}(\gamma) + \epsilon t_1^{(1)}(\gamma, r_0) + \epsilon^2 t_1^{(2)}(\gamma, r_0) + \dots, \tag{6.76}$$

allows us to identify a continuous transition when $t_1^{(1)}$ changes sign, *i.e.*, when the effect of a small ϵ is to decrease t_1 compared with the equilibrium case. If $t_1^{(1)} < 0$ and if the next order term $t_1^{(2)}$ is > 0 and $\gg |t_1^{(1)}|$, one can determine the value of ϵ that minimizes the MFPT, while the terms of order ϵ^3 or higher can be neglected. In the spirit of the

Ginzburg-Landau theory of phase transitions, we expand t_{eq} and the coefficients $t_1^{(i)}$ by taking γ near γ_c (with $0 < \gamma - \gamma_c \ll 1$) and r_0 near r_c. As the critical point fulfills $t_1^{(1)}(\gamma_c, r_c) = 0$ and $\partial_{r_0} t_1^{(1)}|_{\gamma_c, r_c} = 0$, Eq. (6.76) becomes

$$t_1(\gamma, \epsilon, r_0) = t_{eq}(\gamma_c) + (\gamma - \gamma_c) \left.\frac{\partial t_{eq}}{\partial \gamma}\right|_{\gamma_c} + \epsilon(\gamma - \gamma_c) \left.\frac{\partial t_1^{(1)}}{\partial \gamma}\right|_{\gamma_c, r_c} + \epsilon^2 t_1^{(2)}(\gamma_c, r_c) + ... \quad (6.77)$$

at order $\gamma - \gamma_c$. Minimization of the last two terms at fixed γ gives ϵ^*, or:

$$r_1^*(\gamma) = -(\gamma - \gamma_c) r_c \frac{\left.\frac{\partial t_1^{(1)}}{\partial \gamma}\right|_{\gamma_c, r_c}}{2 t_1^{(2)}(\gamma_c, r_c)} + O\left((\gamma - \gamma_c)^2\right), \quad (6.78)$$

where we have replaced r_0 by r_c at leading order in $\gamma - \gamma_c$. The calculation of $t_1^{(2)}$ can be performed as in Section 6.1.4, from the knowledge of $t_1^{(1)}$ for all x. With the help of Mathematica, we obtained the expression given in the Appendix C, for $x = 0$. Numerical evaluation of (6.78) gives,

$$r_1^*(\gamma) = 32.91301557...(\gamma - \gamma_c) + ... \quad (6.79)$$

which is the result (6.54) that we obtained from the numerical analysis of the full exact solution. Eq. (6.78) shows that the "order parameter" r_1^* grows linearly and very rapidly near γ_c. Renoting $\epsilon^* = c(\gamma - \gamma_c)$, $c = -\left.\frac{\partial t_1^{(1)}}{\partial \gamma}\right|_{\gamma_c, r_c} / 2 t_1^{(2)}(\gamma_c, r_c)$ and substituting into Eq. (6.77), we obtain

$$t_1^*(\gamma) = t_{eq}(\gamma_c) + (\gamma - \gamma_c) \left.\frac{\partial t_{eq}}{\partial \gamma}\right|_{\gamma_c} + (\gamma - \gamma_c)^2 \left\{ \frac{1}{2} \left.\frac{\partial^2 t_{eq}}{\partial \gamma^2}\right|_{\gamma_c} + c \left.\frac{\partial t_1^{(1)}}{\partial \gamma}\right|_{\gamma_c, r_c} + c^2 t_1^{(2)}(\gamma_c, r_c) \right\} + ... \quad (6.80)$$

where t_{eq} has been expanded further. Numerical evaluation of the prefactors leads to Eq. (6.53), in very good agreement with the exact solution near γ_c. It is clear from (6.80) that the first derivative of t_1^* is continuous across the transition, whereas the second derivative is discontinuous.

6.1.5 Optimal MFPT t_0^*

For the MFPT t_0 of the particle starting with free diffusion phase, one observes a different behaviour, that contrasts with t_1. In this case, the optimal time

$$t_0^*(\gamma) = \min_{r_0, r_1} t_0(\gamma, r_0, r_1) \quad (6.81)$$

undergoes a "first-order" transition at a potential steepness $\gamma_c' = 1.698768...$, larger than γ_c (see Figure 6.4a). By "first-order", we mean that the corresponding corresponding optimal rates r_0^* and r_1^* (Figs. 6.4b and 6.4c) are discontinuous at γ_c'. Below, we summarize the results, based on analyzing the exact solution and on the perturbative theory, and refer the reader to the end of this section for some derivations.

For $\gamma < \gamma_c'$, $r_1^*(\gamma) = 0$ and $r_0^*(\gamma)$ is finite and given by the minimum of the function

$$f_\gamma(r_0) = \frac{1 - e^{-\sqrt{r_0}}}{r_0} - \frac{2e^{-\sqrt{r_0}}\left(\cosh\sqrt{r_0} + \frac{\gamma}{\sqrt{r_0}}\sinh\sqrt{r_0} - e^{\gamma}\right)}{r_0 - \gamma^2}, \tag{6.82}$$

whereas the optimal MFPT reads

$$t_0^*(\gamma) = t_{eq}(\gamma) + f_\gamma(r_0^*(\gamma)) < t_{eq}(\gamma), \tag{6.83}$$

where $r_0^*(\gamma)$ is the parameter r_0 that minimizes Eq. (6.82) at fixed gamma. It is clear from Fig. 6.4a that t_0^* is non-monotonic with γ, unlike t_1^*.

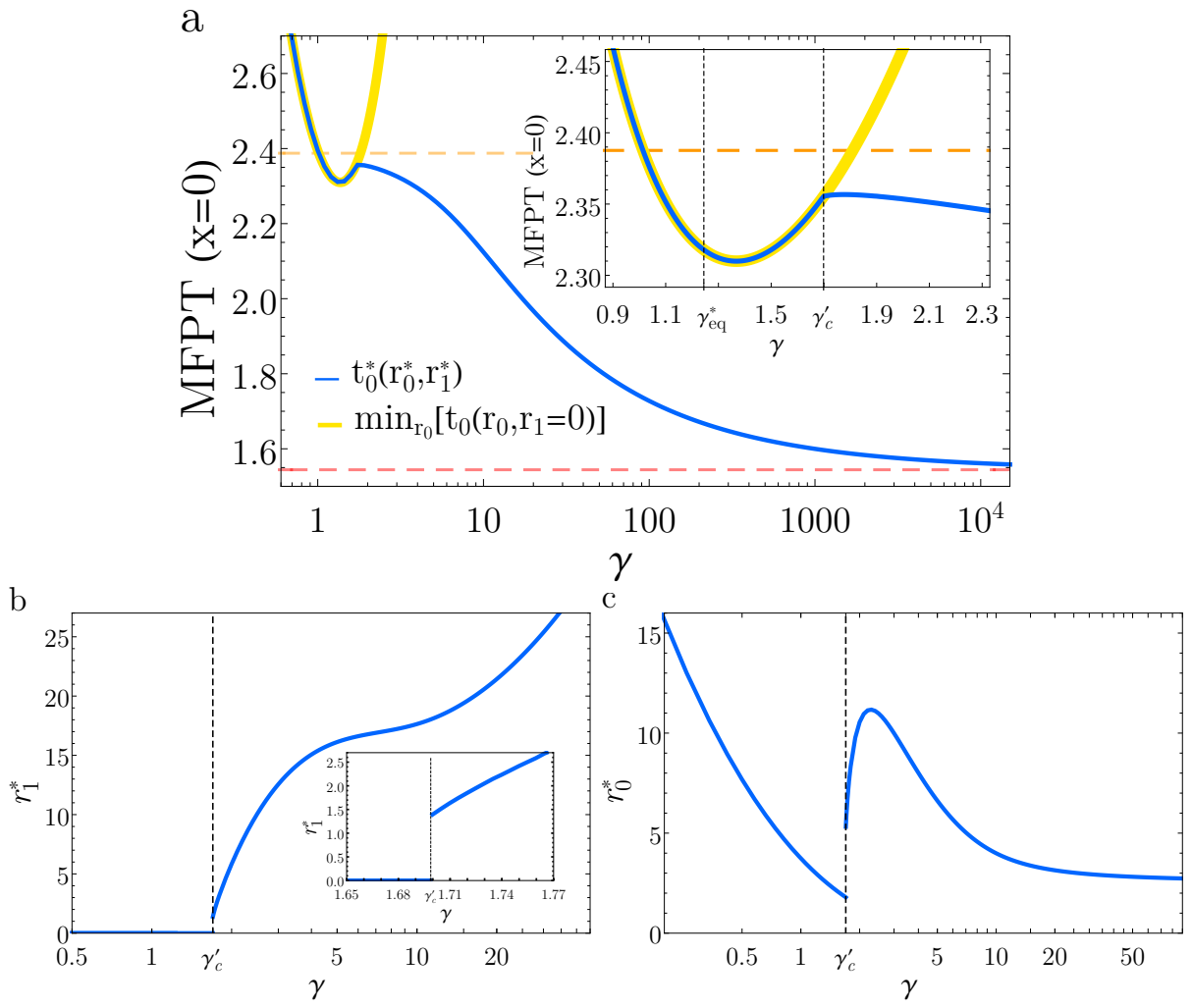

Figure 6.4: a) Minimal MFPT t_0^* (in blue) at fixed γ, and (b and c) their corresponding optimal rates r_0^* and r_1^* for t_1^*. For $\gamma \leq \gamma_c' = 1.683762...$, the optimal t_0^* is reached at $r_1^* = 0$, whereas above γ_c, $r_1^* > 0$. The yellow line in (a) is given by Eq. (6.83). Again, the optimal MFPT of the instantaneous resetting problem (red dotted line) is reached as $\gamma \to \infty$.

For $\gamma > \gamma_c'$, r_1^* becomes positive and t_0^* closely follows the curve of t_1^* displayed in Fig. 6.2. Strikingly, despite of leading to similar MFPTs, the optimal protocols with and without potential at $t = 0$ differ widely in the transition region: for instance, from Eq. (6.82) one finds that $r_0^*(\gamma_c') = 1.795904...$ for the potential off at $t = 0$, a value smaller

than the one in Eq. 6.55 for the potential on at $t = 0$. Interestingly, we find that, at any potential strength, t_0^* slightly outperforms t_1^*: the target can be found faster if one lets the particle diffuse freely initially, instead of starting with the potential on. The former initial condition is actually that of usual resetting processes, which start with a diffusing phase.

The discontinuous transition of the intermittency rates we observed in Figs. 6.4b and 6.4c arises from the fact that t_0, unlike t_1, admits two local minima in the (r_0, r_1)-plane when γ is close to γ_c'. These minima are clear from Figure 6.5, which displays $\min_{r_1} t_0(\gamma, r_0, r_1)$ as a function of r_0. For $\gamma < \gamma_c'$, one notices the existence of a metastable minimum at a larger r_0, which becomes the absolute minimum when $\gamma > \gamma_c'$, causing a discontinuity for r_0^*. Similarly, the function $\min_{r_0} t_0(\gamma, r_0, r_1)$ admits a metastable minimum at a positive r_1 when γ is close to and below γ_c', and causing a discontinuity in r_1^*, too.

At large gamma, both $t_0^*(\gamma)$ and $t_1^*(\gamma)$ tend to the optimum value of the standard resetting problem of [55], which is given by $t^* = 1.544138...$, see Fig. 6.2a-c and 6.4a-c. The time t^* is the global minimum of t_0 and t_1 in parameter space: here, no resetting protocol or potential slope can produce a MFPT lower than the optimal MFPT of stochastic resetting to the origin, which therefore represents a limiting case of a more general class of non-equilibrium searches.

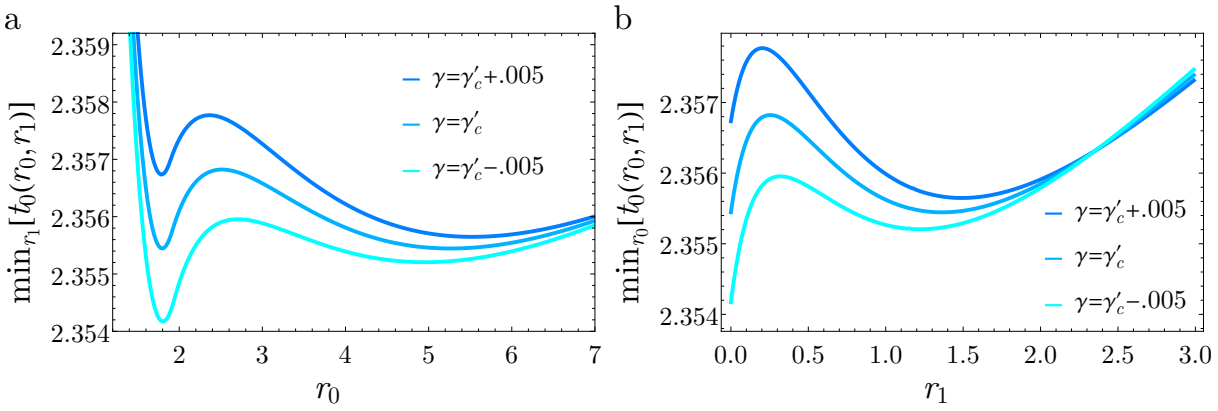

Figure 6.5: a) $\min_{r_0} t_0(r_0, r_1)$ as a function of r_0 and b) $\min_{r_1} t_0(r_0, r_1)$ as a function of r_1. In both cases, one can observe metastability near γ_c'. which generates a discontinuity in r_0^* and r_1^*.

MFPT in the absence of potential at $t = 0$ and with $r_1 = 0$

To derive the expressions (6.82)-(6.83), we can We can further insert the solution (6.71)-(6.72) for $t_1^{\pm(1)}$ into Eq. (6.74), which gives the exact expression of $t_0(x)$ with $r_1 = 0$ ($\epsilon = 0$). This is the MFPT of an initially free particle where the potential is applied once at rate r_0 and is never switched off again afterwards. For $x > 0$ we get:

$$t_0^+(x, \gamma, r_0, r_1 = 0) = \frac{2(e^\gamma - 1) - (1 - x)\gamma}{\gamma^2} + \frac{1 - e^{-\sqrt{r_0}(x+1)}}{r_0} - \frac{2e^{-\sqrt{r_0}(x+1)}\left(\frac{\gamma}{\sqrt{r_0}}\sinh\sqrt{r_0} + \cosh\sqrt{r_0} - e^\gamma\right)}{r_0 - \gamma^2}, \tag{6.84}$$

and for $-1 \leq x < 0$,

$$t_0^-(x,\gamma,r_0,r_1=0) = \frac{2\left(e^{\gamma}-e^{-x\gamma}\right)-(1+x)\gamma}{\gamma^2} + \frac{1-e^{-\sqrt{r_0}(x+1)}}{r_0} - \frac{2e^{-\sqrt{r_0}}\left[\left(\frac{\gamma}{\sqrt{r_0}}-1\right)\sinh\sqrt{r_0}(x+1)+e^{-x\gamma+\sqrt{r_0}}-e^{\gamma-\sqrt{r_0}x}\right]}{r_0-\gamma^2}. \tag{6.85}$$

At $x = 0$, the above relations reduce to

$$t_0(\gamma,r_0,r_1=0) = t_{eq}(\gamma) + \frac{1-e^{-\sqrt{r_0}}}{r_0} - \frac{2e^{-\sqrt{r_0}}\left(\frac{\gamma}{\sqrt{r_0}}\sinh\sqrt{r_0}+\cosh\sqrt{r_0}-e^{\gamma}\right)}{r_0-\gamma^2}. \tag{6.86}$$

This result shows that t_0 deviates from the equilibrium case. At fixed γ, the above expression can be minimized with respect to r_0, see Eq. (6.82)-(6.83). The corresponding t_0^* and r_0^* are shown in Figs. 6.4a and c, for $\gamma < \gamma_c'$. In its present form, the perturbative theory does not allow to predict the first order transition in t_0^*, though, and so far we have not found a simple way to address this problem.

6.1.6 Optimal potentials at fixed rates

Up to this section we have been mainly interested in the optimal mean first passage time that can be reached only by varying the transition rates, thinking that these parameters can be well controlled in an experimental device. Equally interesting is to notice that the MFPT exhibits a non-monotonous behaviour with γ for some values of r_0 and r_1, arising the question of how weak or strong the strength potential must be tuned in order to optimize the MFPT once one has fixed the intermittentcy rates.

To address this question, let us define the optimal MFPT

$$t_1^\star(r_0,r_1) = \min_\gamma t_1(\gamma,r_0,r_1), \tag{6.87}$$

where r_0 and r_1 are fixed and $\gamma^\star(r_0,r_1)$ is the corresponding optimal strength. Minimizing the exact solution of the MFPT with Mathematica, we numerically find a remarkable result, depicted in figure 6.6a: when r_1 is small enough, the mean time $t_1(\gamma,r_0,r_1)$ admits an absolute minimum at a finite value of γ. This minimum becomes metastable and further disappears as r_1 increases. In this second regime, the MFPT reaches its minimum at $\gamma = \infty$. The optimal $\gamma^\star$ (or the potential width $1/\gamma^\star$) is thus discontinuous at a critical value of r_1 which depends on r_0 and that we denote as $r_1^c(r_0)$, see Fig. 6.6b. In Figure 6.6a one can see this metastable state for the particular case in which $r_0 = 0.1$, and where we find that $r_1^c(r_0=0.1) = 0.7852182....$ This figure clearly illustrates the abrupt transition of the global minima from $\gamma^\star < \infty$ to $\gamma^\star = \infty$ when r_1 passes from $r_1 < r_1^c$ to $r_1 > r_1^c$. The analytical curves are compared with MC simulations, finding a great agreement between them.

By varying the intermittent dynamical rates in the (r_0,r_1)-plane one can construct the phase diagram in which the optimal strength change from finite to infinite values. This diagram is depicted in Figure 6.7a, whereas Figure 6.7b shows the variations of $t_1^\star$.

The phase transition can be understood from the fact that, in the diffusion process with intermittent potential, two distinct effects are competing: at fixed r_0, a finite potential minimizes the MFPT when $r_1 < r_1^c(r_0)$, meaning that applying a weak confinement

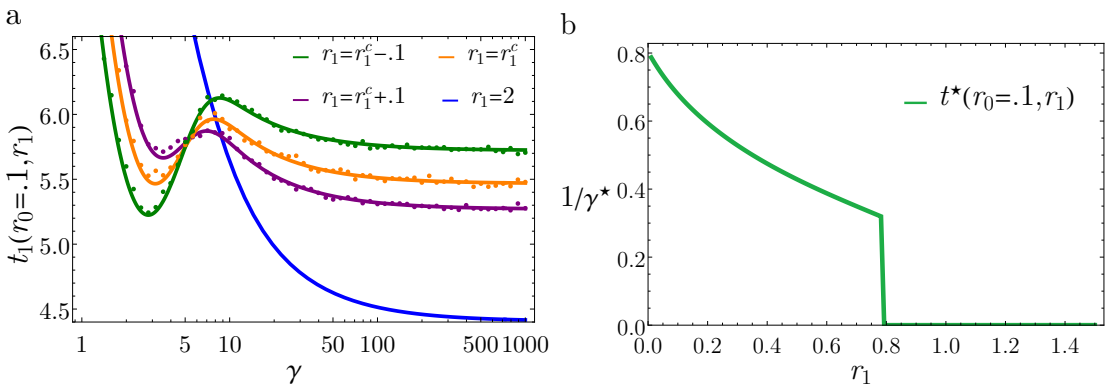

Figure 6.6: Variations of t_1 with the potential strength at fixed rates. (a) Metastability with γ at fixed $r_0 = 0.1$ and several r_1 around the critical value $r_1^c(r_0 = 0.1) = 0.7852182....$ Symbols represent results from MC simulations; each point averages over 2×10^5 realizations. (b) Inverse of the optimal γ vs. r_1 deduced from (a).

for long times ($\sim 1/r_1$) benefits target encounters. In this situation, if we increase the potential strength, the particle will remain close to the origin and won't be able to adequately explore the target region, and in the limiting case $\gamma = \infty$, the particle will stay immobile at each resetting during a time of mean duration $1/r_1$, without searching. However, when r_1 is higher that r_1^c, since the potential is not applied for a long time, it is better to bring back the particle to the origin as rapidly as possible (with gamma=infty), which cuts off the diffusive excursions that explore regions of space far from the target.

A surprising result is the existence of a critical rate $r_0^\infty = 5.539492...$, such that $r_1^c(r_0^\infty) = \infty$ (Fig. 6.7a). If $r_0 > r_0^\infty$, only a finite potential strength minimizes the MFPT, and the phase $\gamma^* = \infty$ disappears.

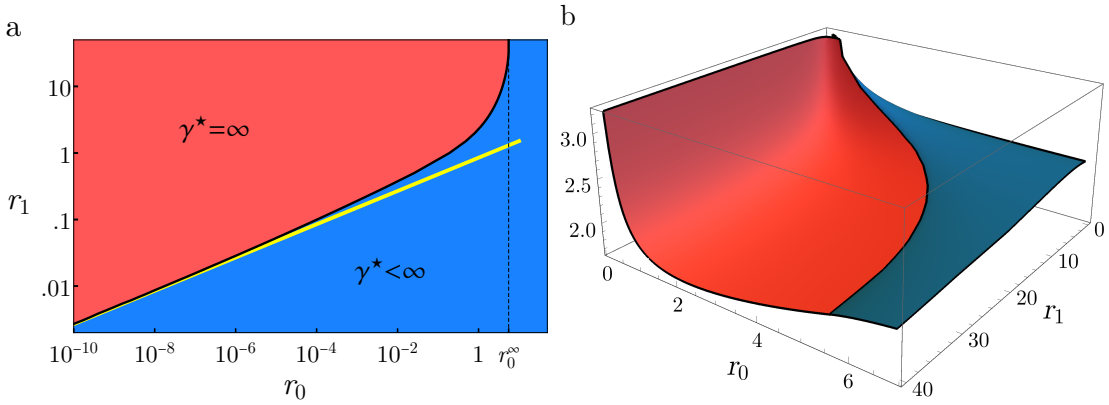

Figure 6.7: (a) Phase diagram in the (r_0, r_1)-plane. The yellow line represents the approximation given by (6.100). (b) Optimized MFPT as a function of (r_0, r_1).

The results discussed above were obtained from the numerical minimization of the exact expression for $t_1(\gamma, r_0, r_1, x = 0)$ exposed in Section 6.1.3. Although it represents a great advance in the light of a better understanding the behaviour of the MFPT, we want to go further in our characterization of the system dynamics and seek for an analytical description for the metastability phenomenon and the discontinuous transition in the optimal potential strength that we observe.

To achieved this goal we notice from Figure 6.7a that r_1 is often $\gg r_0$ at the transition, especially in the small rate region. This suggests a way in which the analysis can be done. In the following we will use this property to obtain an approximate expression of the MFPT. We start by deducing the MFPT with $\gamma = \infty$ (at any rates) from a backward Fokker-Planck equation, and check the agreement with the full exact expression in the limit $\gamma \to \infty$. In a second step, we take γ finite (of order 1) and obtain from the full solution a simplified expression for t_1 within the assumption $\sqrt{r_0} \ll r_1 \ll 1$, showing explicitly the existence of a local minimum at a finite strength. Finally, the two mean times are compared to obtain the absolute minimum and the transition line in the small r_0 regime.

If the potential has infinite strength, the diffusive particle returns to the origin infinitely fast once the potential is turned on, and remains still during a random time of mean $1/r_1$ until the next restart. Hence, the MFPT with the initial condition $\sigma(t=0)=1$ is independent of x, and longer by an amount $1/r_1$ than the MFPT with $\sigma(t=0)=0$ and $x=0$:

$$t_1(\gamma=\infty,x) = t_0(\gamma=\infty,x=0) + \frac{1}{r_1}, \tag{6.88}$$

Substituting this expression in Eq. (6.20) one obtains

$$\frac{\partial^2 t_0^+(\gamma=\infty,x)}{\partial x^2} - r_0 t_0^+(\gamma=\infty,x) = -\frac{r_0+r_1}{r_1} - r_0 t_0^+(\gamma=\infty,x=0). \tag{6.89}$$

as well as a similar equation for $t_0^-(\gamma=\infty,x)$. In Eq. (6.89), we notice that the function $\frac{r_1}{r_0+r_1} t_0^+(\gamma=\infty,x)$ satisfies the same backward equation than the MFPT in diffusion with resetting at rate r_0 without refractory period, whose expression reads $(e^{\sqrt{r_0}}-1)/r_0$ in our dimensionless units and for $x=0$ [54]. We deduce

$$t_0(\gamma=\infty,x=0) = \frac{r_0+r_1}{r_0 r_1}\left(e^{\sqrt{r_0}}-1\right), \tag{6.90}$$

and, from Eq. (6.88),

$$t_1(\gamma=\infty) = \frac{e^{\sqrt{r_0}}}{r_1} + \frac{e^{\sqrt{r_0}}-1}{r_0}. \tag{6.91}$$

This expression agrees with the findings of [56]. It can also be recovered from the limit $\gamma=\infty$ of the exact solution exposed in Section 6.1.3. When we take the limit $\gamma \to \infty$ in Eqs. (6.33)-(6.35), the λ's take the simple form

$$\lambda_1 \simeq \gamma,\ \lambda_2 \simeq -\sqrt{r_0},\ \lambda_3 \simeq \sqrt{r_0}. \tag{6.92}$$

Therefore, given that at $x=0$ the exact solution writes $t_1^+ = A_0^+ + A_2^+$, where A_0 and A_2 read from Eqs. (6.47)-(6.48). The exponential terms with λ_1 become dominant in both factors, and one finds $A_2^+ \simeq (r_0+r_1)/[\gamma (r_0)^{3/2}] \to 0$ and

$$A_0^+ \simeq \frac{(r_0+r_1)e^{\sqrt{r_0}} - r_1}{r_0 r_1}, \tag{6.93}$$

which is Eq. (6.91).

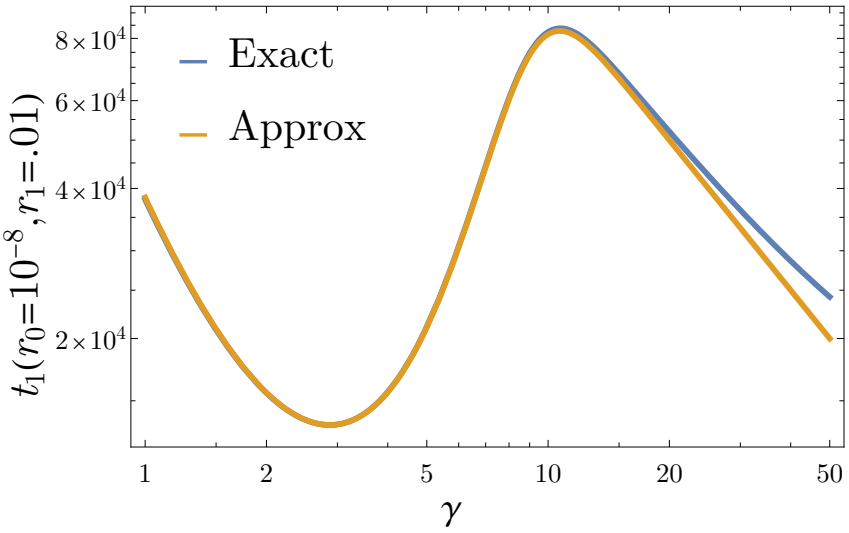

Figure 6.8: t_1 with $(x = 0)$ as a function of γ for $r_0 = 10^{-8}$ and $r_1 = 10^{-2}$. The exact solution (blue line) is compared with the approximation Eq. (6.96) (orange line).

We now turn to the case of a γ of order unity and $r_0 \ll r_1 \ll 1$. In the expressions for the roots given by Eq. (6.33)-(6.35), we set $r_0 = 0$ and expand at first order in r_1 to obtain the approximations

$$\lambda_1 \simeq \frac{r_1}{\gamma} + \gamma, \ \lambda_2 \simeq -\frac{r_1}{\gamma}, \ \lambda_3 \simeq 0. \tag{6.94}$$

Replacing these values into Eqs. (6.47)-(6.48) but keeping $r_0 \neq 0$ elsewhere, one obtains

$$t_1 \simeq \frac{r_0 + r_1}{\gamma r_0} + \frac{\gamma^2\left(\gamma^2 + 2r_1\right)}{r_0 r_1\left(\gamma^2 + r_1\right)}\left(\frac{r_0 + r_1 - (2r_0 + r_1)\, e^{\frac{r_1}{\gamma}}}{\gamma^2 + 2r_1 e^{\gamma + \frac{2r_1}{\gamma}}} + \frac{r_0}{\gamma^2 + 2r_1}\right). \tag{6.95}$$

We notice that the terms proportional to $1/r_0$ are dominant compared to those proportional to $1/r_1$. Eq. (6.95) further simplifies to

$$t_1 \simeq \frac{1}{r_0}\left[\frac{r_1}{\gamma} - \frac{\gamma^2\left(e^{\frac{r_1}{\gamma}} - 1\right)\left(\gamma^2 + 2r_1\right)}{\left(\gamma^2 + r_1\right)\left(\gamma^2 + 2r_1 e^{\gamma + \frac{2r_1}{\gamma}}\right)}\right]. \tag{6.96}$$

As illustrated in Figure 6.8 where $r_0 \ll r_1$, Eq. (6.96) agrees very well with the exact solution at intermediate γ, where a local minimum exists. We next expand the expression (6.96) at small r_1, assuming $r_1 \ll \gamma$, $r_1 \ll \gamma^2$ and $r_1 e^{\gamma}/\gamma^2 \ll 1$; these three inequalities are fulfilled if γ is $O(1)$ and $r_1 \ll 1$. The first non-zero term turns out to be of second order in r_1, and we get the simple expression:

$$t_1 \simeq \frac{r_1^2}{r_0}\left(\frac{4e^{\gamma} - \gamma - 2}{2\gamma^3}\right). \tag{6.97}$$

At fixed rates, the above expression is non-monotonic with γ and reaches a minimum at a value of γ independent of (r_0, r_1), and such that $2e^{\gamma}(\gamma - 3) + \gamma + 3 = 0$. A unique

solution $\gamma_{min} = 2.827641...$ is found, and the local minimum of the MFPT is given by

$$t_1(\gamma_{min}) \simeq 1.388733... \frac{r_1^2}{r_0}. \tag{6.98}$$

One can then compare this expression to the MFPT at $\gamma = \infty$ to find the transition line separating $\gamma^\star = \infty$ from $\gamma^\star < \infty$. We further assume that $\sqrt{r_0} \ll r_1$ near the transition (an assumption to be verified *a posteriori*), hence Eq. (6.91) reduces to $t_1(\gamma = \infty) \simeq 1/\sqrt{r_0}$. Therefore,

$$\frac{t_1(\gamma_{min})}{t_1(\gamma = \infty)} \simeq 1.388733... \frac{r_1^2}{\sqrt{r_0}}, \text{ for } \sqrt{r_0} \ll r_1 \ll 1. \tag{6.99}$$

At the transition this ratio is exactly unity, which gives the critical switch-off rate:

$$r_1^c(r_0) = 0.848575... r_0^{1/4}. \tag{6.100}$$

One checks from Eq. (6.100) that $\sqrt{r_0} \ll r_1^c(r_0)$. Summarizing, we have found the analytical criteria that explains the phenomenon of metastability and the discontinuous transition of the global minimum $\gamma^\star$. We obtained a relation between the rates r_0 and r_1 of the intermittent dynamics at the transition in the small rates regime, namely, for $r_0 \ll 1$. If one chooses a rate r_1 below $r_1^c(r_0)$, the optimal strength will be $\gamma^\star \simeq 2.827641$, while above this point the minimum becomes metastable and $\gamma^\star = \infty$.

6.1.7 Monte Carlo simulations

We would like to conclude the part concerning the MFPT by showing some results from Monte Carlo simulations that are in an excellent agreement with the theoretical ones, in addition to Fig. 6.6 that was shown above. Figures 6.9a depicts the average MFPT t_{av} as a function of r_0 and r_1, for a fixed γ. Particularly interesting is to notice the minima that this function reaches and the good agreement between theory and simulations. Similar results are observed for $t_0(x = 0)$ and $t_1(x = 0)$ separately (not shown).

Figure 6.9b shows $t_1(x = 0)$, as a function of r_1 when r_0 and γ are fixed. A minimum is reached at a finite r_1, and the curves with different r_0 reach the same value at $r_1 = 0$, as they should: this point corresponds to the equilibrium case where the potential is always present and thus r_0 plays no role for t_1.

6.1.8 Non-equilibrium steady states

Finally, in this section we calculate the stationary density of the particle position on the infinite line and in the absence of the absorbing barrier. We recall that, when we introduced in Section 2 the model of free diffusion with stochastic resetting to the origin, we saw that in the absence of the absorbing barrier, the system reaches a non-equilibrium steady state (NESS) [55], in which the particle position X follows the probability density distribution

$$P(X) = \frac{\sqrt{r/D}}{2} e^{-\sqrt{r/D}|X|}, \tag{6.101}$$

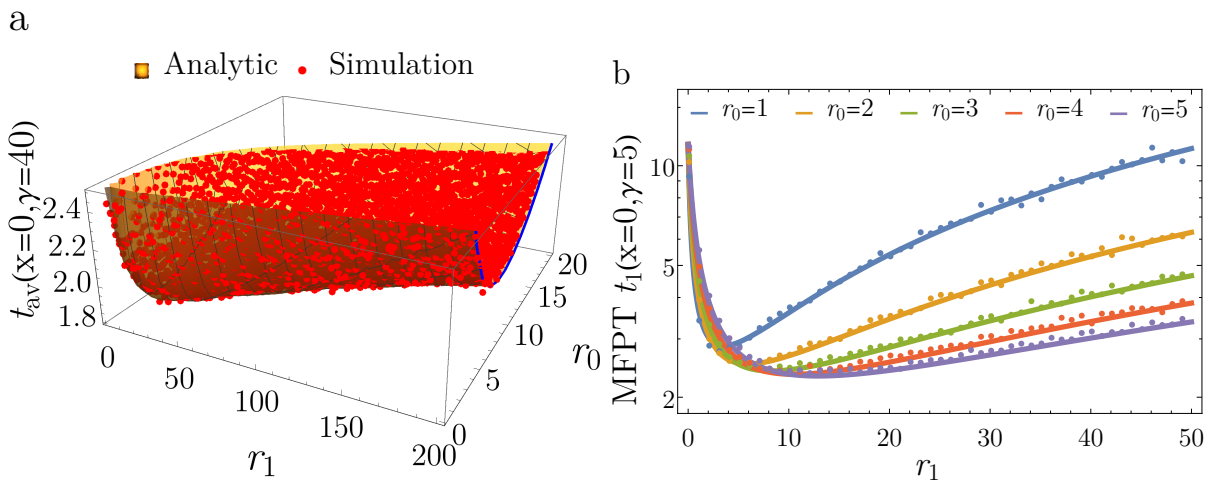

Figure 6.9: MFTP of a MC simulation as a function of r_0 and r_1 for a fixed value of $\gamma = 40$. (a) Red points represents simulation results. A minimum is reached for some rates r_0^* and r_1^*. (b) MFPT as a function of r_1 for several values of r_0 and fixed $\gamma = 5$ and $x = 0$. Points represent simulation results. The curves are calculated numerically from the analytic solution.

where r is the resetting rate and D the diffusion constant. In contrast, when the diffusing particle is in the present of a stationary confining potential of the form $V(X) = \mu|X|$ (without resetting), the system reaches an equilibrium steady state where the particle position follows the Gibbs-Boltzmann equilibrium distribution

$$P(X) = \frac{\mu}{2D} e^{-\mu|X|/D}. \tag{6.102}$$

We will see that, in the limit of large γ, the stationary density can be written as an average of the equilibrium and the NESS of diffusion with instantaneous resetting.

Let us start the analysis using the original dimensional variables and parameters. We define $P_\sigma(X,t)$ as the probability density that the particle is around X and the potential in the state σ (with $\sigma = 0$ or 1) at time t. These two densities satisfy the forward Fokker-Planck equation

$$\frac{\partial}{\partial t}P_0(X,t) = D\frac{\partial^2}{\partial X^2}P_0(X,t) - R_0 P_0(X,t) + R_1 P_1(X,t), \tag{6.103}$$

$$\frac{\partial}{\partial t}P_1(X,t) = D\frac{\partial^2}{\partial X^2}P_1(X,t) + \frac{\partial}{\partial X}\left(\frac{1}{\alpha}V'(X)P_1(X,t)\right) - R_1 P_1(X,t) + R_0 P_0(X,t). \tag{6.104}$$

The first term of the right hand side (r.h.s.) of Eq. (6.103) accounts for the free diffusion of the particle without any external force, whereas the second and third terms represent, respectively, the negative flux of probability out of the state $\sigma = 0$ at rate r_0 and the positive flux into the same state at rate r_1. On the other hand, the first two terms in the r.h.s. of Eq. (6.104) represent the diffusion of the particle with an advection term caused by the external force, the third and fourth terms are, again, probability fluxes between the states $\sigma = 0$ and $\sigma = 1$.

Like in the previous sections, we employ the dimensionless parameter $x = X/L$, where L is an arbitrary length. We do the same for the intermittent parameters r_0 and r_1 and

the strength potential γ, defined by Eqs. 6.3-6.5. The densities of $x = X/L$ are $p_0(x,t)$ and $p_1(x,t)$. Denoting $p_\sigma^+(x,t) \equiv p_\sigma(x,t)$ with $x > 0$, Eqs. (6.103)-(6.104) become

$$\frac{\partial p_0^+}{\partial t} = \frac{\partial^2 p_0^+}{\partial x^2} - r_0 p_0^+ + r_1 p_1^+, \tag{6.105}$$

$$\frac{\partial p_1^+}{\partial t} = \frac{\partial^2 p_1^+}{\partial x^2} + \gamma \frac{\partial p_1^+}{\partial x} - r_1 p_1^+ + r_0 p_0^+. \tag{6.106}$$

The densities $p_0^-(x,t)$ and $p_1^-(x,t)$ for $x < 0$ obey the same equations, except that γ is substituted by $-\gamma$ in (6.106).

At the beginning of section 6.1 we said that, due to the action of the external potential that confines the movement of the particle, we expect to find a non-equilibrium steady state for the position density. This assertion can be proven by seeking stationary solutions of the system (6.105)-(6.106). By symmetry, in the steady state we have that $p_\sigma(x) = p_\sigma(-x)$, then we solve only for $x > 0$. Setting the time derivatives to zero and looking for solutions $p_0(x)$ and $p_1(x)$ proportional to $\exp(-\lambda x)$, we find from Eqs. (6.105)-(6.106) that λ must be the root of the polynomial (6.32) already found in the context of the mean first passage times. The roots are $\lambda_0 = 0$ and λ_k given by Eq. (6.33), with $k = \{1, 2, 3\}$.

Seeking for solutions that do not diverge exponentially as $x \to \infty$, we deduce that the coefficient of $exp(-\lambda_2 x)$ must be zero, since we have already proven that λ_2 is the only negative root [see Eq. (6.36)]. For the densities to be normalized, we also require that there are no constant terms. Therefore, the acceptable solutions for p_1^+ take the form

$$p_1^+(x) = A_1 e^{-\lambda_1 x} + A_3 e^{-\lambda_3 x}, \tag{6.107}$$

while p_0^+ follows from Eq. (6.106) with $\partial/\partial t = 0$:

$$p_0^+(x) = \frac{r_1 + \lambda_1(\gamma - \lambda_1)}{r_0} A_1 e^{-\lambda_1 x} + \frac{r_1 + \lambda_3(\gamma - \lambda_3)}{r_0} A_3 e^{-\lambda_3 x}. \tag{6.108}$$

Constants A_1^+, A_3^+ will be determined from normalization

$$2\int_0^\infty dx [p_0^+(x) + p_1^+(x)] = 1, \tag{6.109}$$

where $p(x) = p_0(x) + p_1(x)$ is the total density, and from the boundary condition

$$\left.\frac{\partial p_1^+}{\partial x}\right|_{x=0} = -\gamma p_1^+(x=0). \tag{6.110}$$

The latter boundary condition asserts that in a vicinity around $x = 0$, the slope of $p_1(x)$ at $x = 0$ is discontinuous. This can be seen directly from taking the integral $\int_{-\epsilon}^{\epsilon} dx$ of Eq. (6.104), noticing that by symmetry one has $\partial_x p_1^+(\epsilon) = -\partial_x p_1^-(-\epsilon)$, $p_1^+(\epsilon) = p_1^-(-\epsilon)$ and $p_0^+(\epsilon) = p_0^-(-\epsilon)$, to then use continuity of the densities and take the limit $\epsilon \to 0$.

The conditions (6.109) and (6.110) yield two equations for A_1 and A_3, that are solved as:

$$A_1 = \frac{\lambda_1\lambda_3(\gamma - \lambda_3) r_0}{2\lambda_2(\lambda_3 - \lambda_1)(r_0 + r_1)}, \tag{6.111}$$

$$A_3 = -\frac{\lambda_1\lambda_3(\gamma - \lambda_1) r_0}{2\lambda_2(\lambda_3 - \lambda_1)(r_0 + r_1)}, \tag{6.112}$$

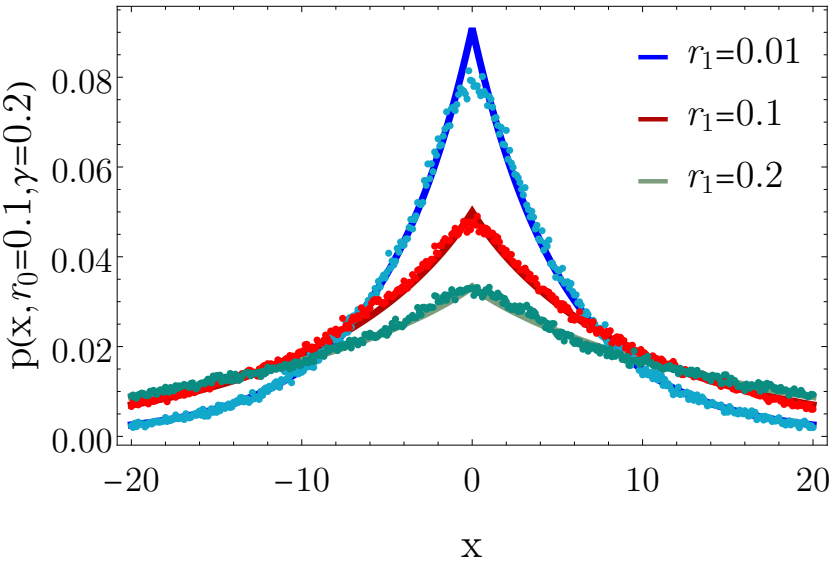

Figure 6.10: Non-equilibrium steady states. The dots represent Monte Carlo simulations and the solid lines Eq. (6.113).

where λ_2 appears as we have used the identity $\lambda_1 + \lambda_2 + \lambda_3 = \gamma$. The total density $p_0(x) + p_1(x)$ reads

$$p(x) = \frac{r_0\gamma}{2(r_0+r_1)}\left(\frac{\lambda_3(\gamma-\lambda_3)}{\lambda_2(\lambda_3-\lambda_1)}e^{-\lambda_1|x|} - \frac{\lambda_1(\gamma-\lambda_1)}{\lambda_2(\lambda_3-\lambda_1)}e^{-\lambda_3|x|}\right) \tag{6.113}$$

for $x \in \mathbb{R}$. It is displayed in Figure 6.10 in a few examples and compared with numerical simulations of the Langevin equation (6.2). The agreement is very good.

One can analyze the behavior of the distribution in the limit of large γ, where $\lambda_1 \simeq \gamma + \frac{r_1}{\gamma}$, $\lambda_2 \simeq -\sqrt{r_0} - \frac{r_1}{2\gamma}$ and $\lambda_3 \simeq \sqrt{r_0} - \frac{r_1}{2\gamma}$. Inserting these expressions into Eq. (6.113) we have

$$p(x) \simeq \frac{r_0\gamma}{2(r_0+r_1)}e^{-\gamma|x|} + \frac{\sqrt{r_0}r_1}{2(r_0+r_1)}e^{-\sqrt{r_0}|x|}, \tag{6.114}$$

which is an average of the NESS of free diffusion with instantaneous resetting at rate r_0 (first term of the r.h.s) and the Gibbs-Boltzmann equilibrium distribution (second term of the r.h.s).

In the limit $\gamma = \infty$, this expression becomes

$$p_{\gamma=\infty}(x) = \frac{r_0}{r_0+r_1}\delta(x) + \frac{\sqrt{r_0}r_1}{2(r_0+r_1)}e^{-\sqrt{r_0}|x|}. \tag{6.115}$$

We recover with this expression the NESS of a resetting process with refractory periods, where the particle remains at the origin for some time after each resetting [58]. If we then take the limit $r_1 \to \infty$, corresponding to a fast switch-off of the potential after attracting the particle back to the origin, the refractory period disappears and the above expression becomes

$$p_{\gamma=\infty,r_1=\infty}(x) = \frac{\sqrt{r_0}}{2}e^{-\sqrt{r_0}|x|}, \tag{6.116}$$

which coincides with the NESS of a particle with unit diffusion constant and resetting rate r_0 to the origin [55].

6.2 General potentials

In this section we extend our analysis of the MFPT to an absorbing target by a Brownian particle in the presence of a general external intermittent potential. The work is orgenized as follows: in Section 6.2.1 we introduce the model and write down the equations of motion that govern the dynamics of two quantities that characterize the statistical properties of the first passage time to a target site, namely, the survival probability in the Laplace domain and the MFPT. These equations are deduced for a general external potential $v(x)$. Due to the difficulty of exactly solving the problem in the general case, in section 6.2.2 we present a perturbative method that allows us to establish when an intermittent potential improves the mean search time. Section 6.2.4 is devoted to the analysis of the particular case in which $v(x) = k|x - x_0|^n/n$. This includes the harmonic case ($n = 2$) and the linear potential ($n = 1$). Both cases are treated separately in Sections 6.2.5 and 6.2.6, respectively. In Section 6.2.7 we analyze the NESS that the system reaches in the absent of the absorbing target.

6.2.1 Governing equations

In the domain, an external potential $V(X)$ is applied intermittently in time, and the state of the potential is characterized by a binary function $\sigma(t)$ which takes the value $\sigma = 0$ when the potential is switched off and $\sigma = 1$ when it is applied. The two-state process $\sigma(t)$ is characterized by two constant transition rates, R_0 (for the transition $0 \to 1$) and R_1 (for $1 \to 0$). A reflecting wall is placed at the position $X = C$, with $C > 0$. The unbounded domain case can be simply obtained by taking the limit $C \to \infty$.

The evolution of the particle position $X(t)$ in the potential $\sigma(t)V(X)$ is given by the over-damped Langevin equation:

$$\frac{dX(t)}{dt} = -\frac{1}{\Gamma}\sigma(t)V'[X(t)] + \xi(t), \tag{6.117}$$

where Γ is the friction coefficient of the particle and $\xi(t)$ a Gaussian white noise of zero mean and correlations $\langle \xi(t)\xi(t')\rangle = 2D\delta(t - t')$, with D the diffusion coefficient.

In the following, it is convenient to introduce the dimensionless space and time variables $x = X/L$ and $t/(L^2/D)$ (which we re-note as t), where L is an arbitrary length. If $V(X)$ has a single minimum, L can be chosen as the distance between the potential minimum and the target placed at $X = 0$. Let us define the dimensionaless parameters:

$$r_0 = R_0L^2/D, \tag{6.118}$$
$$r_1 = R_1L^2/D, \tag{6.119}$$

the re-scaled "on" and "off" rates, respectively. The re-scaled potential is given by $v(x) = V(xL)/(\Gamma D) = V(xL)/(k_BT)$. The reflecting wall is placed at $x = c$ with $c = C/L$.

Let us define $Q_0(x, t)$ as the probability that the particle has not hit the boundary up to time t, given an initial position $x > 0$ and initial potential state $\sigma(t = 0) = 0$. Similarly, $Q_1(x, t)$ corresponds to a potential initially on. These survival probabilities satisfy the

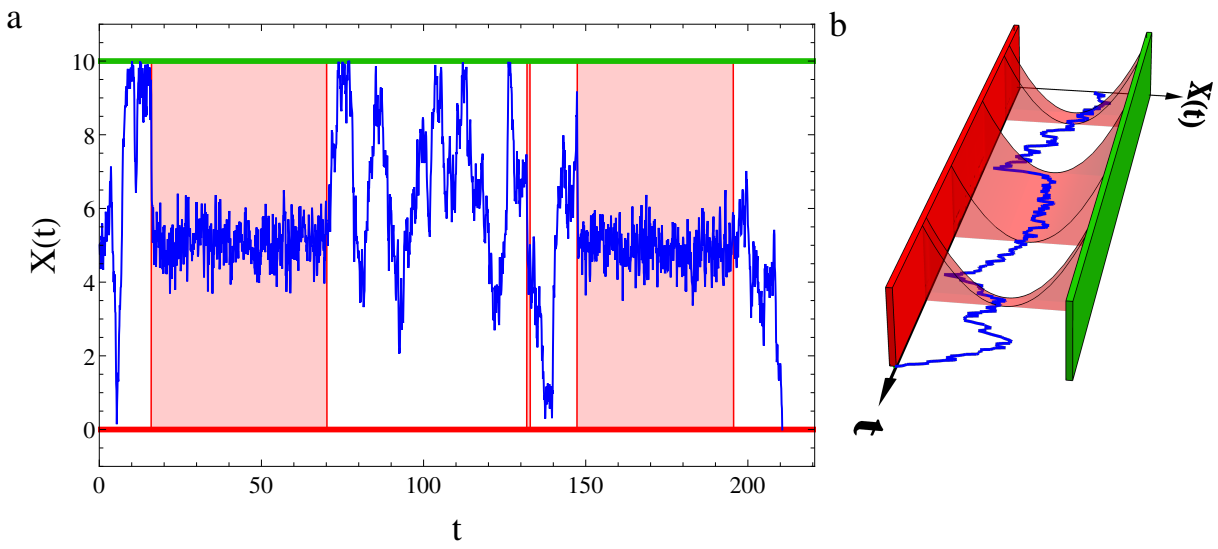

Figure 6.11: a) Trajectory of a diffusive particle with diffusion constant $D = 1$, in an intermittent harmonic potential of the form $V(X) = \frac{K(X-5)^2}{2}$ with $K = 5$. The shaded zones represent the time intervals when the potential is turned on (here $R_0 = R_1 = 0.02$). An absorbing boundary is placed at $X = 0$ (red line) and a reflective wall at $X = 10$ (green line). b) $3D$ view of a particle trajectory and the same harmonic potential.

backward Fokker–Planck equations

$$\frac{\partial Q_1}{\partial t} = \frac{\partial^2 Q_1}{\partial x^2} - v'(x)\frac{\partial Q_1}{\partial x} + r_1(Q_0 - Q_1), \tag{6.120}$$

$$\frac{\partial Q_0}{\partial t} = \frac{\partial^2 Q_0}{\partial x^2} + r_0(Q_1 - Q_0). \tag{6.121}$$

Defining the Laplace transform $\widetilde{Q}(x,s) = \int_0^\infty e^{-st} Q(x,t)dt$, Eqs. (6.120)-(6.121) become

$$-1 = \frac{\partial^2 \widetilde{Q}_1}{\partial x^2} - v'(x)\frac{\partial \widetilde{Q}_1}{\partial x} - (s + r_1)\widetilde{Q}_1 + r_1\widetilde{Q}_0, \tag{6.122}$$

$$-1 = \frac{\partial^2 \widetilde{Q}_0}{\partial x^2} - (s + r_0)\widetilde{Q}_0 + r_0\widetilde{Q}_1, \tag{6.123}$$

from which we deduce the relations for the corresponding MFPTs $t_0(x)$ and $t_1(x)$:

$$-1 = \frac{\partial^2 t_1(x)}{\partial x^2} - v'(x)\frac{\partial t_1(x)}{\partial x} - r_1\left[t_1(x) - t_0(x)\right], \tag{6.124}$$

$$-1 = \frac{\partial^2 t_0(x)}{\partial x^2} - r_0\left[t_0(x) - t_1(x)\right], \tag{6.125}$$

where we have used the fact that $t_i(x) = \widetilde{Q}_i(x, s = 0)$.

The functions $t_0(x)$ and $t_1(x)$ will satisfy the following boundary conditions

$$t_\sigma(x = 0) = 0, \tag{6.126}$$

$$\left.\frac{\partial t_\sigma(x)}{\partial x}\right|_{x=c} = 0, \tag{6.127}$$

where the initial state of the potential is $\sigma = \{0, 1\}$. The first relation enforces the absorption at $x = 0$, whereas the second one follows from imposing a zero flux through the reflective wall placed at $x = c$ [61].

6.2.2 Perturbative method for a general potential

Although the system of differential equations (6.124)-(6.125) may not be solvable in the general case, we develop here an exact perturbative theory by expanding the solutions t_0 and t_1 in powers of $\epsilon \equiv r_1/r_0$, assuming $r_1 \ll r_0$. Let us define the function $S(x) = t_0(x) - t_1(x)$ and write Eqs. (6.124)-(6.125) in terms of $t_1(x)$, $S(x)$ and the parameter ϵ as

$$\frac{\partial^2 t_1(x)}{\partial x^2} - v'(x)\frac{\partial t_1(x)}{\partial x} = -1 - \epsilon r_0 S(x), \tag{6.128}$$

$$\frac{\partial^2 S(x)}{\partial x^2} - r_0 S(x) = -1 - \frac{\partial^2 t_1(x)}{\partial x^2}. \tag{6.129}$$

We look for solutions of the form:

$$t_1(x) = t_1^{(0)}(x) + \epsilon t_1^{(1)}(x) + \dots. \tag{6.130}$$

$$S(x) = S^{(0)}(x) + \epsilon S^{(1)}(x) + \dots. \tag{6.131}$$

at small ϵ. The function $t_1^{(0)}$ is related to the classic Kramers' problem of first passage over a steady potential barrier. The functions $t_1^{(1)}, \dots, S^{(0)}, S^{(1)}, \dots$, depend on the potential shape and r_0, and can be determined recursively. We will particularly focus on the the first order coefficient $t_1^{(1)}(x)$, the so-called "dispersion relation", as it is directly linked to a new phenomenon exhibited by flashing potentials: when this coefficient changes sign, a phase transition between two types of behaviors occurs for t_1. Given a potential initially "on" and a starting position x for the Brownian particle, if

$$t_1^{(1)}(x) > 0 \text{ for any } r_0, \tag{6.132}$$

then switching the potential off and on back and forth (*i.e.*, setting $\epsilon > 0$) will always result in delaying target encounter on average compared to the case with the potential permanently applied, or $\epsilon = 0$. Conversely, if

$$t_1^{(1)}(x) < 0 \text{ for some values of } r_0, \tag{6.133}$$

then the intermittent dynamics of the potential can help to shorten the mean search time.

By construction, the function $S(x)$ satisfies the boundary conditions

$$S(x = 0) = 0, \tag{6.134}$$

$$\left.\frac{\partial S(x)}{\partial x}\right|_{x=c} = 0. \tag{6.135}$$

Eqs. (6.128)-(6.129) can be rewritten in the following form

$$e^{v(x)}\frac{\partial}{\partial x}\left(e^{-v(x)}\frac{\partial}{\partial x}t_1(x)\right) = -1 - \epsilon r_0 S(x), \tag{6.136}$$

$$e^{\sqrt{r_0}x}\frac{\partial}{\partial x}\left(e^{-2\sqrt{r_0}x}\frac{\partial}{\partial x}e^{\sqrt{r_0}x}S(x)\right) = -1 - \frac{\partial^2 t_1(x)}{\partial x^2}, \tag{6.137}$$

which allows to integrate directly each equation and obtain the coupled general solutions $t_1(x)$ and $S(x)$:

$$t_1(x) = C_1 \int_0^x d\tau\ e^{v(\tau)} + C_2 - \int_0^x dy\ e^{v(y)} \int_0^y dz\ e^{-v(z)} \left[1 + \epsilon r_0 S(z)\right], \tag{6.138}$$

$$S(x) = C_3 e^{-\sqrt{r_0}x} + C_4 e^{\sqrt{r_0}x} + \frac{1}{r_0} - e^{-\sqrt{r_0}x} \int_0^x dy\ e^{2\sqrt{r_0}y} \int_0^y dz\ e^{-\sqrt{r_0}z} \frac{\partial^2 t_1(z)}{\partial z^2} \tag{6.139}$$

where the constants C_i are determined from the boundary conditions. Integrating by parts, we can simplify the double integral in Eq. (6.139) to a single integral:

$$S(x) = C_3 e^{-\sqrt{r_0}x} + C_4 e^{\sqrt{r_0}x} + \frac{1}{r_0} - \int_0^x dy\ \frac{\partial t_1(y)}{\partial y} \cosh \sqrt{r_0}(x-y). \tag{6.140}$$

The integral of the r.h.s. can be integrated by parts again and written in terms of t_1 instead of its derivative. However, for the numerical evaluation of these expressions, it is more convenient to keep Eq. (6.140), as we will see later.

Imposing the boundary conditions (6.126)-(6.127) and (6.134)-(6.135) we obtain

$$t_1(x) = \int_0^x dy\ e^{v(y)} \int_y^c dz\ e^{-v(z)} + \epsilon r_0 \int_0^x dy\ e^{v(y)} \int_y^c dz\ e^{-v(z)} S(z), \tag{6.141}$$

$$\begin{aligned} S(x) =& \frac{1}{r_0} - \frac{\cosh \sqrt{r_0}(c-x)}{r_0 \cosh \sqrt{r_0} c} + \sinh \sqrt{r_0} x \int_0^c dy \frac{\partial t_1(y)}{\partial y} \frac{\sinh \sqrt{r_0}(c-y)}{\cosh \sqrt{r_0} c} \\ & - \int_0^x dy \frac{\partial t_1(y)}{\partial y} \cosh \sqrt{r_0}(x-y). \end{aligned} \tag{6.142}$$

Up to this point we have not made any approximation. Although we have obtained a formal solution of the system (6.128)-(6.129), the expressions are still coupled and difficult to write explicitly. However, one can insert the expansions (6.130)-(6.131) into (6.141)-(6.142) and obtain the sought coefficients.

a) Leading order in ϵ

At leading order we have

$$t_1^{(0)}(x) = \int_0^x dy \int_y^c dz\ e^{v(y)-v(z)}, \tag{6.143}$$

$$\begin{aligned} S^{(0)}(x) =& \frac{1}{r_0} - \frac{\cosh \sqrt{r_0}(c-x)}{r_0 \cosh \sqrt{r_0} c} + \sinh \sqrt{r_0} x \int_0^c dy \int_y^c dz\ e^{v(y)-v(z)} \frac{\sinh \sqrt{r_0}(c-y)}{\cosh \sqrt{r_0} c} \\ & - \int_0^x dy \int_y^c dz\ e^{v(y)-v(z)} \cosh \sqrt{r_0}(x-y). \end{aligned} \tag{6.144}$$

The solution of $t_1^{(0)}(x)$ in Eq. (6.143) corresponds to the MFPT of the standard problem for a particle in a potential $v(x)$ [61]. It is related to the the Kramers escape problem in equilibrium. Eqs. (6.143)-(6.144) yields $t_0^{(0)}(x)$, which corresponds physically to the MFPT at the origin of the particle starting at x, with the potential initially "off" and which transits only once to the "on" state at a rate r_0.

b) Higher orders in ϵ

At linear order in ϵ, one obtains the aforementioned dispersion relation, one of the main results of this paper:

$$\begin{aligned} t_1^{(1)}(x) =& t_1^{(0)}(x) - \int_0^x dy \int_y^c dz\ e^{v(y)-v(z)} \frac{\cosh\sqrt{r_0}(c-z)}{\cosh\sqrt{r_0}c} \\ &+ r_0 \left[\int_0^c dy \int_y^c dz\ e^{v(y)-v(z)} \frac{\sinh\sqrt{r_0}(c-y)}{\cosh\sqrt{r_0}c}\right] \left[\int_0^x dy \int_y^c dz\ e^{v(y)-v(z)} \sinh\sqrt{r_0}z\right] \\ &- r_0 \int_0^x dy \int_y^c dz \int_0^z du \int_u^c dw\ e^{v(y)-v(z)+v(u)-v(w)} \cosh\sqrt{r_0}(z-u), \end{aligned} \tag{6.145}$$

and

$$S^{(1)}(x) = \sinh\sqrt{r_0}x \int_0^c dy\ \frac{\partial t_1^{(1)}(y)}{\partial y} \frac{\sinh\sqrt{r_0}(c-y)}{\cosh\sqrt{r_0}c} - \int_0^x dy\ \frac{\partial t_1^{(1)}(y)}{\partial y} \cosh\sqrt{r_0}(x-y). \tag{6.146}$$

At order ϵ^n, with n an integer greater than one, Eqs. (6.141)-(6.142) lead to

$$t_1^{(n)}(x) = r_0 \int_0^x dy\ e^{v(y)} \int_y^c dz\ e^{-v(z)} S^{(n-1)}(z), \tag{6.147}$$

$$S^{(n)}(x) = \sinh\sqrt{r_0}x \int_0^c dy\ \frac{\partial t_1^{(n)}(y)}{\partial y} \frac{\sinh\sqrt{r_0}(c-y)}{\cosh\sqrt{r_0}c} - \int_0^x dy\ \frac{\partial t_1^{(n)}(y)}{\partial y} \cosh\sqrt{r_0}(x-y), \tag{6.148}$$

Hence, there exists a "simple" relation between the functions $t_1^{(n)}$ and $S_1^{(n-1)}$ which allows us to recursively compute any n-th order term in principle. As the expressions rapidly become complicated, we will limit our analysis to the terms of order ϵ, which are sufficient for our purpose.

6.2.3 Semi-infinite line

Before proceeding to the analysis of different potentials, we write the above expressions for the case of the semi-infinite line. This can be achieved by letting the position c of the reflective wall tend to infinity. The expressions (6.143)-(6.144) become

$$t_1^{(0)}(x) = \int_0^x dy \int_y^\infty dz\ e^{v(y)-v(z)}, \tag{6.149}$$

$$\begin{aligned} S^{(0)}(x) =& \frac{1-e^{-\sqrt{r_0}x}}{r_0} + \sinh\sqrt{r_0}x \int_0^\infty dy \int_y^\infty dz\ e^{v(y)-v(z)} e^{-\sqrt{r_0}y} \\ &- \int_0^x dy \int_y^\infty dz\ e^{v(y)-v(z)} \cosh\sqrt{r_0}(x-y), \end{aligned} \tag{6.150}$$

whereas at order one

$$t_1^{(1)}(x) = t_1^{(0)}(x) - \int_0^x dy \int_y^\infty dz\ e^{v(y)-v(z)-\sqrt{r_0}z} + r_0 \left[\int_0^\infty dy \int_y^\infty dz\ e^{v(y)-\sqrt{r_0}y-v(z)}\right]\left[\int_0^x dy \int_y^\infty dz\ e^{v(y)-v(z)} \sinh\sqrt{r_0}z\right] - r_0 \int_0^x dy \int_y^\infty dz \int_0^z du \int_u^\infty dw\ e^{v(y)-v(z)+v(u)-v(w)} \cosh\sqrt{r_0}(z-u), \quad (6.151)$$

$$S^{(1)}(x) = \sinh\sqrt{r_0}x \int_0^\infty dy\ \frac{\partial t_1^{(1)}(y)}{\partial y} e^{-\sqrt{r_0}y} - \int_0^x dy\ \frac{\partial t_1^{(1)}(y)}{\partial y} \cosh\sqrt{r_0}(x-y), \quad (6.152)$$

In the following we compute these expressions [and Eqs. (6.143)-(6.146) at finite c] for different potential shapes.

6.2.4 Potential of the type $v(x) = k|x-1|^n/n$

Let us consider symmetric confining potentials of the form $v(x) = k|x-1|^n/n$, with $n > 0$ and k a dimensionless potential stiffness. As the target is located at the origin, the minimum of this potential is at a distance unity from the target. Although we obtained expressions for any value of the starting position x, we will focus on the case $x = 1$, *i.e.*, the particle starting at the minimum of the potential. The particular case with $n = 1$ for the semi-infinite line has been already analyzed in Section 6.1 by direct resolution of the first passage equations. Here we extend our results to more general potentials and to confined domains ($1 \le c < \infty$).

For the following, let us define the function

$$G_n(x,c) = e^{\frac{k}{n}|x-1|^n} \int_x^c dy\ e^{-\frac{k}{n}|y-1|^n} = e^{\frac{k}{n}|x-1|^n} \frac{\gamma_{\frac{1}{n}}\left(\frac{k}{n}(c-1)^n\right) - \frac{|x-1|}{x-1}\gamma_{\frac{1}{n}}\left(\frac{k}{n}|x-1|^n\right)}{n^{1-\frac{1}{n}}k^{\frac{1}{n}}}, \quad (6.153)$$

where $\gamma_a(x) = \int_0^x dz\ z^{a-1}e^{-z}$ is the lower incomplete gamma function. With this notation, inserting $v(x) = k|x-1|^n/n$ into Eq. (6.143), one gets

$$t_1^{(0)}(x) = \int_0^x dy\ G_n(y,c). \quad (6.154)$$

Substituting the above expression into Eq. (6.144) we obtain

$$S^{(0)}(x) = \frac{1}{r_0} - \frac{\cosh\sqrt{r_0}(c-x)}{r_0\cosh\sqrt{r_0}c} - \int_0^x dy\ G_n(y,c)\cosh\sqrt{r_0}(x-y) + \sinh\sqrt{r_0}x \int_0^c dy\ G_n(y,c)\frac{\sinh\sqrt{r_0}(c-y)}{\cosh\sqrt{r_0}c}. \quad (6.155)$$

From Eq. (6.145), the dispersion relation reads

$$t_1^{(1)}(x) = t_1^{(0)}(x) - r_0 \int_0^x dy \int_y^c dz \int_0^z du \int_u^c dw\ e^{\frac{k}{n}(|y-1|^n-|z-1|^n+|u-1|^n-|w-1|^n)} \cosh\sqrt{r_0}(z-u) - \int_0^x dy \int_y^c dz\ e^{\frac{k}{n}|y-1|^n-\frac{k}{n}|z-1|^n}\left(\frac{\cosh\sqrt{r_0}(c-z)}{\cosh\sqrt{r_0}c} - r_0\sinh\sqrt{r_0}z\left[\int_0^c du\ G_n(u,c)\frac{\sinh\sqrt{r_0}(c-u)}{\cosh\sqrt{r_0}c}\right]\right). \quad (6.156)$$

6.2.5 Harmonic potentials

In this section we consider the generic case $n = 2$, in which the switching potential is harmonic, or $v(x) = k(x-1)^2/2$, with k the re-scaled stiffness. The latter is given by

$$k = \frac{KL^2}{\Gamma D}, \tag{6.157}$$

with K the stiffness in physical units. When the potential is permanently applied, the particle follows an Orstein-Uhlenbeck (OU) process of unit mean [112], and the MFPT from x to the origin is given by

$$t_1^{(0)}(x) = \int_0^x dy\; e^{\frac{k}{2}(y-1)^2} \int_y^c dz\; e^{-\frac{k}{2}(z-1)^2}. \tag{6.158}$$

As mentioned earlier, all the numerical results below correspond to the starting position $x = 1$.

Before discussing the effects of the on-off potential dynamics, one can deduce from the above expression that $t_1^{(0)}(x = 1)$ increases monotonically with k when the position of the reflecting wall c is below a particular value c_0. In this case, the MFPT is minimal at $k = 0$, *i.e.*, without any external force and $t_1^{(0)}(k = 0, c) = c - \frac{1}{2}$. On the other hand, when $c > c_0$, the MFPT $t_1^{(0)}$ exhibits a non-monotonic behaviour with k and reaches a minimum at a certain $k_{OU} > 0$, see further the blue curve of Fig. 6.13a. The exact value of c_0 corresponds to the point in which the slope of $t_1^{(0)}(k, c)$ at $k = 0$ changes from positive to negative values, *i.e.*,

$$\left.\frac{\partial t_1^{(0)}(k, c_0)}{\partial k}\right|_{k=0} = 0. \tag{6.159}$$

Solving the above relation for c_0 using Eq. (6.158) we obtain

$$c_0 = 2.19148\ldots \tag{6.160}$$

Here, we will first assume that the domain size is sufficiently large, or $c > c_0$, and will discuss the case $c < c_0$ afterwards. Taking $n = 2$ in Eq. (6.153), the function $G_2(x, c)$ can be recast as

$$G_2(x, c) = e^{\frac{k}{2}(x-1)^2} \sqrt{\frac{\pi}{2k}} \left[\mathrm{erf}\left(\sqrt{k/2}(c-1)\right) - \mathrm{erf}\left(\sqrt{k/2}(x-1)\right)\right], \tag{6.161}$$

where $\mathrm{erf}(x) = \frac{2}{\sqrt{\pi}} \int_0^z dz\; e^{-z^2}$ is the error function. Now we can replace the form of $G_2(x, c)$ into Eq. (6.156) and then compute $t_1^{(1)}(x)$. We show below the main results obtained from numerical evaluations of the integrals.

Figure 6.12a displays the dispersion relation as a function of r_0, obtained from evaluating $t_1^{(1)}(x)$ at $x = 1$, $c = 3$ and fixing k. We notice that this function is non-monotonic. When the potential stiffness is below a certain critical value, or $k < k_c(c) = 1.49823\ldots$ for $c = 3$, the function $t_1^{(1)}$ always stays positive. This means that turning alternatively the potential off (at a small rate r_1) and on (at any rate r_0) will always increase the mean search time compared with the Kramers' case $r_1 = 0$ (or $t_1 > t_1^{(0)}$). At the marginal

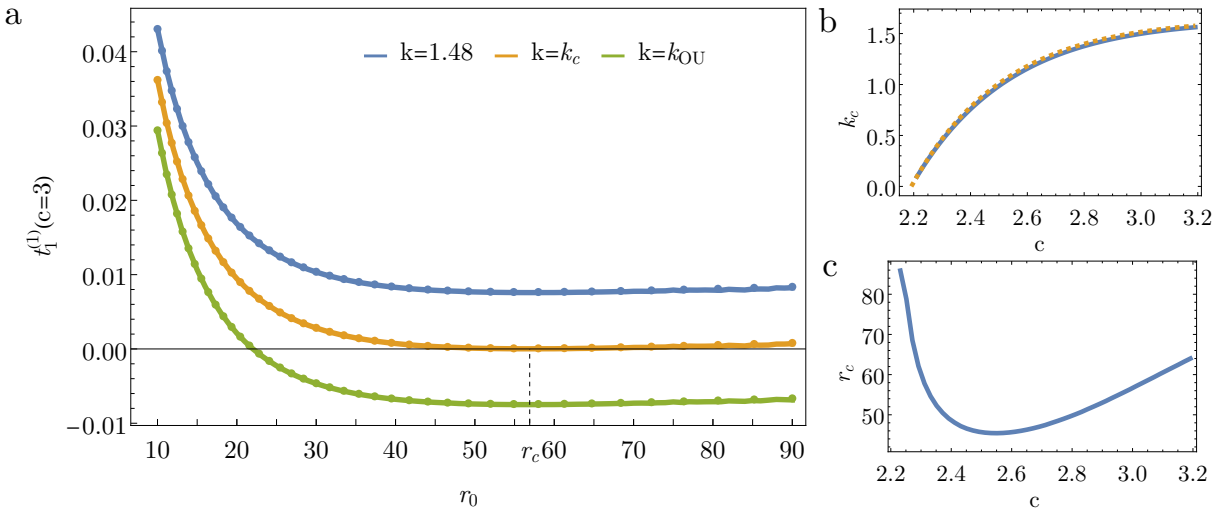

Figure 6.12: Searches starting from $x = 1$ and with the harmonic potential on at $t = 0$. (a) Coefficient of the first correction in the series expansion of t_1 near $r_1 = 0$ (the "dispertion relation") as a function of r_0 and at the fixed value $c = 3$, for various k near $k_c(c = 3) = 1.49819\ldots$. The points represent the results from numerically solving Eqs. (6.124)-(6.125) by using a finite differences scheme. (b) and (c): Critical potential stiffness k_c (next to k_{OU} shown with the dotted line) and optimal switch-off rate r_c as a function of the domain size c, respectively.

case $k = k_c$, the curve of $t_1^{(1)}$ becomes tangent to the $x-$axis, at a critical resetting rate $r_0 = r_c$. For the case $c = 3$, one finds $r_c = 56.66926\ldots$. If the potential stiffness is above k_c, there exists a window of values of r_0 around r_c for which $t_1^{(1)}$ is negative. Therefore, setting $r_0 \simeq r_c$ and r_1 small but > 0 will shorten the mean search time (or $t_1 < t_1^{(0)}$). The agreement between the theory and a direct numerical solution of Eqs. (6.124)-(6.125) [see AppendixD] is excellent.

In figures 6.12b-c are displayed the behaviour of k_c and r_c as a function of the domain size c. The variations of k_{OU} are also shown. It is quite remarkable that k_c is lower than k_{OU} but always very close to it. For instance, for $c = 3$, we find $k_{OU} = 1.51603\ldots$, to be compared to the value $k_c = 1.49823\ldots$ mentioned above. Another surprising property is that r_c is $\gg 1$: in dimensional units, the value of r_0 that minimizes t_1 is thus much larger than the inverse diffusion time.

For $c < c_0$, one has $k_{OU} = 0$ and a marginal dispersion relation cannot be found, therefore the pair (k_c, r_c) cannot be defined. Numerical investigations indicate that $t_1^{(1)}$ is negative for all values of k and r_0 in this case.

The results of Fig. 6.12a demonstrate the existence in large enough domains of a phase transition in the optimal parameters (r_0^*, r_1^*), *i.e.*, the parameters (r_0, r_1) that minimize the MFPT t_1, at a non-trivial value k_c of the potential stiffness. For $k < k_c$, we have $r_1^* = 0$; whereas $r_1^* > 0$ for $k > k_c$. Likewise, r_0^* is not defined below k_c, while $r_0^* \simeq r_c$ for k in the vicinity of k_c from above. Determining the behavior of $r_1^*(k)$ slightly above k_c would require an expansion at the following order ϵ^2 in Eqs. (6.130)-(6.131). We can alternatively solve Eqs. (6.124)-(6.125) numerically by using an implicit finite difference scheme (see Appendix D for details). From this numerical solution, one obtains in Fig. 6.13b-c the optimal rates r_0^* and r_1^*, for $x = 1$, as a function of the potential stiffness k. Fig. 6.13a shows the corresponding minimum MFPT reached, $t_1^*(k)$, which decreases with k.

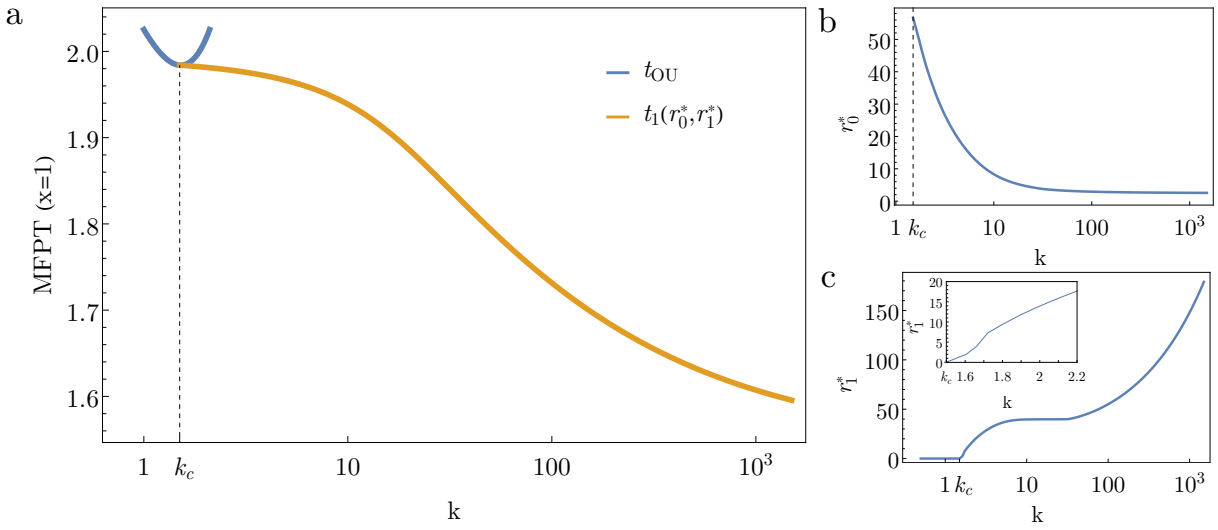

Figure 6.13: Searches starting from $x = 1$ and with the harmonic potential on at $t = 0$ and with $c = 3$. (a) Minimal MFPT t_1^* as a function of the potential stiffness k. The orange line is obtained from numerical minimization of the numerical solution with respect to (r_0, r_1). The blue line represents t_1 for a particle in a steady potential ($r_1 = 0$). (b) and (c): optimal rates $r_1^*(k)$ and $r_0^*(k)$.

Above k_c, this time becomes much smaller than $t_{OU}(k)$, which typically keeps increasing exponentially with k. In the limit $k \to \infty$, one recovers the problem of diffusion with instantaneous stochastic resetting to the origin, where $t_1^* \to 1.5451\ldots$ and $r_0^* \to 2.5396\ldots$ [55].

6.2.6 Piecewise linear potential

In the case $n = 1$, the switching potential is of the form $v(x) = k|x - 1|$, with k the re-scaled potential strength, given by

$$k = \frac{KL}{\Gamma D}, \tag{6.162}$$

where K is the strength in physical units. The results are qualitatively similar to the harmonic case, see Fig. 6.14. We have addressed this problem in Section 6.1 for the semi-infinite line case. Setting $n = 1$ in the expression for $G_n(x, c)$ in (6.153) we get

$$G_1(x, c) = \frac{e^{k|x-1|}}{k}\left(1 - e^{-k(c-1)} - \frac{|x-1|}{x-1}\left(1 - e^{-k|x-1|}\right)\right). \tag{6.163}$$

In the following we denote as $t_1^{(0)}(x, -)$ the solution in the range $0 \le x < 1$ and $t_1^{(0)}(x, +)$ the solution in $1 < x < c$. Replacing the expression of $G_1(x, c)$ in Eq. (6.154) we obtain

$$t_1^{(0)}(x, -) = \frac{\left(2 - e^{-k(c-1)}\right)\left(e^k - e^{-k(x-1)}\right) - xk}{k^2}, \tag{6.164}$$

$$t_1^{(0)}(x, +) = \frac{2(e^k - 1) + (x-2)k + e^{-k(c-1)}(2 - e^k) - e^{-k(c-x)}}{k^2}. \tag{6.165}$$

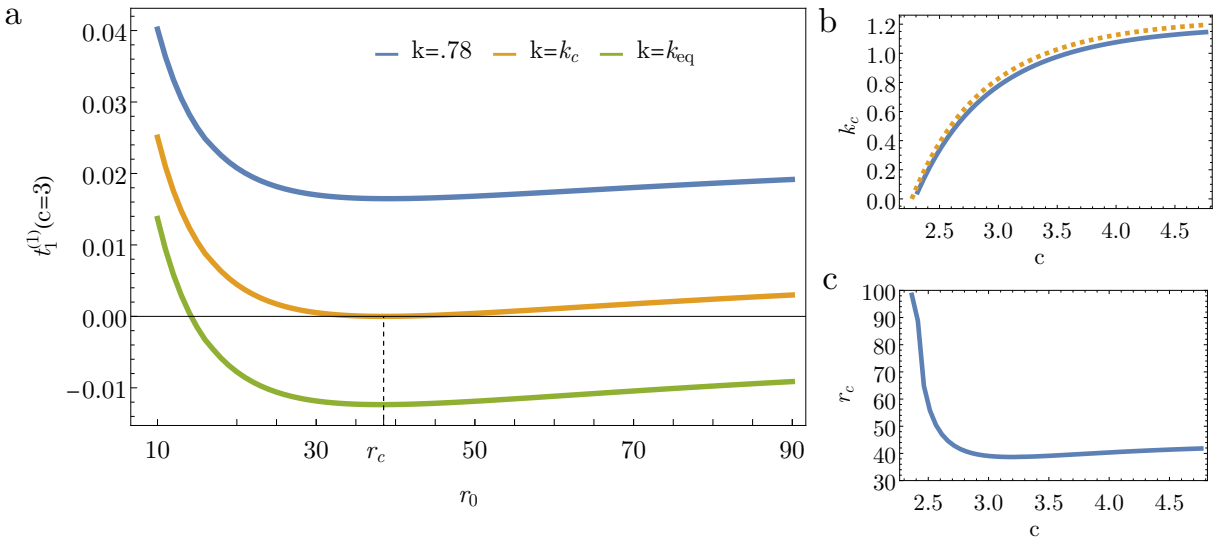

Figure 6.14: Searches starting from $x = 1$ and with the potential on at $t = 0$. (a) Coefficient of the first correction in the series expansion of t_1 near $r_1 = 0$ (the "dispertion relation") as a function of r_0 and at the fixed value $c = 3$, for various k near $k_c(c = 3) = 0.806777\ldots$. (b) and (c): Critical potential stiffness k_c (next to k_{OU} shown with the dotted line) and optimal switch-off rate r_c as a function of the domains size c, respectively.

It is easy to check the continuity of the MFPT in $x = 1$, or $t_1^{(0)}(1,-) = t_1^{(0)}(1,+)$. The complete expressions of $S^{(0)}(x)$ and $t_1^{(1)}(x)$ are somehow intricate and we do not write them here. Again, in the following we show the main results from the numerical analysis of these quantities for the special case in which the particle starts diffusing at the minimum of the potential ($x = 1$).

Taking $x = 1$ in Eq. (6.164) one gets

$$t_1^{(0)}(k,c) = \frac{\left(2 - e^{-k(c-1)}\right)\left(e^k - 1\right) - k}{k^2}, \tag{6.166}$$

where we have made explicit the dependency of the MFPT t_1 with the variables k and c.

As in the case of the harmonic potential, there exists a critical value c_0 such that (i) if $c < c_0$ the minimum of the MFPT $t_1^{(0)}$ is achieved only at $k = 0$ and, (ii) if $c > c_0$, there is a finite potential strength k at which the MFPT $t_1^{(0)}$ is minimum. The value c_0 satisfies

$$\left.\frac{\partial t_1^{(0)}(k,c_0)}{\partial k}\right|_{k=0} = 0. \tag{6.167}$$

Solving the above relation for c_0 and using Eq. (6.166) we obtain

$$c_0 = 2.26376\ldots \tag{6.168}$$

If we let $c \to \infty$, the equations (6.164)-(6.165) reduce to the simple form

$$t_1^{(0)}(x,-) = \frac{2e^k\left(1 - e^{-kx}\right) - xk}{k^2}, \tag{6.169}$$

$$t_1^{(0)}(x,+) = \frac{2(e^k - 1) + (x-2)k}{k^2}. \tag{6.170}$$

With the above result and using Eq. (6.150) we can calculate the leading order $S^{(0)}$ for the semi-infinite line. After some algebra we get

$$S^{(0)}(x,-) = \frac{1-e^{-\sqrt{r_0}x}}{r_0} + \frac{2e^k\left(e^{-kx}-e^{-\sqrt{r_0}x}\right)}{k^2-r_0} + \frac{2e^{-\sqrt{r_0}}\sinh\sqrt{r_0}x}{\sqrt{r_0}(k+\sqrt{r_0})}, \tag{6.171}$$

$$S^{(0)}(x,+) = \frac{1-e^{-\sqrt{r_0}x}}{r_0} + \frac{2e^{-\sqrt{r_0}x}\left(\frac{k}{\sqrt{r_0}}\sinh\sqrt{r_0}+\cosh\sqrt{r_0}-e^k\right)}{k^2-r_0}. \tag{6.172}$$

Recalling that $t_0(x) = S(x) + t_1(x)$, we can compute the first passage time with the initial condition $\sigma(t=0)=0$:

$$t_0^{(0)}(x,-) = \frac{1-e^{-\sqrt{r_0}x}}{r_0} + \frac{2e^k\left(1-e^{-kx}\right)-xk}{k^2} + \frac{2e^k\left(e^{-kx}-e^{-\sqrt{r_0}x}\right)}{k^2-r_0} + \frac{2e^{-\sqrt{r_0}}\sinh\sqrt{r_0}x}{\sqrt{r_0}(k+\sqrt{r_0})}, \tag{6.173}$$

$$t_0^{(0)}(x,+) = \frac{1-e^{-\sqrt{r_0}x}}{r_0} + \frac{2(e^k-1)+(x-2)k}{k^2} + \frac{2e^{-\sqrt{r_0}x}\left(\frac{k}{\sqrt{r_0}}\sinh\sqrt{r_0}+\cosh\sqrt{r_0}-e^k\right)}{k^2-r_0}. \tag{6.174}$$

The above results agree with those computed in Section 6.1 for the piecewise linear potential.

6.2.7 Stationary density with an intermittent harmonic potential

In this section we now study the probability density $P(X,t)$ of the position X of the Brownian particle on the infinite line. We present the full result for the non-equilibrium steady state $\lim_{t\to\infty} P(X,t)$ when the intermittent potential is harmonic.

Let us introduce $P_\sigma(X,t)$, the joint probability that the particle is around X and the potential in state $\sigma = \{0,1\}$ at time t, the initial conditions being implicit. For a general intermittent potential $V(X)$, these densities satisfy the forward Fokker-Planck equations

$$\frac{\partial}{\partial t}P_0(X,t) = D\frac{\partial^2}{\partial X^2}P_0(X,t) - R_0P_0(X,t) + R_1P_1(X,t), \tag{6.175}$$

$$\frac{\partial}{\partial t}P_1(X,t) = D\frac{\partial^2}{\partial X^2}P_1(X,t) + \frac{1}{\Gamma}\frac{\partial}{\partial X}\left[V'(X)P_1(X,t)\right] - R_1P_1(X,t) + R_0P_0(X,t). \tag{6.176}$$

For a harmonic potential $V(X) = \frac{K}{2}X^2$ (we now place the minimum of the potential at the origin), Eqs. (6.175)-(6.176) read

$$\frac{\partial}{\partial t}P_0(X,t) = D\frac{\partial^2}{\partial X^2}P_0(X,t) - R_0P_0(X,t) + R_1P_1(X,t), \tag{6.177}$$

$$\frac{\partial}{\partial t}P_1(X,t) = D\frac{\partial^2}{\partial X^2}P_1(X,t) + \frac{K}{\Gamma}\frac{\partial}{\partial X}\left(XP_1(X,t)\right) - R_1P_1(X,t) + R_0P_0(X,t). \tag{6.178}$$

We again employ the dimensionless space and time variables $x = X/L$ and $t/(L^2/D)$ (re-noted as t), and the dimensionless "on" and "off" rates r_0 and r_1. The re-scaled potential stiffness k reads

$$k = \frac{KL^2}{\Gamma D}, \tag{6.179}$$

The joint densities associated to $x = X/L$ are denoted as $p_0(x,t)$ and $p_1(x,t)$. In the steady state limit, we set the time derivatives to zero in Eqs. (6.177)-(6.178) to obtain, in adimensional units,

$$\frac{\partial^2 p_0(x)}{\partial x^2} - r_0 p_0(x) + r_1 p_1(x) = 0, \tag{6.180}$$

$$\frac{\partial^2 p_1(x)}{\partial x^2} + k\frac{\partial}{\partial x}\left(x p_1(x)\right) - r_1 p_1(x) + r_0 p_0(x) = 0. \tag{6.181}$$

Let us take the space Fourier transform $\widetilde{f}(\nu) = \int_{-\infty}^{\infty} dx\ e^{-i\nu x} f(x)$ of Eqs. (6.180)-(6.181),

$$-\left(\nu^2 + r_0\right)\widetilde{p}_0(\nu) + r_1\widetilde{p}_1(\nu) = 0, \tag{6.182}$$

$$-\left(\nu^2 + r_1\right)\widetilde{p}_1(\nu) - k\nu\frac{\partial}{\partial \nu}\widetilde{p}_1(\nu) + r_0\widetilde{p}_0(\nu) = 0, \tag{6.183}$$

where we have use the identities $\widetilde{\frac{\partial f(x)}{\partial x}} = i\nu\widetilde{f}(\nu)$ and $\widetilde{xf(x)} = i\frac{\partial \widetilde{f}(\nu)}{\partial \nu}$. Combining Eqs. (6.182)-(6.183) gives

$$\frac{\partial \widetilde{p}_1(\nu)}{\partial \nu} + \frac{\nu\left(\nu^2 + r_0 + r_1\right)}{k\left(\nu^2 + r_0\right)}\widetilde{p}_1(\nu) = 0, \tag{6.184}$$

which is solved as

$$\widetilde{p}_1(\nu) = Ae^{-\int^{\nu} a(\tau)d\tau}, \tag{6.185}$$

where

$$a(\tau) = \frac{\tau\left(\tau^2 + r_0 + r_1\right)}{k\left(\tau^2 + r_0\right)}, \tag{6.186}$$

and A is a constant to be determined from the normalization condition. We therefore obtain

$$\widetilde{p}_1(\nu) = Ae^{-\frac{\nu^2 + r_1 \ln\left(\nu^2 + r_0\right)}{2k}} = \frac{Ae^{-\frac{\nu^2}{2k}}}{\left(\nu^2 + r_0\right)^{\frac{r_1}{2k}}}. \tag{6.187}$$

From Eq. (6.182) one deduce the density $p_0(\nu)$,

$$\widetilde{p}_0(\nu) = \frac{r_1}{\nu^2 + r_0}\widetilde{p}_1(\nu) = \frac{Ar_1 e^{-\frac{\nu^2}{2k}}}{\left(\nu^2 + r_0\right)^{\frac{r_1}{2k}+1}}. \tag{6.188}$$

The normalization condition imposes

$$\widetilde{p}_0(\nu = 0) + \widetilde{p}_1(\nu = 0) = \int_{-\infty}^{\infty} dx\left[p_0(x) + p_1(x)\right] = 1, \tag{6.189}$$

from which we deduce

$$A = \frac{r_0^{\frac{r_1}{2k}+1}}{r_0 + r_1}. \tag{6.190}$$

The full position density $\widetilde{p}(\nu) = \widetilde{p}_0(\nu) + \widetilde{p}_1(\nu)$ therefore reads

$$\widetilde{p}(\nu) = \frac{r_0^{\frac{r_1}{2k}+1}\left(\nu^2 + r_0 + r_1\right)e^{-\frac{\nu^2}{2k}}}{\left(r_0 + r_1\right)\left(\nu^2 + r_0\right)^{\frac{r_1}{2k}+1}}. \tag{6.191}$$

In the following we consider a few limiting cases, where this expression simplifies.

a) Limits $r_0 = \infty$ and $r_1 = 0$

In this limit, the potential always stays in the "on" state. Setting $r_0 = \infty$ and $r_1 = 0$, Eq. (6.191) becomes

$$\widetilde{p}(\nu, r_0 = \infty, r_1 = 0) = e^{-\frac{\nu^2}{2k}}, \tag{6.192}$$

which is easily inverted as

$$p(x, r_0 = \infty, r_1 = 0) = p_{OU}(x) = \sqrt{\frac{k}{2\pi}}e^{-\frac{kx^2}{2}}. \tag{6.193}$$

One recovers the equilibrium distribution $p_{OU}(x)$ for the Ornstein-Uhlenbeck process [112].

b) Limit $r_1 \ll k$

In the steep potential limit, or $r_1/k \approx 0$, the probabilities $\widetilde{p}_0$ and $\widetilde{p}_1$ in Eqs. (6.187)-(6.188) can be approximated by

$$\widetilde{p}_1(\nu) = \frac{r_0}{r_0 + r_1}e^{-\frac{\nu^2}{2k}}, \tag{6.194}$$

$$\widetilde{p}_0(\nu) = \frac{r_1}{r_0 + r_1}\left(\frac{r_0 e^{-\frac{\nu^2}{2k}}}{\nu^2 + r_0}\right). \tag{6.195}$$

The inverse Fourier transform of Eq. (6.194) reduces to the Ornstein-Uhlenbeck distribution (6.193), weighted by the probability that the potential is turned on. On the other hand, the inverse transform of Eq. (6.195) can be obtained from the convolution theorem if we notice that the inverse Fourier transform of $r_0/(\nu^2 + r_0)$ is $\frac{\sqrt{r_0}}{2}e^{-\sqrt{r_0}|x|}$, whereas the inverse transform of $e^{-\nu^2/2k}$ is again given by Eq. (6.193). Therefore

$$p_0(x) = \frac{r_1}{r_0 + r_1}\int_{-\infty}^{\infty}\left(\sqrt{\frac{k}{2\pi}}e^{-\frac{ky^2}{2}}\right)\frac{\sqrt{r_0}}{2}e^{-\sqrt{r_0}|x-y|}dy. \tag{6.196}$$

One recognizes in this result the probability distribution of an instantaneous resetting process with rate r_0, averaged over a equilibrium Orstein-Uhlenbeck distribution of resetting points, $p_{OU}(y) = \sqrt{\frac{k}{2\pi}}e^{-\frac{ky^2}{2}}$, which is itself weighted by the probability that the potential is turned off [55]. Then, in this steep potential limit, the total probability density $p(x) = p_0(x) + p_1(x)$ reads

$$p(x) = \frac{r_0}{r_0 + r_1}\sqrt{\frac{k}{2\pi}}e^{-\frac{kx^2}{2}} + \frac{r_1}{r_0 + r_1}\int_{-\infty}^{\infty}\left(\sqrt{\frac{k}{2\pi}}e^{-\frac{ky^2}{2}}\right)\frac{\sqrt{r_0}}{2}e^{-\sqrt{r_0}|x-y|}dy. \tag{6.197}$$

We rewrite the integral in Eq. (6.196) as

$$\begin{aligned} p_0(x) &= \frac{r_1}{2(r_0+r_1)}\sqrt{\frac{r_0 k}{2\pi}}\left(\int_{-\infty}^{x} e^{-\frac{ky^2}{2}-\sqrt{r_0}(x-y)}dy + \int_{x}^{\infty} e^{-\frac{ky^2}{2}-\sqrt{r_0}(y-x)}dy\right) \\ &= \frac{r_1 e^{\frac{r_0}{2k}}}{2(r_0+r_1)}\sqrt{\frac{r_0 k}{2\pi}}\left(e^{-\sqrt{r_0}x}\int_{-\infty}^{x} e^{-\frac{k(y-\sqrt{r_0}/k)^2}{2}}dy + e^{\sqrt{r_0}x}\int_{x}^{\infty} e^{-\frac{k(y+\sqrt{r_0}/k)^2}{2}}dy\right) \\ &= \frac{r_1\sqrt{r_0}e^{\frac{r_0}{2k}}}{4(r_0+r_1)}\left(e^{-\sqrt{r_0}x}\,\mathrm{erfc}\left(\frac{\sqrt{r_0}-kx}{\sqrt{2k}}\right) + e^{\sqrt{r_0}x}\,\mathrm{erfc}\left(\frac{\sqrt{r_0}+kx}{\sqrt{2k}}\right)\right). \end{aligned} \tag{6.198}$$

At large z, we use erfc(z) $\approx e^{-z^2}/\sqrt{\pi}z$ and erfc(-z) $\approx 2 - e^{-z^2}/\sqrt{\pi}z$. This allow us to obtain the large x behavior

$$p_0(x) \approx \frac{r_1\sqrt{r_0}e^{\frac{r_0}{2k}}}{2(r_0+r_1)}\left(e^{-\sqrt{r_0}x} - \frac{\sqrt{2r_0 k}e^{-\frac{kx^2}{2}-\frac{r_0}{2k}}}{\sqrt{\pi}(k^2x^2-r_0)}\right) \approx \frac{r_1 e^{\frac{r_0}{2k}}}{r_0+r_1}\left(\frac{\sqrt{r_0}e^{-\sqrt{r_0}x}}{2}\right). \tag{6.199}$$

This expression is exponential in x and dominant over the Gaussian *OU* distribution $p_1(x)$. Hence, the total probability density $p(x)$ at large x is also given by

$$p(x) \approx \frac{r_1\sqrt{r_0}e^{\frac{r_0}{2k}-\sqrt{r_0}x}}{2(r_0+r_1)}. \tag{6.200}$$

c) General case

To tackle the general case for arbitrary rates r_0 and r_1, we take advantage of the convolution theorem again, noticing that the inverse Fourier transform of the $(\nu^2+r_0)^{-a}$ is [1]

$$\frac{1}{2\pi}\int_{-\infty}^{\infty}\frac{e^{i\nu x}d\nu}{(\nu^2+r_0)^a} = \frac{1}{\pi}\int_0^{\infty}\frac{\cos(\nu x)d\nu}{(\nu^2+r_0)^a} = \frac{\left(2\sqrt{r_0}|x|^{-1}\right)^{\frac{1}{2}-a}}{\sqrt{\pi}\Gamma(a)}\mathbb{K}\left(a-\frac{1}{2},\sqrt{r_0}|x|\right), \tag{6.201}$$

where $\mathbb{K}(\alpha,x)$ is the modified Bessel function of the second kind and $\Gamma(\cdot)$ the Gamma function. From Eq. (6.191) we obtain

$$\begin{aligned} p(x) =& \frac{r_1}{r_0+r_1}\left[\frac{2^{-\frac{r_1+k}{2k}}r_0^{\frac{r_1+3k}{4k}}}{\sqrt{\pi}\Gamma(\frac{r_1}{2k}+1)}\right]\int_{-\infty}^{\infty}\left(\sqrt{\frac{k}{2\pi}}e^{-\frac{ky^2}{2}}\right)|x-y|^{\frac{r_1+k}{2k}}\mathbb{K}\left(\frac{r_1+k}{2k},\sqrt{r_0}|x-y|\right)dy \\ &+ \frac{r_0}{r_0+r_1}\left[\frac{2^{-\frac{r_1-k}{2k}}r_0^{\frac{r_1+k}{4k}}}{\sqrt{\pi}\Gamma(\frac{r_1}{2k})}\right]\int_{-\infty}^{\infty}\left(\sqrt{\frac{k}{2\pi}}e^{-\frac{ky^2}{2}}\right)|x-y|^{\frac{r_1-k}{2k}}\mathbb{K}\left(\frac{r_1-k}{2k},\sqrt{r_0}|x-y|\right)dy. \end{aligned} \tag{6.202}$$

The large x behavior can be obtained by using $\mathbb{K}(\alpha,z) \approx \sqrt{\pi}e^{-z}/\sqrt{2z}$ at large z, or

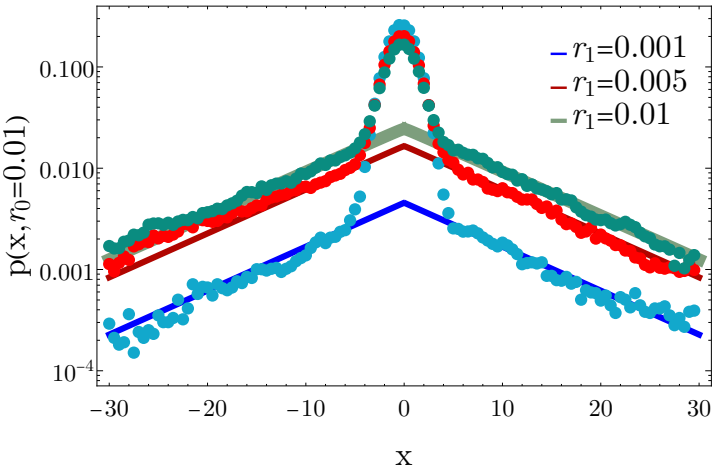

Figure 6.15: Particle density for an intermittent potential of the form $v(x) = \frac{k}{2}x^2$, with fixed rate $r_0 = 0.01$ and stiffness $k = 1$, and for several values of r_1. The lines are given by the approximation (6.205) and symbols represent simulation results.

$$\begin{aligned}
&\int_{-\infty}^{\infty}\left(\sqrt{\frac{k}{2\pi}}e^{-\frac{ky^2}{2}}\right)|x-y|^{\frac{r_1+k}{2k}}\mathbb{K}\left(\frac{r_1+k}{2k},\sqrt{r_0}|x-y|\right)dy\\
&\approx\int_{-\infty}^{\infty}\left(\frac{\sqrt{k}e^{-\frac{ky^2}{2}}}{2}\right)r_0^{-\frac{1}{4}}(x-y)^{\frac{r_1}{2k}}e^{-\sqrt{r_0}(x-y)}dy\\
&\approx r_0^{-\frac{1}{4}}x^{\frac{r_1}{2k}}e^{\frac{r_0}{2k}-\sqrt{r_0}x}\int_{-\infty}^{\infty}\left(\frac{\sqrt{k}e^{-\frac{k(y-\sqrt{r_0}/k)^2}{2}}}{2}\right)dy=r_0^{-\frac{1}{4}}x^{\frac{r_1}{2k}}e^{\frac{r_0}{2k}-\sqrt{r_0}x}\sqrt{\frac{\pi}{2}},
\end{aligned}\tag{6.203}$$

similarly,

$$\int_{-\infty}^{\infty}\left(\sqrt{\frac{k}{2\pi}}e^{-\frac{y^2}{2}}\right)|x-y|^{\frac{r_1-k}{2k}}\mathbb{K}\left(\frac{r_1-k}{2k},\sqrt{r_0}|x-y|\right)dy\approx r_0^{-\frac{1}{4}}x^{\frac{r_1}{2k}-1}e^{\frac{r_0}{2k}-\sqrt{r_0}x}\sqrt{\frac{\pi}{2}}.\tag{6.204}$$

Combining the expressions (6.203)-(6.204) one obtains

$$p(x)\approx\frac{r_0^{\frac{r_1+2k}{4k}}x^{\frac{r_1}{2k}}e^{\frac{r_0}{2k}-\sqrt{r_0}x}}{2^{\frac{r_1}{2k}}\Gamma(\frac{r_1}{2k})(r_0+r_1)}\left(k+\frac{\sqrt{r_0}}{x}\right)\approx\frac{r_0^{\frac{r_1+2k}{4k}}kx^{\frac{r_1}{2k}}e^{\frac{r_0}{2k}-\sqrt{r_0}x}}{2^{\frac{r_1}{2k}}\Gamma(\frac{r_1}{2k})(r_0+r_1)}.\tag{6.205}$$

We conclude that the exponential tail of the non-equilibrium steady state distribution now exhibits an algebraic prefactor, or $p(x)\sim x^{\frac{r_1}{2k}}e^{-\sqrt{r_0}x}$. Notice that in the limit $r_1\approx 0$, $\Gamma(\frac{r_1}{2k})\approx\frac{2k}{r_1}$ and Eq. (6.205) reduces to Eq. (6.200). Our results are in very good agreement with numerical simulations, as displayed in Fig. 6.15.

Chapter 7

Conclusions

The content of the present manuscript is part of the research work that we have done during the Ph.D. program in physics. In the following we point out the main conclusions of our work and discuss the scope of its content, as well as possible extensions and applications. The content of our work is divided in two topics: in Chapter 5 we study the first hitting time properties of a diffusive search to a target that intermittently switches between a reactive and a non-reactive state; In Chapter 6 we have investigated the dynamics of a diffusive particle in the presence of an external potential that intermittently is turned on and off.

In Section 5.1 we addressed the problem of a particle diffusing on the infinite line and hitting an intermittent target placed at the origin. We have deduced the Fokker-Planck equations that govern the evolution of the survival probabilities, from which we calculated the exact first hitting time distribution. We analyzed the asymptotic behaviour of the FHTD for large times, finding a new time regime that appears when the target is mostly inactive. This asymptotic time scales as $\sim t^{-1/2}$, in addition to the standard decay $\sim t^{-3/2}$, characteristic of symmetric diffusive processes. The crossover time τ_c that separates the two regimes depends on the rates of the target dynamics α and β, and is given by Eq. (5.61). On time scales smaller than τ_c, the search process is slow in the sense that the survival probability decays much more slowly than in the standard case of a perfectly reactive target.

In Section 5.2 we have studied the statistical properties of the first hitting time between a diffusing particle undergoing stochastic resetting to the initial position and an intermittent target. We have calculated the mean time it takes for the particle to hit the target for the first time in its reactive state, and have shown that this quantity can be minimized with respect to the resetting rate. This feature is also characteristic of many resetting processes with perfectly absorbing targets. The MFHT increases due to the intermittent dynamics of the target. The minimal MFHT can thus be very high when the target is mostly non-reactive, which is intuitive since the task of searching an intermittent target is much more challenging.

It is also worth noting that the coefficient of variation of the search time is not unity at optimality, in contrast with resetting problems that have a complete renewal structure. Here, the coefficient of variation can reach values much larger than one at the optimal resetting rate, specially for targets that spend a moderate fraction of time in the inactive state but long periods of time in each state. Other situations are analogous to the different

resetting protocols of the stochastic gate. For instance, a run-and-tumble particle can be stochastically reset to its initial position, or may also have its velocity reset according to a given distribution [57]. In continuous time random walks, both the position and the waiting time may be subject to reset, or only the position [79]. The scaled Brownian motion model has also been studied under complete [23] or incomplete [22] resetting protocols.

Section 5.3 is devoted to the study of the first hitting time statistics between a run-and-tumble particle and an intermittent target. When the system is confined between two reflective walls, we have focused our attention on the mean first hitting time, which can be calculated exactly. For any values of the rates a and b of the intermittent dynamics, the particle should opt for a ballistic motion ($\gamma = 0$) in order to minimize the mean search time. Less persistent motion not only increases, on average, the time of first target encounter, but also makes this time less predictable, *i.e.*, with larger relative fluctuations around the mean. According to the results of section 5.3.3, the relative variance of the first hitting time exhibits a non-monotonic behaviour with respect to the intermittent parameters and the turning rate. When the transition rates become slow compared to the tumbling rate ($a, b \ll \gamma$), the coefficient of variation takes larger values compared with the steady target case.

When the particle motion is unbounded, our findings extend the results of Section 5.1 on Brownian motion and an intermittent target on the infinite line. We have found that the target dynamics drastically affect the scaling of the first hitting times distribution, whose most unusual feature is an extended intermediate regime in $t^{-1/2}$, previous to the standard $t^{-3/2}$ asymptotic decay.

Regarding simple diffusion or diffusion with stochastic resetting, we found that, when the target becomes highly intermittent, *i.e.*, when the transitions between the reactive and the non-reactive state occur over a time-scale much smaller than the diffusion time, the model of intermittent targets is equivalent to the problem of a partially absorbing target. We could establish a relationship between the target rates, the diffusion coefficient and the effective absorption velocity of the radiation boundary condition. Such equivalence between partially absorbing and dynamical boundaries has been observed in other search processes [80, 81], but it does not hold in general. For instance, in the problem of diffusion with stochastic resetting when the target transition rates are comparable to the inverse diffusion time, the optimal resetting rate exhibits distinctive features, such as a non-monotonic behaviours.

For the run-and-tumble dynamics, the expression of the global MFPT in bounded domains in our problem takes the same form as for the RT with partial absorption, although the two problems are clearly different. Particularly interesting is to notice that the crossover time t_c can be recast under a simple form as $t_c = 2\gamma\epsilon^{-2}$, where ϵ is the absorption coefficient given by Eq. (5.149) it the limit $\ell = \infty$. Therefore, the crossover time can be redefined in terms of the tumble rate and the effective absorption coefficient. As soon as t is $\gg$ than t_{ta} and t_{tb} (the target relaxation and particle turning times, respectively), the scaling behaviour of the first hitting time distribution and all the subsequent conclusions remain valid for the problem of partial absorption.

We have also addressed the problem of random searches in fluctuating media. In Section 6.1 we study the dynamics of a diffusive particle in one dimension under the action of an intermittent potential. We first study the implementation of a piecewise linear

potential with a minimum at the origin and that is turned on and off intermittently. This problem extends well-known models of diffusion with stochastic resetting to the origin, which are recovered in some limits. Its implementation in experiments employing optical tweezers is possible, and would not require specific micro-manipulations such as bringing the particle back to the origin. In Section 6.2 we extend the scope of our work to more general potentials, particularly for potentials of the form $v(x) = k|x - x_0|^n/n$. With this, we were able to generalize our results, finding that the first passage properties of the system with a general potential power $n > 0$ behaves as similar as the linear potential ($n = 1$) in Section 6.1. Therefore, the following conclusions are valid in the general case with $v(x) = k|x - x_0|^n/n$:

We have shown that the presence of the potential, although intermittent in time, always leads to a non-equilibrium steady state and renders the mean first passage time to a target finite. The MFPT can be further minimized with respect to the re-scaled switch-on (r_0) and switch-off (r_1) rates. Since the problem involves two rates instead of one as usual in resetting processes, we have found a rather rich phenomenology.

If the particle starts at the potential minimum, below a critical potential strength, the protocol that minimizes the MFPT to a target located at a certain distance consists in always keeping the potential on ($r_1 = 0$), whereas for stronger potentials the two optimal rates are non-zero. In the latter case, the dynamics are fully out-of-equilibrium and the trajectories a succession of free and biased diffusive phases. The transition in the optimal rates is continuous or discontinuous at the critical potential strength, depending on whether the potential is initially on or off. Above threshold, the optimal MFPT is nearly always lower than the lowest Kramers' time, a result that generalizes previous comparisons between the efficiency of equilibrium and non-equilibrium searches [58, 65]. Likewise, when one seeks to minimize the MFPT with respect to the potential strength at fixed rates, another discontinuous transition occurs and a phase diagram can be drawn in the (r_0, r_1)-plane.

Near the continuous transition mentioned above, a perturbative theory allows to decompose the MFPT into an equilibrium part (which depends only on the potential strength) and a rate dependent part. The latter is non-monotonous with respect to r_0 and reaches a minimum at a value $\gg 1$ which contrasts with the optimal re-scaled rates of order unity found in usual resetting problems. Importantly, this contribution to the MFPT can take negative values above the critical strength, a regime where minimization leads to non-trivial rates in a way analogous to a second order Ginzburg-Landau transition.

In the vicinity of the discontinuous transitions, we have unveiled metastable behaviors as the rates or the strength are varied. Metastability in a resetting process was recently reported and confirmed experimentally with optical traps in [21] using a quite different setup and protocol. Hence, this new property is likely to be generic in resetting processes.

In summary, for the problem of random searches of fluctuating targets, we have shown that diffusive search processes can be severely affected by the intermittent switching dynamics of a target site, a situation often met in noisy complex media. A new, rate controlled scaling regime with exponent $-1/2$ emerges at high target crypticity, and the problem can be mapped onto a radiation boundary problem at large times. These results can be readily extended to higher spatial dimensions with the same formalism. Further study should consider other transport processes, as well as non-exponential distributions

of activity times. Interestingly, biological on-off processes such as DNA looping and ion channel dynamics often exhibit substantial non-Markov effects [40, 85, 66]. We also mention that the decay of the survival probability in unconfined space plays an important role for the large volume scaling of the FHT distribution in confined environments [82]. The intermediate regime for cryptic targets should thus have important consequences for confined walks [41].

In the context of resetting processes, our results highlight how target internal dynamics, a widely observed feature in natural systems, affect the optimisation of random searches by resetting. The scope of this work can be extended to the study of non-Poissonian resetting/target switching, as well as to anomalous diffusion processes. Although we have considered here the resetting of a single particle in the presence of an intermittent target, our results can be generalized to extended systems that can be reset to a specific configuration. An illustrative example is the growth of an interface which is stochastically interrupted by resetting to a certain profile, as occurring in mammalian tumors that are reduced to their initial size when a chemical is applied [69]. It would be interesting to study interface growth under resetting when the system is surrounded by fluctuating boundaries. Our study brings further understanding on non-equilibrium particles diffusing in fluctuating environments, where target encounters depend on both internal noises and fluctuations external to the particle dynamics.

Our findings point toward intermittent dynamics as a way of regulating first passage processes in the cell. They can also have implications in foraging ecology, where animals are able to be cryptic and undetectable by predators for long period of times by camouflaging themselves [131], or adopting a subterranean lifestyle [49, 114, 62, 104]. According to Eq. (5.70), to avoid predators and fulfill the constraint of spending a certain fraction of time outside, animals should space out consecutive exits in time, a behaviour actually observed in female ground squirrels [144, 145]. Macroscopic search experiments with dynamical targets can be achieved by means of mobile robots with a limited sensing range and fixed sources emitting intermittent electromagnetic signals [128, 127].

Regarding our work on random searches in fluctuating media, our study shows that incorporating physical constraints into idealized resetting models (which often assume instantaneous relocations, for instance) can lead to new phenomena. Our calculations were performed with a linear potential as well as for more general potentials. We got a similar conclusions with harmonic or other confining potentials, at least qualitatively. The distribution of the first passage times remains unknown and could be investigated through the calculation of higher moments. A first-passage distribution with spectacular spikes was found and explained theoretically in optical trap experiments with periodic resetting [21]. Resetting protocols at periodic times [106, 35, 103] that act on a potential deserve further study.

Although we have advanced in the understanding of the first passage properties of diffusing systems in fluctuating media, many questions remain unanswered. One of these questions concerns the study of anomalous diffusion particles hitting intermittent targets. The interest in these systems is motivated by the universality of the Sparre Andersen theorem, which is valid for $1d$ random walks with symmetric and continuous step length distributions [60]. We would like to check whether the scaling behaviour $\sim t^{-1/2}$ of the first hitting time distribution observed in the Brownian case and for cryptic targets can also emerge in anomalous diffusion or if another scaling law depending on the step length

distribution appears.

Systems in which searching particles perform anomalous diffusion, such as Lévy flight [139, 138, 140] have been widely studied and observed in natural phenomena. Non-Brownian diffusion in fluctuating environments has been studied as well [17, 52, 7, 4]. In addition to this, we want to extent our results to targets that fluctuate with a non-Markovian internal dynamics, as has been observed in DNA looping or ion channel dynamics [40, 85, 66].

We are also interested in extending our results of the problem of diffusion in fluctuating environments to more general time-dependent potentials with different shapes. We would also like to combine the two problems, the intermittent target and intermittent potentials, with the aim of modeling more complex systems.

Finally, we would like to mention that most of the work presented in the current manuscript has been published in different scientific journals [96, 99, 97, 98], as well as in national and international schools such as the "2019 Arnold Sommerfeld School: The Physics of Life" at the Arnold Sommerfeld Center for Theoretical Physics in Munich, Germany, and in the "2019 Mexican School of Statistical Physics and Complex System", at the National Autonomous University of Mexico. In the latter school, the presented poster was prized as one of the three best posters. In addition, the study on the linear intermittent potential was developed in collaboration with the researchers Satya N. Majumdar and Grégory Schehr. This collaboration gave rise to an article that has been accepted for publication in the "Journal of Statistical Mechanics: theory and experiment" [99].

Appendix A

Governing equations of the survival probabilities

A.1 Simple diffusion

To derive the set of equations (5.120), let us first suppose that at time $t = 0$ the particle starts with velocity $+v$ and the target is in the invisible state or $\sigma(t = 0) = 0$. During the small time interval $[0, \Delta t]$ there is a probability $a\Delta t$ for the target to change to the state $\sigma = 1$ and a probability $1 - a\Delta t$ to remain in the state $\sigma = 0$. On the other hand, with a probability $\gamma\Delta t$ the particle will change its velocity to $-v$, or will remain with $+v$ with probability $1 - \gamma\Delta t$. If we sum these contributions, the survival probability can be written as

$$\begin{aligned} Q_0^+(x, t + \Delta t) =& (1 - a\Delta t)(1 - \gamma\Delta t)Q_0^+(x + v\Delta t, t) \\ &+ a\Delta t(1 - \gamma\Delta t)Q_1^+(x + v\Delta t, t) \\ &+ \gamma\Delta t(1 - a\Delta t)Q_0^-(x + v\Delta t, t) \\ &+ a\gamma\Delta t^2 Q_1^-(x + v\Delta t, t). \end{aligned} \tag{A.1}$$

Expanding the r.h.s. of (A.1) in Taylor series and retaining only the terms of order Δt, we obtain

$$\frac{\partial Q_0^+}{\partial t} = v\frac{\partial Q_0^+}{\partial x} - a(Q_0^+ - Q_1^+) - \gamma(Q_0^+ - Q_0^-), \tag{A.2}$$

which is the first equation in (5.120). The other three equations for Q_0^-, Q_1^+ and Q_1^- can be deduced in a similar way.

A.2 Diffusion with resetting

In this section we derive Eqs. (5.71) and (5.72), for a particle located at x_0 at $t = 0$. Let us first suppose that the target is initially non-reactive. In a realization of the search process, during a small time interval $[0, \Delta t]$, with probability $\alpha\Delta t$ the target will switch to the reactive state, and with probability $1 - \alpha\Delta t$ it will remain non-reactive. Meanwhile, with probability $r\Delta t$, the particle will reset to the position x_r and with probability $1 - r\Delta t$, it will diffuse and reach a new position $x_0 + \xi$, where ξ is a small random displacement due to Brownian diffusion during Δt. The position at Δt (x_r or $x_0 + \xi$) is considered as a new

starting position, from which the particle may survive during the interval $[\Delta t, t+\Delta t]$, which is of length t. Summing the contributions of the various eventualities, we obtain the evolution of the survival probability at $t+\Delta t$, starting from x_0:

$$\begin{aligned} Q_0(x_0, t+\Delta t) = \; & (1-r\Delta t)\left[\alpha\Delta t \int d\xi Q_1(x_0+\xi, t)P_{\Delta t}(\xi) + (1-\alpha\Delta t)\int d\xi Q_0(x_0+\xi, t)P_{\Delta t}(\xi)\right] \\ & + r\Delta t\left[\alpha\Delta t Q_1(x_r, t) + (1-\alpha\Delta t)Q_0(x_r, t)\right] \end{aligned} \tag{A.3}$$

where $P_{\Delta t}(\xi)$ is the density of ξ.

We expand the survival probabilities in the right-hand-side in series of ξ, which is Gaussian distributed with first moment $\langle\xi\rangle = 0$ and second moment $\langle\xi^2\rangle = 2D\Delta t$, with D the diffusion coefficient. The integrals in Eq. (A.4) are $\langle Q(x_0+\xi, t)\rangle_\xi \approx Q(x_0, t) + D\Delta t\frac{\partial^2 Q(x_0,t)}{\partial x_0^2}$. Neglecting the terms of order higher than Δt, one obtains

$$Q_0(x_0, t+\Delta t) = Q_0(x_0, t) + \Delta t\left\{D\frac{\partial^2 Q_0(x_0,t)}{\partial x_0^2} + \alpha Q_1(x_0,t) - (r+\alpha)Q_0(x_0,t) + rQ_0(x_r,t)\right\} \tag{A.4}$$

Similarly, for the initial target state $\sigma = 1$, we have

$$Q_1(x_0, t+\Delta t) = Q_1(x_0, t) + \Delta t\left\{D\frac{\partial^2 Q_1(x_0,t)}{\partial x_0^2} + \beta Q_0(x_0,t) - (r+\beta)Q_1(x_0,t) + rQ_1(x_r,t)\right\} \tag{A.5}$$

In the limit $\Delta t \to 0$, Eqs. (A.4) and (A.4) become (5.71) and (5.72), repectively.

A.3 Run-and-tumble

To derive the set of equations (5.120), let us first suppose that at time $t = 0$ the particle starts with velocity $+v$ and the target is in the invisible state or $\sigma(t=0) = 0$. During the small time interval $[0, \Delta t]$ there is a probability $a\Delta t$ for the target to change to the state $\sigma = 1$ and a probability $1 - a\Delta t$ to remain in the state $\sigma = 0$. On the other hand, with a probability $\gamma\Delta t$ the particle will change its velocity to $-v$, or will remain with $+v$ with probability $1-\gamma\Delta t$. If we sum these contributions, the survival probability can be written as

$$\begin{aligned} Q_0^+(x, t+\Delta t) = & (1-a\Delta t)(1-\gamma\Delta t)Q_0^+(x+v\Delta t, t) \\ & + a\Delta t(1-\gamma\Delta t)Q_1^+(x+v\Delta t, t) \\ & + \gamma\Delta t(1-a\Delta t)Q_0^-(x+v\Delta t, t) \\ & + a\gamma\Delta t^2 Q_1^-(x+v\Delta t, t). \end{aligned} \tag{A.6}$$

Expanding the r.h.s. of (A.6) in Taylor series and retaining only the terms of order Δt, we obtain

$$\frac{\partial Q_0^+}{\partial t} = v\frac{\partial Q_0^+}{\partial x} - a(Q_0^+ - Q_1^+) - \gamma(Q_0^+ - Q_0^-), \tag{A.7}$$

which is the first equation in (5.120). The other three equations for Q_0^-, Q_1^+ and Q_1^- can be deduced in a similar way.

Appendix B

MFHT for a ballistic particle

In the ballistic limit $\gamma = 0$, the motion of the RTP becomes deterministic; once the particle starts moving, it will cross the origin periodically, with period $T = 2L/v$, until it coincides with the target in the visible state. Then, in order to compute the survival probability it is enough to find the probability that the target is hidden at a succession of times periodically spaced. We also set $x = 0$, as we can see from Eq. (5.146) for a searcher with $\gamma > 0$ that $t_G = t(x = 0)$. For a ballistic particle starting at $x > 0$, the first crossing of the origin occurs at time x/v for the initial velocity $-v$ and $(2L - x)/v$ for the initial velocity $+v$, which gives the average time of $2L/v$, independent of x. We therefore choose $x = 0$. With this initial condition the contribution to the survival probability for the initial velocity $-v$ is zero when the target initial state is $\sigma_0 = 1$, *i.e.*, $Q_1^- = 0$. Also by symmetry one has that $Q_0^+ = Q_0^-$. In the following we focus on the calculation of Q_0^+ and Q_1^+.

Let us consider a Poisson point process Π_{a+b} with rate $a+b$ in dimensional units. The probability that an a-event is followed by a b-event is $p = a/(a+b)$, whereas $q = b/(a+b)$ is the probability that the b-event is followed by an a-event. We can take each case as a Bernoulli realization with probability of success p and failure q, and the number of realizations will be distributed in time as Π_{a+b}. The probability that at time t the target is invisible given the initial target state $\sigma(t = 0) = \sigma_0$ is

$$P\left[\sigma(t) = 0|\sigma_0\right] = \frac{b}{a+b}\left(1 + C_{\sigma_0} e^{-(a+b)t}\right), \tag{B.1}$$

where $C_0 = a/b$ and $C_1 = -1$. For $\sigma_0 = 0$, Eq. (B.1) is the probability that the last event occurred is not a, whereas for $\sigma_0 = 1$ it is the probability that the last event occurred is b.

Similarly, the probability that the target is visible at time t given the initial state σ_0 is

$$P\left[\sigma(t) = 1|\sigma_0\right] = \frac{a}{a+b}\left(1 + B_{\sigma_0} e^{-(a+b)t}\right) \tag{B.2}$$

where $B_0 = -1$ and $B_1 = a/b$.

As mentioned, the searcher will cross the origin at times $t_n = nT$ for $n \in \{1, 2, \dots\}$ and from Eq. (B.1) the survival probability at time t_n given the initial velocity $+v$ and the initial target state $\sigma_0 = 0$ is $P\left[\sigma(t) = 0|\sigma_0 = 0\right]^n$ or

$$Q_0^+ = \left(\frac{b}{a+b} + \frac{a e^{-(a+b)T}}{a+b}\right)^n \tag{B.3}$$

For the initial condition $\sigma_0 = 1$ one has

$$Q_1^+ = \frac{b}{a+b}\left(1 - e^{-(a+b)T}\right)\left(\frac{b}{a+b} + \frac{ae^{-(a+b)T}}{a+b}\right)^{n-1} \tag{B.4}$$

which is the probability that the target has switched to invisible at the first passage of the particle and is invisible at the following $n-1$ passages.

Averaging over the initial velocities and target initial conditions, with $Q_1^- = 0$ and $Q_0^+ = Q_0^-$, the average survival probability up to time $t_n = nT$ will be

$$\begin{aligned} Q_{av}(n) = {} & \frac{ab}{(a+b)^2}\left[\frac{b}{a} + e^{-(a+b)T/2}\cosh\frac{(a+b)T}{2}\right] \\ & \times \left(\frac{b}{a+b} + \frac{ae^{-(a+b)T}}{a+b}\right)^{n-1} \end{aligned} \tag{B.5}$$

where $n \in \{1, 2, \dots\}$.

As expected, for $n = 0$ the survival probability is $Q_{av}(n=0) = \frac{b}{a+b} + \frac{a}{2(a+b)}$, since there is a probability $b/(a+b)$ that at time $t = 0$ the target is invisible, and a probability $a/(2(a+b))$ that at time $t = 0$ the target is visible but the searcher starts moving with velocity $+v$.

From Eq. (B.5), the global MFHT will be

$$\begin{aligned} t_G &= \sum_{n=0}^{\infty} t_n P_{av}(t_n) = T\sum_{n=0}^{\infty} n P_{av}(n) = T\sum_{n=0}^{\infty} Q_{av}(n) \\ &= \left(a + b + b\coth\frac{L(a+b)}{v}\right)\frac{L}{av}, \end{aligned} \tag{B.6}$$

and Eq. (5.157) is recovered.

Appendix C

Expressions for $t_1^{(1)}$ and $t_1^{(2)}$ for the piece-wise linear potential

The solution $t_1^{(1)}(x)$ for $x \in [0, \infty)$ is given by

$$
\begin{aligned}
t_1^{(1)}(x,+) = &\left(\frac{\sqrt{r_0} e^{-\sqrt{r_0}} \left(1 - 2e^{\gamma} - \frac{\gamma^2}{r_0}\right) + \gamma + \sqrt{r_0}}{\left(\sqrt{r_0} - \gamma\right)\left(\sqrt{r_0} + \gamma\right)^2} + \frac{e^{-2\sqrt{r_0}}}{\left(\sqrt{r_0} + \gamma\right)^2} \right) \left(e^{-\sqrt{r_0}x} - 1\right) \\
&- \gamma \frac{\partial t_1^{+(0)}(x)}{\partial \gamma} + \frac{r_0 \gamma^2 \left[\frac{4e^{\gamma}}{\sqrt{r_0}\gamma} - \left(\frac{2e^{\gamma}-1}{\gamma} + \frac{\gamma}{r_0}\right)\left(\frac{2e^{\gamma}-1}{\gamma} + \frac{1}{\sqrt{r_0}}\right) e^{-\sqrt{r_0}}\right]}{\left(r_0 - \gamma^2\right)^2} \\
&+ \frac{\gamma\sqrt{r_0}\left(\frac{2e^{\gamma}-1}{\gamma} - \frac{2e^{\sqrt{r_0}}-1}{\sqrt{r_0}}\right) e^{-2\sqrt{r_0}}}{\left(\gamma + \sqrt{r_0}\right)\left(r_0 - \gamma^2\right)} - \frac{2e^{\gamma}(\gamma - 1) + \frac{\gamma}{\sqrt{r_0}} + 2}{r_0 - \gamma^2},
\end{aligned}
\tag{C.1}
$$

and the solution in the interval $x \in [-1, 0]$ is:

$$
\begin{aligned}
t_1^{(1)}(x,-) = &\left(\frac{4r_0 e^{\gamma - \sqrt{r_0}}}{\left(r_0 - \gamma^2\right)^2} - \frac{2\left(e^{-\sqrt{r_0}} + 1\right)\left(\gamma + \sqrt{r_0} e^{-\sqrt{r_0}}\right)}{\left(\sqrt{r_0} + \gamma\right)\left(r_0 - \gamma^2\right)} \right) \left(e^{-\gamma x} - 1\right) - \frac{e^{\sqrt{r_0}x} - 1}{\left(\gamma + \sqrt{r_0}\right)^2} \\
&- \frac{e^{-2\sqrt{r_0}}\sqrt{r_0}\left(\frac{\gamma^2}{r_0} e^{\sqrt{r_0}} + \frac{\gamma}{\sqrt{r_0}} + 1 - \left(1 - 2e^{\gamma}\right) e^{\sqrt{r_0}}\right)\left(e^{-\sqrt{r_0}x} - 1\right)}{\left(\sqrt{r_0} - \gamma\right)^2\left(\gamma + \sqrt{r_0}\right)} - \frac{2\gamma x e^{-x\gamma}}{r_0 - \gamma^2} \\
&- \gamma \frac{\partial t_1^{-(0)}(x)}{\partial \gamma} + \frac{r_0 \gamma^2 \left[\frac{4e^{\gamma}}{\sqrt{r_0}\gamma} - \left(\frac{2e^{\gamma}-1}{\gamma} + \frac{\gamma}{r_0}\right)\left(\frac{2e^{\gamma}-1}{\gamma} + \frac{1}{\sqrt{r_0}}\right) e^{-\sqrt{r_0}}\right]}{\left(r_0 - \gamma^2\right)^2} \\
&+ \frac{\gamma\sqrt{r_0}\left(\frac{2e^{\gamma}-1}{\gamma} - \frac{2e^{\sqrt{r_0}}-1}{\sqrt{r_0}}\right) e^{-2\sqrt{r_0}}}{\left(\gamma + \sqrt{r_0}\right)\left(r_0 - \gamma^2\right)} - \frac{2e^{\gamma}(\gamma - 1) + \frac{\gamma}{\sqrt{r_0}} + 2}{r_0 - \gamma^2}.
\end{aligned}
\tag{C.2}
$$

For the coefficient of the term of order ϵ^2, at $x = 0$, we obtain:

$$
\begin{aligned}
t_1^{(2)}(\gamma, r_0) =& \frac{\gamma^5 r_0^2 e^{-3\sqrt{r_0}} \left(\frac{1}{r_0^2} + 2\frac{e^\gamma - 2}{r_0^{3/2}\gamma} + 4\frac{e^\gamma + 1}{r_0\gamma^2} + 2\frac{e^\gamma(6e^\gamma - 5)}{\sqrt{r_0}\gamma^3} - \frac{(1-2e^\gamma)^2}{\gamma^4} \right)}{2\left(\gamma - \sqrt{r_0}\right)^3 \left(\gamma + \sqrt{r_0}\right)^4} \\
&+ \frac{e^{-4\sqrt{r_0}} r_0 \gamma^2 \left(\frac{1-2e^\gamma}{\gamma} - \frac{1}{\sqrt{r_0}} \right)}{2\left(\sqrt{r_0} - \gamma\right)\left(\gamma + \sqrt{r_0}\right)^4} + \frac{r_0^2 \gamma^2 e^{-2\sqrt{r_0}}}{\left(r_0 - \gamma^2\right)^2} \left(\frac{4e^{2\gamma}\left(\frac{\gamma^2}{r_0} + \frac{\gamma}{\sqrt{r_0}} - 2\right) + 8e^{3\gamma}}{\left(r_0 - \gamma^2\right)^2} \right. \\
&- 2e^\gamma \left(\frac{3}{r_0} + \frac{2}{\gamma} + \frac{\gamma - 1}{\gamma\sqrt{r_0}} + \frac{\sqrt{r_0} + 1}{\gamma^2} \right) - \frac{2\gamma^2}{r_0^2} - \frac{\gamma}{2r_0^{3/2}} + \frac{3}{r_0} - \frac{2\gamma + 7}{2\gamma\sqrt{r_0}} \\
&\left. + \frac{1 + \sqrt{r_0}}{\gamma^2} \right) + \frac{\gamma^6 r_0^3 e^{-\sqrt{r_0}}}{\left(r_0 - \gamma^2\right)^4} \left(\frac{\left(1 - 2e^\gamma\right)^2 \left(\sqrt{r_0} + 2\right)}{2\gamma^6} - \frac{\sqrt{r_0} - 4}{2r_0^3} + \frac{3e^\gamma + 1}{\gamma r_0^2} \right. \\
&+ \frac{e^\gamma \left(9\sinh(\gamma) + 11\cosh(\gamma) - 5 + \frac{7 - 4\sinh(\gamma)}{\sqrt{r_0}} \right)}{\gamma^5} - \frac{5e^\gamma + 2}{\gamma r_0^{5/2}} \\
&- \frac{2\left(e^\gamma\left(5e^\gamma\left(\sqrt{r_0} + 1\right) - 4\sqrt{r_0} - 5\right) - 6\right)}{\gamma^3 r_0^{3/2}} - \frac{2e^\gamma\left(\frac{2e^\gamma - 1}{\sqrt{r_0}} + 2\right) - \frac{7}{2}\left(1 - \frac{2}{\sqrt{r_0}}\right)}{\gamma^2\sqrt{r_0}} \\
&\left. - \frac{2e^\gamma\left(e^\gamma\left(\sqrt{r_0} - 10\right) - 3\sqrt{r_0} + 5\right) + \frac{7}{2}\sqrt{r_0} + 8}{\gamma^4 r_0} \right) + \frac{\gamma^6 r_0^4}{\left(r_0 - \gamma^2\right)^4} \left(\frac{8e^\gamma + 1}{2\gamma r_0^{7/2}} \right. \\
&- \frac{2\left(e^\gamma((\gamma - 5)\gamma + 5) - 5\right)}{\gamma^6 r_0} - \frac{4e^\gamma(2\gamma + 5) - 5}{2\gamma^5 r_0^{3/2}} + \frac{2e^\gamma((\gamma - 10)\gamma + 10) - 21}{2\gamma^4 r_0^2} \\
&\left. + \frac{2e^\gamma(2\gamma - 7) - 3}{\gamma^3 r_0^{5/2}} + \frac{2e^\gamma(\gamma + 1) + 3}{\gamma^2 r_0^3} + \frac{e^\gamma((\gamma - 2)\gamma + 2) - 2}{\gamma^8} - \frac{1}{2r_0^4} \right). \quad \text{(C.3)}
\end{aligned}
$$

Appendix D

Numerical solution of the MFHTs t_0 and t_1 for a general potential

In this section we present the method we followed to obtain the numerical solution of the system of equations (6.125)-(6.124), which is based on a finite difference scheme for the two-point boundary value problem.

First, we discretize the interval $[0, c]$ into N equal parts, where n is a positive integer. Let $h = c/N$ be the step-size of the grid given by the points $x_i = ih$, where $0 \leq i \leq N$. For the numerical approximation of the MFHT t_0 and t_1 we use the notation $y_i = t_0(x_i)$ and $z_i = t_1(x_i)$, with $0 \leq i \leq N$.

For the derivatives of t_0 in x we will use the following scheme:

$$t_0'(x_i) = \frac{y_{i+1} - y_{i-1}}{2h} + \mathcal{O}(h^2), \tag{D.1}$$

$$t_0''(x_i) = \frac{y_{i+1} - 2y_i + y_{i-1}}{h^2} + \mathcal{O}(h^2), \tag{D.2}$$

Similarly for t_1 we write

$$t_1'(x_i) = \frac{z_{i+1} - z_{i-1}}{2h} + \mathcal{O}(h^2), \tag{D.3}$$

$$t_1''(x_i) = \frac{z_{i+1} - 2z_i + z_{i-1}}{h^2} + \mathcal{O}(h^2). \tag{D.4}$$

With the above definitions and dropping the terms $\mathcal{O}(h^2)$, the system of equations (6.124)-(6.125) becomes, with the harmonic potential $v(x) = k(x-1)^2/2$:

$$-1 = \frac{y_{i+1} - 2y_i + y_{i-1}}{h^2} - r_0 \left[y_i - z_i\right], \tag{D.5}$$

$$-1 = \frac{z_{i+1} - 2z_i + z_{i-1}}{h^2} - k(x_i - 1)\frac{z_{i+1} - z_{i-1}}{2h} - r_1 \left[z_i - y_i\right], \tag{D.6}$$

for $1 \leq i \leq N-1$. Rearranging the above expression we get

$$-h^2 = y_{i+1} - \left(2 + h^2 r_0\right) y_i + y_{i-1} + h^2 r_0 z_i, \tag{D.7}$$

$$-h^2 = \left(1 - \frac{hk(x_i - 1)}{2}\right) z_{i+1} - \left(2 + h^2 r_1\right) z_i + \left(1 + \frac{hk(x_i - 1)}{2}\right) z_{i-1} + h^2 r_1 y_i, \tag{D.8}$$

Imposing the absorbing boundary conditions $y_0 = 0$ and $z_0 = 0$ at $i = 0$, we have, from Eqs. (D.7)-(D.8),

$$-h^2 = y_2 - \left(2 + h^2 r_0\right) y_1 + h^2 r_0 z_1, \tag{D.9}$$

$$-h^2 = \left(1 - \frac{hk(x_1 - 1)}{2}\right) z_2 - \left(2 + h^2 r_1\right) z_1 + h^2 r_1 y_1. \tag{D.10}$$

The reflecting boundary conditions at $x = c$ can be set in a finite difference scheme of second-order accuracy as

$$t_0'(c) = \frac{3y_N - 4y_{N-1} + y_{N-2}}{2h} = 0, \tag{D.11}$$

$$t_1'(c) = \frac{3z_N - 4z_{N-1} + z_{N-2}}{2h} = 0, \tag{D.12}$$

which leads to

$$y_N = \frac{4y_{N-1} - y_{N-2}}{3}, \tag{D.13}$$

$$z_N = \frac{4z_{N-1} - z_{N-2}}{3}. \tag{D.14}$$

With the above results and setting $i = N - 1$ into Eqs. (D.7)-(D.8),

$$-h^2 = -\left(\frac{2}{3} + h^2 r_0\right) y_{N-1} + \frac{2}{3} y_{N-2} + h^2 r_0 z_{N-1}, \tag{D.15}$$

$$-h^2 = -\left(\frac{2}{3} + \frac{2hk(x_{N-1} - 1)}{3} + h^2 r_1\right) z_{N-1} + \frac{2}{3}\left[1 + hk(x_{N-1} - 1)\right] z_{N-2} + h^2 r_1 y_{N-1}. \tag{D.16}$$

Finally, we get the finite difference system

$$\mathbb{A}\mathbf{w} = \mathbf{b}, \tag{D.17}$$

where the numerical solution vector is defined as

$$\mathbf{w}^T = (y_1, y_2, \ldots, y_{N-1}, z_1, z_2, \ldots, z_{N-1}) \tag{D.18}$$

and the constant vector given by

$$\mathbf{b}^T = -h^2 (1, 1, \ldots, 1), \tag{D.19}$$

and the coefficient matrix $\mathbb{A}$ with its entries given by the coefficients in Eqs. (D.7)-(D.8), together with the special cases for $i = 1$ and $i = N - 1$, given by the Eqs. (D.9)-(D.10) and Eqs. (D.15)-(D.16):

$$\mathbb{A} = \begin{pmatrix} -(2+h^2r_0) & 1 & 0 & \cdots & 0 & 0 \\ 1 & -(2+h^2r_0) & 1 & \cdots & 0 & 0 \\ \vdots & \vdots & \vdots & \ddots & \vdots & \vdots \\ 0 & 0 & 0 & \cdots & \frac{2}{3} & -\left(\frac{2}{3}+h^2r_0\right) \\ h^2r_1 & 0 & 0 & \cdots & 0 & 0 \\ 0 & h^2r_1 & 0 & \cdots & 0 & 0 \\ \vdots & \vdots & \vdots & \ddots & \vdots & \vdots \\ 0 & 0 & 0 & \cdots & 0 & h^2r_1 \end{pmatrix}$$

$$\begin{pmatrix} h^2r_0 & 0 & 0 \\ 0 & h^2r_0 & 0 \\ \vdots & \vdots & \vdots \\ 0 & 0 & 0 \\ -(2+h^2r_1) & 1-\frac{hk(x_1-1)}{2} & 0 \\ 1+\frac{hk(x_1-1)}{2} & -(2+h^2r_1) & 1-\frac{hk(x_1-1)}{2} \\ \vdots & \vdots & \vdots \\ 0 & 0 & 0 \end{pmatrix}$$

$$\begin{pmatrix} \cdots & 0 & 0 \\ \cdots & 0 & 0 \\ \cdots & \vdots & \vdots \\ \cdots & 0 & h^2r_0 \\ \cdots & 0 & 0 \\ \cdots & 0 & 0 \\ \cdots & \vdots & \vdots \\ \cdots & \frac{2}{3}\left(1+hk(x_{N-1}-1)\right) & -\left(\frac{2}{3}+\frac{2hk(x_{N-1}-1)}{3}+h^2r_1\right) \end{pmatrix} \tag{D.20}$$

Now we can find the solution $\mathbf{w}$ by numerically inverting the system (D.17):

$$\mathbf{w} = \mathbb{A}^{-1}\mathbf{b}. \tag{D.21}$$

From this vector $\mathbf{w}$ we obtain the numerical solution of the MFPTs t_0 and t_1 at any specified starting point x. It is straightforward to generalize the matrix $\mathbb{A}^{-1}$ to an arbitrary external potential.

Bibliography

[1] M. Abramowitz and I. A. Stegun. *Handbook of mathematical functions: with formulas, graphs, and mathematical tables*, volume 55. Courier Corporation, 1965.

[2] E. S. Andersen. On the fluctuations of sums of random variables. *Mathematica Scandinavica*, pages 263–285, 1954.

[3] E. S. Andersen. On the fluctuations of sums of random variables II. *Mathematica Scandinavica*, pages 195–223, 1955.

[4] L. Angelani. Run-and-tumble particles, telegrapher's equation and absorption problems with partially reflecting boundaries. *Journal of Physics A: Mathematical and Theoretical*, 48(49):495003, Nov 2015.

[5] L. Angelani. Confined run-and-tumble swimmers in one dimension. *Journal of Physics A: Mathematical and Theoretical*, 50(32):325601, Jul 2017.

[6] L. Angelani, A. Costanzo, and R. D. Leonardo. Active ratchets. *Europhysics Letters*, 96(6):68002, Dec 2011.

[7] L. Angelani, R. Di Leonardo, and M. Paoluzzi. First-passage time of run-and-tumble particles. *The European Physical Journal E*, 37(7):59, 2014.

[8] G. B. Arfken, H. J. Weber, and F. E. Harris. Chapter 20 - integral transforms. In G. B. Arfken, H. J. Weber, and F. E. Harris, editors, *Mathematical Methods for Physicists (Seventh Edition)*, pages 963 – 1046. Academic Press, Boston, seventh edition edition, 2013.

[9] G. B. Arfken, H. J. Weber, and F. E. Harris. Chapter 9 - partial differential equations. In G. B. Arfken, H. J. Weber, and F. E. Harris, editors, *Mathematical Methods for Physicists (Seventh Edition)*, pages 401 – 445. Academic Press, Boston, seventh edition edition, 2013.

[10] F. Bartumeus, J. Catalan, U. L. Fulco, M. L. Lyra, and G. M. Viswanathan. Optimizing the Encounter Rate in Biological Interactions: Lévy versus Brownian Strategies. *Physical Review Letters*, 88:097901, Feb 2002.

[11] L. Batsilas, A. M. Berezhkovskii, and S. Y. Shvartsman. Stochastic model of autocrine and paracrine signals in cell culture assays. *Biophysical Journal*, 85(6):3659–3665, 2003.

[12] J. M. Beggs and D. Plenz. Neuronal Avalanches in Neocortical Circuits. *Journal of Neuroscience*, 23(35):11167–11177, 2003.

[13] S. Belan. Restart could optimize the probability of success in a bernoulli trial. *Physical Review Letters*, 120:080601, Feb 2018.

[14] E. Ben-Naim, S. Redner, and G. Weiss. Partial absorption and "virtual" traps. *Journal of Statistical Physics*, 71(1-2):75–88, 1993.

[15] O. Bénichou, M. Coppey, M. Moreau, P.-H. Suet, and R. Voituriez. Optimal Search Strategies for Hidden Targets. *Physical Review Letters*, 94:198101, May 2005.

[16] O. Bénichou, B. Gaveau, and M. Moreau. Resonant diffusion in a linear network of fluctuating obstacles. *Physical Review E*, 59:103–116, Jan 1999.

[17] O. Bénichou, C. Loverdo, M. Moreau, and R. Voituriez. Intermittent search strategies. *Reviews of Modern Physics*, 83:81–129, Mar 2011.

[18] O. Bénichou, M. Moreau, and G. Oshanin. Kinetics of stochastically gated diffusion-limited reactions and geometry of random walk trajectories. *Physical Review E*, 61:3388–3406, Apr 2000.

[19] A. M. Berezhkovskii, Y. A. Makhnovskii, M. I. Monine, V. Y. Zitserman, and S. Y. Shvartsman. Boundary homogenization for trapping by patchy surfaces. *The Journal of Chemical Physics*, 121(22):11390–11394, 2004.

[20] H. C. Berg. *E. coli in Motion*. Springer Science & Business Media, 2008.

[21] B. Besga, A. Bovon, A. Petrosyan, S. N. Majumdar, and S. Ciliberto. Optimal mean first-passage time for a brownian searcher subjected to resetting: Experimental and theoretical results. *Physical Review Research*, 2:032029, Jul 2020.

[22] A. S. Bodrova, A. V. Chechkin, and I. M. Sokolov. Nonrenewal resetting of scaled brownian motion. *Physical Review E*, 100:012119, Jul 2019.

[23] A. S. Bodrova, A. V. Chechkin, and I. M. Sokolov. Scaled brownian motion with renewal resetting. *Physical Review E*, 100:012120, Jul 2019.

[24] A. S. Bodrova and I. M. Sokolov. Brownian motion under noninstantaneous resetting in higher dimensions. *Physical Review E*, 102:032129, Sep 2020.

[25] A. S. Bodrova and I. M. Sokolov. Resetting processes with noninstantaneous return. *Physical Review E*, 101:052130, May 2020.

[26] W. E. Boyce, R. C. DiPrima, and D. B. Meade. *Elementary differential equations*. John Wiley & Sons, 2017.

[27] A. J. Bray, S. N. Majumdar, and G. Schehr. Persistence and first-passage properties in nonequilibrium systems. *Advances in Physics*, 62(3):225–361, 2013.

[28] P. Bressloff and J. Newby. Directed intermittent search for hidden targets. *New Journal of Physics*, 11(2):023033, Feb 2009.

[29] P. C. Bressloff. *Stochastic processes in cell biology*, volume 41. Springer, 2014.

[30] P. C. Bressloff. Diffusive search for a stochastically-gated target with resetting. *Journal of Physics A: Mathematical and Theoretical*, 53(42):425001, oct 2020.

[31] P. C. Bressloff and S. D. Lawley. Stochastically gated diffusion-limited reactions for a small target in a bounded domain. *Physical Review E*, 92:062117, Dec 2015.

[32] C. E. Budde, M. O. Cáceres, and M. A. Ré. Transient behaviour in the absorption probability distribution in the presence of a non-markovian dynamic trap. *Europhysics Letters*, 32(3):205–210, Oct 1995.

[33] T. W. Burkhardt. Dynamics of absorption of a randomly accelerated particle. *Journal of Physics A: Mathematical and General*, 33(45):L429–L432, Nov 2000.

[34] M. O. Cáceres, C. E. Budde, and M. A. Ré. Theory of the absorption probability density of diffusing particles in the presence of a dynamic trap. *Physical Review E*, 52:3462–3468, Oct 1995.

[35] A. Chechkin and I. M. Sokolov. Random search with resetting: A unified renewal approach. *Physical Review Letters*, 121:050601, Aug 2018.

[36] A. V. Chechkin, R. Metzler, J. Klafter, V. Y. Gonchar, et al. Introduction to the theory of Lévy flights. *Anomalous Transport*, pages 129–162, 2008.

[37] Y.-J. Chen, S. Johnson, P. Mulligan, A. J. Spakowitz, and R. Phillips. Modulation of DNA loop lifetimes by the free energy of loop formation. *Proceedings of the National Academy of Sciences*, 111(49):17396–17401, 2014.

[38] T. Chou and M. R. D'Orsogna. First passage problems in biology. In *First-Passage Phenomena and Their Applications*, pages 306–345. World Scientific, 2014.

[39] F. C. Collins and G. E. Kimball. Diffusion-controlled reaction rates. *Journal of Colloid Science*, 4(4):425 – 437, 1949.

[40] D. Colquhoun and B. Sakmann. Fluctuations in the microsecond time range of the current through single acetylcholine receptor ion channels. *Nature*, 294(5840):464, 1981.

[41] S. Condamin, O. Bénichou, V. Tejedor, R. Voituriez, and J. Klafter. First-passage times in complex scale-invariant media. *Nature*, 450(7166):77, 2007.

[42] M. Coppey, O. Bénichou, R. Voituriez, and M. Moreau. Kinetics of Target Site Localization of a Protein on DNA: A Stochastic Approach. *Biophysical Journal*, 87(3):1640 – 1649, 2004.

[43] T. Cui, J. Ding, and J. Z. Y. Chen. Mean first-passage times of looping of polymers with intrachain reactive monomers: Lattice monte carlo simulations. *Macromolecules*, 39(16):5540–5545, 2006.

[44] D. A. Darling, A. Siegert, et al. The first passage problem for a continuous markov process. *The Annals of Mathematical Statistics*, 24(4):624–639, 1953.

[45] M. de Jager, F. J. Weissing, P. M. J. Herman, B. A. Nolet, and J. van de Koppel. Lévy Walks Evolve Through Interaction Between Movement and Environmental Complexity. *Science*, 332(6037):1551–1553, 2011.

[46] A. Dhar, A. Kundu, S. N. Majumdar, S. Sabhapandit, and G. Schehr. Run-and-tumble particle in one-dimensional confining potentials: Steady-state, relaxation, and first-passage properties. *Physical Review E*, 99:032132, Mar 2019.

[47] B. S. Donahue and R. Abercrombie. Free diffusion coefficient of ionic calcium in cytoplasm. *Cell Calcium*, 8(6):437 – 448, 1987.

[48] A. Eberharter and P. B. Becker. Histone acetylation: a switch between repressive and permissive chromatin. *EMBO Reports*, 3(3):224–229, 2002.

[49] M. Edmunds. The evolution of cryptic coloration. *Insect Defenses: Adaptive Mechanisms and Strategies of Prey and Predators*, pages 3–21, 1990.

[50] A. W. F. Edwards. Pascal's Problem: The 'Gambler's Ruin'. *International Statistical Review / Revue Internationale de Statistique*, 51(1):73–79, 1983.

[51] J. Elgeti and G. Gompper. Run-and-tumble dynamics of self-propelled particles in confinement. *Europhysics Letters*, 109(5):58003, Mar 2015.

[52] I. Eliazar, T. Koren, and J. Klafter. Searching circular DNA strands. *Journal of Physics: Condensed Matter*, 19(6):065140, Jan 2007.

[53] G. B. Ermentrout and D. H. Terman. *Mathematical foundations of neuroscience*, volume 35. Springer Science & Business Media, 2010.

[54] M. R. Evans and S. N. Majumdar. Diffusion with optimal resetting. *Journal of Physics A: Mathematical and Theoretical*, 44(43):435001, Oct 2011.

[55] M. R. Evans and S. N. Majumdar. Diffusion with Stochastic Resetting. *Physical Review Letters*, 106:160601, Apr 2011.

[56] M. R. Evans and S. N. Majumdar. Effects of refractory period on stochastic resetting. *Journal of Physics A: Mathematical and Theoretical*, 52(1):01LT01, Nov 2018.

[57] M. R. Evans and S. N. Majumdar. Run and tumble particle under resetting: a renewal approach. *Journal of Physics A: Mathematical and Theoretical*, 51(47):475003, Oct 2018.

[58] M. R. Evans, S. N. Majumdar, and K. Mallick. Optimal diffusive search: nonequilibrium resetting versus equilibrium dynamics. *Journal of Physics A: Mathematical and Theoretical*, 46(18):185001, Apr 2013.

[59] M. R. Evans, S. N. Majumdar, and G. Schehr. Stochastic resetting and applications. *Journal of Physics A: Mathematical and Theoretical*, 53(19):193001, Apr 2020.

[60] W. Feller. *An introduction to probability theory and its applications*, volume 2. John Wiley & Sons, 2008.

[61] C. Gardiner. *Handbook of Stochastic Methods for Physics, Chemistry, and the Natural Sciences*. Springer complexity. Springer, 2004.

[62] R. P. Gendron and J. E. R. Staddon. Searching for Cryptic Prey: The Effect of Search Rate. *The American Naturalist*, 121(2):172–186, 1983.

[63] D. T. Gillespie. A general method for numerically simulating the stochastic time evolution of coupled chemical reactions. *Journal of Computational Physics*, 22(4):403 – 434, 1976.

[64] J. Gillis. Substrate colour-matching cues in the cryptic grasshopper Circotettix rabula rabula (Rehn & Hebard). *Animal Behaviour*, 30(1):113 – 116, 1982.

[65] L. Giuggioli, S. Gupta, and M. Chase. Comparison of two models of tethered motion. *Journal of Physics A: Mathematical and Theoretical*, 52(7):075001, Jan 2019.

[66] I. Goychuk and P. Hänggi. Fractional diffusion modeling of ion channel gating. *Physical Review E*, 70:051915, Nov 2004.

[67] B. Grant and R. J. Howlett. Background selection by the peppered moth (Biston betularia Linn.): individual differences. *Biological Journal of the Linnean Society*, 33(3):217–232, 01 2008.

[68] D. S. Grebenkov. Spectral theory of imperfect diffusion-controlled reactions on heterogeneous catalytic surfaces. *The Journal of Chemical Physics*, 151(10):104108, 2019.

[69] S. Gupta, S. N. Majumdar, and G. Schehr. Fluctuating interfaces subject to stochastic resetting. *Physical Review Letters*, 112:220601, Jun 2014.

[70] S. E. Halford and J. F. Marko. How do site-specific DNA-binding proteins find their targets?. *Nucleic Acids Research*, 32(10):3040–3052, 05 2004.

[71] T. H. Harris, E. J. Banigan, D. A. Christian, C. Konradt, E. D. T. Wojno, K. Norose, E. H. Wilson, B. John, W. Weninger, A. D. Luster, et al. Generalized Lévy walks and the role of chemokines in migration of effector CD8+ T cells. *Nature*, 486(7404):545–548, 2012.

[72] A. L. Hodgkin and A. F. Huxley. Resting and action potentials in single nerve fibres. *The Journal of physiology*, 104(2):176, 1945.

[73] T. Hu and B. I. Shklovskii. How a protein searches for its specific site on DNA: The role of intersegment transfer. *Physical Review E*, 76:051909, Nov 2007.

[74] P. W. Jones and P. Smith. *Stochastic processes: an introduction*. CRC Press, 2017.

[75] E. Kagan and I. Ben-Gal. *Search and Foraging: Individual Motion and Swarm Dynamics*. CRC Press, 06 2015.

[76] R. Kawano, Y. Tsuji, K. Sato, T. Osaki, K. Kamiya, M. Hirano, T. Ide, N. Miki, and S. Takeuchi. Automated parallel recordings of topologically identified single ion channels. *Scientific reports*, 3(1):1–7, 2013.

[77] H. A. Kramers. Brownian motion in a field of force and the diffusion model of chemical reactions. *Physica*, 7(4):284–304, 1940.

[78] P. L. Krapivsky, S. Redner, and E. Ben-Naim. *A kinetic view of statistical physics*. Cambridge University Press, 2010.

[79] Ł. Kuśmierz and E. Gudowska-Nowak. Subdiffusive continuous-time random walks with stochastic resetting. *Physical Review E*, 99:052116, May 2019.

[80] S. D. Lawley and J. P. Keener. A new derivation of robin boundary conditions through homogenization of a stochastically switching boundary. *SIAM Journal on Applied Dynamical Systems*, 14(4):1845–1867, 2015.

[81] S. D. Lawley, J. C. Mattingly, and M. C. Reed. Stochastic switching in infinite dimensions with applications to random parabolic pde. *SIAM Journal on Mathematical Analysis*, 47(4):3035–3063, 2015.

[82] N. Levernier, O. Bénichou, T. Guérin, and R. Voituriez. Universal first-passage statistics in aging media. *Physical Review E*, 98:022125, Aug 2018.

[83] N. Levernier, J. Textor, O. Bénichou, and R. Voituriez. Inverse Square Lévy Walks are not Optimal Search Strategies for $d \geq 2$. *Physical Review Letters*, 124:080601, Feb 2020.

[84] D. R. Lide. *CRC Handbook of Chemistry and Physics*, volume 85. CRC press, 2004.

[85] L. S. Liebovitch, J. Fischbarg, and J. P. Koniarek. Ion channel kinetics: a model based on fractal scaling rather than multistate markov processes. *Mathematical Biosciences*, 84(1):37–68, 1987.

[86] S. N. Majumdar. Universal first-passage properties of discrete-time random walks and Lévy flights on a line: Statistics of the global maximum and records. *Physica A: Statistical Mechanics and its Applications*, 389(20):4299–4316, 2010. Proceedings of the 12th International Summer School on Fundamental Problems in Statistical Physics.

[87] S. N. Majumdar and A. J. Bray. Persistence with Partial Survival. *Physical Review Letters*, 81:2626–2629, Sep 1998.

[88] S. N. Majumdar, P. Mounaix, and G. Schehr. Survival probability of random walks and lévy flights on a semi-infinite line. *Journal of Physics A: Mathematical and Theoretical*, 50(46):465002, Oct 2017.

[89] K. Malakar, V. Jemseena, A. Kundu, K. V. Kumar, S. Sabhapandit, S. N. Majumdar, S. Redner, and A. Dhar. Steady state, relaxation and first-passage properties of a run-and-tumble particle in one-dimension. *Journal of Statistical Mechanics: Theory and Experiment*, 2018(4):043215, Apr 2018.

[90] K. Martens, L. Angelani, R. Di Leonardo, and L. Bocquet. Probability distributions for the run-and-tumble bacterial dynamics: An analogy to the Lorentz model. *The European Physical Journal E*, 35(9):84, 2012.

[91] R. J. Mashl, Y. Tang, J. Schnitzer, and E. Jakobsson. Hierarchical Approach to Predicting Permeation in Ion Channels. *Biophysical Journal*, 81(5):2473 – 2483, 2001.

[92] A. Masó-Puigdellosas, D. Campos, and V. Méndez. Transport properties of random walks under stochastic noninstantaneous resetting. *Physical Review E*, 100:042104, Oct 2019.

[93] J. Masoliver, J. M. Porrà, and G. H. Weiss. Solution to the telegrapher's equation in the presence of reflecting and partly reflecting boundaries. *Physical Review E*, 48:939–944, Aug 1993.

[94] H. H. McAdams and A. Arkin. Stochastic mechanisms in gene expression. *Proceedings of the National Academy of Sciences*, 94(3):814–819, 1997.

[95] J. A. McCammon and S. H. Northrup. Gated binding of ligands to proteins. *Nature*, 293(5830):316–317, 1981.

[96] G. Mercado-Vásquez and D. Boyer. First Hitting Times to Intermittent Targets. *Physical Review Letters*, 123:250603, Dec 2019.

[97] G. Mercado-Vásquez and D. Boyer. First hitting times between a run-and-tumble particle and a stochastically gated target. *Physical Review E*, 103:042139, Apr 2021.

[98] G. Mercado-Vásquez and D. Boyer. Search of stochastically gated targets with diffusive particles under resetting. *Journal of Physics A: Mathematical and Theoretical*, 54(44):444002, oct 2021.

[99] G. Mercado-Vásquez, D. Boyer, S. N. Majumdar, and G. Schehr. Intermittent resetting potentials. *Journal of Statistical Mechanics: Theory and Experiment*, 2020(11):113203, Nov 2020.

[100] R. Metzler, G. Oshanin, and S. Redner (Eds.). *First-passage phenomena and their applications*. World Scientific, 2014.

[101] E. W. Montroll and G. H. Weiss. Random walks on lattices. II. *Journal of Mathematical Physics*, 6(2):167–181, 1965.

[102] B. Munsky, G. Neuert, and A. van Oudenaarden. Using gene expression noise to understand gene regulation. *Science*, 336(6078):183–187, 2012.

[103] A. Nagar and S. Gupta. Diffusion with stochastic resetting at power-law times. *Physical Review E*, 93:060102, Jun 2016.

[104] W. J. O'brien, H. I. Browman, and B. I. Evans. Search Strategies of Foraging Animals. *American Scientist*, 78(2):152–160, 1990.

[105] A. Pal, I. P. Castillo, and A. Kundu. Motion of a Brownian particle in the presence of reactive boundaries. *Physical Review E*, 100:042128, Oct 2019.

[106] A. Pal, A. Kundu, and M. R. Evans. Diffusion under time-dependent resetting. *Journal of Physics A: Mathematical and Theoretical*, 49(22):225001, Apr 2016.

[107] A. Pal and S. Reuveni. First passage under restart. *Physical Review Letters*, 118:030603, Jan 2017.

[108] S. Redner. *A Guide to First-Passage Processes*. Cambridge University Press, 2001.

[109] L. E. Reichl. *A Modern Course in Statistical Physics*. Wiley, 2nd edition, 1998.

[110] J. Reingruber and D. Holcman. Gated Narrow Escape Time for Molecular Signaling. *Physical Review Letters*, 103:148102, Sep 2009.

[111] S. Reuveni. Optimal stochastic restart renders fluctuations in first passage times universal. *Physical Review Letters*, 116:170601, Apr 2016.

[112] H. Risken. Fokker-planck equation. In *The Fokker-Planck Equation*. Springer, 1996.

[113] F. Rojo, P. A. Pury, and C. E. Budde. Intermittent pathways towards a dynamical target. *Physical Review E*, 83:011116, Jan 2011.

[114] G. D. Ruxton, T. N. Sherratt, M. P. Speed, M. P. Speed, M. Speed, et al. *Avoiding attack: the evolutionary ecology of crypsis, warning signals and mimicry*. Oxford University Press, 2004.

[115] B. Sakmann. *Single-channel recording*. Springer Science & Business Media, 2013.

[116] H. Sano and M. Tachiya. Partially diffusion-controlled recombination. *The Journal of Chemical Physics*, 71(3):1276–1282, 1979.

[117] E. Schrödinger. Zur theorie der fall-und steigversuche an teilchen mit brownscher bewegung. *Physikalische Zeitschrift*, 16:289–295, 1915.

[118] R. D. Schumm and P. C. Bressloff. Search processes with stochastic resetting and partially absorbing targets. *Journal of Physics A: Mathematical and Theoretical*, 54(40):404004, sep 2021.

[119] C. J. Schwiening. A brief historical perspective: Hodgkin and Huxley. *The Journal of physiology*, 590(Pt 11):2571, 2012.

[120] M. Sheinman and Y. Kafri. The effects of intersegmental transfers on target location by proteins. *Physical Biology*, 6(1):016003, Jan 2009.

[121] M. F. Shlesinger. Origins and applications of the Montroll-Weiss continuous time random walk. *The European Physical Journal B*, 90(5):93, 2017.

[122] A. J. F. Siegert. On the First Passage Time Probability Problem. *Physical Review*, 81:617–623, Feb 1951.

[123] D. W. Sims, E. J. Southall, N. E. Humphries, G. C. Hays, C. J. Bradshaw, J. W. Pitchford, A. James, M. Z. Ahmed, A. S. Brierley, M. A. Hindell, et al. Scaling laws of marine predator search behaviour. *Nature*, 451(7182):1098–1102, 2008.

[124] A. Singer, Z. Schuss, A. Osipov, and D. Holcman. Partially Reflected Diffusion. *SIAM Journal on Applied Mathematics*, 68(3):844–868, 2008.

[125] P. Singh, S. Sabhapandit, and A. Kundu. Run-and-tumble particle in inhomogeneous media in one dimension. *Journal of Statistical Mechanics: Theory and Experiment*, 2020(8):083207, aug 2020.

[126] M. Slutsky and L. A. Mirny. Kinetics of protein-dna interaction: Facilitated target location in sequence-dependent potential. *Biophysical Journal*, 87(6):4021–4035, 2004.

[127] D. Song, C. Kim, and J. Yi. On the Time to Search for an Intermittent Signal Source Under a Limited Sensing Range. *IEEE Transactions on Robotics*, 27(2):313–323, 2011.

[128] D. Song, C.-Y. Kim, and J. Yi. Stochastic modeling of the expected time to search for an intermittent signal source under a limited sensing range. *Robotics: Science and Systems VI*, page 275, 2011.

[129] S. Song and J. Song. A Note on the History of the Gambler's Ruin Problem. *Communications for Statistical Applications and Methods*, 20(2):157–168, 2013.

[130] M. R. Spiegel. *Laplace transforms*. McGraw-Hill New York, 1965.

[131] M. Stevens and S. Merilaita. Animal camouflage: current issues and new perspectives. *Philosophical Transactions of the Royal Society B: Biological Sciences*, 364(1516):423–427, 2009.

[132] R. Stocker. Reverse and flick: Hybrid locomotion in bacteria. *Proceedings of the National Academy of Sciences*, 108(7):2635–2636, 2011.

[133] D. Swigon, B. D. Coleman, and W. K. Olson. Modeling the Lac repressor-operator assembly: The influence of DNA looping on Lac repressor conformation. *Proceedings of the National Academy of Sciences*, 103(26):9879–9884, 2006.

[134] A. Szabo, K. Schulten, and Z. Schulten. First passage time approach to diffusion controlled reactions. *The Journal of Chemical Physics*, 72(8):4350–4357, 1980.

[135] A. Szabo, D. Shoup, S. H. Northrup, and J. A. McCammon. Stochastically gated diffusion-influenced reactions. *The Journal of Chemical Physics*, 77(9):4484–4493, 1982.

[136] T. Tian and K. Burrage. Stochastic models for regulatory networks of the genetic toggle switch. *Proceedings of the National Academy of Sciences*, 103(22):8372–8377, 2006.

[137] T. Troscianko, C. P. Benton, P. G. Lovell, D. J. Tolhurst, and Z. Pizlo. Camouflage and visual perception. *Philosophical Transactions of the Royal Society of London B: Biological Sciences*, 364(1516):449–461, 2009.

[138] G. M. Viswanathan, F. Bartumeus, S. V. Buldyrev, J. Catalan, U. Fulco, S. Havlin, M. da Luz, M. Lyra, E. Raposo, and H. Eugene Stanley. Lévy flight random searches in biological phenomena. *Physica A: Statistical Mechanics and its Applications*, 314(1):208 – 213, 2002. Horizons in Complex Systems.

[139] G. M. Viswanathan, S. V. Buldyrev, S. Havlin, M. Da Luz, E. Raposo, and H. E. Stanley. Optimizing the success of random searches. *Nature*, 401(6756):911–914, 1999.

[140] G. M. Viswanathan, M. G. E. da Luz, E. P. Raposo, and H. E. Stanley. *The Physics of Foraging: An Introduction to Random Searches and Biological Encounters*. Cambridge University Press, 2011.

[141] M. Von Smoluchowski. Notiz uiber die Berechnung der Brownschen Molekularbewegung bei der Ehrenhaft-Millikanschen Versuchsanordning. *Physikalische Zeitschrift*, 16:318–321, 1915.

[142] G. H. Weiss. Some applications of persistent random walks and the telegrapher's equation. *Physica A: Statistical Mechanics and its Applications*, 311(3):381–410, 2002.

[143] J. Whitehouse, M. R. Evans, and S. N. Majumdar. Effect of partial absorption on diffusion with resetting. *Physical Review E*, 87:022118, Feb 2013.

[144] C. T. Williams, K. Wilsterman, A. D. Kelley, A. R. Breton, H. Stark, M. M. Humphries, A. G. McAdam, B. M. Barnes, S. Boutin, and C. L. Buck. Light loggers reveal weather-driven changes in the daily activity patterns of arboreal and semifossorial rodents. *Journal of Mammalogy*, 95(6):1230–1239, 12 2014.

[145] C. T. Williams, K. Wilsterman, V. Zhang, J. Moore, B. M. Barnes, and C. L. Buck. The secret life of ground squirrels: accelerometry reveals sex-dependent plasticity in above-ground activity. *Royal Society Open Science*, 3(9):160404, 2016.

[146] C. Wu. Chromatin remodeling and the control of gene expression. *Journal of Biological Chemistry*, 272(45):28171–28174, 1997.

[147] Y. Zhang and O. K. Dudko. First-Passage Processes in the Genome. *Annual Review of Biophysics*, 45(1):117–134, 2016.

[148] R. Zwanzig. Diffusion-controlled ligand binding to spheres partially covered by receptors: an effective medium treatment. *Proceedings of the National Academy of Sciences*, 87(15):5856–5857, 1990.